Advances in Production Engineering & Management

Identification Statement

APEM Editorial

Advances in Production Engineering & Management

Contents

Scope and topics

Advances in Production Engineering & Management (*APEM journal*) is an interdisciplinary refereed international academic journal published quarterly by the *Chair of Production Engineering* at the *University of Maribor*. The main goal of the *APEM journal* is to present original, high quality, theoretical and application-oriented research developments in all areas of production engineering and production management to a broad audience of academics and practitioners. In order to bridge the gap between theory and practice, applications based on advanced theory and case studies are particularly welcome. For theoretical papers, their originality and research contributions are the main factors in the evaluation process. General approaches, formalisms, algorithms or techniques should be illustrated with significant applications that demonstrate their applicability to real-world problems. Although the *APEM journal* main goal is to publish original research papers, review articles and professional papers are occasionally published.

Fields of interest include, but are not limited to:

Additive Manufacturing Processes
Advanced Production Technologies
Artificial Intelligence in Production
Assembly Systems
Automation
Big Data in Production
Computer-Integrated Manufacturing
Cutting and Forming Processes
Decision Support Systems
Deep Learning in Manufacturing
Discrete Systems and Methodology
e-Manufacturing
Evolutionary Computation in Production
Fuzzy Systems
Human Factor Engineering, Ergonomics
Industrial Engineering
Industrial Processes
Industrial Robotics
Intelligent Manufacturing Systems
Joining Processes
Knowledge Management

Logistics in Production
Machine Learning in Production
Machine Tools
Machining Systems
Manufacturing Systems
Materials Science, Multidisciplinary
Mechanical Engineering
Mechatronics
Metrology in Production
Modelling and Simulation
Numerical Techniques
Operations Research
Operations Planning, Scheduling and Control
Optimisation Techniques
Project Management
Quality Management
Risk and Uncertainty
Self-Organizing Systems
Statistical Methods
Supply Chain Management
Virtual Reality in Production

Bottleneck identification and alleviation in a blocked serial production line with discrete event simulation: A case study

Li, G.Z.[a,b,c,*], Xu, Z.G.[a,c], Yang, S.L.[a,c,d], Wang, H.Y.[e], Bai, X.L.[a,c], Ren, Z.H.[b]

[a]State Key Laboratory of Robotics, Shenyang Institute of Automation, Chinese Academy of Science, Shenyang, P.R. China
[b]School of Mechanical Engineering and Automation, Northeastern University, Shenyang, P.R. China
[c]Institutes for Robotics and Intelligent Manufacturing, Chinese Academy of Sciences, Shenyang, P.R. China
[d]University of Chinese Academy of Sciences, Beijing, P.R. China
[e]Shanghai Aerospace Chemical Engineering Institute, Huzhou, P.R. China

A B S T R A C T

Aiming at the gap between theoretical research and practical application in the production bottleneck field, we apply five bottleneck identification methods in a serial production line in aerospace industry based on discrete event simulation and Plant Simulation software, meanwhile discuss the influence of the bottleneck machine quantity on the system performance. This paper evaluated the practicability, accuracy and limitation of various bottleneck identification methods at the practical level. The results of the bottleneck alleviation manifest that increasing the number of bottleneck machines can effectively improve the system performance, but the more machine quantity, the smaller performance improvement. More importantly, the paper studies the influence mechanism and function relationship of the bottleneck machine quantity on the maximum completion time from an interesting actual phenomenon for the first time. The function obtains the condition that the maximum completion time achieve the minimum. The research and conclusion of this paper have essential reference significance for production guidance and theoretical research, and can also contribute to narrow the gap between theory and application of the production bottleneck field.

1. Introduction

The bottleneck is the machine or resource that affects the production capacity of the system in a period, which directly restricts the throughput of the whole system [1-6]. Therefore, bottleneck identification and alleviation are a vitally important production problem and the first step of production management, and it is of considerable significance to improve production efficiency, economic benefit and reduce energy consumption. The definition of the bottleneck is distinct for different production systems, and the bottleneck identification methods proposed in most researches are often not universal [7, 8]. The bottleneck is also a dynamic process that may move from one machine to another [9, 10]. Therefore, it is very complicated and challenging to apply the bottleneck identification theory to actual production.

To the best of our knowledge, bottleneck identification methods in most studies are proposed by two approaches: computer simulation [11-14] or mathematical analysis [15-18]. The conventional identification methods include as follows:

- The subsequent machine of the buffer with the highest average work-in-progress quantity is the bottleneck [11],
- The most utilized or least idle machine is the bottleneck [19],
- The next machine to the station with the highest blocking rate is the bottleneck [20],
- The machine with the longest average activity time is the bottleneck [21],
- The machine that processes the least variance or means absolute deviation of the inter-departure time is the bottleneck [14, 22], and
- The most sensitive machine to the system throughput is the bottleneck [23].

The purpose of bottleneck identification is to alleviate the bottleneck and improve system productivity. However, how to alleviate the bottleneck is a problem involving specific scenarios, and the methods to alleviate the bottleneck are also different for specific systems. The general alleviation methods include as follows:

- Increase the number of bottleneck machines [11, 21],
- Increase the buffer capacity before the bottleneck station [14], and
- Improve the production efficiency or reduce the processing time of the bottleneck machine [11, 24].

Although many researchers have established different bottleneck identification methods for various production systems, the practical application of these theories is rare. The reason is reflected in the complexity and uncertainty of the actual production system, such as limited buffer capacity, blocked, random interference, unique scenes. Moreover, these characteristics are difficult to be truly reflected by the theoretical model. Actual case studies on bottleneck alleviation are also rare, the effectiveness of alleviation methods has not been fully verified, and the general conclusions are still lacking. Therefore, there is a gap between the bottleneck theory and the practical application, which may be due to the fact that most papers focus on one or more practical problems at a time, and it is a challenge to apply the theory to various practical environments.

This paper aims to provide a case study that fully considers various bottleneck identification and alleviation methods, hoping to draw general conclusions for practice and theory, and also to narrow the gap between theory and application. The rest of the article is organized as follows. Section 2 proposes the materials and methods of the case study. Section 3 describes the system and establishes a virtual model based on Plant Simulation software. Section 4 shows the simulation results. Section 5 discusses the results of section 4. The summary and general conclusions will be presented in section 6.

2. Materials and methods

The serial production line, as the basic form of other types of production lines, is a typical discrete event dynamic system. The ideal serial production line model is shown in Fig. 1.
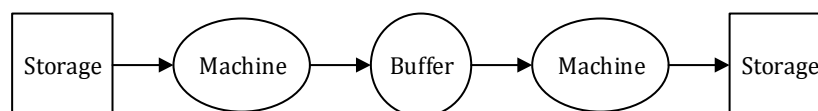
Fig. 1 The ideal model of the serial production line

The production activity in the serial production line is a dynamic process so that the bottleneck will change with this dynamic process. That means there is more than one bottleneck in the production process. Nevertheless, the primary bottleneck in a period is always significant and prominent, which is widely recognized by bottleneck theory and practical. Therefore, it is feasible to determine the most significant bottleneck based on the actual situation.

With the advent of Industry 4.0, computer simulation has become an important tool for production optimization [25]. Compared with mathematical modelling and algorithms, computer simulation can accurately reflect the system characteristics when faced with complex and dynamic production problems [26-29]. Simulation as a powerful tool to guide decision-making in

an uncertain environment can simulate the whole production cycle by processing a series of discrete event points on the time axis successively. Recent literature also points out that discrete event simulation is an effective means to solve discrete event systems [30, 31]. Therefore, we adopt the method of discrete event simulation to carry out the case study.

The research method of this paper can be described as follows, and the Plant Simulation software was used for creation of virtual model.

- Analysis layout and material flow of the system, and collect the time information of each process.
- Determines the feasible bottleneck identification method according to the actual system information.
- Establishes and verifies the simulation model of the system.
- Analysis system bottleneck based on the simulation model and identification method.
- Determines the appropriate bottleneck alleviation methods according to the actual system and the identified bottleneck machine, then discusses the performance of the alleviation method.
- Summarizes and concludes.

3. System analysis and modelling

3.1 Problem description

The case study involved a product processing and testing system in the aerospace field. The production layout is shown in Fig. 2. The system is mainly composed of the warehouse, four frame manipulators, two sets of transmission devices, some composite processing platforms (CP) and a series of auxiliary process platforms.
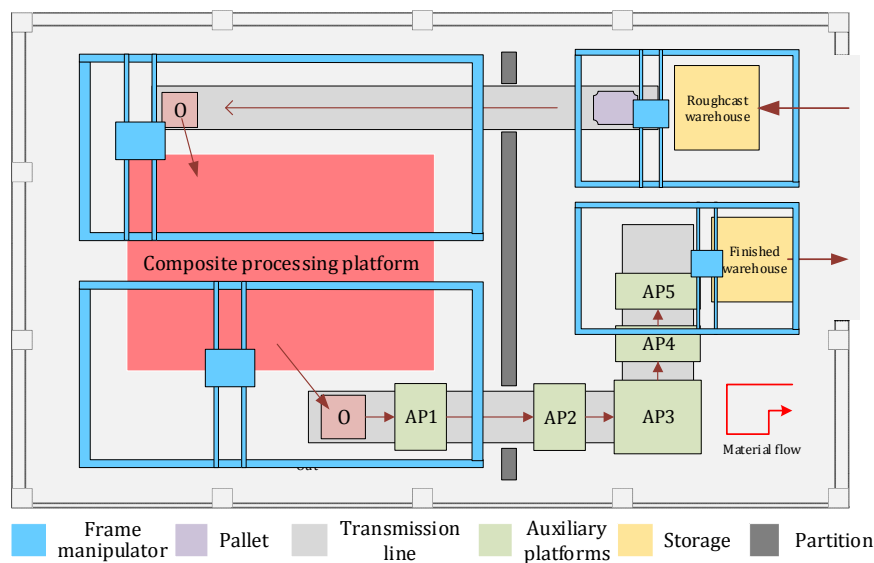
Fig. 2 The layout of the system

The material flow process can be described as follows:

- The frame manipulator carries the parts from the roughcast warehouse (RW) to the pallet until the pallet is filled, then the transport line begins to move with the pallet to the leftmost side of the track. The pallet capacity is 2. 15 s is needed for each part to be transported from the warehouse to pallet. The length of the transport line is 12 m, and the speed is 0.3 m/s.
- The second frame manipulator (FM, feeding manipulator) carries the parts from the pallet to the composite processing platform for processing, which requires 85 s for each frame manipulator to carry, and the processing time of the compound platform is 568 s.

- After the completion of the composite processing platform, the parts are carried by the third frame manipulator (BM, blanking manipulator) to the starting point of another transmission line, and each frame manipulator in this stage needs 57 s.
- The transmission line carries the parts through 5 auxiliary platforms (AP1, AP2, AP3, AP4, AP5) in turn, and the fourth frame manipulator (OM, offline manipulator) carries it to the finished product warehouse (FW). The processing time of the five stations is 10 s, 10 s, 10 s, 30 s, 30 s. The time of the frame manipulator off the line is 40 s.

Besides, if there are multiple compound processing platform, the feeding and blanking manipulator may face the problem of multiple targets, then the feeding to take the principle of proximity, the blanking to take the "first finished parts first blanking" strategy.

3.2 Problem assumption

According to the problem description, the system is a blocked serial production line system, which has no buffers. To facilitate the case study and the establishment of the simulation model, we suggest the following hypotheses in the case study:

1) The system is completely reliable and will not break down;
2) Due to the high degree of automation and the stable machining efficiency, the processing time is regarded as an absolute constant;
3) The finished product warehouse has enough capacity;
4) The number of parts stored in the roughcast warehouse is 40 and evaluates the production performance by the production indicators when 40 parts were all processed.

Six bottleneck identification methods are mentioned in the introduction, but the system has no buffer, so it is not feasible by the average work-in-progress of the buffer. The other five methods are all available, which will be applied to our practical case.

3.3 Model construction

Plant Simulation is used in this paper, and it is an object-oriented discrete event simulation software that can significantly reduce the difficulty of modelling and analysis with the characteristics of inheritance, encapsulation and visualization.

Establish machine objects, control strategies and data collection strategies for each process according to the system layout and material flow process. After repeated adjustments and modifications, the final simulation model is shown in Fig. 3. The object of "BF1", "BF2" and "BF3" was created for ease of modelling and had no impact on the simulation logic.
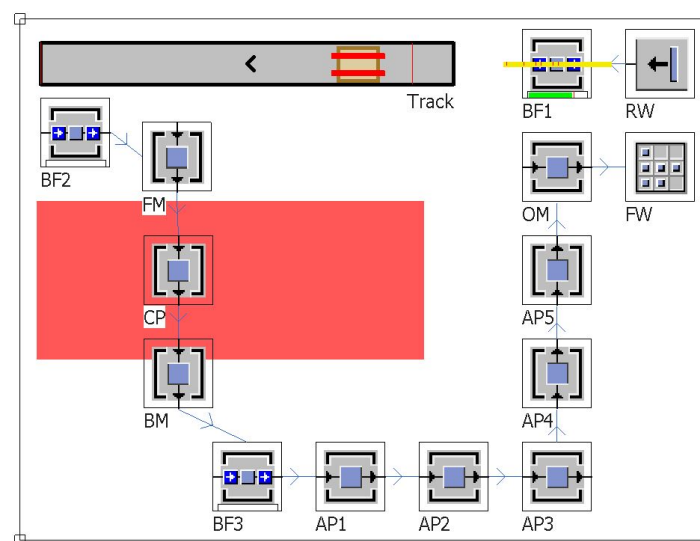
Fig. 3 The simulation model in plant simulation software

3.4 Model validation

The validity of the model is the premise of drawing correct results and conclusions. We allege that the established model is valid based on the following facts:

- The model runs correctly until all 40 parts are offline.
- The time of each production process is discussed and determined repeatedly by the planners after taking full account of the actual situation.
- The planners consider that the simulation logic is consistent with the actual production logic described in 3.1 by observing the simulation animation.
  (https://www.bilibili.com/video/av82436626/)

4. Results of the simulation

For the case study, the five available bottleneck identification methods are the most utilized or least idle machine (BT_1); The next machine to the station with the highest blocking rate (BT_2); The machine with the longest average activity time (BT_3); The machine that processes the least variance or mean absolute deviation of the inter-departure time (BT_4); The most sensitive machine to the system throughput (BT_5).

The evaluation indexes of BT_1, BT_2, BT_3 and BT_4 are machine utilization rate (MUR) or machine idle rate (MIR), machine blocking rate (MBR), average activity time (ACT), average absolute deviation (ITA) or variance (ITV) of inter-departure time.

BT_5 is the natural explanation of the bottleneck, but this concept is relatively vague, and the evaluation index is difficult to establish. Literature [21] solved the problem of job shop bottleneck identification through complex mathematical models and algorithms, but the authenticity and accuracy of mathematical modelling in diverse and complex environments could not be guaranteed. Therefore, we propose an intuitive mean that observe the Gantt chart to judge the most sensitive machine for throughput.

Collecting time information in the whole production cycle through model simulation, obtaining the indexes and shown in Table 1.

Table 1 shows that the bottlenecks identified by BT_1 and BT_3 are CP. However, the evaluation indexes of BT_2 and BT_4 do not show the difference on the machine, and the bottleneck is not distinguished. The result of BT_5 is also CP, its Gantt chart and specific discussion will be put in Section 5.

Then consider the measure to alleviate the bottleneck after CP is determined as the bottleneck. There is no buffer in the case study, so it is not feasible to increase the buffer capacity in front of the bottleneck. Besides, all the work is done by automatic equipment, so the production efficiency can hardly be accelerated. Therefore, the measure to alleviate the bottleneck is to increase the number of composite processing platforms.

Table 1 Evaluation indexes of the BT_1, BT_2, BT_3, BT_4

Machine	BT_1		BT_2	BT_3	BT_4	
	MUR, %	MIR, %	MBR, %	ACT, s	ITA	ITV
FM	12.9	87.1	0	85	0	0
CP	**86.3**	**13.7**	0	**568**	0	0
BM	8.7	91.3	0	57	0	0
AP1	1.5	98.5	0	10	0	0
AP2	1.5	98.5	0	10	0	0
AP3	1.5	98.5	0	10	0	0
AP4	4.6	95.4	0	30	0	0
AP5	4.6	95.4	0	30	0	0
OM	6.1	93.9	0	40	0	0

To determine the impact of the bottleneck machine quantity on the system performance, we consider a total of five scenarios, corresponding to the number of composite machining platforms of 1, 2, 3, 4, 5, then established the simulation model and control strategy for each scenario. The evaluation indexes in each scenario are completion time of the first part (FAT, first arrival time), completion time of the last part (FCT, final completion time), mean time interval between the part entering the finished warehouse (MCT, mean cycle time), utilization of the composite processing platform (CPU), utilization of feeding manipulator (FMU), utilization of blanking manipulator (BMU), maximum machine utilization (MMU), average machine utilization (AMU). The simulation results of those indexes are shown in Table 2.

Table 2 System performance evaluation in each scenario

Scenario No.	FAT, s	FCT, s	MCT, s	CPU, %	FMU, %	BMU, %	MMU, %	AMU, %
1	865	26332	653.1	86.3	12.9	8.7	86.3	15.9
2	865	13357	320.3	85	25.5	17.1	85	27.9
3	865	9354	217.7	80.9	36.3	24.4	80.9	35.9
4	865	6997	157.2	81.1	48.6	32.6	81.1	43.7
5	865	5776	125.9	78.6	58.8	39.5	78.6	48.9

5. Discussion

5.1 Evaluation of each bottleneck identification method

There are four machine states: working, waiting, blocked and failed. From the results in Table 1, it can be seen that the three states other than the working do not necessarily exist, such as the blocked state of the machine in our case study.

Machine utilization represents the working state, is the natural characteristic of the machine. Using machine utilization as an indicator to identify the bottleneck can determine the use degree of the machine. High usage means that parts are stacked in front of it, forming bottlenecks.

Average activity time is correlated with the machine utilization. With the total completion time is equal, the higher the machine utilization, the longer time the part stays on each machine, which is also the average activity time.

The inter-departure time of each part arrive at each machine in the case is shown in Fig. 4. The abscissa represents the sequence of parts arriving at each machine, and the ordinate represents the corresponding arrival time. It can be seen that the part arrival time of each machine is proportional to the part arrival sequence, which means that the processing interval time of all the part begins in each machine is equal.
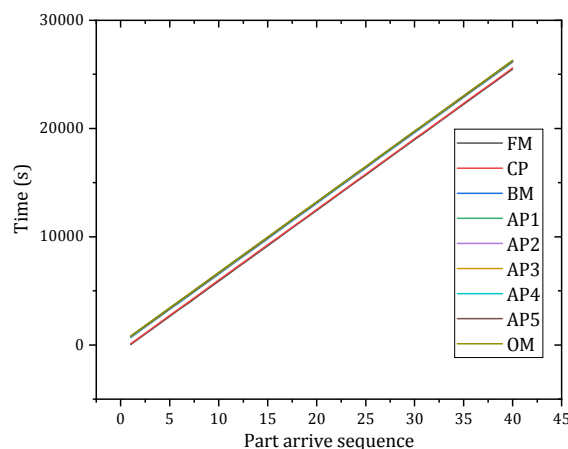
Fig. 4 The inter-departure time of each part arrive at each machine
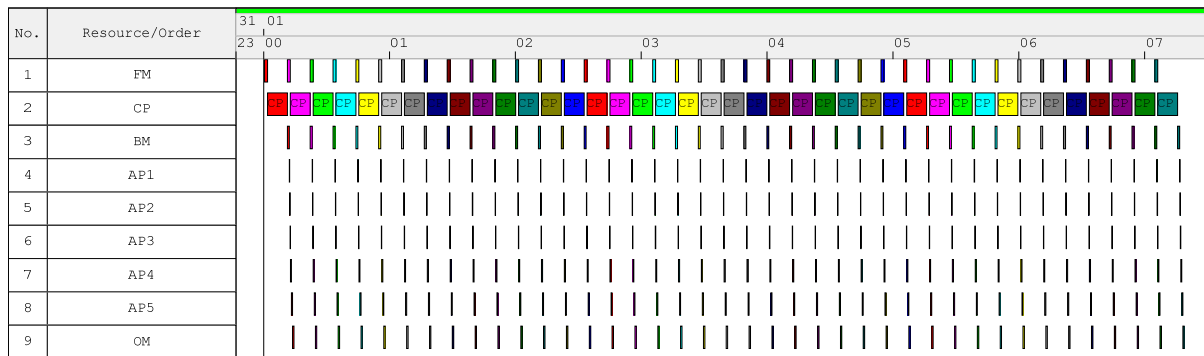
Fig. 5 The Gantt chart of the system

The Gantt chart is shown in Fig. 5. The abscissa is time (unit: h), and the ordinate is machine sequence. Each block in the Gantt chart represents the starting processing time and processing duration of the corresponding part on the corresponding machine. It can be seen that the processing duration of the parts in the CP is the longest, which has a more significant impact on the final completion time and throughput than other machines. Therefore, the composite processing platform is the most sensitive machine to the throughput, means it is the bottleneck machine.

It should be noted that the practicability, accuracy and limitation of these bottleneck identification methods are specific to this case study, which does not mean that these methods are wrong in principle, but indicates that there is a gap between theory and application.

5.2 The impact of the bottleneck machine quantity on system performance

The FAT represents the speed of the system laying, the FCT and the MCT represent production efficiency, and the machine utilization represents the degree of efficient output. Besides, the factory is very concerned about the utilization of the CP, FM and the BM. Therefore, we selected a total of eight indicators in Table 2 to evaluate the system performance.

The completion time curves and mean cycle time under five scenarios are shown in Fig. 6. According to Fig. 6(a), it can be known that the first completion time of the five scenarios is the same, while the maximum completion time presents a downward trend, which means increase the bottleneck machine quantity cannot improve the system laying speed, but can effectively improve the production efficiency. It can be seen from Fig. 6(b) that the relationship between the mean cycle time and the number of bottleneck machines presents a decreasing trend with decreasing acceleration. It can be inferred from this trend that as the number of bottlenecks continues to increase, the final completion time and the mean cycle time will hardly decrease once the threshold is reached.
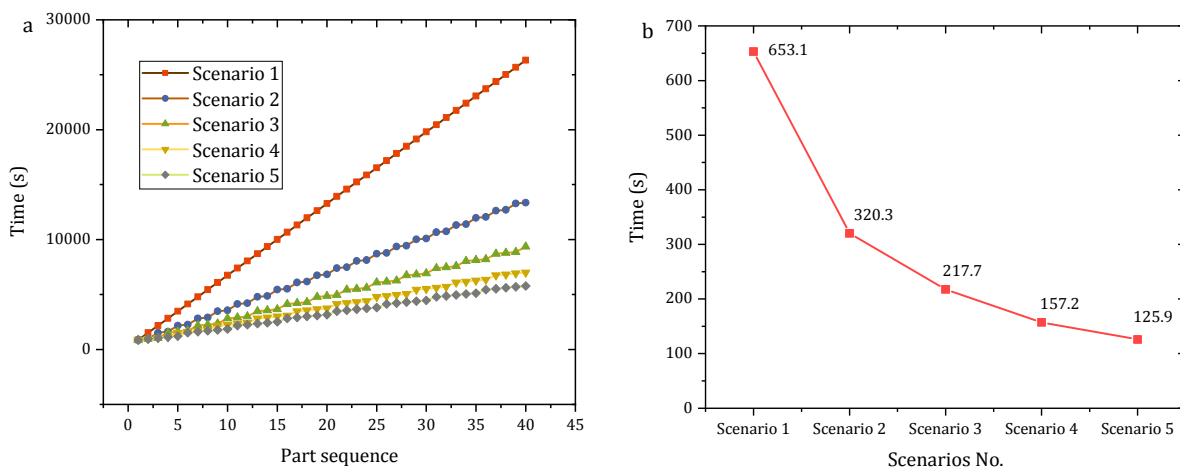
Fig. 6 (a) The completion time of each part in each scenario; (b) The mean cycle time of each scenario

The utilization rate of each machine under five scenarios is shown in Fig. 7. It can be seen in Fig. 7(a) that with the increase of the bottleneck machine quantity, the mean utilization rate of the composite processing platform (MCP) decreases with a small range, while the utilization rate of the non-bottleneck station increases significantly. It can be seen in Fig. 7(b) that with the increase of the bottleneck machine quantity, the maximum machine utilization rate decreases slightly, while the average machine utilization rate increases significantly, which indicates that increasing the bottleneck machine quantity can improve the balance of the whole serial production line system.

From the above analysis, it can be drawn that increasing the number of bottleneck machines can effectively alleviate the bottleneck. However, the alleviate ability decreases with the machine quantity increases. The more bottleneck machines, the smaller the performance improvement to the production system. At the same time, increasing the machine quantity will bring more resource consumption and economic investment, which means that the bottleneck machine quantity should meet the requirements of both system performance and economy, and there must be a balance between the two. For the case study, the number of bottleneck machines was ultimately determined to be 3.
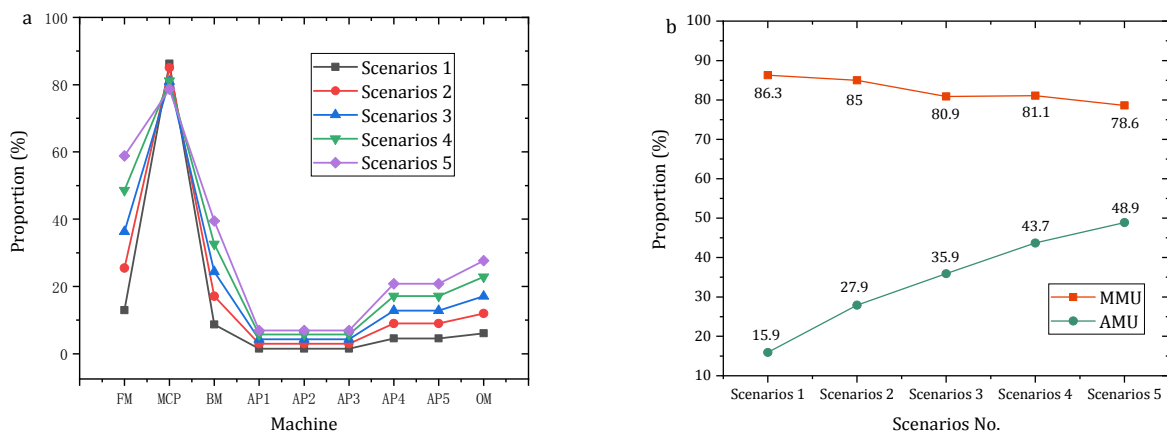
Fig. 7 (a) Machine utilization in each scenario; (b) The maximum and average machine utilization in each scenario

5.3 The function between final completion time and bottleneck machine quantity

According to Fig. 6(a), when the bottleneck machine quantity is greater than 1, the interval of part completion time is not equal. This phenomenon can be explained as the group warehousing under different quantity of bottleneck machine, which means the parts are completed in groups, and the number of parts per group is equal to the bottleneck machine quantity. The completion time curve in scenarios 5 is shown in Fig. 8, which intuitively shows the phenomenon that five parts are put into storage as a group, with short completion interval time within the group and long completion interval time between the groups.
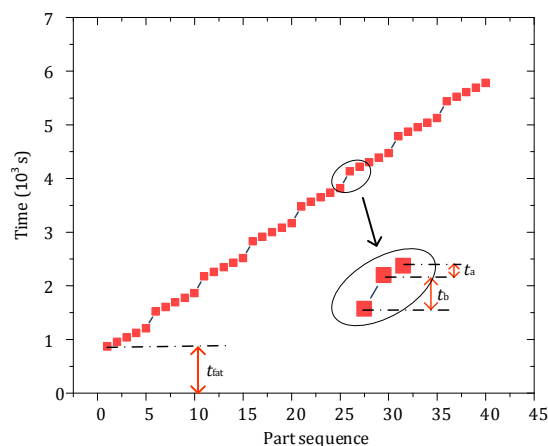
Fig. 8 The completion time of each part in scenarios 5

According to Fig. 8, the final completion time is related to five factors: completion time of the first part denoted by t_{fat}, the completion interval time within the group denoted by t_a, the completion interval time between the groups denoted by t_b, the number of times t_a appears denoted by n_a, the number of times t_b appears denoted by n_b. Besides, there is only t_b when the number of bottleneck machines is 1. The objective function can be preliminarily expressed as follows.

$$C_{max} = \begin{cases} t_{fat} + n_{bi} \times t_{bi} + n_{ai} \times t_{ai} & i > 1 \\ t_{fat} + n_{bi} \times t_{bi} & i = 1 \end{cases} \tag{1}$$

where

$$t_{fat} = \sum_{k=1}^{m} t_k \tag{2}$$

$$n_{bi} = \begin{cases} floor\left(\frac{y}{i}\right) - 1 & mod\left(\frac{y}{i}\right) = 0 \\ floor\left(\frac{y}{i}\right) & mod\left(\frac{y}{i}\right) \neq 0 \end{cases} \tag{3}$$

$$n_{ai} = \begin{cases} y - floor\left(\frac{y}{i}\right) & mod\left(\frac{y}{i}\right) = 0 \\ y - floor\left(\frac{y}{i}\right) - 1 & mod\left(\frac{y}{i}\right) \neq 0 \end{cases} \tag{4}$$

Where C_{max} is the final completion time, i is the number of bottleneck machines (i is a positive integer), t_k is the processing time of the machine k, m is the total process quantity, y is the number of parts needs to be processed; "*floor*" means rounding down, "*mod*" means remainder.

The Gantt chart of the first two groups in the feeding manipulator (M1, machine no.1) and composite processing platform (M2, machine No.2) is shown in Fig. 9. All scenarios can be described in Fig. 9, t_a can be regarded as the completion interval of the part in the second group, while t_b can be regarded as the time between the last part in the first group and the first part in the second group.
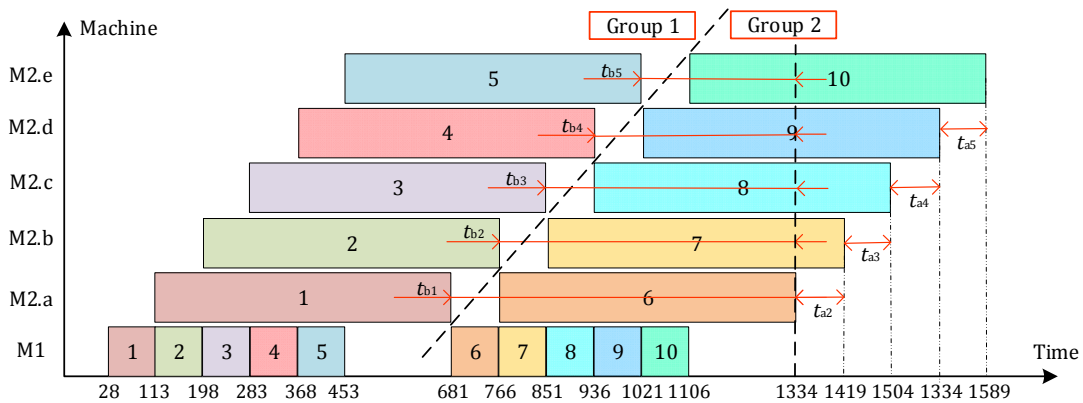
Fig. 9 The Gantt chart of the first two groups

For instance, parts 1 and 6 describe scenarios 1. Since the feeding frame manipulator needs to wait for the completion of the composite processing platform to continue feeding, the process (6, 1) (representing the processing of part No. 6 on machine No. 1) shall not begin until the process (1, 2) is completed. It means that the period from the end of the process (1, 2) to the end of the process (6, 2) is the interval time between the groups in scenario 1, which denoted by t_{b1}.

Parts 1, 2, and 6, 7 represent scenarios 2. Since there are two CP at scenarios 2, process (2, 1) can be started immediately after the process (1, 1) completes, while (6, 1) can only start after the processes (1, 2) and (2, 2) all complete. Then the period from the end of the process (2, 2) to the end of the process (6, 2) is the interval time between the groups in scenario 2, which denoted by t_{b2}. The interval time within the group can represent the time from the end of the process

(6, 2) to the end of the process (7, 2) and denoted by t_{a2}. Similarly, the corresponding t_{a2}, t_{a3}, t_{a4}, t_{a5} and t_{b1}, t_{b2}, t_{b3}, t_{b4}, t_{b5} can be obtained and has been shown in Fig. 9.

For analysis and representation comprehensible, we introduce the concept of the secondary bottleneck to distinguish the most significant bottleneck. A fundamental principle of the secondary bottleneck is that as the number of bottleneck machines increases, the bottleneck will move from the current bottleneck to the secondary bottleneck. The identification method of the secondary bottleneck is similar to the primary bottleneck. Sort the indexes in table 1, and the second one is the secondary bottleneck. According to Table 2, FM is the secondary bottleneck machine in the case study.

According to the above analysis and Fig. 9, with the increase of the bottleneck machine quantity, t_a remains unchanged and is equal to the processing time of the FM. However, every time the number of bottleneck machines increases by one, t_b reduces the processing time of a secondary bottleneck. t_a and t_b can be expressed as follows.

$$t_{ai} = t_{sb} \quad i > 1 \tag{5}$$

$$\begin{aligned} t_{bi} &= t_{pb} + t_{sb} - (i-1) \times t_{sb} \\ &= t_{pb} - (i-2) \times t_{sb} \end{aligned} \tag{6}$$

Where t_{sb} is the processing time of secondary bottleneck, t_{pb} is the processing time of primary bottleneck. Although we can only know from Fig. 9 that t_{ai} is equal to the processing time of FM, and t_{bi} is equal to the processing time of CP. Nevertheless, through further analysis by changing the time of each station, we found that t_{sb} is always equal to the processing time of secondary bottleneck, and t_{pb} is always equal to the processing time of primary bottleneck. Then the C_{max} can be expressed as follows.

$$C_{i\max} = \begin{cases} \sum_{k=1}^{m} t_k + \left[y - floor\left(\frac{y}{i}\right)\right] \times t_{sb} + \left[floor\left(\frac{y}{i}\right) - 1\right] \times (t_{pb} - (i-2) \times t_{sb}) & i > 1, mod\left(\frac{y}{x}\right) = 0 \\ \sum_{k=1}^{m} t_k + \left[y - floor\left(\frac{y}{i}\right) - 1\right] \times t_{sb} + floor\left(\frac{y}{i}\right) \times (t_{pb} - (i-2) \times t_{sb}) & i > 1, mod\left(\frac{y}{x}\right) \neq 0 \\ \sum_{k=1}^{m} t_k + \left[floor\left(\frac{y}{i}\right) - 1\right] \times (t_{pb} - (i-2) \times t_{sb}) & i = 1 \end{cases} \tag{7}$$

After arrangement

$$C_{i\max} = \begin{cases} \sum_{k=1}^{m} t_k + floor\left(\frac{y}{i}\right) \times (t_{pb} - (i-1) \times t_{sb}) + (y + i - 2) \times t_{sb} - t_{pb} & i > 1, mod\left(\frac{y}{x}\right) = 0 \\ \sum_{k=1}^{m} t_k + floor\left(\frac{y}{i}\right) \times (t_{pb} - (i-1) \times t_{sb}) + (y - 1) \times t_{sb} & i > 1, mod\left(\frac{y}{x}\right) \neq 0 \\ \sum_{k=1}^{m} t_k + [y - 1] \times (t_{pb} + t_{sb}) & i = 1 \end{cases} \tag{8}$$

According to Eq. 8, when $t_{pb} - (i-1) \times t_{sb} = 0$, the $C_{i\max}$ gets the minimum value. Then according to Eq. 8, the condition can be expressed as the Eq. 9 and Eq. 10 after the arrangement.

$$i = mod\left(\frac{t_{pb}}{t_{sb}} + 1\right) \tag{9}$$

$$\frac{t_{pb}}{i-1} = t_{sb} \tag{10}$$

From Eq. 8, we can draw that when making the production plan, the number of the part batch should be an integer multiple of the bottleneck machine quantity. From Eq. 9, we can get the optimal configuration number of the bottleneck machine. The final completion time achieves the minimum value when Eq. 10 is valid.

6. Conclusion

This paper applied the bottleneck theory to studied a blocked serial production line system in the aerospace field based on discrete event simulation, meanwhile discussed the performance of five bottleneck identification methods, the effect of the bottleneck machine quantity on system performance, obtained the function between final completion time and bottleneck machine quantity. Through the case study in this paper, we have reached the following conclusions:

- The bottleneck identification method based on machine utilization or average activity time is universal and practical. The method which is based solely on the machine idle rate, blockage rate, and the average absolute deviation or variance of the inter-departure time of the machine has some limitations. The method based on the sensitivity of throughput is the most natural interpretation of the bottleneck, which is most accurate but difficult to apply.
- Increasing the bottleneck machine quantity can accelerate the production efficiency and improve the utilization rate of non-bottleneck machine and system balance. However, the alleviation capacity decreases as the number of machines increases.
- The general function between the final completion time and bottleneck machine quantity in the blocked serial production line is obtained, which shows that the production efficiency is determined by the primary bottleneck and the secondary bottleneck. It also manifests that the condition of the final completion time gets the minimum value.

The main contribution of this paper is it evaluates the performance of various bottleneck identification and alleviation methods with a practical case, and discusses the relationship between the final completion time and the bottleneck machine quantity in the blocked serial production line for the first time, which has important significance to actual production guidance. Also, the case study indicates that some bottleneck identification methods may not be available to solve some practical problems, which also proves that there is a gap between theoretical research and practical application. Therefore, another contribution of this paper is it provides a practical case for theoretical researchers to reflect and use for reference.

The limitation of this paper is that it only provides some general conclusions in the blocked serial production line. Our next work is to introduce the buffer based on this paper, and research the effect between the system performance, the bottleneck machine quantity and the buffer capacity.

Acknowledgement

References

[1] Watson, K.J., Blackstone, J.H., Gardiner, S.C. (2007). The evolution of a management philosophy: The theory of constraints, *Journal of Operations Management*, Vol. 25, No. 2, 387-402, doi: 10.1016/j.jom.2006.04.004.

[2] Wang, Y., Zhao, Q., Zheng, D. (2005). Bottlenecks in production networks: An overview, *Journal of Systems Science and Systems Engineering*, Vol. 14, No. 3, 347-363, doi: 10.1007/s11518-006-0198-3.

[3] Sims, T., Wan, H.-D. (2017). Constraint identification techniques for lean manufacturing systems, *Robotics and Computer-Integrated Manufacturing*, Vol. 43, 50-58, doi: 10.1016/j.rcim.2015.12.005.

[4] Yan, H.-S., An, Y.-W., Shi, W.-W. (2010). A new bottleneck detecting approach to productivity improvement of knowledgeable manufacturing system, *Journal of Intelligent Manufacturing*, Vol. 21, No. 6, 665-680, doi: 10.1007/s10845-009-0244-3.

[5] Scholz-Reiter, B., Windt, K., Liu, H. (2010). Modelling dynamic bottlenecks in production networks, *International Journal of Computer Integrated Manufacturing*, Vol. 24, No. 5, 391-404, doi: 10.1080/0951192X.2010.511655.

[6] Li, L., Chang, Q., Ni, J., Biller, S. (2009). Real time production improvement through bottleneck control, *International Journal of Production Research*, Vol. 47, No. 21, 6145-6158, doi: 10.1080/00207540802244240.

[7] Shi, W.-W., Yan, H.-S. (2006). Method of shifting bottleneck analysis in knowledge-oriented manufacturing system, *Computer Integrated Manufacturing Systems*, Vol. 12, No. 2, 271-279, doi: 10.13196/j.cims.2006.02.113.shiww.020.

[8]   Li, X., Yuan, Y., Sun, W., Feng, H. (2016). Bottleneck identification in job-shop based on network structure charac-teristic, *Computer Integrated Manufacturing Systems*, Vol. 22, No. 4, 1088-1096, doi: 10.13196/j.cims.2016.04.023.

[9]   Liu, M., Tang, J., Ge, M., Jiang, Z., Hu, J., Ling, L. (2009). Dynamic prediction method of production logistics bottle-neck based on bottleneck index, *Chinese Journal of Mechanical Engineering*, Vol. 22, No. 5, 710-716, doi: 10.3901/CJME.2009.05.710.

[10]   Zhou, F.L., Wang, X., He, Y.D., Goh, M. (2017). Production lot-sizing decision making considering bottle-neck drift in multi-stage manufacturing system, *Advances in Production Engineering & Management*, Vol. 12, No. 3, 213-220, doi: 10.14743/apem2017.3.252.

[11]   Zhou, J., Deng, J.X., Huang, P.L., Liu, Z.Q., Ai, X. (2006). Integrated analysis method: Visual modelling, simulation, diagnosis and reduction for bottleneck processes of production lines, *Iranian Journal of Science & Technology, Transaction B, Engineering*, Vol. 30, No. B3, 363-375.

[12]   Pehrsson, L., Ng, A.H.C., Bernedixen, J. (2016). Automatic identification of constraints and improvement actions in production systems using multi-objective optimization and post-optimality analysis, *Journal of Manufacturing Systems*, Vol. 39, 24-37, doi: 10.1016/j.jmsy.2016.02.001.

[13]   Li, H.Y., Gui, C., Xiao, K. (2018). Simulation of multivariate scheduling optimization for open production line based on improved genetic algorithm, *International Journal of Simulation Modelling*, Vol. 17, No. 2, 347-358, doi: 10.2507/IJSIMM17(2)CO9.

[14]   Betterton, C.E., Silver, S.J. (2012). Detecting bottlenecks in serial production lines-a focus on interdeparture time variance, *International Journal of Production Research*, Vol. 50, No. 15, 4158-4174, doi: 10.1080/00207543.2011.596847.

[15]   Hajmirfattahtabrizi, M., Song, H. (2019). Investigation of bottlenecks in supply chain system for minimizing total cost by integrating manufacturing modelling based on MINLP approach, *Applied Sciences*, Vol. 9, No. 6, Article No. 1185, doi: 10.3390/app9061185.

[16]   Kang, Y., Ju, F. (2019). Integrated analysis of productivity and machine condition degradation: Performance evaluation and bottleneck identification, *IISE Transactions*, Vol. 51, No. 5, 501-516, doi: 10.1080/24725854.2018.1494867.

[17]   Kefeli, A., Uzsoy, R. (2016). Identifying potential bottlenecks in production systems using dual prices from a mathematical programming model, *International Journal of Production Research*, Vol. 54, No. 7, 2000-2018, doi: 10.1080/00207543.2015.1076182.

[18]   Lei, Q., Li, T. (2017). Identification approach for bottleneck clusters in a job shop based on theory of constraints and sensitivity analysis, *Proceedings of the Institution of Mechanical Engineers, Part B: Journal of Engineering Manufacture*, Vol. 231, No. 6, 1091-1101, doi: 10.1177/0954405415583884.

[19]   Lawrence, S.R., Buss, A.H. (1994). Shifting production bottlenecks: Causes, cures, and conundrums, *Production and Operations Management*, Vol. 3, No. 1, 21-37, doi: 10.1111/j.1937-5956.1994.tb00107.x.

[20]   Kikolski, M. (2016). Identification of production bottlenecks with the use of Plant Simulation software, *Engineering Management in Production and Services,* Vol. 8, No.4, 103-112, doi: 10.1515/emj-2016-0038.

[21]   Roser, C., Nakano, M., Tanaka, M. (2001). A practical bottleneck detection method, In: *Proceedings of the 2001 Winter Simulation Conference*, Arlington, USA, 949-953, doi: 10.1109/WSC.2001.977398.

[22]   Sengupta, S., Das, K., VanTil, R.P. (2008). A new method for bottleneck detection, In: *Proceedings of the 2008 Winter Simulation Conference*, Miami, USA, 1741-1745, doi: 10.1109/WSC.2008.4736261.

[23]   Zhang, R., Wu, C. (2012). Bottleneck machine identification method based on constraint transformation for job shop scheduling with genetic algorithm, *Information Sciences*, Vol. 188, 236-252, doi: 10.1016/j.ins.2011.11.013.

[24]   Li, G., Xu, Z., Ren, Z. (2019). Simulation and optimization of plant production takt, In: *Proceedings of the 2019 International Conference on Modeling, Simulation and Big Data Analysis,* Wuhan, China, 98-103, doi: 10.2991/msbda-19.2019.16.

[25]   Ojstersek, R., Lalic, D., Buchmeister, B. (2019). A new method for mathematical and simulation modelling inter-activity: A case study in flexible job shop scheduling, *Advances in Production Engineering & Management*, Vol. 14, No. 4, 435-448, doi: 10.14743/apem2019.4.339.

[26]   Zhang, Z., Wang, X., Wang, X., Cui, F., Cheng, H. (2019). A simulation-based approach for plant layout design and production planning, *Journal of Ambient Intelligence and Humanized Computing*, Vol. 10, No. 3, 1217-1230, doi: 10.1007/s12652-018-0687-5.

[27]   Jia, Y., Tian, H., Chen, C., Wang, L. (2017). Predicting the availability of production lines by combining simulation and surrogate model, *Advances in Production Engineering & Management*, Vol. 12, No. 3, 285-295, doi: 10.14743/apem2017.3.259.

[28]   Khalid, R., Nawawi, M.K.M., Kawsar, L.A., Ghani, N.A., Kamil, A.A, Mustafa, A. (2013). A discrete event simulation model for evaluating the performances of an M/G/C/C state dependent queuing system, *Plos One*, Vol. 8, No. 4, Article No. e58402, doi: 10.1371/journal.pone.0058402.

[29]   Ištoković, D., Perinić, M., Doboviček, S., Bazina, T. (2019). Simulation framework for determining the order and size of the product batches in the flow shop: A case study, *Advances in Production Engineering & Management*, Vol. 14, No. 2, 166-176, doi: 10.14743/apem2019.2.319.

[30]   Silva, M. (2018). On the history of discrete event systems, *Annual Reviews in Control*, Vol. 45, 213-222, doi: 10.1016/j.arcontrol.2018.03.004.

[31]   de Sousa Junior, W.T., Montevechi, J.A.B., de Carvalho Miranda, R., Campos, A.T. (2019). Discrete simulation-based optimization methods for industrial engineering problems: A systematic literature review, *Computers & Industrial Engineering*, Vol. 128, 526-540, doi: 10.1016/j.cie.2018.12.073.

Comparison of artificial neural network, fuzzy logic and genetic algorithm for cutting temperature and surface roughness prediction during the face milling process

Savkovic, B.[a,*], **Kovac, P.**[a], **Rodic, D.**[a], **Strbac, B.**[a], **Klancnik, S.**[b]

[a]University of Novi Sad, Faculty of Technical Sciences, Department of Production Engineering, Novi Sad, Serbia
[b]University of Maribor, Faculty of Mechanical Engineering, Production Engineering Institute, Maribor, Slovenia

A B S T R A C T

This paper shows the possibility of applying artificial intelligence methods in milling, as one of the most common machining operations. The main goal of the research is to obtain reliable intelligent models for selected output characteristics of the milling process, depending on the input parameters of the process: depth of cut, cutting speed and feed to the tooth. One of the problems is certainly determining the value of input parameters of the processing process depending on the objective function, i.e. the output characteristics of the milling process. The selected objective functions in this paper are the temperature in the cutting zone and arithmetic mean roughness of the machined surface. The paper examines the accuracy of three models based on artificial intelligence, obtained through artificial neural networks, fuzzy logic, and genetic algorithms. Based on the mean percentage error of deviation, conclusions were drawn as to which of the three models is most adequately applied and implemented in appropriate process systems, which are based on artificial intelligence.

1. Introduction

There is a need to improve the machining process by applying knowledge from advanced modeling techniques, such as simulation, which certainly involves modeling using artificial intelligence methods. The developed models are used for the analysis, management and selection of optimal process parameters, which represent a picture of complex relationships between the input and output parameters of the milling process. The obtained models can be used with sufficient accuracy in adaptive management and monitoring of processes and decision making in real time, which is of great importance in the exploitation of intelligent manufacturing systems. It is also possible to optimize the input process parameters based on the processing constraints set in order to achieve one or more target functions such as reducing cutting forces and/or minimizing the roughness of the machined surface, which have the greatest practical value and meaning from a technical point of view. In terms of quality of the machined surface, the emphasis on the roughness test as well as the influence of the corresponding parameters was given by a large number of authors [1-4].

Applying methods and techniques of artificial intelligence together with modeling, simulation and optimization of production processes lead to the generation of new and better solutions

during manufacturing [5-8]. Their application leads to the development of intelligent processing systems that automatically perform complex production problems, freeing people not only from physical but also intellectual work, leaving them to do expert and creative jobs.

Artificial intelligence can be considered an experimental doctrine where experiments are performed on a computer within the models that are expressed in programs and whose testing and upgrading achieve some models of human intelligence. By algorithm it is usually meant a finite set of precisely defined operations that can be performed on a computer. One of the areas of artificial intelligence, together with its sub-areas, is computer intelligence *(soft computing).* It is a basic artificial intelligence tool that involves series of methods and techniques for the conception, design and use of an intelligent system. As such, the tool is certainly attractive for creating various models that describe certain phenomena in the production process.

The objective of this paper is to determine the optimal model obtained on the basis of artificial intelligence for predicting the roughness of the machined surface, i.e. the temperature in the cutting zone during of the face milling process. The proposed models are realized as a function of processing parameters: cutting speed, feed per tooth and cutting depth. The most common artificial intelligence methods are surely: fuzzy logic, artificial neural networks and genetic algorithms. Accordingly, it is necessary to determine which of these three types for model creation most closely describes the change in the output characteristics of the process.

2. Literature review

Artificial neural networks (ANN) are nowadays used in almost all fields of science and technology, including mechanical engineering. Technological processing parameters are values that depend on a large number of factors. There are no exact forms and procedures for determining processing parameters, so in most cases, experience values are used, like various books, tables, graphics, etc. Therefore, neural networks can be of great use. Instead of a detailed calculation of the processing parameters, a neural network is created that can predict the unknown machining parameters, after a properly training process [9]. Today, artificial neural networks are widely used in the industrial sector to solve problems [10-12].

An example of the implementation of ANN can be seen in the paper [13]. The application of neural networks for the calculation of cutting force, torque and monitoring of tool wear during the drilling process is presented there. Also, these principles of neural networks application can be seen in other kinds of cutting material process. This primarily refers to the milling process as one of the most common cutting process [14]. There are papers showing the application of the network structure in the milling process for variables such as tool geometry and machining regimes [15].

In their research, Lin and Liu present the methodology of creating the neural network structure, emphasizing the type of function as well as the number of hidden layers in the network itself. It should be pointed out that it is very important which type of neural network, i.e. the number of nodes in individual layers, is the most appropriate to choose and to obtain a sufficiently reliable model. Based on the analysis of the papers [16, 17], it can be concluded that the back-propagation neural network is sufficiently reliable. Also, it was noticed that the faster convergence is achieved using a two-hidden-layer network than using a one-hidden-layer network, with the same number of nodes.

The neural networks application is also present in the adaptive control of the spindle milling process [18]. ANN are used for on-line determination of optimal milling parameters, specifically feed per tooth, based on the values of measured cutting forces.

Next, a certainly not less important tool of artificial intelligence is Fuzzy logic. It represents the generalization of the classical Boolean logic. Systems based on fuzzy logic and fuzzy sets can be observed as a generalization of expert systems based on rules. Fuzzy systems manifest both symbolic and numerical features.

It can also be said that fuzzy logic and fuzzy systems represent an effective techniques to identify and control complex non-linear systems. Fuzzy logic is also used for prediction. The theory of fuzzy logic, which has been initiated Zadeh [19], is still helpful for the operation with

uncertain and inaccurate information. Fuzzy logic is especially attractive because of its ability to solve problems in the absence of precise mathematical models. This theory has proved to be an effective tool for describing objectives expressed through linguistic terms, such as *small*, *medium* and *high*, which may be defined as the fuzzy sets [20].

Application of fuzzy logic to solve problems in the cutting process is very common and it can be seen through the overview of following papers. Rajasekaran *et al.* [21] investigated the influence of combinations of processing parameters in order to obtain a good quality when finishing machining by turning. They used the fuzzy modeling to predict the value of surface roughness. Other literature sources also show the application of the adaptive approach based on the network of fuzzy logic system (ANFIS), set to show the correlation of surface roughness when machining by turning or milling [22, 23]. The implementation of fuzzy logic in surface roughness modeling when finishing machining has also been discussed in paper [24]. It can be stated that the fuzzy logic is a recognizable system, sufficiently developed and widely used [25].

Surface roughness modelling when face milling is considered a complex process. The concept of fuzzy reasoning for four inputs and one output fuzzy logic unit (singleton) is excellently presented in [26]. Cutting speed, feed per tooth, cutting depth and flank wear were set as input variables, while the output variable was the roughness of the machined surface.

Similar issues were described by the authors in paper [27], where the cutting speed, feed per tooth, cutting depth and flank wear were taken as input parameters as well, but this time the output variables were tool life and cutting temperature.

At the end of this review of artificial intelligence application, it is necessary to analyze genetic algorithms (GA). Genetic algorithms are an effective way to quickly find a solution to a complex problem. They are certainly not fast but they do a great job of searching large areas. They are also most effective when searching an area which is very little known or not known at all. Terminology and operators are taken from the field of population genetics. The basic object of genetic algorithms is the chromosome, and they represent an instantaneous approximation of the solution for the set goal function. Each chromosome is encoded and has a certain quality – fitness. During initialization, the initial population is generated, which is a solution obtained by another optimization method. Then follows a repetitive process until the stop condition is met. This process consists of the execution of genetic operators of selection, crossover and mutation. By multiple application of the selection operator, mostly bad individuals become extinct, and better ones stay alive, and the next step is crossing over between the good individuals. The characteristics of parents are transferred to children by crossover operator. Mutation changes the characteristics of individuals by random change of genes. One such procedure enables the average quality of the population to grow from generation to generation. Essentially, this is a heuristic optimization method that solves certain computer problems by simulating the mechanism of natural evolution.

Accordingly, it can be stated that the mechanism on which GA is based, can be used in order to optimize or to model the value that occur in certain production processes. Thus, in addition to the wide domain of application of the genetic algorithm, they also found their implementation in designing of CNC control [28]. When it comes to artificial intelligence, specifically based on genetic algorithms, it has found its application in machining processes where material is removed. Thus, there is an example of using genetic algorithms to perform optimization of parameters in the examination of surface morphology [29]. Genetic algorithms are also used for modeling the cutting force in machining process of hard materials such as titanium alloys [30]. They have also found their application in the processing of aluminium, specifically for the optimization of processing parameters [31]. There are also papers in which the authors deal with modeling the temperature during milling with the help of GA [32].

3. Materials and methods

Conditions for predicting the appropriate machinability values are created by defining the model. Those conditions allow the technologist or CNC programmer to select the appropriate machining regimes long before the actual machining. By knowing these values of machinability, the
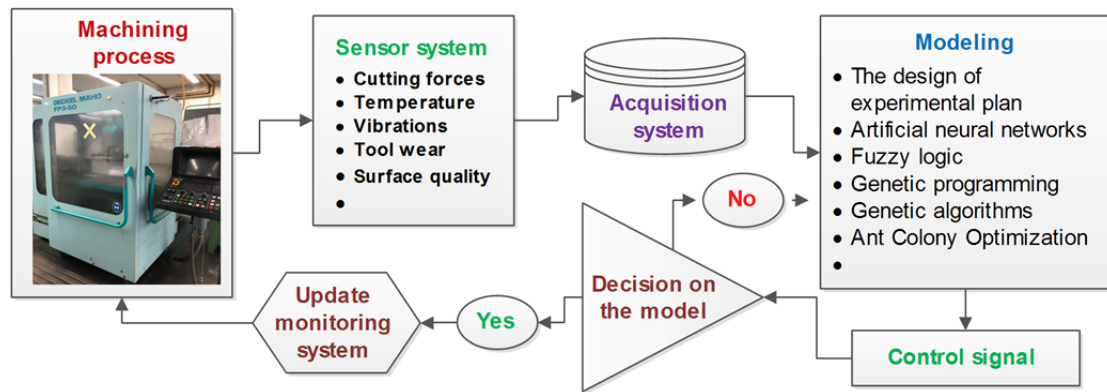
Fig. 1 Monitoring, modeling and control signal in machining process

conditions are created to achieve control of machining systems. Certainly, assuming that the best production process was previously selected in relation to the set criteria [33]. Fig. 1 shows the scheme of intelligent control and monitoring of the machining process. The figure shows that the part for modeling collected data is located at the central part of the system.

Experimental setup

The material used for workpiece was aluminum alloy. It is an alloy from 7000 series which contains a high percentage of zinc (Zn), as the main alloying element, and magnesium (Mg) as the second alloying element. Beside Zn and Mg, the alloy code 7075 also contains copper (Cu) as a fourth alloying element, i.e. it is a multicomponent Al-Zn-Mg-Cu alloy. The alloys 7075 have high mechanical properties, good machinability and heat-treated process, and also good corrosion resistance [34]. They belong to the group of *hard alloys*. They are usually used in the aviation and military industry. The forms they are usually used are: sheets, plates, wires, rods, extruded products, structural shapes, pipes, forgings etc. [35].

Fig. 2 shows the typical microstructure of the tested samples of Al 4.4 % Cu alloys obtained by conventional casting. Table 1 shows the chemical composition of the tested alloys.

The experiments was performed on a vertical milling machine FSS-GVK-3 with a face milling head diameter of ϕ100 mm, with removable inserts following characteristics: number of teeth t = 5, entrance angle κ = 75°, rake angle γ = 0°. Inserts are made of tungsten carbide quality K20, the following characteristics (l = IC = 12.7 mm; s = 3.18 mm; b_s = 1.4 mm; b_ε = 1.4 mm).

Measurement of cutting temperature was performed using the measuring acquisition system shown in Fig 3. The central part of the system is virtual instrumentation.
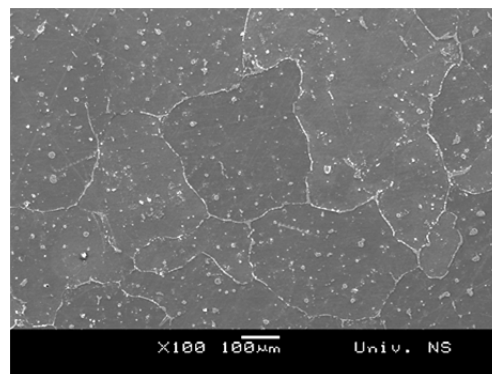
Fig. 2 Microstructure of tested aluminum alloy

Table 1 Chemical composition of the alloy 7075

Alloy designation	Basic element	Zn	Mg	Cu	Cr	Fe	Si	Mn	Ti
7075	Al	5.8	2.52	1.65	0.2	0.18	0.1	0.025	0.025

In the case of milling, unlike turning, there are problems of transmitting the signal from the tool to the measuring instrument. Due to the fact that the milling tool moves in a circular motion during the process, it is not possible to directly manage the thermocouple wire directly to the measuring instrument. Thermocouple wire connects to copper rings, which together with graphite brushes provide sliding contact. Contact with copper rings is provided by springs. Thermovoltage occurring when measuring temperature between 10 to 50 mV, so small losses also mean large measurement errors. The thermocouple is made of Ni and CrNi wire with diameter of 0.1 mm. In the high-temperature zone, the wires were insulated using a ceramic tube of 0.9 mm in diameter, Fig. 4. The length of the tube was about 10 mm, and the insulation was PVC.

Apart of the measurement and acquisition system, temperature measurement was also performed by the ThermoPro TP8S thermal camera, which served as another verification of reliable temperature measurement. For the purposes of this research, i.e. measuring the roughness of the machined surface, it was used the device called „MarSurf PS1". The maximum measuring range is 350 µm (from -200 µm to + 150 µm). This device also meets the standards of the International Organization for Standardization DIN EN ISO 3.274.

The factor variation is performed at 5 level values, so that each mean value between adjacent levels of the geometric mean of these values. The selected levels of factors are shown in Table 2.
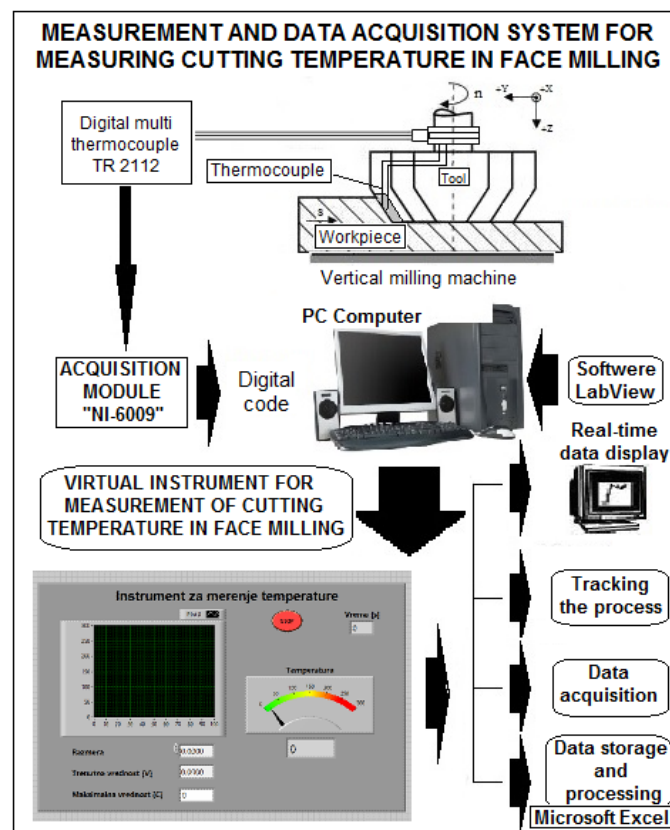
Fig. 3 Scheme of the measurement in face milling process
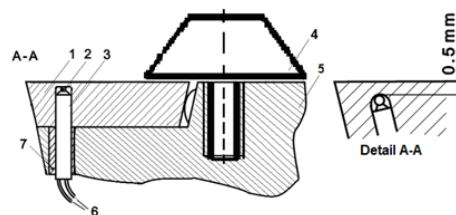
Fig. 4 Prepared cutting insert with thermocouple installed in the body of the milling head

1 – polygonal inserts, 2 – welded top of the thermocouple, 3 – ceramic tube, 4 – a screw that secures the insert, 5 – tool body, 6 – thermocouple PVC insulated, 7 – glue

Table 2 Levels of the experimental parameters for face milling

Levels (Functions of affiliation)		Cutting speed v (m/min)	Cutting speed v (m/s)	Feed to the tooth s_1 (mm/t)	Depth of cut a (mm)	Spindle speed n (min^{-1})
Highest	+1.41	351.86	5.864	0.223	2.6	1120
High	+1	282.74	4.712	0.177	1.72	900
Medium	0	223.05	3.717	0.141	1.14	710
Low	-1	175.93	2.932	0.112	0.75	560
Lowest	-1.41	141.37	2.356	0.089	0.5	450

4. Modeling using artificial intelligence methods

The realization of the model using artificial intelligence-based tools was done by using programs that have artificial neural networks, fuzzy logic (mamdani model) and genetic algorithms in their structure. Experimental data with a set of 21 experiments shown in the Table 3 were used to train these systems.

Table 4 shows the experimental data that were used for the test for further analysis of the models obtained.

Table 3 A plan of experimental testing with measured values for the process of training models based on artificial intelligence during face milling

No.	Factor			Measured values	
	v (m/s)	s_1 (mm/t)	a (mm)	Q (°C)	R_a (µm)
1	2.93	0.112	0.75	46	1.074
2	4.71	0.112	0.75	52	1.081
3	2.93	0.177	0.75	53	1.743
4	4.71	0.177	0.75	56	1.645
5	2.93	0.112	1.72	60	1.058
6	4.71	0.112	1.72	67	1.023
7	2.93	0.177	1.72	70	1.898
8	4.71	0.177	1.72	77	1.734
9	3.71	0.141	1.14	60	1.205
10	2.35	0.141	1.14	54	1.133
11	5.86	0.141	1.14	65	1.244
12	3.71	0.089	1.14	55	0.995
13	3.71	0.223	1.14	66	2.522
14	3.71	0.141	0.5	47	1.242
15	3.71	0.141	2.6	76.5	1.229
16	2.35	0.089	0.5	51	0.915
17	2.35	0.223	2.6	108	1.705
18	3.71	0.223	0.5	66	2.023
19	5.86	0.089	2.6	98	0.969
20	5.86	0.141	0.5	66	1.258
21	5.86	0.223	1.14	94	1.94

Table 4 Experimental data for testing the artificial intelligence model

No.	Factor			Measured values	
	v (m/s)	s_1 (mm/t)	a (mm)	Q (°C)	R_a (µm)
1	3.71	0.141	0.75	51	1.222
2	3.71	0.141	1.72	69	1.28
3	3.71	0.112	1.14	55	1.037
4	3.71	0.177	1.14	62	1.583
5	2.93	0.141	1.14	57	1.263
6	4.71	0.141	1.14	60	1.734

4.1 Neural network-based model

Training and testing are the most important features of a neural network (NN) which at the same time determine the characteristics of NN. The training will determine whether the neural network can provide the expected response or not. If that is not possible, NN will be trained again. The basic architecture of the artificial neural network consists of an input function, which can be in the form of binary, continuous or normalized data [36].

The distribution of data used for network training, validation or testing was as follows: 70 % of the data is training, 15 % data for validation, and 15 % for test data. A two-layer NN with sigmoid transfer function in hidden layers and linear transfer function in output layer (fit net) can arbitrarily incorporate multidimensional mapping problems, regarding consistent data and sufficient neurons in its hidden layer. The used NN has one hidden layer with 10 neurons. The network is trained with Levenberg-Markuard's return propagation algorithm (trainlm). This algorithm usually requires more memory, but less time. Cutting speed v (m/s), the feed per tooth s_1 (mm/t) and the cutting depth a (mm) are used as input data. These input data are grouped into one whole that is indicated $IN = (v, s_1, a)$. Output data are Q and R_a are not grouped, but a new network is created for each one individually. Due to that, models that were made were type 3-1, three inputs and one output, Fig. 5.

Fig. 6 shows a regression diagram in the neural network training process, where the goal is to set the value of the regression coefficient to be close to 1, the regression line should be at an angle of 45°, while most of the data from which the network is trained with should be along the line of regression.

When the network training is completed, simulation of the neural network can be performed. It is necessary to define inputs (*TestIn*), which are created on the base of Table 4, and based on those inputs to perform simulation and get new generated output process characteristics (*Test_outputs*).
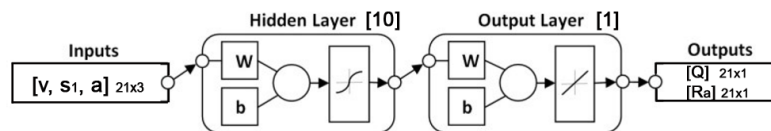
Fig. 5 Model of formed neural networks
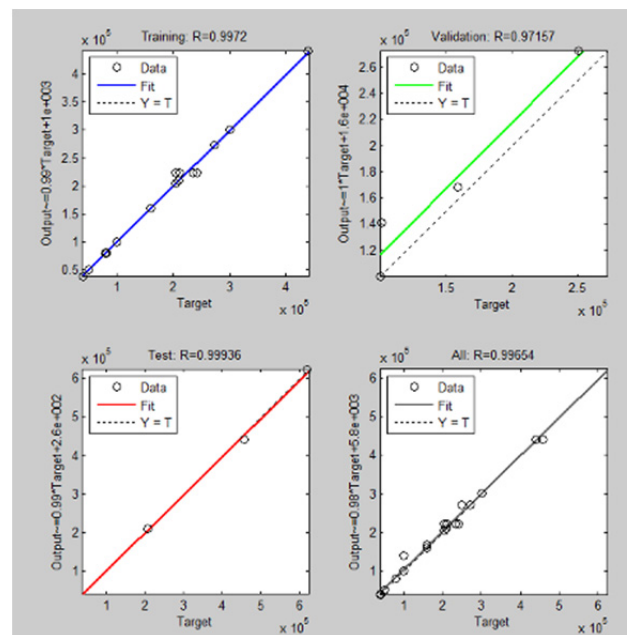
Fig. 6 Diagram of regression in the process of training a neural network

4.2 Fuzzy logic-based model

Implementation of the model based on fuzzy logic of the Mamdani type consists of several steps, where it is necessary to give a contribution in terms of editing membership functions and appropriate rules. On these bases, the fuzzy inference system comes to an editing, and there is a graphical representation of the appropriate solutions. Mamdani type implies that the language values of the output variable are regular fuzzy sets, where it is necessary to define the number of inputs, the names of the input and output variables. As with the neural network, there are three input variables (v, s_1, a) and the two output variables (Q, R_a) in face milling.
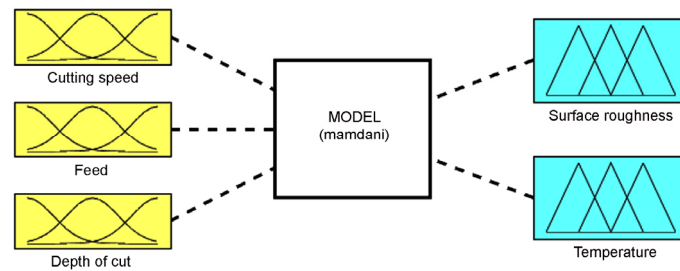
Fig. 7 Editor of fuzzy inference system

Editor of membership function enables the display and modification of all membership functions, input and output variables for the entire fuzzy inference system, Fig 7.

For the set problem, the Gaussian (gaussmf) membership function for each variable is defined. Gaussian membership function is the function most commonly used in modelling by using the fuzzy inference system [26, 27]. This symmetric Gaussian function depends on two parameters σ and C that need to be defined in the process of modeling, Eq. 1.

$$f(x; \sigma, c) = e^{\frac{-(x-c)^2}{2\sigma^2}} \tag{1}$$

After accepting the rules comprehensible to the program package, that is, the highest value of the input parameter is represented numerically +1.41 written in an attribute form with *Highest*, respectively: +1 with *High*, 0 with *Medium*, -1 with *Low* and -1.41 with *Lowest* defining appropriate fuzzy set is performed.

The rules are defined so that the data that define the cutting temperature are divided into 6 fuzzy subsets labelled (A, B, C, D, E, F) that group the approximate output values arranged by the Gaussian distribution. For the second output process characteristic, 9 fuzzy sets (A, B, C, D, E, F, G, H, I) are defined according to the same principle.

Accordingly, the final rule understandable for fuzzy logic is: if *speed is* lower and *feed* is lower and *depth* is lower, then surface roughness in the set C, this is the first order. This way, the other rules, all 21 of them, are defined, Table 5.

Table 5 The modified table with corresponding subsets

No.	Factor			Measured values	
	v (m/s)	s_1 (mm/t)	a (mm)	Q (°C)	R_a (µm)
1	-1	-1	-1	A	C
2	1	-1	-1	B	D
3	-1	1	-1	B	G
4	1	1	-1	B	F
5	-1	-1	1	C	C
6	1	-1	1	D	C
7	-1	1	1	D	H
8	1	1	1	E	G
9	0	0	0	C	E
10	-1.41	0	0	B	D
11	1.41	0	0	D	E
12	0	-1.41	0	B	B
13	0	1.41	0	D	I
14	0	0	-1.41	A	E
15	0	0	1.41	E	E
16	-1.41	-1.41	-1.41	B	A
17	-1.41	1.41	1.41	F	G
18	0	1.41	-1.41	D	H
19	1.41	-1.41	1.41	F	B
20	1.41	0	-1.41	D	E
21	1.41	1.41	0	F	H

4.3 Genetic algorithm-based model

Predefined second-order model, obtained based on a previous regression analysis based on the design of the experiment, was used to model the function of Q (cutting temperature) and Ra (arithmetic mean roughness):

$$Q = C_1 \cdot v^{x_1} \cdot s_1^{x_2} \cdot a^{x_3} \qquad (2)$$

$$R_a = C_2 \cdot v^{x_4} \cdot s_1^{x_5} \cdot a^{x_6} \qquad (3)$$

When determining the appropriate shape of the model, the genetic algorithm method starts from the initial random population $P(t)$. Population $P(t)$ is composed of organisms. Each organism is one of the possible solutions to the problem and consists of real constants (gens): C_1, x_1, x_2, x_3, C_2, x_4, x_5, x_6.

Based on already performed examinations and calculations based on regression analysis, as well as due to faster detection of the optimal solution, the limits in the search area have been introduced. Thus, the positioning of possible solutions, the coefficients for determining tool stability, are localized to: $60 \leq C_1 \leq 80$; $0.1 \leq x_1 \leq 0.5$; $0.1 \leq x_2 \leq 0.5$; $0.1 \leq x_3 \leq 0.5$.

After generating the initial population, the iterative procedure of selection, recombination (crossover) and mutation is carried out until the convergence criterion is satisfied, Fig. 8.
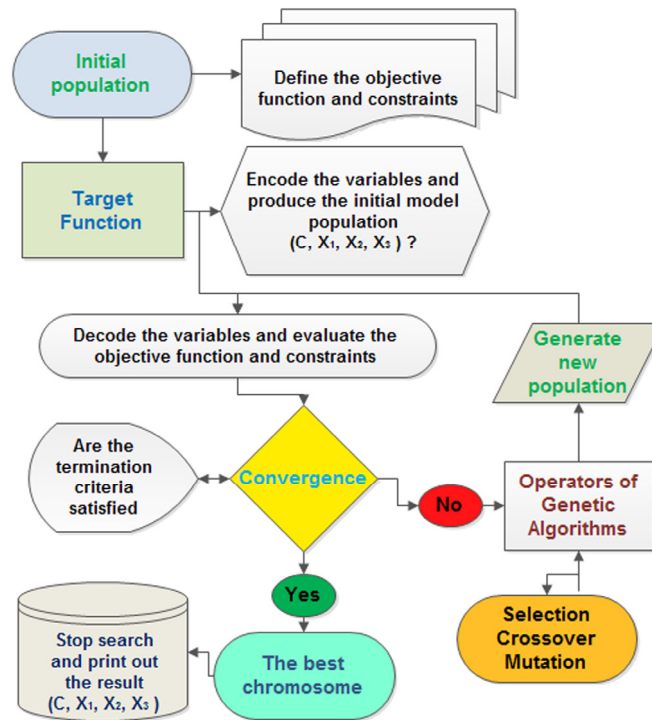
Fig. 8 Principle of the genetic algorithm

Determining the interactions that occur among different GA parameters has a direct impact on the quality of the solution and keeping parameters values *balanced* improves the solution of the GA. For machining process modeling, GA with the following parameters was used: population size 150, crossover rate 0.8, mutation rate 0.03 and number of generations 1000.

The only difference between modelling the function for cutting temperature and arithmetic mean roughness is precisely in the values of the search area limits. Thus, the determination of the coefficients that are represented in the equation for the arithmetic mean roughness are set to the constraints in terms of the limits: $10 \leq C_2 \leq 20$; $-0.5 \leq x_4 \leq 0.5$; $1 \leq x_5 \leq 1.5$; $-0.5 \leq x_6 \leq 0.5$.

After generating the optimal constants through the genetic algorithms, the Eqs. 4 and 5 have the final form:

$$Q = 72.551 \cdot v^{0.305} \cdot s_1^{0.297} \cdot a^{0.311} \qquad (4)$$

$$R_a = 12.337 \cdot v^{-0.059} \cdot s_1^{1.088} \cdot a^{-0.018} \qquad (5)$$

5. Results and discussion

The quantitative predictive potential E, the Eq. 6 is evaluated due to percentage of deviation between the obtained values (using the corresponding model) and the expected (experimental) values for the temperature in the cutting zone Q and the surface roughness R_a for the data on the basis of which the training of corresponding models of artificial intelligence was performed. The results presented are given in Table 6 and Table 7. The verification of the accuracy of these models was performed on the basis of 6 additional experiments performed according to the plan given in the second part of Tables 6 and 7.

Based on the average percentage error, it can be concluded that in both output characteristics of the process for the data used in the training of the corresponding model, this percentage error does not exceed 10 %. The situation is similar with test data where models used for cutting temperatures Q are also below 10 %, while in arithmetic main roughness R_a obtains a maximum deviation of 14 % using an artificial neural network-based model. Comparing all three models, it is concluded that looking at both output characteristics of the process, the smallest error was made by the model based on fuzzy logic. Consequently, it is recommended that the knowledge base, based on artificial intelligence is recommend built into the appropriate process systems.

$$E = \frac{|Y_{i\,\text{mod}} - Y_{i\,\text{exp}}|}{Y_{i\,\text{exp}}} * 100 \text{ \%}; i = 1 \dots n, \ Y_i = \theta_i; \ R_{a_i} \qquad (6)$$

Table 6 Comparison of NN, FL, and GA predictive models for cutting temperature Q

	No.	$\theta_{Exp.}$ (°C)	$\theta_{N.N.}$ (°C)	E (%)	$\theta_{F.L.}$ (°C)	E (%)	$\theta_{G.A.}$ (C°)	E (%)
Training data	1	46	48.80	6.1	48.82	6.13	48.06	4.48
	2	52	52.32	0.61	54.17	4.17	55.55	6.82
	3	53	54.24	2.35	54.16	2.18	55.06	3.88
	4	56	56.67	1.19	54.07	3.44	63.64	13.64
	5	60	60.03	0.05	62.29	3.81	62.22	3.69
	6	67	67.13	0.19	67.50	0.74	71.91	7.33
	7	70	69.94	0.09	67.50	3.58	71.27	1.82
	8	77	77.15	0.19	75.98	1.33	82.38	6.98
	9	60	60.64	1.06	61.42	2.38	62.99	4.99
	10	54	53.87	0.24	53.95	0.09	54.81	1.49
	11	65	64.85	0.23	62.03	4.57	72.42	11.41
	12	55	55.16	0.29	53.95	1.91	54.95	0.09
	13	66	79.13	19.89	67.50	2.27	72.18	9.37
	14	47	45.03	4.19	48.94	4.12	48.75	3.73
	15	76.5	75.65	1.11	76.00	0.65	81.41	6.42
	16	51	51.26	0.51	53.48	4.86	36.99	27.46
	17	108	117.68	8.96	101.00	6.48	81.16	24.85
	18	66	59.50	9.84	67.50	2.27	55.86	15.36
	19	98	97.97	0.03	101.00	3.06	81.63	16.69
	20	66	65.99	0.01	67.49	2.26	56.05	15.08
	21	94	93.92	0.08	100.96	7.41	82.98	11.72
	Average error ⇒			2.72		3.22		9.39
Testing data	1	51	48.84	4.23	48.058	5.77	55.30	8.44
	2	69	65.53	5.03	64.94	5.88	71.59	3.76
	3	55	54.98	0.04	55.01	0.02	58.83	6.97
	4	62	54.88	11.48	56.81	8.36	67.39	8.71
	5	57	55.03	3.45	54.54	4.32	58.62	2.84
	6	60	53.96	10.06	56.29	6.18	67.75	12.92
	Average error ⇒			5.72		5.09		7.27

Table 7 Comparison of NN, FL, and GA predictive models for arithmetic mean roughness R_a

	No.	$R_{a\ Exp.}$ (μm)	$R_{a\ N.N.}$ (μm)	E (%)	$R_{a\ F.L.}$ (μm)	E (%)	$R_{a\ G.A.}$ (μm)	E (%)
	1	1.074	1.071	0.24	1.048	2.38	1.075	0.11
	2	1.081	1.075	0.53	1.129	4.53	1.045	3.29
	3	1.743	1.418	18.63	1.707	2.04	1.769	1.49
	4	1.645	1.643	0.09	1.517	7.8	1.720	4.56
	5	1.058	0.617	41.66	1.066	0.74	1.059	0.11
	6	1.023	1.313	28.33	1.057	3.36	1.029	0.68
	7	1.898	1.751	7.74	2.002	5.48	1.742	8.18
	8	1.734	1.733	0.08	1.722	0.68	1.695	2.27
Training data	9	1.205	1.205	0.02	1.244	3.2	1.352 μm	12.19
	10	1.133	1.135	0.21	1.141	0.72	1.389	22.58
	11	1.244	1.245	0.1	1.241	0.26	1.316	5.78
	12	0.995	0.999	0.37	1.003	0.84	0.819	17.64
	13	2.522	2.488	1.35	2.552	1.19	2.226	11.73
	14	1.242	1.237	0.37	1.240	0.14	1.372	10.47
	15	1.229	1.218	0.88	1.240	0.9	1.332	8.38
	16	0.915	0.909	0.68	0.940	2.77	0.850	7.10
	17	1.705	1.707	0.12	1.725	1.17	2.253	32.15
	18	2.023	2.017	0.3	2.011	0.61	2.259	11.68
	19	0.969	1.029	6.21	0.996	2.79	0.786	18.89
	20	1.258	1.259	0.08	1.240	1.41	1.336	6.17
	21	1.94	1.944	0.19	2.011	3.64	2.167	11.69
	Average error ⇒			5.15		2.22		9.39
	1	1.222	1.253	2.51	1.241	1.50	1.362	11.47
	2	1.28	1.022	20.12	1.328	3.73	1.342	4.84
Testing data	3	1.037	0.911	12.12	1.053	1.59	1.052	1.48
	4	1.583	1.763	11.39	1.611	1.79	1.731	9.37
	5	1.263	1.124	10.99	1.143	9.54	1.371	8.54
	6	1.734	1.240	28.46	1.257	27.51	1.333	8.02
	Average error ⇒			14.26		7.61		7.29

Another analysis of the accuracy of the corresponding models was performed based on simple linear regression. Figs. 9 and 10 show diagrams of actual and predicted values as well as the calculated coefficient of determination for each proposed model. Based on the analysis of the coefficient of determination in defining the most accurate model for predicting the cutting temperature Q, the following can be stated: the fuzzy logic model gave the best match of actual and predicted values ($R^2 = 0.982$), next the neural network model ($R^2 = 0.945$), and finally the most unfavourable prediction comes from a model based on GA. In this case, the first two models are acceptable for further implementation in process systems, while the GA model should be avoided.

Fig. 10 also shows an analysis of deviation of the values of the arithmetic mean roughness, where it is concluded that the fuzzy logic model gives a completely correct representation of the actual and predicted values with a very high coefficient of determination. The values for the other two models based on the membership interval belong to the domain of good correlation.
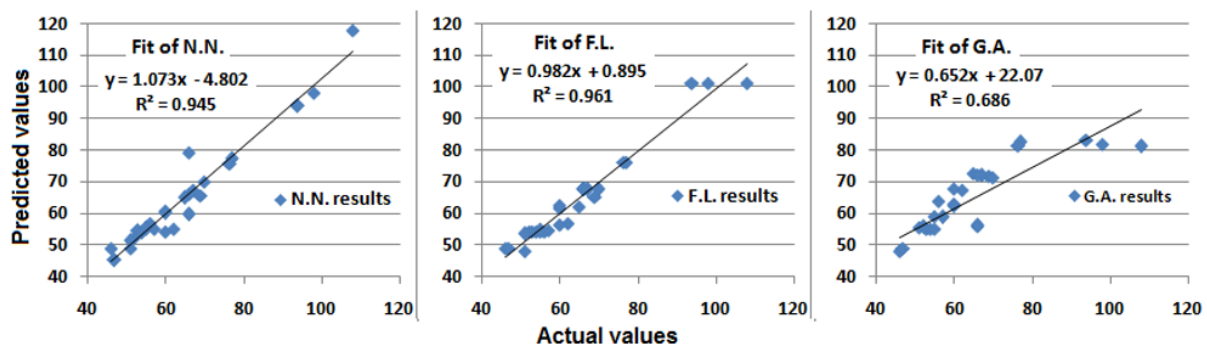
Fig. 9 Diagram of actual and predicted values for cutting temperature
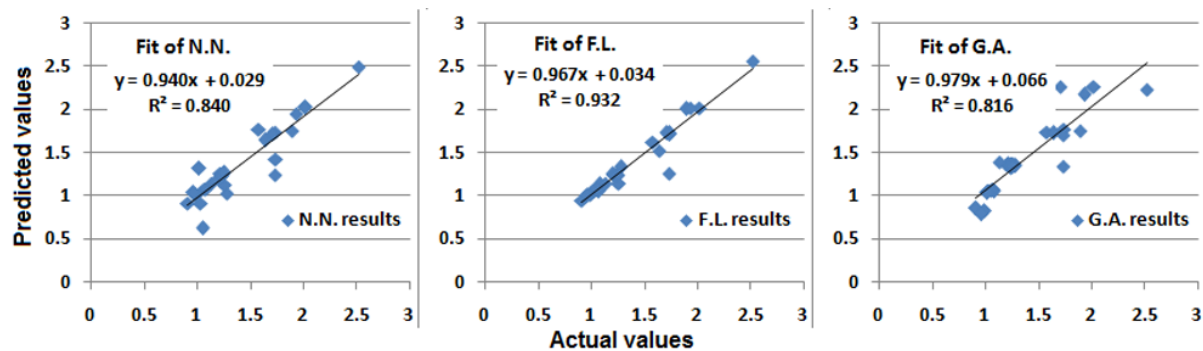
Fig. 10 Diagram of the actual and predicted values for the arithmetic mean roughness

Based on the overall analysis, taking into account the values based on the quantitative predictive potential E as well as the coefficient of determination R^2, it is concluded that the models based on fuzzy logic are the most suitable for further use.

6. Conclusion

By modeling the machinability functions of the milling process, i.e., the machining conditions and the output characteristics of the process, the conditions for a predict control and optimize process parameters have been created. The modeling process was performed using artificial intelligence based methods. Models were realized by artificial neural networks, fuzzy logic and genetic algorithms with the analysis of the accuracy. The obtained models for each machinability function were analyzed and on the basis of least error of deviation, the best model is proposed. An analysis was also performed in terms of the values of the coefficient of determination for each individual model as a function of the corresponding characteristics of the face milling process. The verification of the accuracy of the model was performed on the basis of additional experiments, which were not used in training phase. Based on a comprehensive analysis, it can be concluded that the application of the Fuzzy logic is the most adequate in the examined process. A further recommendation would be in the application of artificial neural networks in the first place, and then genetic algorithms in the second place.

The successful theoretical and experimental research has demonstrated the applicability of new modeling methods to milling processes. Also, models developed using artificial intelligence tools have a potential application in the industry. Consequently, the results of this research have their significance in that view, i.e., they can be integrated into manufacturing systems within which the tools of the integrated memory for the knowledge base are represented.

References

[1] Klancnik, S., Begic-Hajdarevic, D., Paulic, M., Ficko, M., Cekic, A., Husic, M.C. (2015). Prediction of laser cut quality for tungsten alloy using the neural network method, *Strojniški Vestnik – Journal of Mechanical Engineering*, Vol. 61, No. 12, 714-720, doi: 10.5545/sv-jme.2015.2717.

[2] Fulemová, J., Řehoř, J. (2015). Influence of form factor of the cutting edge on tool life during finishing milling, *Procedia Engineering*, Vol. 100, 682-688, doi: 10.1016/j.proeng.2015.01.420.

[3] Simunovic, G., Simunovic, K., Saric, T. (2013). Modelling and simulation of surface roughness in face milling, *International Journal of Simulation Modelling*, Vol. 12, No. 3, 141-153, doi: 10.2507/IJSIMM12(3)1.219.

[4] Perez, C.J.L. (2002). Surface roughness modeling considering uncertainty in measurements, *International Journal of Production Research*, Vol. 40, No. 10, 2245-2268, doi: 10.1080/00207540210125489.

[5] Ferreira, R., Rehor, J., Lauro, H.C., Carou , D., Davim , J.P. (2016). Analysis of the hard turning of AISI H13 steel with ceramic tools based on tool geometry: surface roughness, tool wear and their relation, *Journal of the Brazilian Society of Mechanical Sciences and Engineering*, Vol. 38, 2413-2420, doi: 10.1007/s40430-016-0504-z.

[6] Efkolidis, N., Hernández, C.G., Talón, J.L.H., Kyratsis, P. (2018). Modelling and prediction of thrust force and torque in drilling operations of Al7075 using ANN and RSM methodologies, *Strojniški Vestnik – Journal of Mechanical Engineering*, Vol. 64, No. 6, 351-361, doi: 10.5545/sv-jme.2017.5188.

[7] Hrelja, M., Klancnik, S., Balic, J., Brezocnik, M. (2014). Modelling of a turning process using the gravitational search algorithm, *International Journal of Simulation Modelling*, Vol. 13, No. 1, 30-41, doi: 10.2507/IJSIMM13(1)3.248.

[8]   Ojstersek, R., Lalic, D., Buchmeister, B. (2019). A new method for mathematical and simulation modelling inter-activity: A case study in flexible job shop scheduling, *Advances in Production Engineering & Management*, Vol. 14, No. 4, 435-448, doi: 10.14743/apem2019.4.339.

[9]   Sekulic, M., Pejic, V., Brezocnik, M., Gostimirović, M., Hadzistevic, M. (2018). Prediction of surface roughness in the ball-end milling process using response surface methodology, genetic algorithms, and grey wolf optimizer algorithm, *Advances in Production Engineering & Management*, Vol. 13, No. 1, 18-30, doi: 10.14743/apem2018.1.270.

[10] Meireles, M.R.G., Almeida, P.E.M., Simoes, M.G. (2003). A comprehensive review for industrial applicability of artificial neural networks, *IEEE Transactions on Industrial Electronics*, Vol. 50, No. 3, 585-601, doi: 10.1109/TIE.2003.812470.

[11] Balic, J., Korosec, M. (2002). Intelligent tool path generation for milling of free surfaces using neural networks, *International Journal of Machine Tools and Manufacture*, Vol. 42, No. 10, 1171-1179, doi: 10.1016/S0890-6955(02)00045-7.

[12] Azouzi, R., Gullot, M. (1997). On-line prediction of surface finish and dimensional deviation in turning using neural network based sensor fusion, *International Journal of Machine Tools and Manufacturing*, Vol. 37, No. 9, 1201-1217, doi: 10.1016/S0890-6955(97)00013-8.

[13] Singh, A.K., Panda, S.S., Chakraborty, D., Pal, S.K. (2006). Predicting drill wear using an artificial neural network, *The International Journal of Advanced Manufacturing Technology*, Vol. 28, No. 5, 456-462, doi: 10.1007/s00170-004-2376-0.

[14] Zuperl, U., Cus, F., Zawada-Tomkiewicz, A., Stępień, K. (2020). Neuro-mechanistic model for cutting force prediction in helical end milling of metal materials layered in multiple directions, *Advances in Production Engineering & Management*, Vol. 15, No. 1, 5-17, doi: 10.14743/apem2020.1.345.

[15] Savković, B., Kovac, P., Gerić, K., Sekulić, M., Rokosz, K. (2013). Application of neural network for determination of cutting force changes versus instantaneous angle in face milling, *Journal of Production Engineering*, Vol. 16, No. 2, 1-4.

[16] Lin, S.C., Ting, C.J. (1996). Drill wear monitoring using neural networks, *International Journal of Machine Tools and Manufacture*, Vol. 36, No. 4, 465-475, doi: 10.1016/0890-6955(95)00059-3.

[17] Liu, T.I., Chen, W.Y., Anantharaman, K.S. (1998). Inteligent detection of drill wear, *Mechanical Systems and Signal Procesing*, Vol. 12, No. 6, 863-873, doi: 10.1006/mssp.1998.0165.

[18] Zuperl, U., Čuš, F., Kiker, E. (2006). Intelligent adaptive cutting force control in end-milling, *Tehnički Vjesnik – Technical Gazzete*, Vol. 13, No. 1-2, 15-22.

[19] Zadeh, L.A. (1965). Fuzzy sets, *Information and Control*, Vol. 8, No. 3, 338-353, doi: 10.1016/S0019-9958(65)90241-X.

[20] Sivarao, S., Brevern, P., El-Tayeb, N.S.M., Vengkatesh, V.C. (2009). GUI based Mamdani fuzzy Inference system modeling to predict surface roughness in laser machining, *International Journal of Electrical & Computer Sciences IJECS-IJENS*, Vol. 9, No. 9, 281-288.

[21] Rajasekaran, T., Palanikumar, K., Vinayagam, B.K. (2011). Application of fuzzy logic for modeling surface roughness in turning CFRP composites using CBN tool, *Production Engineering*, Vol. 5, No. 2, 191-199, doi: 10.1007/s11740-011-0297-y.

[22] Savković, B., Kovač, P., Rodic, D., Gostimirovic, M., Pucovski, V., Holešovský, F. (2014). Application of ANFIS for modeling and prediction of the surface roughness for steel dificult to machining, In: *Proceedings of 8st International Scientific Conference on Mechanical Engineering-COMEC*, Faculty of Mechanical and Industrial Engineering, UCLV, Cuba, 1-11.

[23] Lo, S.-P. (2003). An adaptive-network based fuzzy inference system for prediction of workpiece surface roughness in end milling, *Journal of Materials Processing Technology*, Vol. 142, No. 3, 665-675, doi: 10.1016/S0924-0136(03)00687-3.

[24] Ho, S.-Y., Lee, K.-C., Chen, S.-S., Ho, S.-J. (2002). Accurate modeling and prediction of surface roughness by computer vision in turning operations using an adaptive neuro-fuzzy inference system, *International Journal of Machine Tools and Manufacture*, Vol. 42, No. 13, 1441-1446, doi: 10.1016/S0890-6955(02)00078-0.

[25] Hany, F. (2003). Handwriting digit reorganization with fuzzy logic, *Jurnal Teknik Elektro*, Vol. 3, No. 2, 84-87.

[26] Kovac, P., Rodic, D., Pucovsky, V., Savkovic, B., Gostimirovic, M. (2013). Application of fuzzy logic and regression analysis for modeling surface roughness in face milling, *Journal of Intelligent Manufacturing*, Vol. 24, No. 4, 755-762, doi: 10.1007/s10845-012-0623-z.

[27] Kovac, P., Rodic, D., Pucovsky, V., Savkovic, B., Gostimirovic, M. (2014). Multi-output fuzzy inference system for modeling cutting temperature and tool life in face milling, *Journal of Mechanical Science and Technology*, Vol. 28, No. 10, 4247-4256, doi: 10.1007/s12206-014-0938-0.

[28] Balic, J., Kovacic, M., Vaupotic, B. (2006). Intelligent programming of CNC turning operations using genetic algorithm, *Journal of Intelligent Manufacturing*, Vol. 17, No. 3, 331-340, doi: 10.1007/s10845-005-0001-1.

[29] Batish, A., Bhattacharya, A., Kaur, M, Cheema, M.S. (2014). Hard turning: Parametric optimization using genetic algorithm for rough/finish machining and study of surface morphology, *Journal of Mechanical Science and Technology*, Vol. 28, No. 5, 1629-1640, doi: 10.1007/s12206-014-0308-y.

[30] Dorlin, T., Fromentin, G., Costes, J.-P. (2016). Generalised cutting force model including contact radius effect for turning operations on Ti6Al4V titanium alloy, *International Journal of Advanced Manufacturing Technology*, Vol. 86, No. 9-12, 3297-3313, doi: 10.1007/s00170-016-8422-x.

[31] Santos, M.C., Machado, A.R., Barrozo, M.A.S., Jackson, M. J., Ezugwu, E.O. (2015). Multi-objective optimization of cutting conditions when turning aluminum alloys (1350-O and 7075 T6 grades) using genetic algorithm, *Inter-*

national Journal of Advanced Manufacturing Technology, Vol. 76, No. 5-8, 1123-1138, doi: 10.1007/s00170-014-6314-5.

[32] Sivasakthivel, P.S., Sudhakaran, R. (2013). Optimization of machining parameters on temperature rise in end milling of Al 6063 using response surface methodology and genetic algorithm, *The International Journal of Advanced Manufacturing Technology*, Vol. 67, No. 9, 2313-2323, doi: 10.1007/s00170-012-4652-8.

[33] Lukic, D., Milosevic, M., Antic, A., Borojevic, S., Ficko, M. (2017). Multi-criteria selection of manufacturing processes in the conceptual process planning, *Advances in Production Engineering & Management*, Vol. 12, No. 2, 151-162, doi: 10.14743/apem2017.2.247.

[34] Borojević, S., Lukić, D., Milošević, M., Vukman, J., Kramar, D. (2018). Optimization of process parameters for machining of Al 7075 thin-walled structures, *Advances in Production Engineering & Management*, Vol. 13, No. 2, 121-232, doi: 10.14743/apem2018.2.278.

[35] Stojanović, B., Ivanović, L. (2015). Application of aluminium hybrid composites in automotive industry, *Tehnički vjesnik – Technical Gazette*, Vol. 22, No. 1, 247-251, doi: 10.17559/TV-20130905094303.

[36] Kovač, P., Rodić, D., Pucovski, V., Mankova, I., Savkovic, B ., Gostimirović, M. (2012). A review of artificial inteligence approaches applied in inteligent processes, *Journal of Production Engineering*, Vol. 15, No. 1, 1-6.

Multi-criteria decision making in supply chain management based on inventory levels, environmental impact and costs

Žic, J.[a,*], Žic, S.[a]

[a]University of Rijeka, Faculty of Engineering, Rijeka, Croatia

ABSTRACT

Supply chains in a global business environment operate within conflicting aspects. This research analyses correlation and interdependencies between inventory levels, costs and greenhouse gas emissions from replenishments within supply chain echelon. A simulation-based inventory optimisation conducted on 4000 experiments assumes the conditions of stochastic market demand, (R, s, S) inventory policy, target fill rates, predefined lead times and closing days constraint. It verifies the influence of operational and logistic decisions such as frequency of inventory replenishments or vehicle size selection on management objectives. Besides determining the best individual results for the objectives of minimum inventory levels, total costs and emissions, the overall best solutions in terms of three decision models – uniformly valued, cost-oriented and environmentally responsible model, were determined using multi-criteria decision-making methodology. These models are relevant for both scientific and practical managerial settings due to the evident lack of research simultaneously analysing inventory, cost and environmental performances of (R, s, S) policy. This study confirms that it is crucial in practice to perform an extensive simulation experiment analysis for each product to be able to determine its optimal settings. Inventory management software should have a direct influence on operational decisions in order to reduce costs or emissions within the same fill rate.

1. Introduction

According to Cetinkaya *et al*. [1], there are three crucial factors which determine the business environment and the strategy of corporations nowadays: demand (customers and target groups), supply (competitors and suppliers) and general environment (regulations, natural resources, society, etc.). These factors are becoming increasingly complex and dynamic in today's business settings, determining the behaviour of market players. The unique objective of business until recent years was to acquire the maximum economic profit or to improve customer service [2-3]. During the quality revolution of the 1980s and the supply chain (SC) revolution of the 1990s, it has become clear that the best business practices require integration of environmental management with on-going business operations [4]. Severe deterioration of the environment, waste generation and resources depletion, together with legislation and customers' pressure, lead to the development of new concept - Green Supply Chain Management, which is often defined as an approach that implements ecological thinking into traditional supply chain management (SCM), products and services. However, this cannot be done to the detriment of

quality, cost or service level, which leads to the growing need to treat inventory management inseparably from environmental and economic objectives [5-7].

The rest of this paper is organised as follows: a review of relevant literature is presented in Section 2. Section 3 provides a formulation of a simulation model and presents the methods used. In Section 4 the experimental results (inventory levels, costs and emissions) are analysed, together with the multi-criteria decision-making method, used to select the favourable solutions by several decision criteria. Finally, research conclusions are given in Section 5.

2. Literature review

In this research, we study the correlation between several aspects of modern SCM - economic performance, inventory management under (R, s, S) policy and environmental impact, to provide the useful insights for managerial decisions. The environmental impact of SC activities analysed in this work considers greenhouse gases (GHG) emissions resulting from inventory replenishments based on road freight transport, which is a significant contributor to CO_{2eq} emissions [8]. Venkat and Wakeland observed that carbon emissions, as an indicator of the environmental performance of SC, are highly sensitive to the frequency and mode of deliveries, as well as type and amount of stored inventory. This implies that, even though lean SCs typically have lower emissions due to reduced inventory, frequent replenishments generally increase the level of emissions, particularly with longer-distance trade and globalisation [9]. Increasing customer awareness about environmental issues, especially in Europe and the US, requires transport and storage providers to demonstrate their sustainability. At the same time, modern management forces companies to integrate transportation planning in their management decisions to achieve a reduction of costs and improved customer service [10-11]. To be able to move towards reduction of emissions caused by transportation, companies tend to either adopt electric and hybrid vehicles or to optimise their operational decisions, where operational adjustments might be more cost-effective than investing in more carbon-efficient technologies [12-13].

(R, s, S) or periodic review policy is widely present inventory model both in practice and academic literature. Due to its structure, it has been implemented in many business information systems, such as ERP and APS, without the simple algorithms or procedures to determine the optimal characteristic inventory levels in practice [14-15]. Reorder point s and order-up-to level S, together with review period R, are in practical business situations set by inventory managers. Decision-making process becomes even more complicated with opposed, real-life objectives and constraints, such as service or cost-based targets, limited resources and workforce, which is not acknowledged by most of the classic inventory formulas. Additionally, behavioural preference is a substantial factor which affects the decision-making strategies of companies, usually leading to deviations from profit maximisation [16].

Despite the presence of this inventory policy in practice, there is a study gap in the review of the current literature regarding inventory management using (R, s, S) policy and related environmental and economic aspects. In this context, papers analysing Economic Order Quantity (EOQ) or other production-inventory models are much more common. The review of relevant literature is shown in Table 1, with specified factors considered in the listed studies.

Kapalka *et al.* described the approach for determining optimal (R, s, S) policies for inventory management in a practical retail environment, in conditions of stochastic demand and lost sales [17]. Possible benefits are evident in inventory and cost reduction while fulfilling defined service level constraint. Kiesmüller *et al.* compared the economic performance of (R, s, S) and (R, s, t, Q_{min}) policies with new policy (R, S, Q_{min}), taking into an account minimum order quantity (MOQ) parameter [14]. Bijvank and Vis analysed lost sales inventory models with service level constraint, comparing the optimal replenishment policy to (R, s, S) policy [18]. Periodic review inventory systems with service level constraint are also studied in the work of Bijvank [19], showing cost performance similar to the optimal policy, justifying their use in practical settings. Gocken *et al.* used the simulation model to determine optimal inventory parameters and review model between continuous and periodic review (s, S) inventory policies [20]. Their work included cost analysis and selection of the best supplier.

Table 1 Sustainable inventory models; factors considered in the literature

Authors	Year	Periodic review	Continuous review	Deterministic	Stochastic	EOQ/SEOQ model	Lead-time	MOQ constraint	Closing day constraint	Service-based constraint	Inventory impact on carbon emissions (CE)	CE from logistic activities (LA)	Fuel consumption by LA	Carbon policies	Holding costs	Order costs	Penalty/lost sales costs	Backorder costs	Transport costs
Kapalka *et al.*	1999	•			•		•			•					•	•			
Wahab *et al.*	2011					•						•		•	•	•			•
Kiesmüller	2011	•			•		•	•							•	•		•	
Bijvank, Vis	2012	•			•					•					•	•	•		
Chen *et al.*	2013			•		•					•			•	•	•			
Digiesi *et al.*	2013				•	•	•			•		•		•	•		•		•
Benjaafar *et al.*	2013			•	•						•			•	•	•		•	
Konur and Schaefer	2014				•							•		•	•	•			•
Bijvank	2014	•			•		•			•					•	•			
Battini *et al.*	2014				•						•	•			•	•			•
Tang *et al.*	2015	•			•		•				•	•	•		•			•	•
Gocken *et al.*	2017	•	•		•		•								•	•	•		
Akhtari *et al.*	2019	•		•						•		•	•		•	•			•
This study	2020	•			•		•	•	•	•	•	•			•	•	•		•

Only a few papers that study periodic review policy considered the environmental aspects. The research of Tang *et al.* [21] examines the cost of cutting carbon emissions by reducing shipment frequency and adjusting the inventory control decisions. Akhtari *et al.* [22] used a simulation model to compare the main parameters of forest-based biomass SC for two inventory management systems. The results showed that the selection of inventory system slightly impacts demand fulfilment, but has a considerable influence on total costs and carbon emissions. As mentioned, consideration of factors that have environmental and cost impact is more prevalent within the studies using the EOQ model. An environmental approach to traditional EOQ is introduced in a few works as the new "Sustainable Order Quantity" model (SOQ). Digiesi *et al.* [23] analysed SOQ model with stochastic demand in regards to logistic and environmental costs performance, and Battini *et al.* [24] examined all sustainability factors connected to lot sizing, using the life-cycle assessment approach. Benjaafar *et al.* [13] presented how firms could effectively reduce their carbon emissions, without significantly increasing costs, by making only operational adjustments in regards to transportation, production, inventory management, or collaboration with other members of SC. Chen *et al.* [25] used the EOQ model to discuss a similar concept. In their work, emission reductions are achieved by modifications of order quantities without significant cost increase. Konur and Schaefer [26] studied the integrated inventory control using EOQ model and transportation decisions of a retailer under four different carbon emissions regulation policies. Wahab *et al.* [7] explored the problem of determining the optimal production-shipment policy in domestic and international SC with incorporated consideration of the environmental impact of operational decisions such as a number of shipments, shipment size, the return of defected items etc. Papers of Ferretti *et al.,* Darvish *et al.*, and Yu *et al.* [3, 27, 28] contributed to the problem formulation of this research in regards to environmental or economic aspects of SCM.

3. Formulation of the inventory system model

3.1 General inventory model settings

Inventory model considered in this research consists of a single echelon SC system with stochastic market demand. The model observes operating of a distribution centre (DC) in a period of 90 days, using (R, s, S) control policy for managing inventory levels and replenishments from the

supplier to fulfil desired fill rates. Main model settings are specified in Fig. 1. Market demand is generated in software programmed in Python, and confirmed to be normally distributed by D'Agostino-Pearson omnibus K2 test in GraphPad Prism software, with P-value higher than the significance level (α = 0.05). Demand is modelled with a mean of 1000 products per day. Standard deviation of demand is defined as high (σ_H), with a value of 200, and low (σ_L) when it's value is 2. In total, our research is based on 400 simulated market demands, grouped per 200 for each standard deviation of demand. Tolerance of mean daily demand, in total observed period is 0, tolerance of standard deviation of demand is ±0.0001, and inventory fill rate tolerance is +0, −0.0001. Simulation model assumes that days without orders from customers may exist. The service-based constraint imposed on DC is defined with fill rates of 90 % and 100 %, calculated for the total observed period. Market demand, product deliveries and inventory levels are of non-negative, integer values. Inventory level is periodically reviewed at the end of each day.

In (R, s, S) inventory policy, lowest characteristic inventory levels can only be determined by applying exhaustive brute force search. Brute force search method results in a global minimum of characteristic inventory levels s and S at the expense of rapidly growing total number of simulation experiments (SE). In total, $1.13 \cdot 10^{13}$ SEs were tested to determine 4000 SEs with the lowest characteristic inventory levels satisfying boundary conditions for the observed period. For numerical analysis, HP ProLiant DL580 G7 server with four Xeon E7-4870 processors and 256 GB RAM was used. Each processor has 10 cores, and with hyperthreading we were able to conduct 80 separate searches parallelly. Generating 400 normally distributed market demands required approx. 8.5 h and brute force search for the lowest characteristic inventory levels of abovementioned 4000 SEs required approx. 23 h.

As our SC model tends to simulate realistic functioning of market-oriented SCs, Saturday and Sunday are defined as closing days for the supplier, while DC works seven days a week. The constraint of closing days makes the calculations more complex, reflecting on increased inventory levels, number of orders and their size, etc. Even though it is common in practice, one of the rare examples where such constraint can be found in the scientific literature is the study of Janssen *et al.* [29], related to perishable inventory model. Initial inventory level in SE is set to the S level. If current inventory position x at the time of review is equal to, or bellow s, an order of size (S-x) is placed. Average inventory level (AIL) is calculated for each SE as an average value of average daily inventory levels during the total observed period. MOQ is 1 unit of product. Supplier is reliable and supplying complete ordered quantity at predefined lead times of 0, 2, 5, 10 or 15 working days, meaning that products are delivered and available on the stock of DC in that time. Methods used in this paper are simulation modelling, statistical analysis and description and multi-criteria decision making.
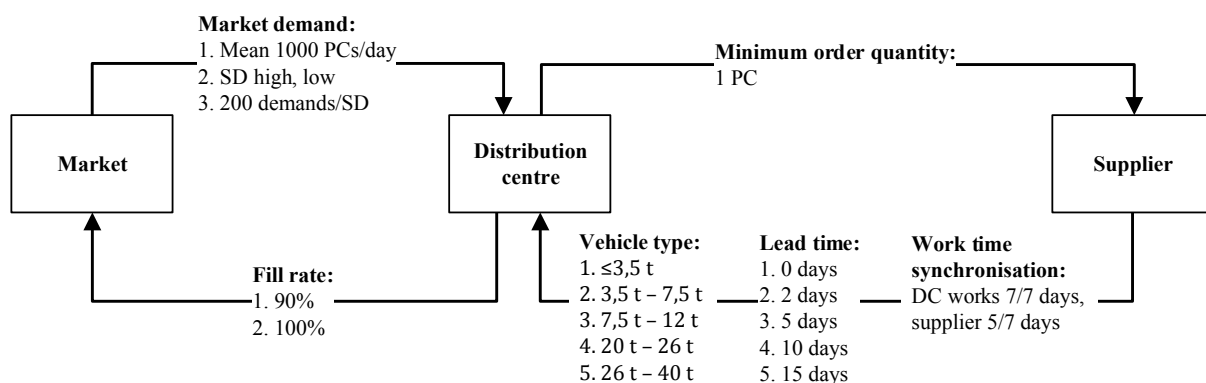
Fig. 1 The settings of the supply-chain echelon simulation model

3.2 Environmental impact of deliveries

Small and heavy-duty trucks together form more than 50 % of the GHG emissions in the transportation sector, which is one of the main contributors to GHG emissions in general [30]. In European Union, between 1990 and 2017, GHG emissions from transport increased by 10 %, although European Commission targets determine that emissions need to fall by around two thirds by 2050, in comparison to 1990 levels, to meet the long-term 60 % GHG emission from transport reduction [31, 32]. Operational decisions that tend to reduce emissions from transport activities can contribute to GHG emission reduction.

In our SC model, product deliveries from the supplier are organised via road freight transport, by five available vehicles of different types and payload capacities as presented in Table 2. The vehicle selection rule assumes using a single vehicle of the lowest category and sufficient payload capacity to transport the complete ordered quantity and weight in one trip. Transported product is of average goods freight type. Fuel used is diesel, emission standard EURO 6. SEs outputs provide information about the number and size of needed deliveries to keep defined fill rates at deterministic lead times. Notation and metrics used in this paper are visible in Table 3. GHG emissions are calculated in compliance with EN 16258, which specifies the methodology for calculation of transport services [33]. The energy consumption calculations are not considered in this study. The European norm EN 16258 prescribes calculation of emissions on tank-to-wheels (TTW) basis, concerning final emission production during vehicle operation, and on well-to-wheels basis (WTW), covering total emissions from the production of energy and vehicle operation. Emission calculations are verified with specialised software tool EcoTransIT by ETW in accordance with EN 16258 [34]. Total well-to-wheels (G_w) and tank-to-wheels GHG emissions (G_t) emitted during the period $i = 90$ days are calculated according to Eq. 1 and Eq. 2:

$$G_w = G_w(VOS) \cdot N_d \tag{1}$$

$$G_t = G_t(VOS) \cdot N_d \tag{2}$$

Well-to-wheels GHG emissions of the vehicle operating system (G_w (VOS)) for a round trip, are calculated according to [28], as in Eq. 3:

$$G_w(VOS) = F(VOS) \cdot g_w \tag{3}$$

Tank-to-wheels GHG emissions of the vehicle operating system (G_t (VOS)) are calculated according to Eq.4:

$$G_t(VOS) = F(VOS) \cdot g_t \tag{4}$$

3.3 The economic impact of inventory management

Costs taken into consideration in this research are the costs associated with holding and procurement of inventory, transportation costs and penalty costs, calculated for the total observed period. We use the following notation:

C_h are the holding costs, calculated by multiplying the average inventory level, as in the work of Urban [35], by the cost of carrying a single unit of inventory during the observed period, as in Eq. 5.

$$C_h = H \cdot i \cdot AIL \tag{5}$$

Table 2 Specification of fixed transport costs per vehicles

Vehicle type	Maximum total weight (MTW) of the vehicle	Maximum payload capacity, [t]	Maximum number of products per delivery,[PC]	Estimated vehicle price, [€]	Fixed transport cost, F_t, [€/vehicle/trip]
Van	≤3.5 t	1.5	1500	25000	24.7
Truck	3.5 t < MTW≤ 7.5t	3.5	3500	30000	29.64
Truck	7.5t< MTW≤ 12 t	6	6000	70000	69.17
Truck	20t< MTW≤ 26 t	17	17000	120000	118.58
Truck	26t< MTW≤ 40 t	26	26000	150000	148.22

<div align="center">Table 3 Notation and metrics used in this paper</div>

Parameters	Values and units	Variables	Units
Observed period (i)	90 days	Holding costs in the observed period (C_h)	€
Demand mean value (μ)	1000 units/day	Ordering costs in the observed period (C_o)	€
Standard deviations of demand (σ_L, σ_H)	2, 200 units/day	Transportation costs in observed period (C_t)	€
Fill rate (β)	90, 100 %	Penalty costs in the observed period (C_p)	€
Minimum order quantity (MOQ)	1 unit	Total costs in the observed period (C_T)	€
Review period (R)	1 day	Number of deliveries in the observed period (N_d)	-
Fixed order cost (K)	20 €/order	Number of orders in the observed period (N_o)	-
Fixed holding cost (H)	0.005 €/unit/day	Average inventory level in observed period (AIL)	units
Fixed penalty cost (P)	0.1 €/unit/period	Total well-to-wheels GHG emissions in the observed period (G_w)	tonne CO_{2e}
Fixed transportation cost (F_t)	24.7, 29.64, 69.17, 118.58, 148.22 €/vehicle/trip	Total tank-to-wheels GHG emissions in the observed period (G_t)	tonne CO_{2e}
Delivery vehicle payload capacity	1.5, 3.5, 6, 17, 26 tonne	Lost sales factor in the observed period (LS)	units/ period
Well-to-wheels GHG emission factor for diesel (g_w)	3.24 kg CO_{2e}/l	Tank-to-wheels GHG emissions of the vehicle operating system (G_t (VOS))	kg CO_{2e}
Tank-to-wheels GHG emission factor for diesel (g_t)	2.67 kg CO_{2e}/l	Well-to-wheels GHG emissions of the vehicle operating system (G_w (VOS))	kg CO_{2e}
Lead time (L)	0, 2, 5, 10, 15 days	Fuel consumption used for the vehicle operating system (F(VOS))	l
Product weight	1 kg	Load factor (L_f)	-
Distance from the supplier to the DC	218 km		

C_o are the order costs, incurred with each replenishment order to the supplier, calculated according to Eq. 6.

$$C_o = K \cdot N_o \tag{6}$$

C_t are the total transportation costs related to inventory replenishments, as in Eq. 7. They consist of a fixed and variable component, as in the work of Bonney and Jaber [6]. In our model, fixed transportation costs are the costs per vehicle per trip (F_t), defined for each vehicle type, as specified in Table 2, calculated with the assumption that the purchasing price of the vehicle will be paid off in 4 years of utilisation. Vehicles are being used for transport activities of deliveries along the SC and in observed echelon are being used once per every working day, which means 1012 days in 4 year period. Variable transportation costs depend on the load factor (L_f).

$$C_t = F_t \cdot N_d \left(1 + L_f \right) \tag{7}$$

C_p are the penalty costs, charged for the lost sales due to the stock-outs, as in Eq. 8. Lost sales are expressed with *LS* factor, representing the number of unsold units in the total observed period due to unmet demand caused by a lack of inventory. In this paper, only penalty costs due to unmet demand will be calculated, not considering the loss of reputation, customers, or similar effects.

$$C_p = P \cdot LS \tag{8}$$

Total costs C_T are calculated according to Eq. 9:

$$C_T = C_h + C_o + C_t + C_p \tag{9}$$

4. Results and discussion

Inventory management parameters and related variables resulting from SEs, examined in this research are average inventory level (AIL), number and the size of inventory replenishments (deliveries), GHG emissions from deliveries and SC costs. All inventory, cost and emission variables are calculated on the level of single SE, and later on, grouped based on a standard deviation of demand, fill rate and lead time for transparency and understanding of the results.

4.1 Average inventory level (AIL)

Influence of lead time, fill rate and demand fluctuations on AIL is visible from Figs. 2 and 3. Expectedly, AIL has the highest value in the scenario of the most extended lead time scenario – L15 days, high fluctuations of demand and fill rate of 100 %. Results indicate that demand oscillations have a medium effect on average AILs. When comparing the values of average AILs, for the change of standard deviation from low to high between the groups of the same lead time and fill rate conditions, we find that they can decrease up to 8 % or increase up to 33.7 %. The peak value of 33.7 % occurs for lead time 0, fill rate of 100 % and change from low to high standard deviation of demand.

The influence of fill rate decreases with longer lead times. The maximum increase of average AILs for the shift in fill rate from 90 % to 100 % occurs for 0 days lead time and high standard deviation of demand. In general, average AILs increase with the increase of lead time, fill rate and standard deviation of demand. The highest percentage of average AIL increase, 105.5 %, dependent on the lead time lengthening from 0 to 2 days, occurs in the case of a 100 % fill rate and low standard deviation of demand. Very high increase of average AILs, from 76.9 % to 99.7 %, depending on the fill rate and demand oscillations, is registered for the change of lead time from 5 to 10 days.

The most significant difference between the minimum and maximum AILs occurs for a lead time of 15 days, 100 % fill rate and high standard deviations of demand, followed by those in the conditions of lead time 5 days, fill rate 90 % and high demand oscillations. It is interesting to mention that, depending on the fill rate and standard deviation of demand, a DC needs to have in average 8.4 times higher AILs in conditions of the lead time of 15 days, than of 0 lead times. Numerical simulations showed that the best solution from the aspect of the lowest average AIL levels would be the set of data with lead time 0, fill rate 90 % and high demand oscillations.

4.2 Costs

The structure of average total costs, and the shares of its components – holding, ordering, transportation and penalty costs, are shown in Figs. 4 and 5. It is evident that the minimum average total costs occur under conditions of lead time 0, fill rate 90 % and high demand oscillations. The highest total average costs occur in terms of lead time of 15 days, 100 % fill rate and high demand oscillations. From Figs. 4 and 5 it is visible that the average holding costs account for the significant share of average total costs, and that it increases with the increase of lead time. This share varies from 13.8 % in case of lead time 0, fill rate 90 % and high demand oscillations, up to 89.8 % when lead time is 15 days, fill rate 100 % and high demand oscillations. The highest average transportation costs, making 58.8 % of average total costs, are registered in the scenario with conditions of 0 lead time, low deviations of demand and fill rate of 100 % what corresponds with the maximum average number of deliveries in the total period.

Penalty costs occur only when market demand is not completely satisfied, meaning in scenarios of fill rate of 90 %. They can reach up to a maximum of 20.4 % of average total costs.
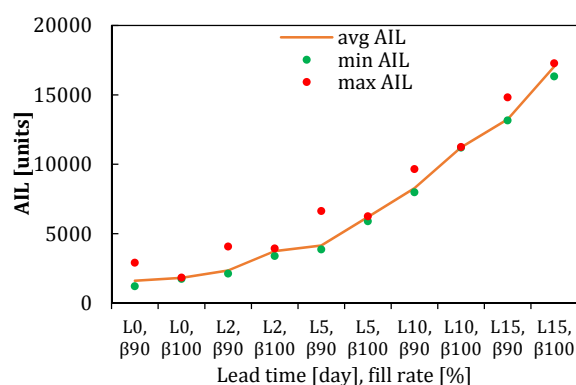
Fig. 2 Average, minimum and maximum AIL$_i$ depending on fill rate and lead times for σ_L
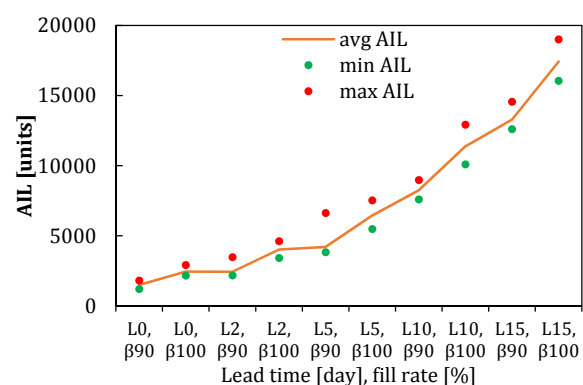
Fig. 3 Average, minimum and maximum AIL$_i$ depending on fill rate and lead times for σ_H
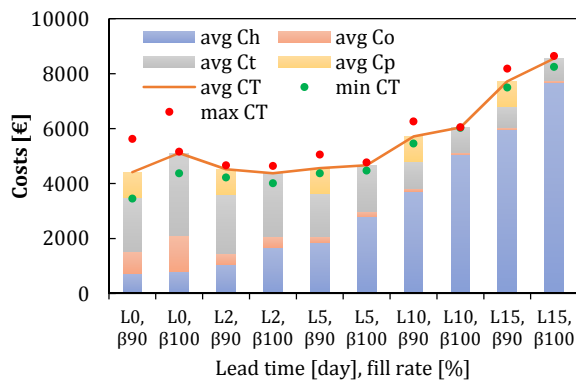
Fig. 4 Minimum, maximum and average total costs and its components for σ_L
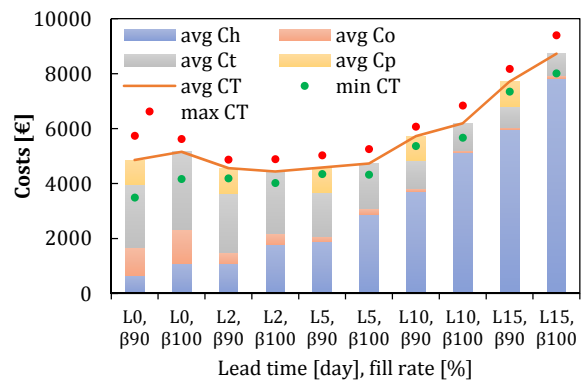
Fig. 5 Minimum, maximum and average total costs and its components for σ_H

Ordering costs have the smallest share, reaching up to maximum 25.2 % of total costs in case of everyday deliveries (lead time 0). Fluctuations of average total costs, depending on demand oscillations, are not significant. There is in average 2 % difference in total costs, when comparing high and low demand oscillations, for the same lead time and fill rate scenarios groups. Fluctuations of average total costs, depending on the fill rate change, are more evident. Per example, the maximum increase of average total costs of 15.8 % occurs for a fill rate increase from 90 % to 100 %, in conditions of lead time 0, and low demand oscillations. The increase in average total costs becomes strongly evident for 5 days lead time and longer. Lead time increase from 5 to 10 days implies the increase of average total costs from 25 % to 30.8 %, and from 10 to 15 days for up to 41.6 %, depending on fill rate and demand. Overall, the lowest average total costs are recorded in conditions of lead time of 2 days, 100 % fill rate and low demand oscillations.

4.3 GHG emissions

The number of deliveries directly influences the amount of GHG emissions. As presented in Figs. 6 and 7, the maximum average number of shipments in the observed period, 63.3, is registered in conditions of the shortest lead time (L0), low deviations of demand, and fill rate of 100 %. The same conditions result in the highest average WTW GHG emissions. Additionally, the lowest total WTW GHG emissions are registered in the situation of the longest lead time; for a lead time of 15 days, 100 % fill rate and low standard deviation of demand. Level of WTW GHG emissions decreases with longer lead times due to reduced frequency and number of deliveries. However, it is necessary to note that the reduction of the average number of deliveries does not cause a linear decrease in emissions. On the other hand, when comparing the average number of deliveries for the lead time of 5 and 10 days, they drop for 52.8 %, while the level of emissions decreases for only 16.3 %. In general, change from low to high demand oscillations within the same lead time and fill rate group, does not significantly influence the level of emissions.
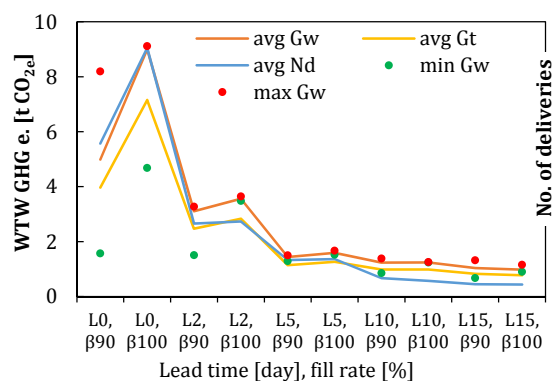
Fig. 6 Minimum, maximum and average total WTW GHG emissions and deliveries for σ_L
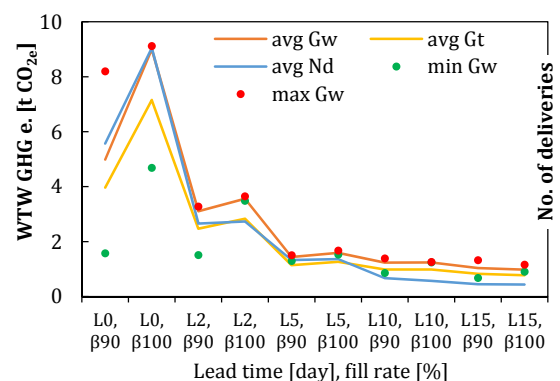
Fig. 7 Minimum, maximum and average total WTW GHG emissions and deliveries for σ_H

Fill rate increase from 90 % to 100 % results in WTW GHG emissions increase, within the same standard deviation of demand and lead time. The highest rise in emissions' level in an amount of 80.4% occurs in the case of the lead time of 0 days and low standard deviation of demand. With longer lead times, it drops to the levels from 14.6 % to 0.3 %. Only lead time group of 15 days differs from this behaviour, where emissions slightly decrease with the increase of fill rate. From this study results, gained from a single echelon model, it is justified to conclude that the frequency of deliveries strongly affects the emitted level of GHG emissions. Therefore, the decrease in deliveries frequency could contribute to deduction of overall emissions.

4.4 Multi-criteria decision making

Trends of the average inventory level, total costs and emissions resulting from SC activities, detailedly analysed in previous chapters, are presented in Figs. 8 and 9. To achieve the overall optimum results in a practical business environment, it is necessary to approach the decision-making process comprehensively, taking into consideration all aspects simultaneously. With this purpose, the weighted sum method (WSM) of multi-criteria decision making (MCDM) was used. Three decision criteria are selected as relevant for the evaluation of alternatives: (i) average inventory levels, (ii) total costs and (iii) WTW GHG emissions. These are all non-beneficial attributes, meaning that minimum value is desired.

In general, for *m* alternatives and *n* criteria, the best alternative is, in the minimisation case, the one that satisfies the Eq. 10:

$$PS^* = \min_i \sum_{j=1}^{n} a_{ij} w_j, for \ i = 1, 2, 3, \ldots, m \tag{10}$$

where PS^* is the performance score of the best alternative, with *n* representing the number of decision criteria, a_{ij} the actual value of the *i*-th alternative in terms of the *j*-th criterion, and w_j the weightage of the *j*-th criterion. In this paper, values of 4000 alternatives resulting from the equivalent number of SEs, per each of the three decision criteria, are normalised according to Eq. 11 and rescaled in the range between 0 and 1 to be mutually comparable.

$$a_{i,norm} = \frac{a_i - a_{min}}{a_{max} - a_{min}} \tag{11}$$

Normalised values of the alternatives for each criterion are multiplied by the corresponding weightage, depending on the decision-making model. To get performance score of each alternative, all weighted normalised performance values for each alternative are summarised, where the best result is the one that yields the minimum total performance value, as per Eq. 10.

Three decision models which are relevant for both managerial practice and further scientific research are defined - uniformly valued, cost-oriented, and environmentally responsible decision model. Models differ based on the dominant aspect, as specified in Table 4.
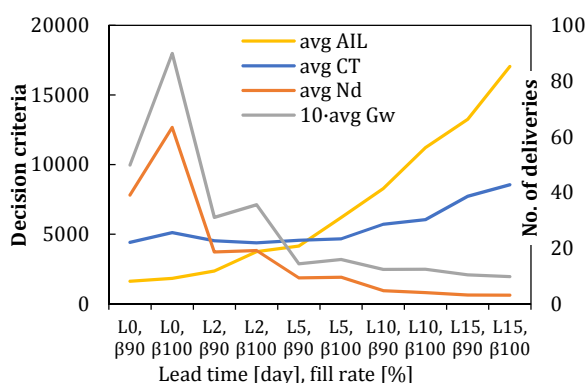
Fig. 8 Number of deliveries and decision criteria in conditions of σ_L
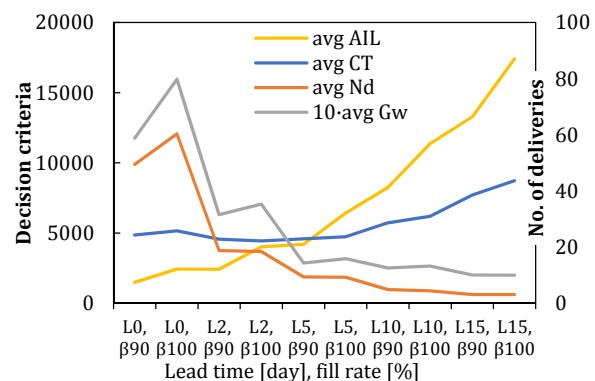
Fig. 9 Number of deliveries and decision criteria in conditions of σ_H

Models are defined based on the goal which wants to be achieved – better environmental or economic performance, or equal performance in regards to inventory levels, costs and emissions.

Weightage factors for uniformly valued decision model are determined according to the objective weighting method – Mean Weight, based on the assumption that all decision criteria are of equal importance. In cost-oriented and environmentally responsible decision model decision criteria are chosen by Point Allocation Method in a way that dominant decision criterion is of the three times higher value than the other two criteria (20-20-60). The number of points allocated to each criterion is assigned by the decision-maker, based on the experience and reasoning. Therefore, subjectivity in this step of the MCDM model, same as in the real world conditions, cannot be avoided entirely. However, there is no subjectivity in all the calculations that precede and follow this step.

Results gained are considerably different within the same lead time, fill rate and standard deviation of demand groups, which is visible from the range width between the maximum and minimum performance score (PS), as shown on Figs. 10 and 11. The difference is even more evident when comparing the overall best ranked (min PS) and worst ranked (max PS) solutions within each decision model. These results are presented in Table 5, together with corresponding decision criteria.

The overall best solution according to the settings of the uniformly valued decision model, occurs in case of shortest lead time and deliveries within the same day (L0), fill rate of 90 % and low standard deviations of market demand. If comparing the performance of the worst solution within the same group (L0, β = 90 %, σ_L), it shows 57.8 % lower AIL, 28 % higher total costs and 416.4 % higher GHG emissions. The overall worst solution would result in 552 % higher AIL, 113.4 % higher total costs and 36.8 % lower GHG emissions.

The overall best solution, according to the cost-oriented decision model, occurs in the same conditions as for uniformly valued decision model: L0, β = 90 %, σ_L. The same conditions, without optimally set parameters, could also result in 27.1 % lower AIL, 62.8 % higher total costs and 93.9 % higher GHG emissions. For the comparison, the overall least favourable solution (with worst performance score) results with 1027 % higher AIL, 171.5 % higher total costs and 76.3 % lower amount of GHG emissions.

The overall best solution according to the environmentally responsible decision model happens in the conditions of the lead time of 5 days, 90 % fill rate and high standard deviation of market demand. In these same conditions significantly worse scenario could occur – that one of 58.6 % higher AIL, 14 % higher total costs and 3.9 % higher GHG emissions. Additionally, when comparing the best solution to the worst-ranked one, the later results in 26.7 % lower AIL, 27.4 % higher total costs and 556.4 % higher GHG emissions. It is visible that the same lead time, fill rate and market demand oscillations level provide optimal solution according to uniformly valued and cost-oriented decision model; the conditions of the lead time of 0 days, fill rate of 90 % and low standard deviation of demand. In an environmentally responsible decision model, the best solution occurs for a lead time of 5 days, fill rate of 90 % and a high standard deviation of demand. In an environmentally responsible decision model, emissions are 302.87 % lower than in cost-oriented decision model, and 113.74 % lower than in uniformly valued decision model. However, this reduction results with 25.8 % higher total costs than in cost-oriented decision model and approximately the same level of the costs as in uniformly valued decision model.

Table 4 Decision-making models and criteria

Decision making model	Uniformly valued decision model (A)	Cost oriented decision model (B)	Environmentally responsible decision model (C)
Model characteristic	each decision criterion has the equal significance	total costs are the dominant decision criterion	environmental impact is dominant decision criterion
Weightage of the decision criteria	AIL : total costs : emissions is $^1/_3 : ^1/_3 : ^1/_3$	AIL : total costs : emissions is $^1/_5 : ^3/_5 : ^1/_5$	AIL : total costs : emissions is $^1/_5 : ^1/_5 : ^3/_5$
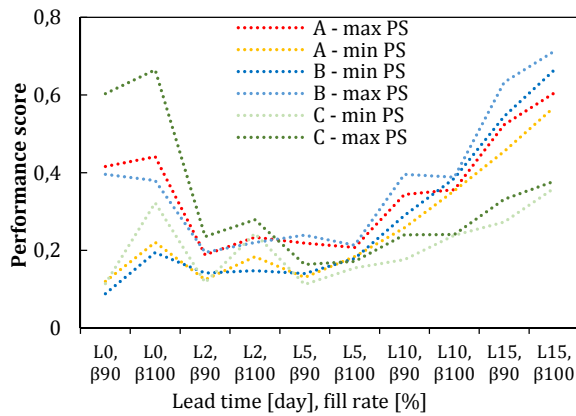
Fig. 10 Minimum and maximum performance scores for each decision model and σL
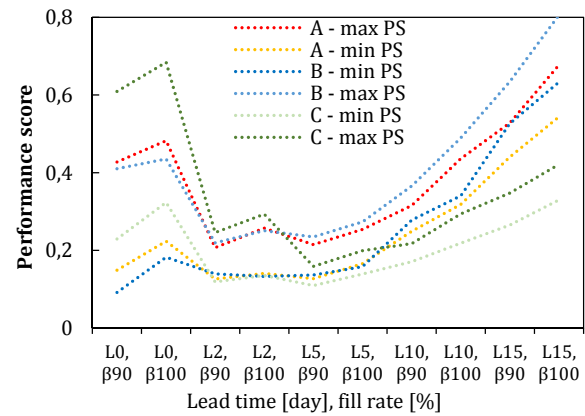
Fig. 11 Minimum and maximum performance scores for each decision model and σ_H

5. Conclusion

In this research, we studied a single echelon inventory system with (*R, s, S*) policy and normally distributed market demand, taking into an account market demand fluctuations, service-based constraints, predefined lead-times and closing days.

In total, 4000 simulation experiments were examined, providing relevant information about the behaviour of various SC performance factors, such as average inventory levels, costs, number and size of inventory replenishments and GHG emissions from delivery activities. To the practitioners in companies operating under (*R, s, S*) inventory policy this offers valuable insights on correlations and interdependencies of characteristic inventory, economic and environmental parameters in conditions of stochastic market demand; information which are not available without the extensive simulation analysis. Research conclusions can be transferred to real-life systems operating in similar situations as defined in our SC model to identify possible improvements for management, find optimal operational settings, enable cost or GHG emissions reduction without jeopardising any operational aspect of SC, etc.

Statistical analysis provides the conclusion about the conditions leading to the individual best solutions in regards to the inventory levels, costs or GHG emissions from transport activities. However, identification of the overall best configuration, considering these three crucial aspects simultaneously, requires a structured analysis of multiple criteria. Therefore, a multi-criteria decision-making method was used to select the optimal results, based on different decision models relevant for managerial business practice – uniformly valued, cost-oriented and environmentally responsible one.

Deviations between the best and the worst-ranked solution (performance score) indicate how much the results can oscillate even within the same lead time, fill rate and demand oscillations group. The results display that even more significant differences occur between the overall worst and best-ranked solution within the same decision model. These differences can reach up to maximum 1127 % for AIL (in cost-oriented decision model), 272 % for total costs (in cost-oriented decision model), and 656 % for GHG emissions (in environmentally responsible decision model), which gives a clear overview on the importance of correct decision-making.

Table 5 The overall best and worst solutions within decision models

Decision model	Rank	L	β	σ	SE	AIL	C_T	G_w	PS
A	the best-ranked score	L0	90	σL	5	2902.7	4399.19	1.57	0.120 (min)
A	the worst-ranked score	L15	100	σ_H	3858	18925.7	9389.03	0.99	0.677 (max)
B	the best-ranked score	L0	90	σL	61	1679.29	3458.16	4.18	0.089 (min)
B	the worst-ranked score	L15	100	σ_H	3858	18925.7	9389.03	0.99	0.806 (max)
C	the best-ranked score	L5	90	σ_H	1930	3816.38	4350.57	1.38	0.110 (min)
C	the worst-ranked score	L0	100	σ_H	761	2797.12	5544.71	9.05	0.684 (max)

Research results imply that it is crucial to perform complete SEs analysis for each product considered in SC echelon to be able to determine its particular optimal inventory management settings. Therefore, for optimal SCM that takes into an account a wide range of influential aspects, we find that continuous monitoring of inventory, demand, logistics, sales and marketing activities is necessary. Inventory management software should be implemented in the business software of the company at the bottom level, with direct influence on operational decisions. The proposed approach should raise the awareness that operational decisions such as the frequency and size of replenishment deliveries, vehicle category choice but also oscillations of market demand, target fill rates, etc., have a significant impact on inventory, economic and environmental performance in SC.

Acknowledgement

References

[1]   Cetinkaya, B., Cuthbertson, R., Ewer, G., Klaas-Wissing, T., Piotrowicz, W., Tyssen, C. (2011). *Sustainable supply chain management*, Springer-Verlag, Berlin Heidelberg, Germany, doi: 10.1007/978-3-642-12023-7.

[2]   Shapiro, J. (2001). *Modelling the supply chain*, Duxbury Press, Pacific Grove, California, USA.

[3]   Ferretti, I., Zanoni, S., Zavanella, L., Diana, A. (2007). Greening the aluminium supply chain, *International Journal of Production Economics*, Vol. 108, No. 1-2, 236-245, doi: 10.1016/j.ijpe.2006.12.037.

[4]   Srivastava, S.K. (2007). Green supply chain management: a state-of-the-art literature review, *International Journal of Management Reviews*, Vol. 9, No. 1, 53-80, doi: 10.1111/j.1468-2370.2007.00202.x.

[5]   Christoper, M., Towill, D.R. (2000). Supply chain migration from lean and functional to agile and customised, *Supply Chain Management*, Vol. 5, No. 4, 206-213, doi: 10.1108/13598540010347334.

[6]   Bonney, M., Jaber, M.Y. (2011). Environmentally responsible inventory models: non-classical models for a non-classical era, *International Journal of Production Economics*, Vol. 133, No. 1, 43-53, doi: 10.1016/j.ijpe.2009.10.033.

[7]   Wahab, M.I.M., Mamun, S.M.H., Ongkunaruk, P. (2011). EOQ models for a coordinated two-level, *Journal of Production Economics*, Vol. 134, No. 1, 151-158, doi: 10.1016/j.ijpe.2011.06.008.

[8]   Demir, E., Bektaş, T., Laporte, G. (2014). A review of recent research on green road freight transportation, *European Journal of Operational Research,* Vol. 237, No. 3, 775-793, doi: 10.1016/j.ejor.2013.12.033.

[9]   Venkat, K., Wakeland, W. (2006). Is lean necessarily green?, In: *Proceedings of the 50th Annual Meeting of the International Society for the Systems Sciences*, Sonoma, California, USA.

[10] Oršič, J., Rosi, B., Jereb, B. (2019). Measuring sustainable performance among logistic service providers in supply chains, *Tehnički Vjestnik – Technical Gazette,* Vol. 26, No. 5, 1478-1485, doi: 10.17559/TV-20180607112607.

[11] Somboonwiwat, T., Khompatraporn, C., Miengarrom, T., Lerdluechachai, K. (2018). A bi-objective environmental-economic optimisation of hot-rolled steel coils supply chain: A case study in Thailand, *Advances in Production Engineering & Management,* Vol. 13, No. 1, 93-106, doi: 10.14743/apem2018.1.276.

[12] Balamurugan, T., Karunamoorthy, L., Arunkumar, N., & Santhosh, D. (2018). Optimisation of inventory routing problem to minimise carbon dioxide emission, *International Journal of Simulation Modelling*, Vol. 17, No. 1, 42-54, doi: 10.2507/IJSIMM17(1)410.

[13] Benjaafar, S., Li, Y., Daskin, M. (2013). Carbon footprint and the management of supply chains: Insights from simple models, *IEEE Transactions on Automation Science and Engineering*, Vol. 10, No. 1, 99-116, doi: 10.1109/TASE.2012.2203304.

[14] Kiesmüller, G.P., de Kok, A.G., Dabia, S. (2011). Single item inventory control under periodic review and a minimum order quantity, *International Journal of Production Economics*, Vol. 133, No. 1, 280-285, doi: 10.1016/j.ijpe.2010.03.019.

[15] Sani, B., Kingsman, B.G. (1997). Selecting the best periodic inventory control and demand forecasting methods for low demand items, *Journal of the Operational Research Society*, Vol. 48, No. 7, 700-713, doi: 10.1057/ palgrave. jors.2600418.

[16] Jian, M., Wang, Y.L. (2018). Decision-making strategies in supply chain management with a waste-averse and stockout-averse manufacturer, *Advances in Production Engineering & Management,* Vol. 13, No. 3, 345-357, doi: 10.14743/apem2018.3.295.

[17] Kapalka, B.A., Katircioglu, K., Puterman, M.L. (1999). Retail inventory control with lost sales, service constraints, and fractional lead times, *Production and Operations Management*, Vol. 8, No. 4, 393-408, doi: 10.1111/j.1937-5956. 1999.tb00315.x.

[18] Bijvank, M., Vis, I.F.A. (2012). Lost-sales inventory systems with a service level criterion, *European Journal of Operational Research*, Vol. 220, No. 3, 610-618, doi: 10.1016/j.ejor.2012.02.013.

[19] Bijvank, M. (2014). Periodic review inventory systems with a service level criterion, *Journal of the Operational Research Society*, Vol. 65, No. 12, 1853-1863, doi: 10.1057/jors.2013.160.

[20] Gocken, M., Dosdogru, A.T., Boru, A. (2017). Optimization via simulation for inventory control policies and supplier selection, *International Journal of Simulation Modelling*, Vol. 16, No. 2, 241-252, doi: 10.2507/IJSIMM16 (2)5.375.

[21] Tang, S., Wang, W., Yan, H., Hao, G. (2015). Low carbon logistics: Reducing shipment frequency to cut carbon emissions, *International Journal of Production Economics*, Vol. 164, 339-350, doi: 10.1016/j.ijpe.2014.12.008.

[22] Akhtari, S., Sowlati, T., Siller-Benitez, D.G., Roeser, D. (2019). Impact of inventory management on demand fulfilment, cost and emission of forest-based biomass supply chains using simulation modelling, *Biosystems Engineering,* Vol. 178, 184-199, doi: 10.1016/j.biosystemseng.2018.11.015.

[23] Digiesi, S., Mossa, G., Mummolo, G. (2013). A sustainable order quantity model under uncertain product demand, *IFAC Proceedings Volumes*, Vol. 46, No. 9, 664-669, doi: 10.3182/20130619-3-RU-3018.00444.

[24] Battini, D., Persona, A., Sgarbossa, F. (2014). A sustainable EOQ model: Theoretical formulation and applications, *International Journal of Production Economics*, Vol. 149, 145-153, doi: 10.1016/j.ijpe.2013.06.026.

[25] Chen, X., Benjaafar, S., Elomri, A. (2013). The carbon-constrained EOQ, *Operations Research Letters*, Vol. 41, No.2, 172-179, doi: 10.1016/j.orl.2012.12.003.

[26] Konur, D., Schaefer, B. (2014). Integrated inventory control and transportation decisions under carbon emissions regulations: LTL vs. TL carriers, *Transportation Research*, Vol. 68, 14-38, doi: 10.1016/j.tre.2014.04.012.

[27] Darvish, M., Archetti, C., Coelho, L.C. (2019). Trade-offs between environmental and economic performance in production and inventory-routing problems, *International Journal of Production Economics*, Vol. 217, 269-280, doi: 10.1016/j.ijpe.2018.08.020.

[28] Yu, W., Hou, G., Xia, P., Li, J. (2019). Supply chain joint inventory management and cost optimisation based on ant colony algorithm and fuzzy model, *Tehnički Vjesnik – Technical Gazette,* Vol. 26, No. 6, 1729-1737, doi: 10.17559/TV-20190805123158.

[29] Janssen, L., Sauer, J., Claus, T., Nehls, U. (2018). Development and simulation analysis of a new perishable inventory model with a closing days constraint under non-stationary stochastic demand, *Computers & Industrial Engineering*, Vol. 118, 9-22, doi: 10.1016/j.cie.2018.02.016.

[30] Bozorgi, A., Pazour, J., Nazzal, D. (2014). A new inventory model for cold items that considers costs and emissions, *International Journal of Production Economics*, Vol. 155, 114-125, doi: 10.1016/j.ijpe.2014.01.006.

[31] Eurostat. Greenhouse gas emission statistics – Emission inventories, from *https://ec.europa.eu/eurostat/ statistics-explained/pdfscache/1180.pdf*, accessed February 11, 2020.

[32] European Environmental Agency (EEA). Greenhouse gas emissions from transport in Europe, from *https://www.eea.europa.eu/data-and-maps/indicators/transport-emissions-of-greenhouse-gases/transport-emissions-of-greenhouse-gases-12*, accessed February 11, 2020.

[33] European Committee for Standardization (CEN), (2012). Methodology for calculation and declaration of energy consumption and GHG emissions of transport services (freight and passengers)*, SS-EN 16258:2012*, CEN, Brussels, Belgium, from:*https://www.sis.se/en/produkter/sociology-services-company-organization/services/services-for-consumers/ssen162582012/*, accessed February 10, 2020.

[34] ifeu, INFRAS, IVE. Ecotransit world: Methodology and data – Update 2019, from *https://www.ecotransit.org/download/EcoTransIT World Methodology Data Update 2019.pdf*, accessed February 10, 2020.

[35] Urban, T.L. (1998). An inventory – Theoretic approach to product assortment and shelf-space allocation, *Journal of Retailing*, Vol. 74, No. 1, 15-35, doi: 10.1016/S0022-4359(99)80086-4.

Development of family of artificial neural networks for the prediction of cutting tool condition

Spaić, O.[a], **Krivokapić, Z.**[b], **Kramar, D.**[c,*]

[a]University in East Sarajevo, Faculty of Production and Management Trebinje, Bosnia and Herzegovina
[b]University in Montenegro, Faculty of Mechanical Engineering Podgorica, Montenegro
[c]University in Ljubljana, Faculty of Mechanical Engineering Ljubljana, Slovenia

ABSTRACT

Recently, besides regression analysis, artificial neural networks (ANNs) are increasingly used to predict the state of tools. Nevertheless, simulations trained by cutting modes, material type and the method of sharpening twist drills (TD) and the drilling length from sharp to blunt as input parameters and axial drilling force and torque as output ANN parameters did not achieve the expected results. Therefore, in this paper a family of artificial neural networks (FANN) was developed to predict the axial force and drilling torque as a function of a number of influencing factors. The formation of the FANN took place in three phases, in each phase the neural networks formed were trained by drilling lengths until the drill bit was worn out and by a variable parameter, while the combinations of the other influencing parameters were taken as constant values. The results of the prediction obtained by applying the FANN were compared with the results obtained by regression analysis at the points of experimental results. The comparison confirmed that the FANN can be used as a very reliable method for predicting tool condition.

1. Introduction

The prediction of the tool condition, i.e. the determination of correlations between the target function and the influencing parameters, is of high importance, since the technological and economic effects of the machining process depend directly on the tool life. However, due to the highly complex phenomena that develop within the cutting zone and are caused by the influence of a number of mutually collinear factors, modeling the cutting process is difficult. One of the most accurate and reliable methods for predicting the tool condition is the experimental-analytical method, in which a regression model for predicting the tool condition is created on the basis of the determined dependence of the target function on the influencing parameters [1]. Nevertheless, regression analysis does not provide satisfactory results when the relationship between the target function and the influencing parameters is non-linear, as is usually the case in cutting, and requires additional experiments. For this reason, many researchers have recently started to apply the principles of ANNs to the modeling of the cutting process.

Krivokapić *et al.* [2], explored the possibility of using ANN to predict the wear of S390 high speed steel twist drills (TD) produced by powder metallurgy (PM), when drilling hardened steel. TD nominal diameter, sharpening mode, number of revolutions, feed rate and drilling length were used as input parameters and the mean value of the wear band width of the back surface

was used as output parameter. Kaya *et al.* [3] presented an effective and efficient model for assessing cutting tool wear when milling the Inconel 718 superalloy, based on ANN. The model trained with components of cutting force in three axes, torque, conditions and cutting time showed a very good correlation between actual and predicted values of tool wear. Also in milling operations, Wu *et al.* [4] compared three machine learning algorithms, including ANNs, SVR, and RFs in predicting tool wear. Performance measures include mean square error, R square, and training time. A number of statistical characteristics have been extracted from cutting forces, vibrations, and acoustic emissions. A similar study using a Response Surface Methodology (RSM), a genetic algorithm (GA) and a Grey Wolf Optimizer (GWO) algorithm to predict surface roughness in ball-end nose milling of hardened steel was conducted by Sekulic *et al.* [5]. Two modeling techniques, RSM and ANN, have been used to develop R_a and *VB* predictive models in turning and their predictive capabilities have been compared in a study by Tamang *et al.* [6]. Netoa *et al.* [7] used two types of ANN to assess the diameter of precision drilled holes in aluminum and titanium alloys. The input parameters were signals of acoustic emission, power and cutting force and vibration. Rao *et al.* [8] used ANN to predict the surface roughness, the tool wear and the workpiece vibration amplitude drilling AISI 316 steel, and their input parameters were tool tip radius, cutting speed, feed rate and the amount of material removed. The application of ANN [9] resulted in a model for monitoring the wear condition depending on the acoustic emission signal. By applying ANN, Kannan *et al.* [10] have monitored the roughness of the machined surface as a function of the influencing parameters when drilling brass plates and have developed a model for monitoring drill wear with optimisation of feed rate, cutting speed, thrust and torque. Benkedjouh *et al.* [11] formed a model for assessing tool condition and predicting its lifetime, based on the properties obtained from the control signals and the support of vector regression to assess and predict tool wear. Drouillet *et al.* [12] developed an ANN-based model for predicting the remaining tool life based on the value of the measured power of the spindle when milling stainless steel workpieces at different cutting speeds. D'Addona *et al.* [13] showed that ANN is a reliable method for monitoring the wear of drill based on the analysis of vibration signals. Patra *et al.* [14] developed an ANN model to predict the number of drill holes based on axial force, cutting speed, drill spindle speed and feed rate. Khorasani and Yazdi [15] developed a general dynamic ANN system for monitoring surface roughness when milling Al 7075 and St 52 using cutting speed, feed rate, material type, coolant, vibration and noise as input parameters. Mikołajczyk *et al.* [16] confirmed that a useful industrial tool for assessing tool life in turning by combining image recognition software and ANN. Wang and Jia [17] developed ANN to express thrust force and delamination factor as a function of drilling parameters. Multi-objective optimization of drilling parameters is than performed based on NSGA-II. In the research of Kumar and Hynes [18] the ANFIS model has been used for predicting surface roughness of drilled galvanized steel, while optimization was performed using the GA method. In Mondal *et al.* [19] the minization of burr formation in drilling process was performed with the application of regression modeling and ANN. In the work of Schorr *et al.* [20] an approach to predict the quality of drilled and reamed bores was presented. The machine learning method of random forest was used to predict the concentricity and the diameter of the bores on the basis of the torque measurements. Yin *et al.* [21] have established the model by backpropagation ANN for the prediction of microhole diameters and hole roundness in laser drilling.

The importance of predicting tool wear at different cutting conditions, possible limitations of regression analysis and the increasing use of ANN in tool condition prediction were the challenges for this research. The aim of the research was to develop a model for a comprehensive prediction of tool wear of TDs as a function of a number of influencing parameters for drill lengths up to the point when TD became worn. Axial force and torque by drilling were chosen as a target function. Both provide the most reliable information about tool wear that can be measured during the cutting process. The input parameters for ANNs were: the material of the TD, sharpening mode and nominal diameter *d*, number of revolutions *n*, feed rate *s* and achieved drilling length L_{max}. The attempt to create the desired model by applying a complex ANN did not lead to a satisfactory result; therefore the idea was to form a family of simple ANNs (FANN).

2. Materials and methods

In order to create a model for predicting the TD condition, backpropagation was performed using ANNs. The modeling was based on the determined correlations between the target functions (drilling force and torque) and the influencing parameters by drilling of quenched and tempered alloy steel 42CrMo4 (43-45 HRC). In the experiments, twist drill bits (DIN 338) made of high-speed steel with increased Co content were used, which were produced in the conventional metallurgical process (C) or in the powder metallurgical process (PM), regularly sharpened with a corrected main cutting blade (CMB) or ground crosswise (CL), see Table 1.

The workpiece dimensions (thickness) were adjusted so that the bore length of $L = 3d$ mm is maintained with uniform distribution of the workpiece hardness over the longitudinal and cross section. The cutting conditions were adjusted to the recommendations for drilling hardened steel.

For cooling and lubrication the 8 % solution of Teolin H/VR in the amount of 1 l/min was used. Axial force and torque were measured with the three-component dynamometer "Kistler", TYP 8152B2, in the range from 100 to 900 kHZ, integrated in the conventional drilling machine TYP FGU-32 and connected to a Global Lab software for data acquisition, as illustrated in Fig. 1. The initial experiment was conducted with four repetitions of drilling tests in the central point according to the matrix plan for three-factor experiment shown in Table 2.

Table 1 Tool material and sharpening modes for TDs

Influential parameters	
Cutting tool material	High-speed steel with 8 % Co, produced in conventional metallurgy process, S2-9-1-8, (C)
	High-speed steel with 8 % Co, produced in powder metallurgy, S390 MICROCLEAN, (PM)
Sharpening mode of drills	Regular with corrected main blade (CMB)
	Cross-like (CL)
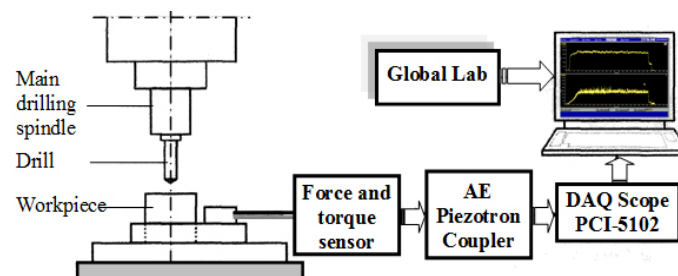
Fig. 1 Set-up for measurement of axial force and torque in drilling [1]

Table 2 Matrix plan of three-factor experiment [1]

Experimental points	Coded values			Real values			Output vectors
	x_1	x_2	x_3	d [mm]	n [rpm]	s [mm/rev]	F_a, M
1	-1	-1	-1	6.0	250	0.027	F_1, M_1
2	+1	-1	-1	10.0	250	0.027	F_2, M_2
3	-1	+1	-1	6.0	500	0.027	F_3, M_3
4	+1	+1	-1	10.0	500	0.027	F_4, M_4
5	-1	-1	+1	6.0	250	0.107	F_5, M_5
6	+1	-1	+1	10.0	250	0.107	F_6, M_6
7	-1	+1	+1	6.0	500	0.107	F_7, M_7
8	+1	+1	+1	10.0	500	0.107	F_8, M_8
9	0	0	0	7.75	355	0.053	F_9, M_9
10	0	0	0	7.75	355	0.053	F_{10}, M_{10}
11	0	0	0	7.75	355	0.053	F_{11}, M_{11}
12	0	0	0	7.75	355	0.053	F_{12}, M_{12}

Based on the matrix plan, measurement of the axial force and the torque for the particular experiment was performed at five measuring points for both tool materials and both sharpening modes. The first measurement was performed while drilling $L = 3d$ mm deep holes with sharp

TD, while the fifth measurement was performed when the drilling lengths were reached, whereby the following predefined maximum allowed flank wear values (h_{max}) for different TD were reached:

- for TD Ø6.0 mm – h_{max} = 0.25 mm,
- for TD Ø7.75 mm – h_{max} = 0.30 mm,
- for TD Ø10.0 mm – h_{max} = 0.35 mm.

The other three measurements were performed upon achievement of the drilling lengths whereat the flank wear of TD remained within the interval $0 < h_i < h_{max}$, and i = 2, 3, 4.

Under different experimental conditions (material of TD, sharpening mode, nominal diameter, number of revolutions and feed rate), TD reached the maximum allowed flank wear at different drilling lengths, as shown in Table 3.

Based on the measurement results of all the TD used in the experiments, diagrams for the axial force and the torque as a function of the drilling length and the cutting regime were generated.

Table 3 Drilling lengths at which drills achieved maximum allowable wear

No.	Drills mate-rial	Sharpe-ning mode	d [mm]	n [rpm]	s [mm/rev]	L_{max} [mm]	No.	Drills mate-rial	Sharpe-ning mode	d [mm]	n [rpm]	s [mm/rev]	L_{max} [mm]
1			6.0	250	0.027	560	25			6.0	250	0.027	630
2			10.0	250	0.027	750	26			10.0	250	0.027	1420
3			6.0	500	0.027	1325	27			6.0	500	0.027	3050
4			10.0	500	0.027	3250	28			10.0	500	0.027	3020
5			6.0	250	0.107	1330	29			6.0	250	0.107	1550
6		CMB	10.0	250	0.107	1050	30		CMB	10.0	250	0.107	2400
7			6.0	500	0.107	3000	31			6.0	500	0.107	4650
8			10.0	500	0.107	800	32			10.0	500	0.107	720
9			7.75	355	0.053	1730	33			7.75	355	0.053	1755
10			7.75	355	0.053	2370	34			7.75	355	0.053	1220
11			7.75	355	0.053	1920	35			7.75	355	0.053	1520
12	S390		7.75	355	0.053	1870	36	S 2-9-1-8		7.75	355	0.053	1480
13			6.0	250	0.027	1300	37			6.0	250	0.027	610
14			10.0	250	0.027	1000	38			10.0	250	0.027	1100
15			6.0	500	0.027	2700	39			6.0	500	0.027	3690
16			10.0	500	0.027	5075	40			10.0	500	0.027	5800
17			6.0	250	0.107	1400	41			6.0	250	0.107	4200
18		CL	10.0	250	0.107	2000	42		CL	10.0	250	0.107	3820
19			6.0	500	0.107	2260	43			6.0	500	0.107	5850
20			10.0	500	0.107	900	44			10.0	500	0.107	800
21			7.75	355	0.053	2650	45			7.75	355	0.053	2750
22			7.75	355	0.053	2530	46			7.75	355	0.053	2340
23			7.75	355	0.053	2650	47			7.75	355	0.053	2400
24			7.75	355	0.053	2850	48			7.75	355	0.053	2440
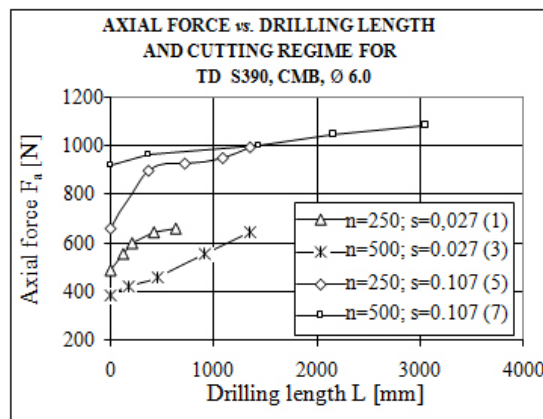
Fig. 2 Axial force *vs.* drilling length and cutting regime for TD S390, CMB, Ø6.0
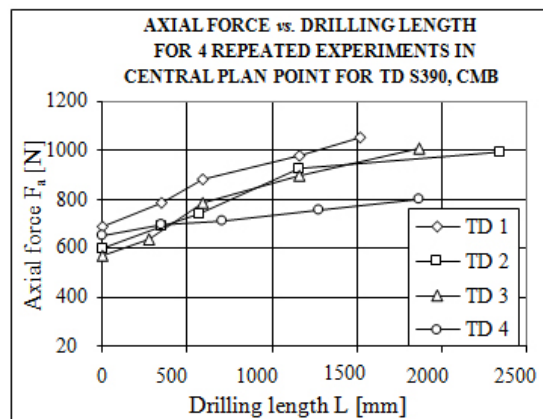
Fig. 3 Axial force *vs.* drilling length for 4 repeated experiments in central plan point (d_4 = 7.75 mm, n_5 = 355 rpm, s_5 = 0.053 mm/rev) for TD S390, CMB

The axial force F_a as a function of the drilling length L for TD Ø6.0 mm, made of S390 PM steel, regularly sharpened (CMB), is shown in Fig. 2 and for TD in the central plan point (d_4 = 7.75 mm, n_5 = 355 rpm, s_5 = 0.053 mm/rev) in Fig. 3. The diagrams show that all the different factors (material of twist drill bits, sharpening mode and cutting regime) had a significant influence on the axial force F_a.

3. Results and discussion

As far as the defined correlation curves are concerned, the trend curves and polynomial equations were defined for their interpretation, thus providing sufficient data sets for the ANN output parameters. After the data research in ANN the tool condition prediction application, a feed-forward back propagation ANN training was conducted in the MATLAB 6.0 software package. The training was performed with six input parameters, three of which were parameters of the cutting regime (nominal diameter d, number of revolutions n, and feed rate s), material type of TD, sharpening mode and drilling length l, and two output parameters – axial drilling force F_a and torque M, as shown in Fig. 4.

What follows is a selection of parameters amongst those offered in back propagation ANN training within MATLAB software package:

1. Training function
2. Adaption learning function
3. Performance function
4. Number of epochs
5. Number of neuron layers, and for each neuron layer
   5.1 Number of neurons in a layer
   5.2 Transfer function
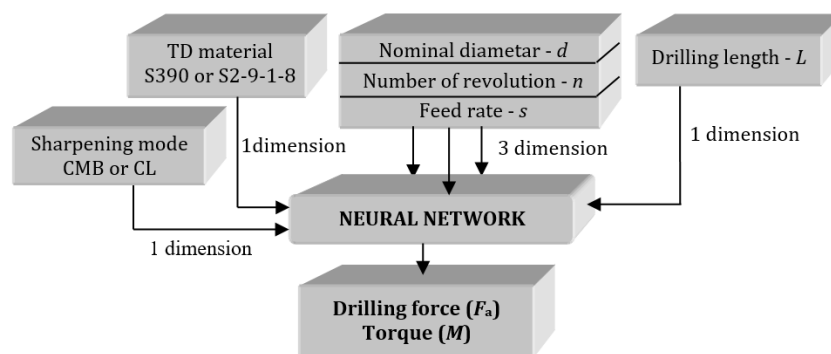
Fig. 4 Complex ANN training scheme [22]

As one of the ways to improve generalization during ANN training, it is suggested to surround each element of the trained family with a low noise level. By applying the above mentioned method, the ANN trainees approached a training error of less than 10^{-10}. After ANN training, it was checked (simulated) with the data relevant to the experiment, but was not used in the training process. However, the simulation of the trainees ANN did not yield the expected results, which indicates that it is impossible to efficiently process a large amount of data for the cutting process using the usual approach with ANN multiple inputs and outputs. This again confirms the fact that predicting the tool condition, which depends on numerous influential parameters, is a delicate matter. The trained ANN had a poor generalization due to the occurrence of the following phenomena:

- depending on the type of TD material, the sharpening mode and the cutting regime (nominal diameter, number of revolutions and feed rate), TD reached the maximum wear at different drilling lengths, as shown in Fig. 2 and Table 3;
- wide dispersion of axial drilling force and torque depending on the type of TD material, sharpening mode and cutting regime; and

- the same type of TD material, the same sharpening mode and the same cutting conditions (nominal diameter, number of revolutions and feed rate) together with different drilling lengths (changing only one of the input parameters while keeping the others constant) are an additional disadvantage for ANN.

3.1 Formation of the family of neural networks (FANN)

Since the trained ANN did not achieve the research goal set for the reasons worked out, the following idea came up: Instead of training a complex ANN with 6 input parameters and axial drilling force F_a and torque M as output parameters, the training of a family of simple ANNs should be carried out with two variable parameters, one of which would always be the drilling length L, while the axial drilling force F_a would be the output parameter.

The formation of a FANN was performed for TD material – PM (high-speed steel produced in powder metallurgy process) and sharpening mode – CBM (regular with corrected main cutting edge), where one of the parameters of the cutting regime (d, n and s) and the drilling length L were variable values, while the combination of the other two parameters was assumed to be constant. As shown in Fig. 5, the formation of FANN (ANNs training) was organised in several phases. In Phase I, the nominal diameter of the TD involved in the experiment ($d_1 = 6.0$ mm and $d_2 = 10.0$ mm) and drilling length L were taken as variables, while the combinations of the following parameters involved in the experiment: type of TD material, sharpening mode, number of revolutions and feed rate, were taken as constant values. Over the course of Phase I, simulation of the trained ANN was performed for nominal TD diameters of $6.0 < d_n < 10.0$ mm ($d_3 = 7.0$, $d_4 = 7.75$ and $d_5 = 9.0$ mm) and drilling length of $L = 0$-2.000 mm.
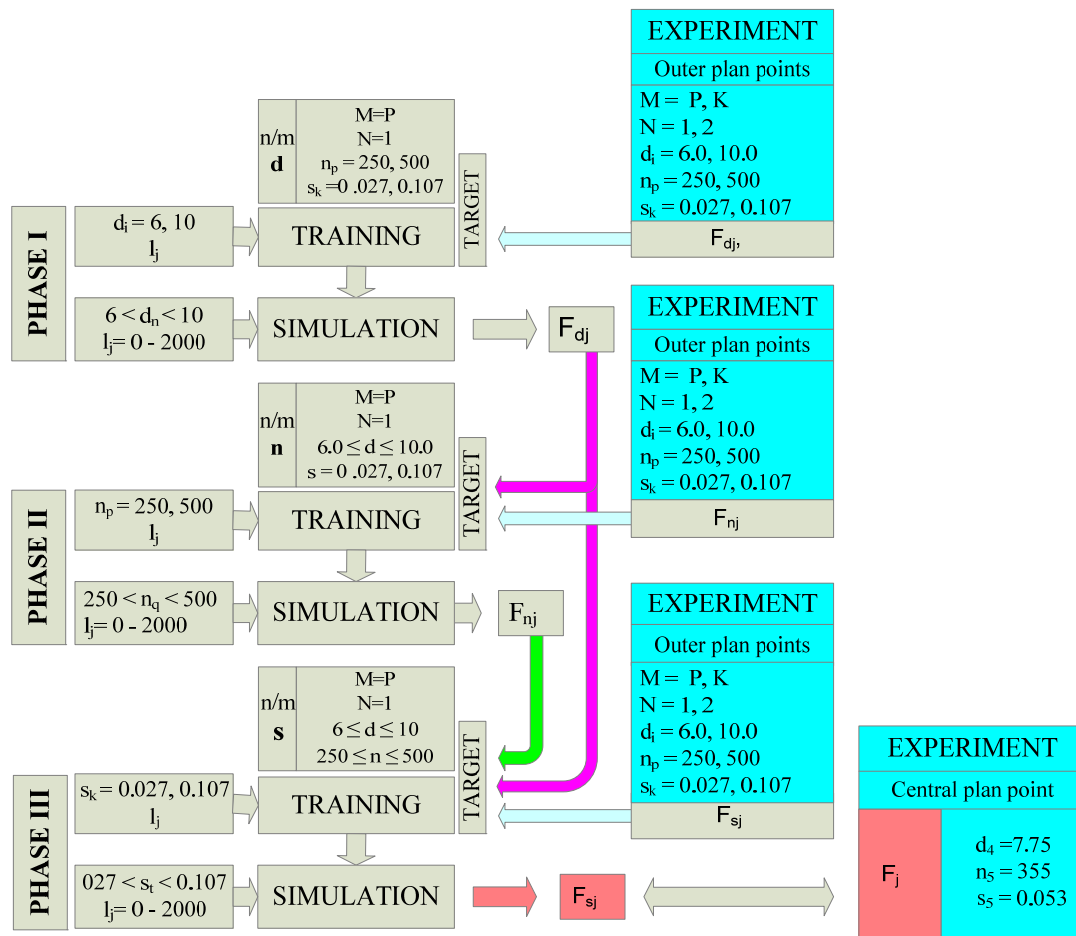
Fig. 5 Development of a family of simple ANNs

During Phase II of ANN formation, values for the number of revolutions n involved in the experiment (n_1 = 250 and n_2 = 500 rpm) and the drilling length L were taken as the variable parameters, while the constant values contained combinations of the following parameters: TD material, sharpening mode and feed rate (s_1 = 0.027 and s_2 = 0.107 mm/rev), and the TD diameters for which the values of the axial forces had been obtained by experimenting and simulating the ANN formed in Phase I ($6.0 \leq d \leq 10.0$ mm). The simulation of ANN in Phase II was performed with the standard number of revolutions within the range $250 < n_q < 500$ (n_3 = 280, n_4 = 315, n_5 = 355, n_6 = 400 and n_7 = 450 rpm) and the drilling length L expressed in mm.

In Phase III, values of the feed rate (s_1 = 0.027 and s_2 = 0.107 mm/rev) and the drilling length L were taken as variable parameters, while the constant values comprised combinations of the following parameters: TD material, sharpening mode, diameters within the range of $6.0 \leq d \leq 10.0$ mm (for which the values of axial force F_a had been obtained by experimenting and simulation of the ANN in Phase I), and standard number of revolutions within the range of $250 \leq n \leq 500$ rpm (for which the values of axial force F_a had been obtained by experimenting and simulation of the ANN in Phase II). The simulation of a trained ANN in Phase III was performed with the standard feed rate within the interval of $0.027 < s_t < 0.107$ (s_3 = 0.033, s_4 = 0.042, s_5 = 0.053, s_6 = 0.067 and s_7 = 0.084 mm/rev) and the drilling length L. The axial drilling force F_a, expressed in N, was chosen as the output parameter of all ANNs.

In Phase I of the FANN formation, only those ANNs were trained which were involved in the experiment with the factor values d_i, n_p and s_k, i.e. the ANN: n11, n21, n12 and n22.
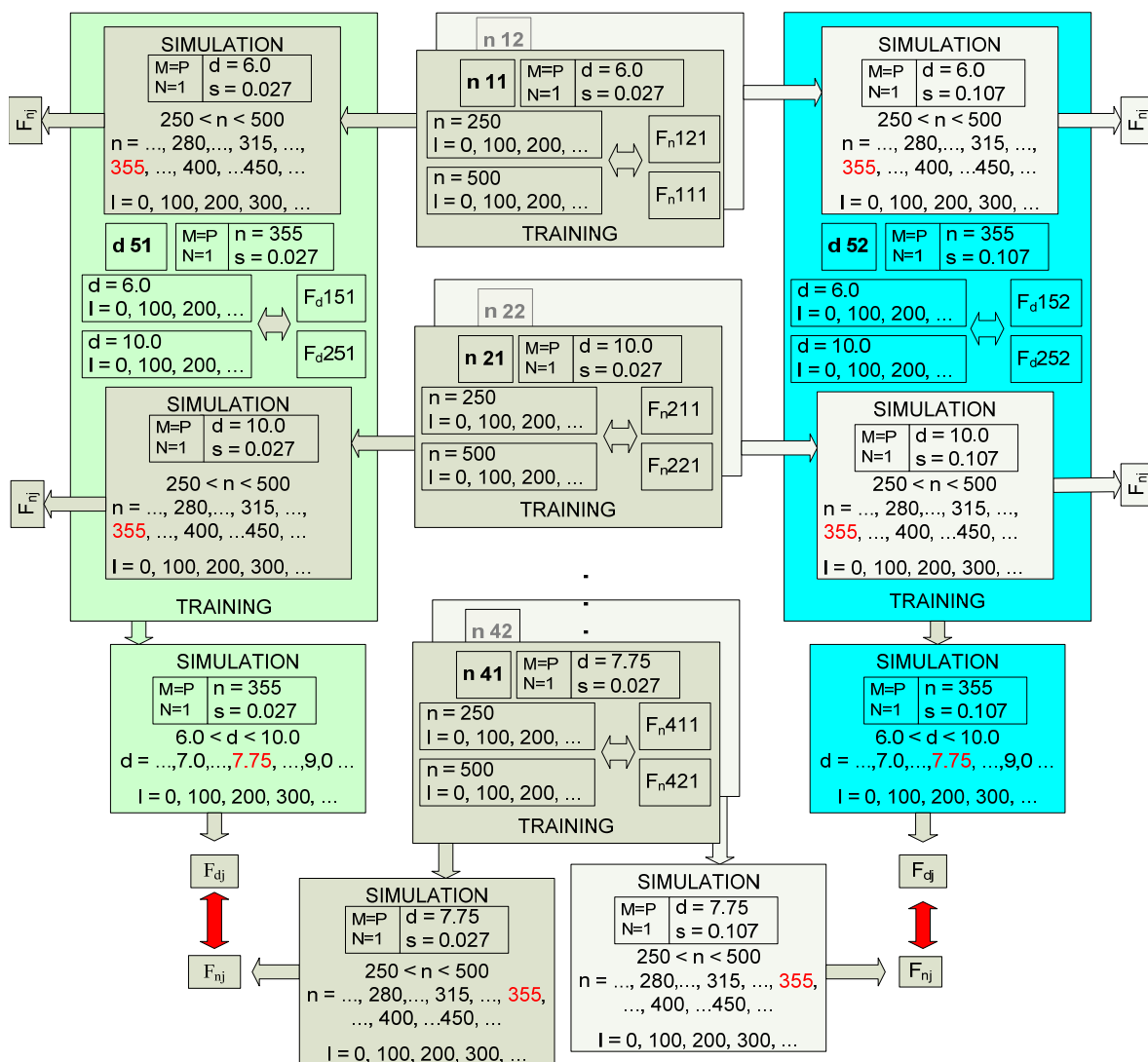
Fig. 6 First model of Phase II of FANN formation

In Phase II, besides the ANN trained with the values of parameters involved in the experiment (n11, n21, n12 and n22), the following ANNs were formed: n41 (n_1 = 250 and n_2 = 500 rpm; d_4 = 7.75 mm; s_1 = 0.027 mm/rev) and n42 (n_1 = 250 and n_2 = 500 rpm; d_4 = 7.75 mm; s_2 = 0.107 mm/rev), as well as control ANNs d51 (d_1 = 6.0 and d_2 = 10.0 mm; n_5 = 355 rpm; s_1 = 0.027 mm/rev) and d52 (d_1 = 6.0 and d_2 = 10.0 mm; n_5 = 355 rpm; s_2 = 0.107 mm/rev), as shown in Fig. 6. The values of the axial force F_a for combinations of influencing parameters of the mentioned ANN were obtained by simulation of ANN in Phase I or by ANN from Phase II, which was trained with the factor values involved in the experiment.

The results of the simulation of ANN n41 for n_5 = 355 rpm (d_4 = 7.75 mm and s_1 = 0.027 mm/rev) shall be consistent with the results of the simulation of control ANN d51 for d_4 = 7.75 mm (n_5 = 355 rpm and s_1 = 0.027 mm/rev), while the results of simulation of ANN n42 for n_5 = 355 rpm shall be consistent with the results of the simulation of the control ANN d52 for d_4 = 7.75 mm.

In Phase III, in addition to the ANNs trained with the factor values involved in the experiment (s11, s21, s12 and s22), the following ANNs were formed: s41 (s_1 = 0.027 and s_2 = 0.107 mm/rev; d_4= 7.75 mm; n_1 = 250 rpm) and s42 (s_1 = 0.027 and s_2 = 0.107 mm/rev; d_4 = 7.75 mm; n_2 = 500 rpm), and the control ANNs d15 (d_1 = 6.0 and d_2 = 10.0 mm; n_1 = 250 rpm; s_5 = 0.053 mm/rev) and d25 (d_1 = 6.0 and d_2 = 10.0 mm; n_2 = 500 rpm; s_5 = 0.053 mm/rev). The values of the axial force F_a for combinations of influencing parameters from the above stated ANNs were obtained by simulating the ANNs from the Phase II, i.e. ANNs of the Phase III which had been trained with the factor values involved in the experiment (s11, s21, s12 and s22). The results of the simulation of ANN s41 for s_5 = 0.053 mm/rev (d_4 = 7.75 mm and n_1 = 250 rpm) must correspond to the results of the simulation of ANN d15 for d_4 = 7.75 mm (n_1 = 250 rpm and s_5 = 0.053 mm/rev), while the results of the simulation of ANN s42 for s_5 = 0.053 mm/rev (d_4 = 7.75 mm and n_2 = 500 rpm) must correspond to those of the simulation of ANN d25 for d_4 = 7.75 mm.

In addition to those ANNs specified in the fifth model in Phase III, the following ANNs were also formed: s15 (s_1 = 0.027 and s_2 = 0.107 mm/rev, d_1 = 6.0 mm and n_5 = 355 rpm), s25 (s_1 = 0.027 and s_2 = 0.107 mm/rev, d_2 = 10.0 mm and n_5 = 355 rpm), s45 (s_1 = 0.027 and s_2 = 0.107 mm/rev; d_4 = 7.75 mm and n_5 = 355 rpm) and control ANNs d55 (d_1 = 6.0 and d_2 = 10.0 mm; n_5 = 355 rpm and s_5 = 0.053 mm/rev) and in the control model also n45 (n_1 = 250 and n_2 = 500 rpm; d_4 = 7.75 mm; s_5 = 0.053 mm/rev), for which the values of the axial force F_a have been obtained by simulating the ANNs from previous phases, as shown in Fig. 7.
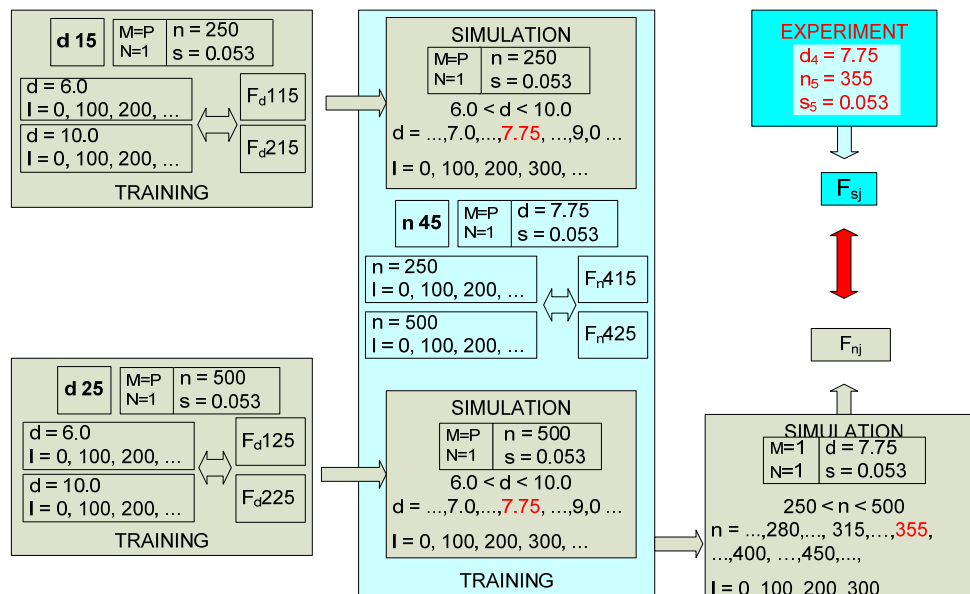
Fig. 7 Control model of FANN formation

Results of the simulation of ANN d55 for d_4 = 7.75 mm (n_5 = 355 rpm, s_5 = 0.053 mm/rev); s45 for s_5 = 0.053 mm/rev (d_4 = 7.75 mm, n_5 =355 355 rpm) and n45 for n_5 = 355 rpm (d_4 = 7.75 mm, s_5 = 0.053 mm/rev) must correspond both to each other and to the results of the experiment in the central plan point (d_4 = 7.75 mm; n_5 = 355 rpm and s_5 = 0.053 mm/rev).

The first training of the ANNs was performed at the outer points of the experiment, using the values of axial force obtained by the experiment as input parameters. The formation of the sequence of ANNs was continued towards the central point of the plan, as shown in Fig. 8, so that the final training was performed in the central point of the plan. As output parameters the values of axial force F_a obtained by the simulation of the ANNs in the previous phases were used.

The values of the axial drilling force F_a as a function of the drilling length and the influencing parameters (type of TD material, sharpening mode, nominal diameter, number of revolutions and feed rate), which were obtained by the simulation of trained ANNs can be graphically displayed, as shown in Figs 9. and 10. Fig. 9. shows the values of the axial force F_a as a function the drilling length obtained by the simulation of ANN d11 (M = PM, SM = CMB, n_1 = 250 rpm, s_1 = 0.027 mm/rev) at the nominal diameters of drills d_3 = 7.0; d_4 = 7.75 and d_5 = 9.0 mm in relation to the values of the axial force determined in the experiment for drills with nominal diameter d_1 = 6.0 and d_2 = 10.0 mm.
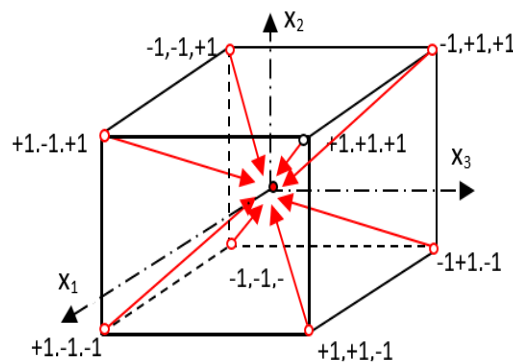
Fig. 8 Direction of development of ANNs
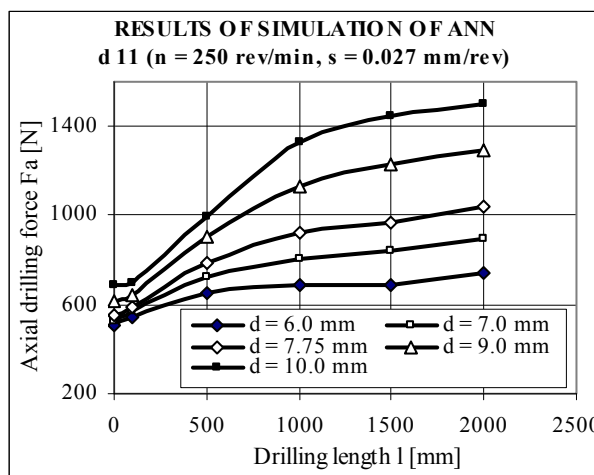
Fig. 9 Results of simulation of ANN d 11
(n_1 = 250 rev/min, s_1 = 0.027 mm/rev)
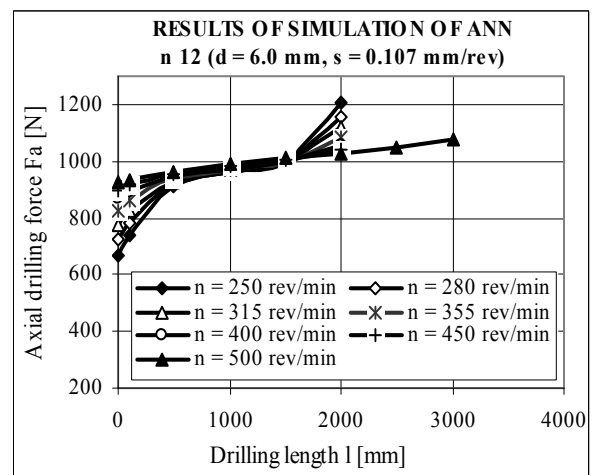
Fig. 10 Results of simulation of ANN n 12
(d_1 = 6.0 mm, s_2 = 0.107 mm/rev)

Fig. 10 shows the values of the axial force F_a as a function of the drilling length obtained by simulating ANN n12 (M = PM, SM = CMB, d_1 = 6.0 rpm, s_2 = 0.107 mm/rev) for the number of revolutions n_3 = 280; n_4 = 315, n_5 = 355, n_6 = 400 and n_7 = 450 rpm, in relation to the value of the axial force at the number of revolutions n_1 = 250 and n_2 = 500 rpm obtained in the experiment. The same principle can be applied to represent the values of axial force as a function of drilling length obtained by simulating others ANNs within the family formed.

Comparison values of the axial drilling force, which were obtained by simulating ANN n41 for n_5 = 355 rpm (d_4 = 7.75 mm, s_1 = 0.027 mm/rev) and control ANN d51 for d_4 = 7.75 mm (n_5 = 355 rpm, s_1 = 0.027 mm/rev) are shown in Fig. 11, while those for ANN s42 for s_5 = 0.053 mm/rev (d_4 = 7.75 mm, n_2 = 500 rpm) and control ANN d25 for d_4 = 7.75 mm (n_2 = 500 rpm, s_5 = 0.053 mm/rev) are shown in Fig. 12. The diagrams show that the results of simulation of control ANN d51 correspond to the results of simulation of ANN n41 with a maximum deviation of 3.14 % for L = 500 mm (Fig. 11), while the results of simulation of control ANN d25 correspond to the results of simulation of ANN s42 with a maximum deviation of 3.95 % for L = 2000 mm (Fig. 12).

The same principle can be used to represent comparative values of axial force obtained by simulation of ANN n42 and control ANN d52 as well as ANN s41 and control ANN d15.
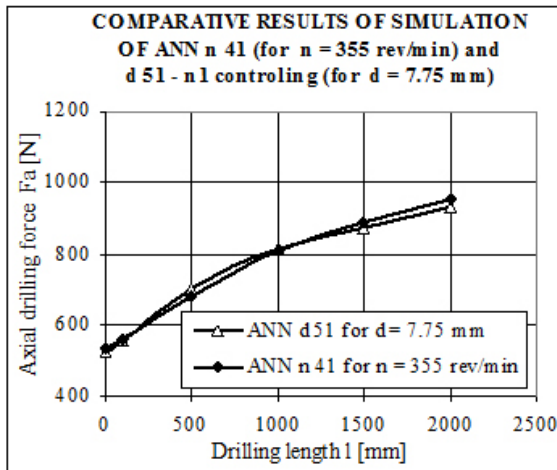
Fig. 11 Comparative results of simulation of ANN n 41 (for n_5 = 355 rpm) and d 51 – n 1 controlling (for d_4 = 7.75 mm)
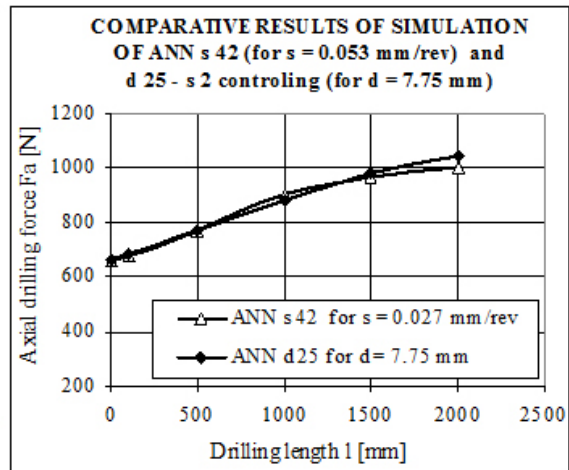
Fig. 12 Comparative results of simulation of ANN s 42 (for s_5 = 0.053 mm/rev) and d 25 – s 2 controlling (for d_4 = 7.75 mm)

The values of the axial drilling force F_a for four repeated experiments in the central plan point and their mean value are shown in Fig. 13. Comparative values of axial drilling force obtained by simulation of ANN s45 for s_5 = 0.053 mm/rev, the control ANN d55 for d_4 = 7.75 mm and n45 for n_5 = 355 rpm, and mean values of the experiments in the central plan point are shown in Fig. 14. The diagrams in Figs 13 and 14 show that the results of the simulation of ANN s45 for s_5 = 0.053 mm/rev and the control ANN d55 for d_4 = 7.75 mm, and n45 for n_5 = 355 rpm correspond to each other and lie within the interval comprising the values of three repeated experimental results in the central plan point.

The results of the fourth repeated experiment deviate both from the results of the other three repeated experiments and from the results obtained by simulating ANN. The comparison of the results of the simulation with the mean value of four experiment results in the central planning point reveals the following:

- the deviation of the results of the simulation of ANN s45 from the mean value of the experimental results is at most 6.598 % for L = 1000 mm;
- the deviation of the results of the simulation of the control ANN d55 from the results of the simulation of ANN s45 is at most 7.89 % for L = 0 mm and from the mean value of the experimental results for four repeated experiments is at most 9.7 % for L = 2000 mm, and
- the deviation of the results of the simulation of the control ANN n45 from the results of the simulation of ANN s45 is maximum 5.596 % and from average of four repeated experiments results maximum of 10.74 % for L = 1000 mm.

The results of the simulation of the ANN central plan point come even closer to the experimental results when compared with the mean value of three instead of all four repeated experiments.
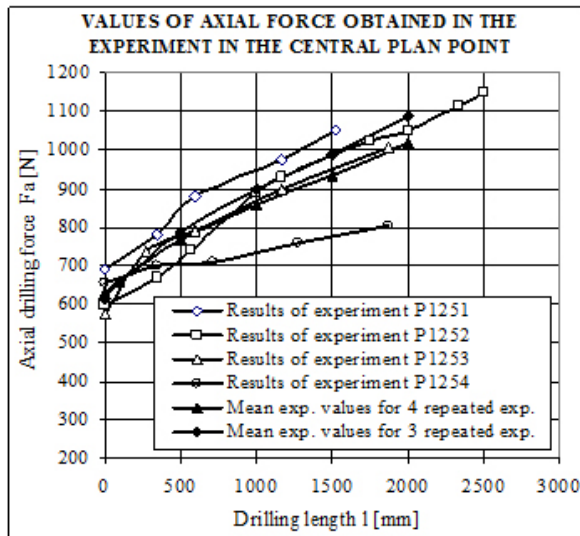
Fig. 13 Value of axial force for four repeated experiments in the central plan point
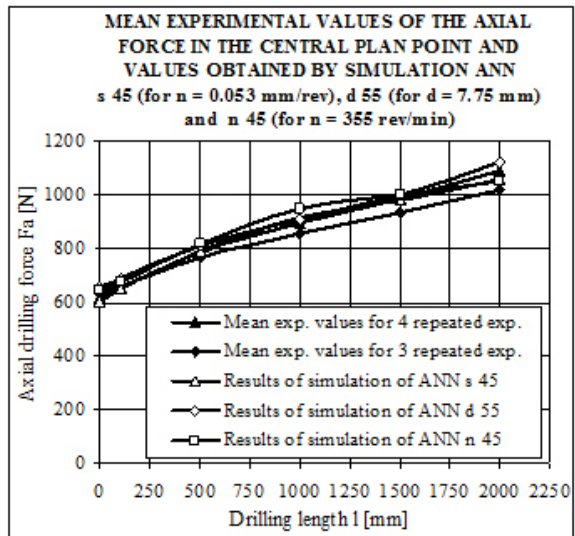
Fig. 14 Comparative values of axial force obtained by simulation of ANN s 45 (for s_5 = 0.053 mm/rev), d 55 (for d_4 =7.75 mm) and n 45 (for n_5 = 355 rev/min) as well as mean values of four, that is to say, three central point

3.2 Comparative analysis of the axial drilling force obtained by ANN and regression analysis

The comparative analysis of the values of the axial drilling force F_a obtained by ANN and regression analysis was performed for the following drilling lengths L = 100, 500 and 1000 mm.

The experimental values of the axial drilling force for the drilling lengths L = 100 mm, L = 500 mm and L = 1000 mm are shown in Table 4.

The axial drilling force F_a, as a target function, can be represented in the form of the complex exponentiation, shown by the Eq. 1.

$$F_a = C_F d^{b_1} n^{b_2} s^{b_3} \tag{1}$$

In order to obtain a regression model that describes which will describe the target function as accurately as possible with respect to Eq. 1, the incomplete second-order three-factor model (incomplete quadratic model) with constant coefficients was applied after completion of the linearization, as shown in Eq. 2.

Table 4 The experimental values of the axial drilling force

EXPERI-MENTAL POINTS	Coded values							Actual values			Experimental F_a values [N]		
	x_1	x_2	x_3	$x_1 x_2$	$x_1 x_3$	$x_2 x_3$	$x_1 x_2 x_3$	d [mm]	n [rpm]	s [mm/rev]	L=100 mm	L=500 mm	L=1000 mm
1	-1	-1	-1	1	1	1	-1	6.0	250	0,027	544,85	649,96	686.90
2	1	-1	-1	-1	-1	1	1	10.0	250	0,027	700,86	996,71	1325.30
3	-1	1	-1	-1	1	-1	1	6.0	500	0,027	401,11	464,31	564.24
4	1	1	-1	1	-1	-1	-1	10	500	0,027	654,23	717,83	768.65
5	-1	-1	1	1	-1	-1	1	6.0	250	0,107	740,32	909,58	959.71
6	1	-1	1	-1	1	-1	-1	10.0	250	0,107	1339,03	1716,27	1907.70
7	-1	1	1	-1	-1	1	-1	6.0	500	0,107	931,98	962,00	989.67
8	1	1	1	1	1	1	1	10.0	500	0,107	1329,16	1531,00	1727.44
9	0	0	0	0	0	0	0	7.75	355	0,053	720,56	838,55	950.36
10	0	0	0	0	0	0	0	7.75	355	0,053	615,73	736,10	870.26
11	0	0	0	0	0	0	0	7.75	355	0,053	633,70	784,84	873.20
12	0	0	0	0	0	0	0	7.75	355	0,053	667,50	703,69	736.60

$$y = b_0 + b_1 x_1 + b_2 x_2 + b_3 x_3 + b_{12} x_1 x_2 + b_{13} x_1 x_3 + b_{23} x_2 x_3 + b_{123} x_1 x_2 x_3 \tag{2}$$

The coding has been performed by the transformation Eq. 3:

$$x_1 = 2\frac{\ln(D)-\ln(D_{max})}{\ln(D_{max})-\ln(D_{min})} + 1 \,, \; x_2 = 2\frac{\ln(n)-\ln(n_{max})}{\ln(n_{max})-\ln(n_{min})} + 1 \text{ and } x_3 = 2\frac{\ln(s)-\ln(s_{max})}{\ln(s_{max})-\ln(s_{min})} + 1 \tag{3}$$

By applying the regression analysis, the coefficients of models for drilling lengths L =100, 500 and 1000 mm, have been obtained and shown in Table 5.

Based on the coefficients shown in Table 5 and the return to the original coordinates, the regression models of the target function (axial drilling force F_a) were obtained through the transformation Eq. 3. To obtain more accurate results, no verification of the significance of the parameters was performed, and no insignificant parameters were omitted, they were all retained in the model. The equation obtained in this way was used to calculate the values of the axial drilling force F_a. The comparison between results obtained by the ANN simulation and the regression model is shown in Table 6.

Table 5 Coefficients of the regression model

Drilling length	Coefficients of the model							
	b_0	b_1	b_2	b_3	b_{12}	b_{13}	b_{23}	b_{123}
$L = 100$	6.5943	0.2111	-0.0190	0.3132	-2.52E-05	0.0258235	0.074737	0.0747443
$L = 500$	6.7604	0.2454	-0.0903	0.2957	-0.02027	0.029545	0.075798	-0.0223
$L = 1000$	6.8742	0.2763	-0.1012	0.2588	-0.05976	0.034711	0.084119	0.027256

Table 6 Comparative values of the axial drilling force

Drilling length L [mm]	Cutting modes			Results of the experiment F_{eksp} [N]	Results of ANN simulation			Results of Regression analysis		Deviation F_{ANN} from F_{ra} [%]
	d [mm]	n [rpm]	s [mm/rev]		F_{ANN} [N]	Error [%]	ANN	F_{ra} [N]	Error [%]	
$L = 100$ mm	6.00	500	0.027	401.11	401.06	-0.012	d 21	380.97	-5.021	5.27
	7.75	250	0.027		590.19		d 11	587.07		0.53
	10.00	250	0.107	1339.03	1338.92	-0.008	d 12	1271.80	-5.021	5.28
	6.00	355	0.027		470.51		n 11	443.21		6.16
	7.75	355	0.027		555.65		n 41	533.99		4.06
					560.25		d 51			
	10.00	250	0.053		863.30		s 21	914.04		-5.55
	7.75	355	0.053	659.37 (middle)	646.89	-1.893	s 45	726.43	10.170	-10.95
					690.34	4.697	d 55			
					675.58	2.458	n 45			
$L = 500$ mm	10.00	500	0.027	717.83	717.86	0.004	d 21	676.18	-5.802	6.16
	10.00	355	0.027		868.87		n 21	795.24		9.26
	6.00	250	0.107	909.58	909.48	-0.011	d 12	856.81	-5.802	6.15
	7.75	250	0.107		1204.08		d 12	1177.71		2.24
	6.00	355	0.107		938.19		n 12	881.44		6.44
	7.75	500	0.053		768.35		s 42	782.88		-1.86
					770.99		d 25			
	7.75	355	0.053	765.80 (middle)	794.40	3.735	s 45	857.34	11.954	-7.34
					808.72	5.605	d 55			
					819.35	6.993	n 45			
$L = 1000$ mm	10.00	250	0.027	1325.30	1325.28	-0.002	d 11	1248.09	-5.826	6.18
	7.75	500	0.027		680.79		d 21	620.39		9.74
	7.75	355	0.027		813.38		n 41	745.24		9.14
					806.83		d 51			
	6.00	500	0.107	989.67	989.78	0.011	d 22	932.01	-5.826	6.20
	6.00	250	0.053		795.76		s 11	762.02		4.43
	10.00	500	0.053		1101.65		s 22	1076.25		2.36
	7.75	355	0.053	857.61 (middle)	914.19	6.598	s 45	961.28	12.089	-4.90
					905.26	5.557	d 55			
					949.72	10.741	n 45			

The comparison made revealed the following:

- The results obtained by simulation of the ANN at the points of experiment for all drilling lengths are fully are fully consistent with the experimental results with a maximum deviation of less than 0.025 %.
- For controlled drilling lengths (L = 100, 500 and 1000 mm), the maximum deviations of the results obtained by simulation of the ANN in the central plan point, if compared to the experimental results, are:
  – for ANN s45 - 6,598 % at drilling length L = 1000 mm;
  – for ANN d55 - 5.557 % at drilling length L = 1000 mm, and
  – for ANN n45 - 10.741 % at drilling length L = 1000 mm.
- For drilling lengths L = 100, 500 and 1000 mm, the values of the axial force obtained by regression analysis deviate from the experimental results as follows:
  In the points of experiment:
  – 5.022 % for L = 100 mm,
  – 5.802 % for L = 500 mm, and
  – 5.826 % for L = 1000 mm,
  and in the central plan point:
  – 10.17 % for L = 100 mm,
  – 11.954 % for L = 500 mm, and
  – 12.089 % for L = 1000 mm,
  which is significantly less favourable compared to the results obtained by the simulation of ANN.
- The results obtained by simulation of neural networks in the plan points which were not included in the experiment also correspond to the results obtained by regression analysis maximum deviation of less than 9.75 %.

The performed analyses of the results obtained by application of a family of ANNs and their comparison with the experimental results and the results obtained by mathematical modelling of multifactor plans show that prediction of tool condition, in conditions of non-linear dependency of the target function and influential parameters, can be additionally enhanced by application of a family of ANNs. Therefore, a family of ANNs can be applied very successfully in prediction of tool condition, in particular in cases of non-linear dependency of the target function and influential parameters when the regression analysis method fails to render satisfactory results and calls for further experimental research.

4. Conclusion

The prediction of tool condition is of high practical importance, since the (technological and economic) effects of the machining process depend directly on the tool life. However, considering that the machining process is a highly complex physico-chemical mechanism of interaction between tool and workpiece under the conditions of scatter of characteristics and properties of the elements of the technological system, modelling this process seems to be very difficult. The application of modern technologies aimed at solving the problems related to modeling, simulation and monitoring of the machining process has recently begun, and the most commonly used ANNs allow to predict changes in the parameters of interest as a function of changes in the input value.

In this paper the axial cutting force F_a was chosen as a target function, i.e. as a source of information about the amount of cutting tool wear. The influencing factors selected included the material of the tool (twist drill), the sharpening mode, the nominal diameter, the number of revolutions, the feed rate and the drilling length until the twist drills are worn out. Based on the established correlations between the target function and the influencing parameters for predicting the wear size of twist drills, a FANN was developed. The results of the prediction obtained by applying a FANN were compared with the results obtained by regression analysis in the experimental points. The comparison showed that the prediction results were consistent.

Furthermore, the prediction results obtained by applying a FANN deviate significantly less from the experimental results. Therefore, the developed model of FANN can be used as a very reliable method for predicting the state of the tool, especially in case of a nonlinear relationship between the target function and the parameters involved, and in cases where the regression analysis does not give satisfactory results and requires additional experimental research.

References

[1] Spaić, O., Krivokapić, Z., Ivanković R. (2013). Mathematical modelling of cutting force as the most reliable information bearer on cutting tools wearing phenomenon, *Journal of Mechanics Engineering and Automation (JMEA)*, Vol. 3, No. 12, 772-777.

[2] Krivokapić, Z., Zogović, V., Spaić O. (2006). Using neural netvorks to follow the wear of a 390 twist drill, *Strojniški vestnik – Journal of Mechanichal Engineering*, Vol. 52, No. 7-8, 437-442.

[3] Kaya, B., Oysu, C., Ertunc, H.M. (2011). Force-torque based on-line tool wear estimation system for CNC milling of Inconel 718 using neural networks, *Advances in Engineering Software*, Vol. 42, No. 3, 76-84, doi: 10.1016/j.advengsoft.2010.12.002.

[4] Wu, D., Jennings, C., Terpenny, J., Gao, R.X., Kumara, S. (2017). A comparative study on machine learning algorithms for smart manufacturing: Tool wear prediction using random forests, *Journal of Manufacturing Science and Engineering*, Vol. 139, 071018-1-071018-9, doi: 10.1115/1.4036350.

[5] Sekulic, M., Pejic, V., Brezocnik, M., Gostimirović, M., Hadzistevic, M. (2018). Prediction of surface roughness in the ball-end milling process using response surface methodology, genetic algorithms, and grey wolf optimizer algorithm, *Advances in Production Engineering & Management*, Vol. 13, No. 1, 18-30, doi: 10.14743/apem2018.1.270.

[6] Tamang, S.K., Chandrasekaran, M. (2015). Modeling and optimization of parameters for minimizing surface roughness and tool wear in turning Al/SiCp MMC, using conventional and soft computing techniques, *Advances in Production Engineering & Management*, Vol. 10, No. 2, 59-72, doi: 10.14743/apem2015.2.192.

[7] Neto, F.C., Gerônimo, T.M., Cruz, C.E.D., Aguiar, P.R., Bianchi, E.E.C. (2013). Neural models for predicting hole diameters in drilling processes, *Procedia CIRP*, Vol. 12, 49-54, doi: 10.1016/j.procir.2013.09.010.

[8] Rao, K.V., Murthy, B.S.N., Rao, N.M. (2014). Prediction of cutting tool wear, surface roughness and vibration of work piece in boring of AISI 316 steel with artificial neural network, *Measurement*, Vol. 51, 63-70, doi: 10.1016/j.measurement.2014.01.024.

[9] Martins, C.H.R., Aguiar, P.R., Frech, A., Bianchi, E.C. (2014). Tool condition monitoring of single-point dresser using acoustic emission and neural networks models, *IEEE Transactions on Instrumentation and Measurement*, Vol. 63, No. 3, 667-679, doi: 10.1109/TIM.2013.2281576.

[10] Kannan, T.D.B., Kannan, G.R., Umar, M., Kumar, S.A. (2015). ANN approach for modelling parameters in drilling operation, *Indian Journal of Science and Technology*, Vol. 8, No. 22, doi: 10.17485/ijst/2015/v8i22/79097.

[11] Benkedjouh, T., Medjaher, K. , Zerhouni, N., Rechak, S. (2015). Health assessment and life prediction of cutting tools based on support vector regression, *Journal of Intelligent Manufacturing*, Vol. 26, No. 2, 213-223, doi: 10.1007/s10845-013-0774-6.

[12] Drouillet, C., Karandikar, J., Nath, C. , Journeaux, A.-C., El Mansori, M., Kurfess, T. (2016): Tool life predictions in milling using spindle power with the neural network technique, *Journal of Manufacturing Processes,* Vol 22, 161-168, doi: 10.1016/j.jmapro.2016.03.010.

[13] D'Addona, D.M., Matarazzo, D., de Aguiar, P.R., Bianchi, E.C., Martins, C.H.R. (2016). Neural networks tool condition monitoring in single-point dressing operations, *Procedia CIRP*, Vol. 41, 431-43, doi: org/10.1016/j.procir.2016.01.001.

[14] Patra, K., Jha, A.K., Szalay, T., Ranjan, J., Monostori, L. (2017). Artificial neural network based tool condition monitoring in micro mechanical peck drilling using thrust force signal, Precision Engineering, Vol. 48, 279-291, doi: org/10.1016/j.precisioneng.2016.12.011.

[15] Khorasani, A.M., Yazdi, M.R.S. (2017). Development of a dynamic surface roughness monitoring system based on artificial neural networks (ANN) in milling operation, *The International Journal of Advanced Manufacturing Technology*, Vol. 93, 141-151, doi: 10.1007/s00170-015-7922-4.

[16] Mikołajczyk, T., Nowicki, K., Bustillo, A., Yu Pimeno, D. (2018). Predicting tool life in turning operations using neural networks and image processing, *Mechanical Systems and Signal Processing*, Vol. 104, 503-513, doi: 10.1016/j.ymssp.2017.11.022.

[17] Wang, Q., Jia, X. (2020). Multi-objective optimization of CFRP drilling parameters with a hybrid method integrating the ANN, NSGA-II and fuzzy C-means, *Composite Structures,* Vol. 235, 111803, doi: 10.1016/j.compstruct.2019.111803.

[18] Kumar, R., Hynes, N.R.J. (2020). Prediction and optimization of surface roughness in thermal drilling using integrated ANFIS and GA approach, *Engineering Science and Technology, an International Journal*, Vol. 23, Vol. 1, 30-41, doi: 10.1016/j.jestch.2019.04.011.

[19] Mondal, N., Mandal, S., Mandal, M.C. (2020). FPA based optimization of drilling burr using regression analysis and ANN model, *Measurement,* Vol. 152, 107327, doi: 10.1016/j.measurement.2019.107327.

[20] Schorr, S., Möller, M., Heib, J., Bähre, D. (2020). Quality prediction of drilled and reamed bores based on torque measurements and the machine learning method of random forest, *Procedia Manufacturing*, Vol. 48, 894-901, doi: 10.1016/j.promfg.2020.05.127.

[21] Yin, C.P., Wu, Z.P., Dong, Y.W., You, Y.C., Liao, T. (2019). Femtosecond laser helical drilling of nickel-base single-crystal super-alloy: Effect of machining parameters on geometrical characteristics of micro-holes, *Advances in Production Engineering & Management*, Vol. 14, No. 4, 407-420, doi: 10.14743/apem2019.4.337.

[22] Spaić, O. (2017). *Teorija rezanja*, Univerzitet u Istočnom Sarajevu, Fakultet za proizvodnju i menadžment Trebinje, Trebinje, Bosnia and Herzegovina.

Fuel gas operation management practices for reheating furnace in iron and steel industry

Chen, D.M.[a,b]**, Liu, Y.H.**[a]**, He, S.F.**[c]**, Xu, S.**[c]**, Dai, F.Q.**[b]**, Lu, B.**[a,*]

[a]School of Civil Engineering and Architecture, Anhui University of Technology, Ma'anshan, P.R. China
[b]The State Key Laboratory of Refractories and Metallurgy, Wuhan University of Science and Technology, Wuhan, P.R. China
[c]Ma'anshan iron and Steel Co., Ltd, Ma'anshan, Anhui, P.R. China

A B S T R A C T

How to evaluate the fuel gas operation (FGO) of various working groups (WGs) and working shifts (WSs) in reheating furnace is still ambiguous problem. In this paper, a novelty time-series FGO evaluation model was proposed. The strategy mainly included: Firstly, the fuel gas per ton steel (FGTS) was calculated in certain time interval; Secondly, the FGTS time-series data set was formulated in statistical period; Thirdly, the FGTS time-series data set was divided according to working schedule; Lastly, the FGO evaluation model was established. Case study showed that: i) The fuel gas operation evaluation results of various WGs in different WSs were accorded with normal distribution; ii) For various WGs, A WG performed best, followed by C WG and D WG. The performance of B WG was the worst due to its violent fluctuation of fuel gas operation evaluation results in three WSs; iii) For different WSs, the day WS and swing WS performed well, whereas the performance of night WS was unsatisfactory. Discussion results showed that the improvement of working skills, working responsibility and working passion, which were effective measure to achieve energy saving in terms of operation, should be enhanced through skills training and the reward and punishment system. Generally, this novelty time-series FGO evaluation method could also be applied to other industrial equipment.

1. Introduction

The iron and steel industry, whose products are widely used in various industries, is the pillar of the manufacturing industry [1]. Therefore, the development of iron and steel industry (whether technological innovation or economic operation) has attracted much attention of many scholars from different countries, such as the United States of America [2], China [3-4], Great Britain [5] etc. With the rapid development of iron and steel industry, the energy consumption is also increasing [6-7] (especially in China, as shown in Fig. 1 [8], million ton coal equivalent (Mtce)). And the energy consumption in iron and steel industry accounts for about 23.6 % of the whole industrial energy consumption in China 2012 [9]. Accordingly, many energy conservation technologies and methods are widely used in iron and steel industry, such as waste energy recovery [10], material flow balance analysis [11] etc. Then, the energy efficiency of iron and steel industry has been greatly improved. However, energy conservation of iron and steel industry should

still be further developed [12]. It has been demonstrated that there is considerable potential for energy conservation and emissions reduction in iron and steel industry [13-14].

Reheating furnace, which is widely applied to rolling process [15], is a very important thermal equipment. The energy consumption of reheating furnace accounts for approximately 15-20 % of the total energy consumption in steel industries and approximately 70 % of the rolling process [16]. Therefore, the energy saving of reheating furnace has been an area of intense investigation.
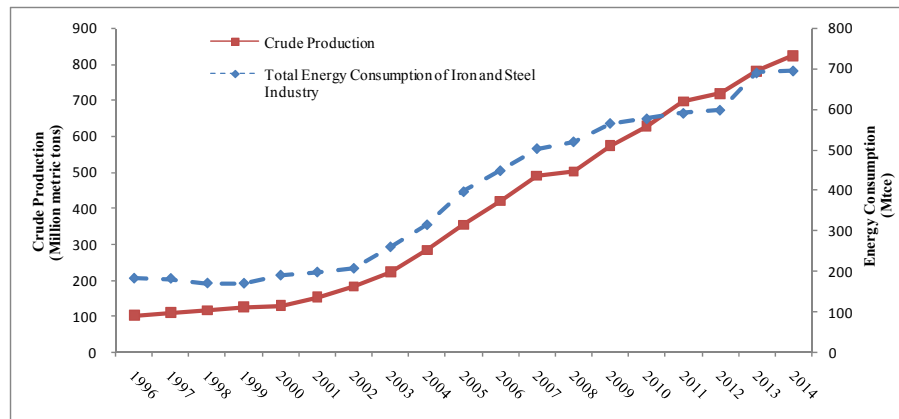
Fig.1 The crude production and energy consumption of Chinese iron and steel industry over the years (Data Source: CHINA STATISTICAL YEARBOOK)

2. Literature review

The research on energy conservation of reheating furnace has been highly valued all the time. Generally, the research work is mainly carried out as follows: thermal regulation optimization, combustion process optimization, waste heat recovery and utilization.

1) Thermal regulation optimization

Energy waste will be effectively reduced, if a reasonable thermal regulation is adopted. Furthermore, thermal regulation optimization can be achieved through billet heat transfer process analysis. The study on billet heat transfer process mainly focus on variation rule of billet heat transfer characteristics under various production rhythm(s) and different loading temperature(s). The reasonable gas supply strategy, which can improve billet heat quality and energy saving, should be formulated in accordance with these variation rules. The numerical analysis method is wildly applied to this field. Mayr *et al*. [17] put forward a time saving simulation of an 18 MW pusher type reheating furnace with a production capacity of 60 t/h and it is fired by natural gas burners. Tang *et al*. [18] developed a transient three-dimensional Computational Fluid Dynamics (CFD) model, which could simulate the flow characteristics, combustion process and multi-scale heat transfer inside the reheating furnace. The validation on an industrial walking beam slab reheating furnace was conducted. Han *et al*. used the finite-volume method to simulate the slab heating characteristics [19]. Although these CFD analyses can be used for accurate prediction of the thermal and combusting fluid characteristics in reheating furnace, it necessitates long computational time and resulting costs due to many governing equations, complexity of the furnace structure and uncertainty of the models [20].

2) Combustion process optimization

Combustion process optimization can improve the fuel gas combustion efficiency through the improvement of burner, the optimization of fuel gas-supply, air-fuel ratio control or other technical means. For example, García and Amel [21] presented a numerical simulation of the effects of using self-recuperative burners, which can utilize heat recovery on the performance of a walking-beam reheating furnace. A transient radiative slab heating analysis was performed to investigate the effect of various fuel mixtures on the performance of an axial-fired reheating furnace

[22]. Meanwhile, the approach, which applied oxy-fuel combustion instead of air-fuel combustion, could enhance combustion efficiency [23]. Moreover, Jian-Guo Wang [24] put forwards a soft-sensing method, which can predict combustion efficiency, since it cannot be measured directly.

3) Waste heat recovery and utilization

Waste heat of flue gas and vaporization cooling system accounts for about 50 % of the energy consumption in reheating furnace [25]. Moreover, the temperature of the flue gas leaving the furnace hearth is about 850 °C [26]. Therefore, the waste heat of flue gas has recovery value. The Organic Ranking Cycle, which has been successfully applied to reheating furnace, is a very effective technology in waste heat recovery [27-28]. Moreover, energy cascade utilization technology has also been applied to recovery of reheating furnace [29].

The above researches mainly concentrated on how to achieve energy saving of reheating furnace through the improvement of technical measures. These technical measures mainly seek new breakthroughs from objective factor. Unfortunately, the influence of subjective factors, which are significant for energy saving of reheating furnace, has not been taken into account. For example, there are differences in the FGO for various WGs in different WSs due to individual operation skills, fatigue state etc. Moreover, Lu *et al.* [30] had proposed an energy apportionment model, which could calculate the energy consumption amount for every billet, in reheating furnace. Then, bottleneck of slab thermal efficiency had been further analyzed [31] and variation of fuel gas consumption had been discussed based on energy consumption model [32] in reheating furnace. However, the FGO for various WGs in different WSs could not be evaluated. This paper proposes a novelty time-series FGO evaluation method, which can evaluate the FGO of various WGs in different WSs.

3. Methodology

3.1 The FGTS in $[T_l, T_{l+1}]$ time interval

Take $[T_l, T_{l+1}]$ time interval as an example, the calculation process of the FGTS is described in detail. Suppose there are f accumulative time segments (ATSs, as shown in reference [30, 32] for the ATS definition) in $[T_l, T_{l+1}]$ time interval (as shown in Fig. 2.), three possible scenarios are as follows:

- G_1 (Starting time: (T_l); Ending time (t_1): the first change moment of billet number (loading time or unloading time) in $[T_l, T_{l+1}]$ time interval);
- G_f (Starting time (t_{f-1}): the last change moment of billet number in $[T_l, T_{l+1}]$ time interval; Ending time: T_{l+1});
- G_i (Starting time (t_{i-1}): the $(i-1)^{\text{th}}$ change moment of billet number; Ending time (t_i): the ith change moment of billet number, $i = 2, 3 \cdots f - 1$).

3.1.1 The fuel gas-supply amount in the ith ATS

Correspondingly, the calculation processes of fuel gas-supply for three scenarios are as follows:

- $i = 1$

$$G_1 = \frac{t_{1,1} - T_l}{T_s} \cdot E_{1,1} \cdot T_s + \sum_{j=1}^{n_1} E_{1,j} \cdot T_s + \frac{t_1 - t_{1,n_1}}{T_s} \cdot E_{2,1} \cdot T_s \tag{1}$$

G_1 is the fuel gas-supply amount in the first ATS in GJ. The other variables are shown in Fig. 2.

- $i = f$

$$G_f = \frac{t_{f,1} - t_{f-1}}{T_s} \cdot E_{f,1} \cdot T_s + \sum_{j=1}^{n_f} E_{f,j} \cdot T_s + \frac{T_{l+1} - t_{f,x}}{T_s} \cdot E_{f,x} \cdot T_s \tag{2}$$

G_f is the fuel gas-supply amount in the fth ATS in GJ. The other variables are shown in Fig. 2.

- Variable description:
- 1. T_l, T_{l+1}: Starting Time and Ending Time;
- 2. T_s: Sampling interval of fuel gas measuring, min;
- 3. t_i: The i th ATS time when the number of billets changes in furnace hearth (loading or unloading);
- 4. $t_{i,j}$: The j th sampling time in the i th ATS time;
- 5. f: The number of billets changes in furnace hearth in $[T_l, T_{l+1}]$;
- 6. $E_{i,j}$: The instantaneous measurement value of gas flow in the j th sampling time of the i th ATS time, GJ/min.

Fig. 2 The calculation process of the FGTS in $[T_l, T_{l+1}]$ time interval

- $i \neq 1 \ \& \ i \neq f$

$$G_i = \frac{t_{i,1} - t_{i-1}}{T_s} \cdot E_{i,1} \cdot T_s + \sum_{j=1}^{n_i} E_{i,j} \cdot T_s + \frac{t_i - t_{i,n_i}}{T_s} \cdot E_{i+1,1} \cdot T_s \qquad (3)$$

G_i is the fuel gas-supply amount in the i th ATS in GJ. The other variables are shown in Fig. 2.

3.1.2 The billets weight of furnace hearth in the ith ATS (including i = 1 and i = f)

According to ATS definition, there is no loading billet or unloading billet in ATS. Therefore, the billets weight of furnace hearth in the i th ATS can be denoted as:

$$M_i = \sum_{k=1}^{N_i} m_{i,k} \qquad (4)$$

M_i is the billets weight of furnace hearth in the i th ATS in tons, $m_{i,k}$ is the k th billet weight of furnace hearth in the i th ATS in tons, and N_i is the billet number of furnace hearth in the i th ATS.

3.1.3 The FGTS value in the ith ATS

The FGTS value can be calculated in the i th ATS:

$$e_i = \frac{G_i}{M_i} \qquad (5)$$

e_i is the FGTS value in the i th ATS, $i = 1 \cdots f$ in GJ/tons.

3.1.4 The FGTS value in $[T_l, T_{l+1}]$ time interval

The FGTS value can be calculated in $[T_l, T_{l+1}]$ time interval:

$$e_{[T_l,T_{l+1}]} = \frac{\sum_{i=1}^{f} e_i}{f} \qquad (6)$$

$e_{[T_l,T_{l+1}]}$ is the FGTS value in $[T_l, T_{l+1}]$ time interval in GJ/tons.

3.2 The FGTS time-series data set in statistical period

The FGTS value can be calculated in $[T_l, T_{l+1}]$ time interval through calculation method in Section 3.1. Then, the statistical period can be divided into several equal time intervals (time intervals: $\Delta T = T_{l+1} - T_l$). Afterwards, the FGTS time-series can be achieved.

Moreover, the FGTS time-series data set can be denoted in statistical period, as shown in Eq. 7.

$$R = \{e_{[T_l,T_{l+1}]} | l \in Integer \ and \ 1 \le l \le r-1\} \qquad (7)$$

R is the FGTS time-series data set, and r is the amount of time-intervals in statistical period.

3.3 The FGTS time-series data set division according to working schedule

Reheating furnace implements 24-hour continuous working schedule. Moreover, this working schedule consists mainly of two important components (WGs and WSs). Therefore, the FGTS time-series data set can be disaggregated by various WGs and WSs. In general, working schedule mainly includes 'Four Shifts Three Operation Production Mode' and 'Three Shifts Two Operation Production Mode'.

'Four Shifts Three Operation Production Mode': 24 hours in one day are divided into day working shift (DWS, from 0 o'clock to 8 o'clock), swing working shift (SWS, from 8 o'clock to 16 o'clock), night working shift (NWS, from 16 o'clock to 24 o'clock). There are four WGs in turn.

'Three Shifts Two Operation Production Mode': 24 hours in one day are divided into DWS (from 8 o'clock to 20 o'clock), NWS (from 20 o'clock to 8 o'clock next day). There are three WGs in turn.

Therefore, the FGTS time-series data set can be divided according to working schedule. Then, the FGTS time-series data sets of various WGs and WSs can be denoted as data set according to the working schedule, as shown in Eq. 8.

$$P_{u,v} = \{e_{[T_l,T_{l+1}]} | l \in Integer \ \& \ 1 \le l \le r-1 \ \& \ [T_l,T_{l+1}] \in the \ u^{th} \ WG \ \& \ [T_l,T_{l+1}] \in the \ v^{th} \ WS\} \qquad (8)$$

$P_{u,v}$ is the FGTS time-series data set of the uth WG in the vth WS, $u = 1 \cdots U$, $v = 1 \cdots V$, $P_{u,v} \in R$.

3.4 The establishment of the FGO evaluation model

These elements in FGTS time-series data sets are continuous data, which is suitable for boxplot analysis [33-34]. The boxplot can qualitatively describe the distribution differences between various data sets. Unfortunately, the quantitative description of these differences is indistinct. Therefore, on the premise of the production process of reheating furnace, the FGO evaluation model, which can quantitatively assess distribution of various data sets, can be established in this paper.

The boxplot parameters of $P_{u,v}$ data set can be recorded as $Q_{2(u,v)}$, $IQR_{(u,v)}$, $UW_{(u,v)}$, $LW_{(u,v)}$. Then, it is should be noted as follows before the FGO evaluation model establishment.

- $Q_{2(u,v)}$, which represents the overall fuel gas consumption level of various data sets, is the benchmark.
- $IQR_{(u,v)}$, which represents data concentration in the 25-75 % range, is the major composition.
- $UW_{(u,v)}$, which represents data concentration in the 75-100 % range, is the supplement.
- $LW_{(u,v)}$, which represents data concentration in the 0-25 % range, is also the supplement.

Data normalization

Data normalization, which can eliminate the influence of magnitude order and dimension, is an effective method. Then, Min-Max Normalization is adopted in this paper. Take Q_2 ($Q_2 =$

$\{Q_{2(1,1)}, \cdots Q_{2(1,V)}, Q_{2(2,1)}, \cdots Q_{2(2,V)}, \cdots Q_{2(U,V)}\}$) data set as an example, data normalization is described in detail, as shown in Eq. 9.

$$Q'_{2(u,v)} = \frac{Q_{2(u,v)} - min(Q_2)}{max(Q_2) - min(Q_2)} \tag{9}$$

$Q'_{2(u,v)}$ is the 50th percentile of the uth WG in the vth WS after normalization, $Q_{2(u,v)}$ is the 50th percentile of the uth WG in the vth WS before normalization. $min(Q_2)$ and $max(Q_2)$ are the minimum value and maximum value in Q_2 data set, respectively. $IQR'_{(u,v)}$ is the interquartile rage of the uth WG in the vth WS after normalization, $UW'_{(u,v)}$ is the upper whisker of the uth WG in the vth WS after normalization, and $LW'_{(u,v)}$ is the lower whisker of the uth WG in the vth WS after normalization.

Modelling

Then, the FGO evaluation model of the uth WG in the vth WS can be defined as follow:

$$ID_{(u,v)} = \alpha_1 \cdot Q'_{2(u,v)} + \alpha_2 \cdot IQR'_{(u,v)} + \alpha_3 \cdot UW'_{(u,v)} + \alpha_4 \cdot LW'_{(u,v)} \tag{10}$$

$ID_{(u,v)}$ is the FGO evaluation value of the uth WG in the vth WS, [0,1]. $\alpha_1, \alpha_2, \alpha_3, \alpha_4$ are the weighting coefficients of $Q'_{2(u,v)}, IQR'_{(u,v)}, UW'_{(u,v)}, LW'_{(u,v)}$, respectively.

According to the weighting description hypotheses, the importance of four variables is shown in descending order.

$$Q'_{2(u,v)} > IQR'_{(u,v)} > UW'_{(u,v)} = LW'_{(u,v)}$$

Therefore, $\alpha_1 > \alpha_2 > \alpha_3 = \alpha_4$ in turn in this FGO evaluation model.

It is worth noting that the FGO evaluation model, which is put forward in this manuscript, is to evaluate the FGO of various WGs and WSs. In order to ensure of the evaluation effectiveness, it is necessary to select the production data of normal production.

4. Case study – Results and discussion

The No. 1 reheating furnace of a rolling mill is considered as research object. The main product of this reheating furnace is medium-plate (length: 8000-10000mm; width: 1200-2000mm; thick: 220-230mm). The production data are analyzed as the basic data sources in June and July 2016. In this period, the production process of No. 1 reheating furnace is relatively stable, which is convenient for FGO evaluation analysis.

4.1 The working schedule of No. 1 reheating furnace

'Four Shifts Three Operation Production Mode' has been adopted in this No. 1 reheating furnace. The working schedule, which derives from the production record, for this reheating furnace in June and July 2016 has also been shown in Table 1.

Table 1 The working schedule of No.1 reheating furnace in June and July 2016

A WG	NWS	NWS	OD	DWS	DWS	SWS	SWS	OD
B WG	OD	DWS	DWS	SWS	SWS	OD	NWS	NWS
C WG	DWS	SWS	SWS	OD	NWS	NWS	OD	DWS
D WG	SWS	OD	NWS	NWS	OD	DWS	DWS	SWS
June								1
	2	3	4	5	6	7	8	9
	10	11	12	13	14	15	16	17
	18	19	20	21	22	23	24	25
	26	27	28	29	30			
July						1	2	3
	4	5	6	7	8	9	10	11
	12	13	14	15	16	17	18	19
	20	21	22	23	24	25	26	27
	28	29	30	31				

Noted: Off-Duty (OD)

As shown in Table 1, the working status of various WGs is presented clearly in different WSs. Due to 24-hour continuous working mode of reheating furnace, the $[T_l, T_{l+1}]$ time interval can be defined as 1 hour for convenient calculation. Furthermore, the FGTS per an hour (FGTSH) can be defined.

4.2 The calculation and discussion of FGTSH

There are 1464 FGTSHs can be achieved through calculation in statistical period. Then, these FGTSHs can be classified according to Section 3.3 (as shown in Table 2). The FGTSH boxplot of various WGs in different WSs is shown in Fig. 3.

It should be noted that the outliers are not under consideration due to their small proportion. The results after normalization and the FGO evaluation value of each WG in various WSs can be calculated through Eqs. 9 and 10 (as shown in Table 3, $\alpha_1 = 0.4$, $\alpha_2 = 0.3$, $\alpha_3 = 0.15$, $\alpha_4 = 0.15$).

Table 2 The FGTSHs division for various WGs and WSs

The number of FGTSH	A WG	B WG	C WG	D WG	Total
The DWS	122	132	111	118	483
The SWS	126	121	119	120	486
The NWS	139	122	108	126	495
Total	387	375	338	364	1464
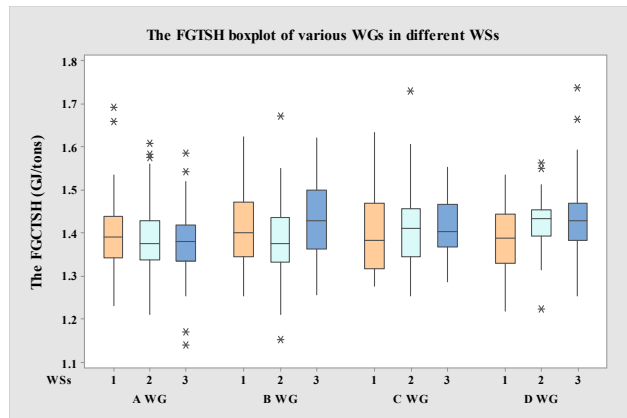
Fig. 3 The FGTSH boxplot of various WGs in different WSs
Noted: 1: DWS; 2: SWS; 3: N WS.
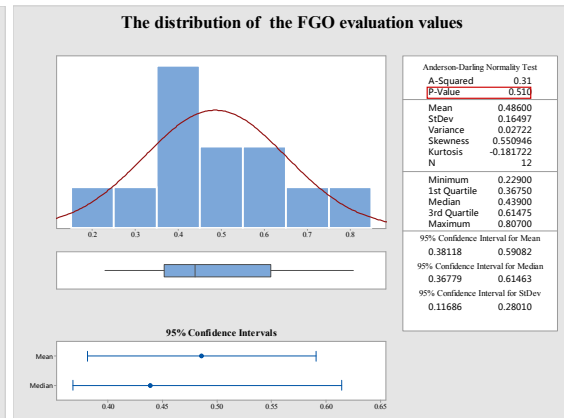
Fig. 4 The FGO evaluation values distribution

Table 3 The value of $Q'_{2(u,v)}$, $IQR'_{(u,v)}$, $UW'_{(u,v)}$, $LW'_{(u,v)}$ and the FGO evaluation value for WGs in various WSs

Type (Normalization)	A WG			B WG			C WG			D WG		
	DWS	SWS	NWS	DWS	SWS	NWS	DWS	SWS	NWS	DWS	SWS	NWS
$Q'_{2(u,v)}$	0.241	0	0.086	0.448	0.017	0.897	0.103	0.603	0.483	0.207	1	0.931
$IQR'_{(u,v)}$	0.097	0.092	0.082	0.697	0.461	0.82	1	0.539	0.382	0.551	0	0.258
$UW'_{(u,v)}$	0.349	0.689	0.415	0.896	0.519	0.594	1	0.858	0.274	0.302	0	0.623
$LW'_{(u,v)}$	0.802	0.965	0.453	0.57	0.93	0.756	0	0.57	0.465	0.826	0.395	1
The FGO evaluation value	0.384	0.346	0.229	0.608	0.362	0.807	0.491	0.617	0.419	0.417	0.459	0.693

4.2.1 The FGO evaluation model validation

The FGO evaluation values of various WGs in different WSs are accorded with normal distribution due to P-Value (0.51) > 0.05 (as shown in Fig. 4, this data analysis has been done in Minitab 17.0). That is, the FGO evaluation values mainly concentrate on [0.2, 0.8] range (account for 91.7 % of total number), especially for [0.2, 0.6] range (account for 66.67 % of total number). Therefore, the FGO evaluation model is reasonable. It is worth mentioning that there are no FGO evaluation values less than 0.2. Thus, there is still room for improvement in the FGO of various WGs in different WSs. Additionally, the FGO evaluation values, which are higher than 0.8, should be emphasized due to the higher fuel gas consumption, such as the NWS of B WG.

4.2.2 The FGO evaluation results analysis

The following analysis results can be achieved.

- The FGO evaluation values analysis of each WG in various WSs

A WG: The FGO of A WG in all WSs is very well due to its lower FGO evaluation values. Nevertheless, there is still room for improvement in the FGO for A WG. Because the Q_2 value is lower than others, the FGO evaluation value is relatively small. Unfortunately, the IQR and whisker are not optimal. Therefore, the enhancement of fuel gas consumption centralization is an effective method to improve the FGO of A WG.

B WG: the FGO of B WG varies greatly in three WSs. Comparing with A WG, the performance of SWS, which is better than the other WSs, still has a certain gap. Because of the high value of Q_2, IQR and whisker in DWS and NWS, the FGO evaluation value has deteriorated further. Therefore, the DWS and NWS should be given more attention, especially for NWS.

C WG and D WG: the FGO evaluation value is mainly distributed in [0.4, 0.7] for C WG and D WG in three WSs. This distribution is determined by the following three conditions: i) The higher Q_2 value, the lower IQR and whisker value, such as the SWS of D WG; ii) The lower Q_2 value, the higher IQR and whisker value, such as DWS of C WG and DWS of D WG; iii) The medium of Q_2, IQR value and whisker value, such as the other WSs of C WG and D WG. Therefore, appropriate energy saving measures should be adopted according to different conditions.

- The FGO evaluation values analysis of each WS in various WGs

DWS: The FGO evaluation values of various WGs are 0.384 (A WG), 0.608 (B WG), 0.491 (C WG), 0.417 (D WG), respectively. The performance of A WG is optimal due to the lower Q_2, IQR and whisker. The Q_2 value of D WG is slightly lower than that of A WG, yet the IQR of D WG is larger than that of A WG. Therefore, the FGO of D WG is still lower than that of A WG. There is not much difference between C WG and D WG. Because the Q_2 value of B WG is more larger than that of others, the performance of B WG is the worst.

SWS: The FGO evaluation values of different WGs are 0.346 (A WG), 0.362 (B WG), 0.617 (C WG), 0.459 (D WG), respectively. The FGO of A WG and B WG performs better than the other WGs. Although the IQR value of D WG is lower than other WGs, the Q_2 value of D WG is much larger than that of the other WGs. Therefore, the performance of D WG is either mediocre. Then, the FGO of C WG is the lowest due to the higher Q_2 value and IQR value.

NWS: The FGO evaluation values of different WGs are 0.229 (A WG), 0.807 (B WG), 0.419 (C WG), 0.693 (D WG), respectively. Obviously, the performance of A WG is much higher than that of other WGs, followed by C WG and D WG due to the medium Q_2 value and IQR value. It is worth mentioning that the FGO of B WG is worst because its Q_2 value and IQR value are much higher than that of the other WGs.

4.3 Main findings

4.3.1 The primary reasons of FGO evaluation values' difference

Actually, the FGO of various WGs in different WSs can be evaluated through two indicators, that is, the average value and the standard deviation value of individual FGTSH data set. On one hand, the average values of various FGTSH data sets indicate fuel gas consumption level of various WGs in different WSs. On the other hand, the standard deviation values of various FGTSH data sets represent gas consumption fluctuation of various WGs in different WSs. Unfortunately, it is inconvenient for these two indicators to evaluate the FGO due to dimensional difference and their uncertain influence degree on the FGO. Therefore, the FGO evaluation model based on box-plot is proposed in this paper. The ranking results of the FGO evaluation values are as follows in ascending order (as shown in Table 3): NWS(A WG:0.229), SWS(A WG:0.346), SWS(B WG:0.362), DWS(A WG:0.384), DWS(D WG:0.417), NWS(C WG:0.419), SWS(D WG:0.459), DWS(C WG:0.491), DWS(B WG:0.608), SWS(C WG:0.617), NWS(D WG:0.693), NWS(B WG:0.807). Then,

the ranking results of the FGO evaluation values, the average values and the standard deviation values of individual FGTSH data sets are all shown in Fig. 5.

There are three possible scenarios between the FGO evaluation values and two indicators (as shown in Fig. 5).

- The FGO evaluation value is relatively lower because of the smaller the average value and the standard deviation value of FGTSH data sets, such as NWS (A WG);
- The FGO evaluation value is relatively higher because of the larger the average value and the standard deviation value of FGTSH data sets, such as NWS (B WG);
- The FGO evaluation value is undetermined due to the uncertainty of the average value and the standard deviation value of FGTSH data sets. For example, although the average value of SWS (B WG) FGTSH data set is higher than that of DWS (A WG) FGTSH data set, the FGO evaluation value of SWS (B WG) is superior to that of DWS (A WG) because of the lower the standard deviation value of SWS (B WG) FGTSH data set. Similarly, this phenomenon also happens between SWS (D WG) and DWS (C WG) etc.

The FGO evaluation values can reflect these two indicators synthetically. Then, the FGO evaluation values can represent the FGO of various WGs in different WSs. Meanwhile, the validation of the FGO evaluation model has also been further verified.
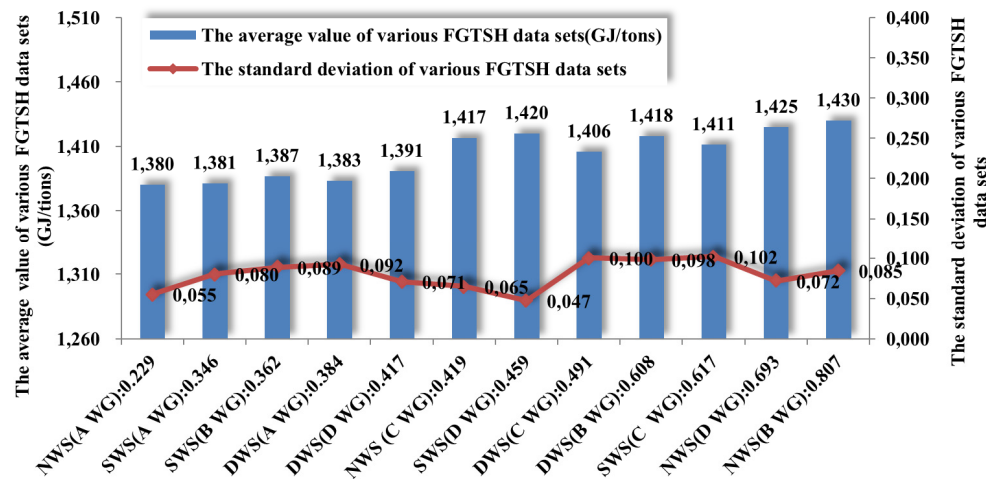
Fig. 5 The FGO evaluation values, the average value and the standard deviation of individual FGTSH data set

4.3.2 The establishment of the reward and punishment system

For improving employees' awareness of energy conservation, the reward and punishment system should be established.

Firstly, the FGO evaluation grade should be formulated. For example, the FGO evaluation grade can be divided into five levels according to FGO evaluation value. That is, [0, 0.2): Excellent grade; [0.2, 0.4): Good grade; [0.4, 0.6): Mean grade; [0.6, 0.8): Poor grade; [0.8, 1]: Failed grade (as shown in Fig. 6).
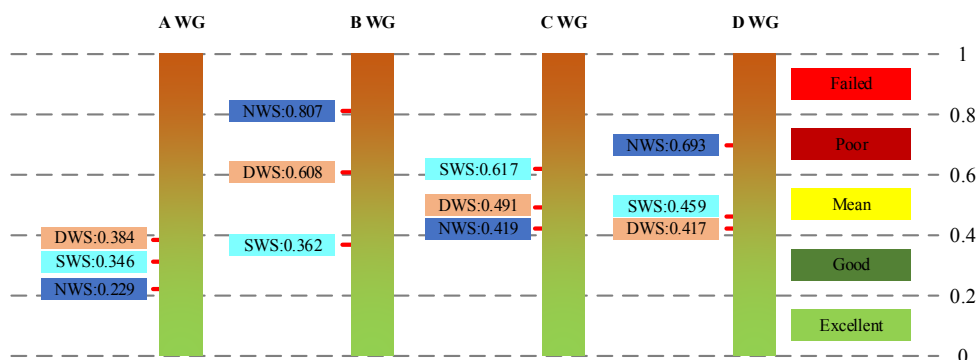
Fig. 6 The FGO evaluation grade of various WGs in different WSs

As shown in Fig. 6, there are four FGTSH data sets in Good grade, DWS (A WG), SWS (A WG), NWS (A WG), SWS (B WG), respectively; four FGTSH data sets in Mean grade, DWS (C WG), NWS (C WG), DWS (D WG) and SWS (D WG), respectively; three FGTSH data sets in Poor grade, DWS (B WG), SWS (C WG), NWS (D WG), respectively; one FGTSH data set in Failed grade, NWS (B WG). Moreover, two points should be concerned about:

- The FGO evaluation grade difference of B WG is obvious in various WSs, DWS (B WG): Poor grade; SWS (B WG): Good grade; NWS (B WG): Failed grade. Therefore, the B WG should be focused on.
- There is no FGCSH data set can reach Excellent grade. Thus, this reheating furnace has great energy saving potential in terms of operation.

Secondly, the reward and punishment system should be established in accordance to FGO evaluation grade.

1) The determination of FGO evaluation period

Generally, wage settlement cycle can be regarded as FGO evaluation period for payment convenience, such as one month (especially for Chinese enterprises).

2) The establishment of reward and punishment rules

i) Evaluation benchmark
Mean grade can be used as evaluation benchmark. That is, neither reward nor punishment will be given when the FGO evaluation grade is Mean grade.

ii) The principle of cascade reward and punishment
The principle of cascade reward and punishment mainly entails a certain proportion of rewards should be given when FGO evaluation grade is higher one level than Mean grade, such as Good grade: 20 % rewards. A higher proportion of rewards should be given when FGO evaluation grade is higher one level than before, such as Excellent grade: 50 % rewards, and vice versa. In order to pursue more profits, employees actively enhance their skills and improve their FGO. Then, the operation energy saving of reheating furnace can be achieved.

4.3.3 The FGO improvement measures

Essentially, the FGO evaluation grades of various FGTSH data sets are determined by their respective FGO evaluation values. Therefore, the FGO evaluation values should be further improved. Generally, there are three ways to improve the FGO evaluation values according to the analysis results of Section 4.2.

- Q_2 value

The lower Q_2 value is the major way to improve FGO evaluation value because of the dominant function in FGO evaluation model. Q_2 values, which are the median in various FGTSH data sets, represent overall FGO. Moreover, working skills, which is the main way to reduce Q_2 values, should be strengthened for every employee.

- IQR value

IQR value represents the concentration of 25-75 % elements in every FGTSH data set. That is, the smaller the IQR value, the higher 25-75 % elements centralization degree, the higher the FGO, and vice versa. Besides working skills, working responsibility, which determines whether employees are willing to do their jobs better, is also very important. If yes, IQR value will be improved, and vice versa.

- Whisker value

The lower whisker value and the upper whisker value represent the concentration of 0-25 % elements and 75-100 % elements in every FGTSH data set, respectively. The smaller the whisker

value, the higher the FGO, and vice versa. However, the lower whisker value and upper whisker value only represent 25 % elements in every FGTSH data set, respectively. Their influence on the FGO evaluation value is relatively limited. Furthermore, working passion determines whether employees want to improve their work better or not. If yes, whisker value will be improved, and vice versa. Therefore, 3W (Working passion, Working responsibility, Working skills) determines the FGO evaluation grade of each FGTSH data set together. That is, the energy saving of reheating furnace in the respect of operation can be achieved through the 3W improvement. How to improve 3W should be paid more attention. Generally, the skills training and the reward and punishment system are the important improvement measures on 3W. The relationship of the improvement measures, the influence object, the influence result is shown in Fig. 7.
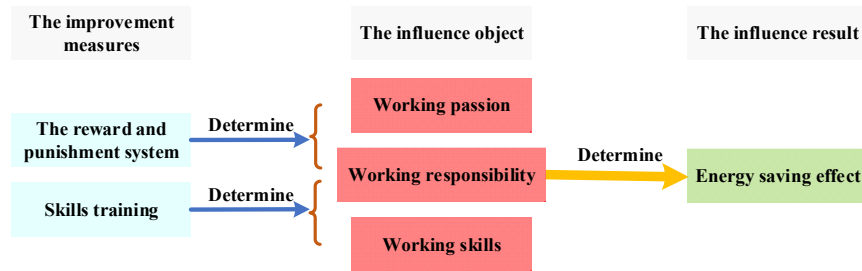
Fig. 7 The relationship between the improvement measures, the influence object and the influence result

5. Conclusion

A new time-series FGO evaluation model, which can evaluate the FGO of various WGs in different WSs, has been established in this paper. This time-series FGO evaluation model mainly includes: i) The FGTS in $[T_l, T_{l+1}]$ time interval; ii) The FGTS time-series data set in statistical period; iii) The FGTS time-series data set division according to working schedule; iv) The establishment of the FGO evaluation model. Then, this FGO evaluation model has been successfully applied to the FGO evaluation for various WGs in different WSs in a reheating furnace.

The main conclusions are as follows:

1) A novelty time-series FGO evaluation model has been put forward in this paper. This model can resolve the problem that FGO of various WGs in different WSs can't be effectively evaluated.

2) Case study shows that the ranking results of the FGO evaluation values are as follows in ascending order in statistical period: NWS (A WG:0.229), SWS (A WG:0.346), SWS (B WG:0.362), DWS (A WG:0.384), DWS (D WG:0.417), NWS (C WG:0.419), SWS (D WG:0.459), DWS (C WG:0.491), DWS (B WG:0.608), SWS (C WG:0.617), NWS (D WG:0.693), NWS (B WG:0.807). The evaluation result shows that:

   - For various WGs, the A WG performs best, followed by C WG and D WG. And the performance of B WG is the worst due to its violent fluctuation of FGO evaluation values in three WSs;
   - For different WSs, the DWS and SWS performs well. Unfortunately, the performance of NWS is unsatisfactory.

3) The discussion results show that:

   - The reward and punishment system should be established according to FGO evaluation grade results;
   - 3W can be enhanced through skills training and the reward and punishment system. The energy saving effect in terms of operation for reheating furnace can be achieved.

Acknowledgement

Reference

[1] Duan, W., Yu, Q., Wang, K., Qin, Q., Hou, L., Yao, X., Wu, T. (2015). ASPEN plus simulation of coal integrated gasification combined blast furnace slag waste heat recovery system, *Energy Conversion and Management*, Vol. 100, 30-36, doi: 10.1016/j.enconman.2015.04.066.

[2] Karali, N., Park, W.Y., McNeil, M. (2017). Modeling technological change and its impact on energy savings in the U.S. iron and steel sector, *Applied Energy*, Vol. 202, 447-458, doi: 10.1016/j.apenergy.2017.05.173.

[3] Chen, Q., Gu, Y., Tang, Z., Wei, W., Sun, Y. (2018). Assessment of low-carbon iron and steel production with CO_2 recycling and utilization technologies: A case study in China, *Applied Energy*, Vol. 220, 192-207, doi: 10.1016/j.apenergy.2018.03.043.

[4] Lu, B., Tang, K., Chen, D., Han, Y., Wang, S., He, X., Chen, G. (2019). A novel approach for lean energy operation based on energy apportionment model in reheating furnace, *Energy*, Vol. 182, 1239-1249, doi: 10.1016/j.energy.2019.06.076.

[5] Griffin, P.W., Hammond, G.P. (2019). Industrial energy use and carbon emissions reduction in the iron and steel sector: A UK perspective, *Applied Energy*, Vol. 249, 109-125, doi: 10.1016/j.apenergy.2019.04.148.

[6] Lu, B., Chen, G., Chen, D., Yu, W. (2016). An energy intensity optimization model for production system in iron and steel industry, *Applied Thermal Engineering*, Vol. 100, 285-295, doi: 10.1016/j.applthermaleng.2016.01.064.

[7] An, R., Yu, B., Li, R., Wei, Y.-W. (2018). Potential of energy saving and CO_2 emission reduction in China's iron and steel industry, *Applied Energy*, Vol. 226, 862-880, doi: 10.1016/j.apenergy.2018.06.044.

[8] Chen, D., Lu, B., Zhang, X., Dai, F., Chen, G., Liu, Y. (2018). Fluctuation characteristic of billet region gas consumption in reheating furnace based on energy apportionment model, *Applied Thermal Engineering*, Vol. 136, 152-160, doi: 10.1016/j.applthermaleng.2018.03.007.

[9] Chen, D., Lu, B., Chen, G., Yu, W. (2017). Influence of the production fluctuation on the process energy intensity in iron and steel industry, *Advances in Production Engineering & Management*, Vol. 12, No. 1, 75-87, doi: 10.14743/apem2017.1.241.

[10] Zhang, Q., Zhao, X., Lu, H., Ni, T., Li, Y. (2017). Waste energy recovery and energy efficiency improvement in China's iron and steel industry, *Applied Energy*, Vol. 191, 502-520, doi: 10.1016/j.apenergy.2017.01.072.

[11] Zhang, Q., Xu, J., Wang, Y., Hasanbeigi, A., Zhang, W., Lu, H., Arens, M. (2018). Comprehensive assessment of energy conservation and CO_2 emissions mitigation in China's iron and steel industry based on dynamic material flows, *Applied Energy*, Vol. 209, 251-265, doi: 10.1016/j.apenergy.2017.10.084.

[12] He, K., Wang, L. (2017). A review of energy use and energy-efficient technologies for the iron and steel industry, *Renewable and Sustainable Energy Reviews*, Vol. 70, 1022-1039, doi: 10.1016/j.rser.2016.12.007.

[13] Peng, J., Xie, R., Lai, M. (2018). Energy-related CO_2 emissions in the China's iron and steel industry: A global supply chain analysis, *Resources, Conservation and Recycling*, Vol. 129, 392-401, doi: 10.1016/j.resconrec.2016.09.019.

[14] Hu, R., Zhang, Q. (2015). Study of a low-carbon production strategy in the metallurgical industry in China, *Energy*, Vol. 90, Part 2, 1456-1467, doi: 10.1016/j.energy.2015.06.099.

[15] McBrien, M., Cabrera Serrenho, A., Allwood, J.M. (2016). Potential for energy savings by heat recovery in an integrated steel supply chain, *Applied Thermal Engineering*, Vol. 103, 592-606, doi: 10.1016/j.applthermaleng.2016.04.099.

[16] Ke, H.-L., Dong, B., Ye, B. (2014). Research and application of slab heating curve in reheating furnace, *Metallurgical Industry Automation*, Vol. 38, No. 3, 50-55, doi: 10.3969/j.issn.1000-7059.2014.03.010.

[17] Mayr, B., Prieler, R., Demuth, M., Moderer, L., Hochenauer, C. (2017). CFD analysis of a pusher type reheating furnace and the billet heating characteristic, *Applied Thermal Engineering*, Vol. 115, 986-994, doi: 10.1016/j.applthermaleng.2017.01.028.

[18] Tang, G., Wu, B., Bai, D., Wang, Y., Bodnar, R., Zhou, C. (2018). CFD modeling and validation of a dynamic slab heating process in an industrial walking beam reheating furnace, *Applied Thermal Engineering*, Vol. 132, 779-789, doi: 10.1016/j.applthermaleng.2018.01.017.

[19] Han, S.H., Chang, D., Kim, C.Y. (2010). A numerical analysis of slab heating characteristics in a walking beam type reheating furnace, *International Journal of Heat and Mass Transfer*, Vol. 53, No. 19-20, 3855-3861, doi: 10.1016/j.ijheatmasstransfer.2010.05.002.

[20] Emadi, A., Saboonchi, A., Taheri, M., Hassanpour, S. (2014). Heating characteristics of billet in a walking hearth type reheating furnace, *Applied Thermal Engineering*, Vol. 63, No. 1, 396-405, doi: 10.1016/j.applthermaleng.2013.11.003.

[21] García, A.M., Amell, A.A. (2018). A numerical analysis of the effect of heat recovery burners on the heat transfer and billet heating characteristics in a walking-beam type reheating furnace, *International Journal of Heat and Mass Transfer*, Vol. 127, Part B, 1208-1222, doi: 10.1016/j.ijheatmasstransfer.2018.07.121.

[22] Han, S.H., Chang, D. (2012). Radiative slab heating analysis for various fuel gas compositions in an axial-fired reheating furnace, *International Journal of Heat and Mass Transfer*, Vol. 55, No. 15-16, 4029-4036, doi: 10.1016/j.ijheatmasstransfer.2012.03.041.

[23] Han, S.H., Lee, Y.S., Cho, J.R., Lee, K.H. (2018). Efficiency analysis of air-fuel and oxy-fuel combustion in a reheating furnace, *International Journal of Heat and Mass Transfer*, Vol. 121, 1364-1370, <u>doi: 10.1016 /j.ijheatmasstransfer.2017.12.110</u>.

[24] Wang, J.-G., Shen, T., Zhao, J.-H., Ma, S.-W., Wang, X.-F., Yao, Y., Chen, T. (2017). Soft-sensing method for optimizing combustion efficiency of reheating furnaces, *Journal of the Taiwan Institute of Chemical Engineers*, Vol. 73, 112-122, <u>doi: 10.1016/j.jtice.2016.09.037</u>.

[25] Zhang, Q. (2017). Application of reheating furnace waste heat integrated utilization technology, *Energy for Metallurgical Industry*. Vol. 36, No. 1, 45-47, <u>doi: 10.3969/j.issn.1001-1617.2017.01.011</u>.

[26] Dal Magro, F., Jimenez-Arreola, M., Romagnoli, A. (2017). Improving energy recovery efficiency by retrofitting a PCM-based technology to an ORC system operating under thermal power fluctuations, *Applied Energy*, Vol. 208, 972-985, <u>doi: 10.1016/j.apenergy.2017.09.054</u>.

[27] Jiménez-Arreola, M., Wieland, C., Romagnoli, A. (2017). Response time characterization of organic rankine cycle evaporators for dynamic regime analysis with fluctuating load, *Energy Procedia*, Vol. 129, 427-434, <u>doi: 10.1016 /j.egypro.2017.09.131</u>.

[28] Pili, R., Romagnoli, A., Spliethoff, H., Wieland, C. (2017). Techno-economic analysis of waste heat recovery with ORC from fluctuating industrial sources, *Energy Procedia*, Vol. 129, 503-510, <u>doi: 10.1016/j.egypro.2017.09.170</u>.

[29] Wang, L. (2016). An example of waste heat recovery of heating furnace based on energy cascade utilization, *Metallurgical Power*, Vol. 1, 30-31, <u>doi: 10.3969/j.issn.1006-6764.2016.01.010</u>.

[30] Lu, B., Chen, D., Chen, G., Yu, W. (2017). An energy apportionment model for a reheating furnace in a hot rolling mill – A case study, *Applied Thermal Engineering*, Vol. 112, 174-183, <u>doi: 10.1016/j.applthermaleng.2016.10.080</u>.

[31] Chen, D., Lu, B., Dai, G.-Q., Chen, G., Zhang, X. (2018). Bottleneck of slab thermal efficiency in reheating furnace based on energy apportionment model, *Energy*, Vol. 150, 1058-1069, <u>doi: 10.1016/j.energy.2018.02.149</u>.

[32] Chen, D., Lu, B., Dai, F.-Q., Chen, G., Yu, W. (2018). Variations on billet gas consumption intensity of reheating furnace in different production states, *Applied Thermal Engineering*, Vol. 129, 1058-1067, <u>doi: 10.1016/ j.applthermaleng.2017.10.096</u>.

[33] Ferreira, J.E.V., Pinheiro, M.T.S., dos Santos, W.R.S., da Silva Maia, R. (2016). Graphical representation of chemical periodicity of main elements through boxplot, *Educación Química,* Vol. 27, No. 3, 209-216, <u>doi: 10.1016/ j.eq.2016.04.007</u>.

[34] Hubert, M., Vandervieren, E. (2008). An adjusted boxplot for skewed distributions, *Computational Statistics & Data Analysis,* Vol. 52, No. 12, 5186-5201, <u>doi: 10.1016/j.csda.2007.11.008</u>.

Appendix

The following abbreviations are used in the paper:

FGO   Fuel gas operation
FGTS   Fuel gas per ton steel
ATS   Accumulative time segment
FGTSH   FGTS per an hour
Mtce   Million ton coal equivalent
CFD   Computational fluid dynamics
WG   Working group
A WG   A working group
B WG   B working group
C WG   C working group
D WG   D working group
WS   Working shift
DWS   Day working shift
SWS   Swing working shift
NWS   Night working shift
OD   Off-Duty

Coordination of dual-channel supply chain with perfect product considering sales effort

Hu, H.[a,*]**, Wu, Q.**[a]**, Han, S.**[a]**, Zhang, Z.**[a]

[a]School of Economics and Management, Yanshan University, Qinghuangdao, P.R. China

A B S T R A C T

As more and more people use e-commerce for shopping, manufacturers are willing to open online sales channels in order to obtain more profits. This paper discusses a dual-channel supply chain (DCSC) composed of a retailer with a traditional channel and a manufacturer with a direct channel. In the external environment of uncertain market demand and defective products produced by manufacturers, manufacturers make efforts to promote online products, and consumers have free rider behaviour. Therefore, three game models under the leadership of manufacturers are established: (a) non-cooperative game model; (b) coordination model under revenue-sharing contract; (c) coordination model under profit-sharing contract. The results indicate that the product defect rate has a certain influence on channel pricing and sale efforts. The competition between the actors of the dual-channel is beneficial to the consumers who pursue the price. Considering the overall profit of the DCSC, the cooperation between the manufacturer and retailer is more profitable than the channel competition, and they are more willing to make product sale efforts. The retailer's expected profit under revenue-sharing contract is less than that under profit-sharing contract, but the total profit of coordination model is more than the latter.

1. Introduction

With the increasing willingness of consumers to shop online, more and more manufacturers are turning to online sales, and the DCSC with both offline and online sales channels will become a long-term market pattern. In 2018, there are about 1.8 billion customers electing shopping online, and the global e-retail sales reached $2.8 trillion, which is grown to $4.2 trillion by 2020 (https://www.statista.com/topics/871/online-shopping/). Some manufacturers use independent online retailers (e.g. amazon and taobao mall) to sell their products, while some brand-name manufacturers (e.g. Apple and Lenovo) build direct online channels to sell their products. The popularity of IT and market demand force manufacturers to choose dual-channel sales products. Compared with the centralized e-market platform, the agent-based platform is distributed and dynamic, which is closer to the natural state of the supply chain [1]. Online trading is more efficient than traditional trading, and products sell to market quickly [2]. Dual-channel supply chain not only brings convenient, comfortable and diversified experience to consumers, but also reduces market risk through profit sharing between the manufacturer and retailer. What's more, the indirect cost of online sales is low, and may make the product globally influential. The manufacturer establishes direct sales channel to improve the performance of the DCSC, and the ability of the DCSC actors to deal with risks can be enhanced [3].

It is impossible for manufacturers to produce high-quality products up to 100%. Therefore, in order to maintain market competitiveness, it is necessary for manufacturers to screen out defective quality products. The products are produced by the supplier. If there are defective products, they cannot be replaced by qualified products quickly [4]. Modak [5] believes that if the sold price of defective products is less than the production cost, the channel members' profit and manufacturer's wholesale price will decrease with the defect rate. When the uncertainty of product quality increases, the buyer will reduce the purchase intention [6]. Li [7] studied how the manufacturer and retailer sell products of different quality levels, among which the manufacturer sell products of low quality. When the retailer implements personalized pricing strategy, direct channel is beneficial to the manufacturer, but it often makes the retailer in trouble. Hu *et al.* [8] established a mathematical model for the detection, tracking and recall of defective products, and concluded that the avoidance of manufacturer's product quality inspection has seriously harmed the profits of retailer, and is not conducive to the long-term stable cooperation between the manufacturer and retailer.

In the actual production and operation, retailers and manufacturers actively carry out various promotional activities to attract consumers, and the continuous promotion has an important long-term impact on the image and market positioning of enterprises. Tsao [9] believes that the promotion cost sharing policy encourages the manufacturer to increase their promotion efforts, so that the retailer can order more products. Giovanni [10] believes that only when the contribution of advertising to goodwill is very large, advertising will be better than the strategy of improving product quality. Pu [11] compared the decentralized system with the centralized system, and found that the sales effort level of retailer and the profit of DCSC under the centralized system were both higher, and both increased with direct channel demand sales effort elasticity coefficient. Li *et al.* [12] studied the advertising cooperation strategies of the manufacturer and retailer in DCSC, and Chen [13] believed that appropriate product sales efforts can promote DCSC coordination and have win-win results. Ranjan [14] found that centralized supply chain management model can always bring the best supply chain profit, and the demand of different channels and the profit of SC can be improved through surplus value sharing mechanism. The incentive for promotion of retailer will reduce if the cost coefficient of sales efforts increases [15].

Supply chain management mainly emphasizes learning ability, and it is difficult to imitate and has creative value [16]. Considering the overall profit of DCSC, decentralized system is less than centralized system [17]. The contradiction among the actors of the DCSC can be adjusted by some contracts, and then the long-term cooperation among members can be promoted; for example, price discounts [18], two-part tariff [19], cost-sharing contract [20]. Liu [21] finds that the retailer almost always hates manufacturer to establish dual channels, and there is no motivation to share the information proved to be valuable to the manufacturer, and enterprises should carefully adopt quality differentiation as a strategy to alleviate channel conflict [22]. Jabarzare [23] thinks that the coordination effect of profits-sharing contract is better, and the competition among channel members is more favourable to consumers. Jafari [24] analyzed three game models: Bertrand, collusion, and Stackelberg, and concluded that the retail price is highest under cooperative game. Due to information asymmetry, the DCSC actors should set online and offline channel prices according to various factors such as demand uncertainty, market size and elasticity of demand to price [25].

This paper builds 3 kinds of game scenarios: non-cooperative game model, coordination model under revenue-sharing contract, and coordination model under profit-sharing contract, and derives the equilibrium result of the decision-making model by using Stackelberg game theory. The purposes of this research include: (a) to show the impact of defect rate on the optimal decision; (b) to analyze the relationship between manufacturer's sales efforts and consumers' free riding; (c) to verify whether the revenue-sharing contract and profits-sharing contract coordinate the DCSC.

2. Description of the problem

This paper studies a DCSC system, which consists of a retailer and a manufacturer which has a direct channel to sell product, and the DCSC structure is shown in Fig. 1. Considering the market environment of uncertain market demand and defective products produced by the manufacturer, it makes efforts to promote online products, and consumers have free riding behavior. This paper mainly considers the game model of DCSC led by the manufacturer, and then uses the method of backward induction method to solve the optimal action combination. The products produced by the manufacturer include the defective products with random ratio, but the defective products and the qualified products will be classified by inspection. The qualified products will flow to the market through online and offline channels, and the defective products will be sold to the secondary market in the form of low price. Market demand of different channel is termed as linear function in this paper, and it is respect to the manufacturer's sales effort and the price of each channel. The online sales price and sales effort level are determined by the manufacturer, while the retailer determines the retail price of the product. The notation and description used in this research is shown in Table 1.

Table 1 Model parameters notation and description

notation	description
ρ	The tendency of customers to buy through offline channels
α	Basic market demand
t	Probability of defective product, random variable
$f(t)$	The probability density function of the random variable t
$E(t)$	The expected probability density of defective products
w	Wholesale prices offered by the manufacturer
g	Product sale efforts level (Manufacturer's decision)
p_m	Online selling price (Manufacturer's decision)
p_r	Offline selling price (Retailer's decision)
τ	Direct channel demand sales effort elasticity coefficient
b	Cross price elasticity coefficient between direct channel and traditional channel
p_l	Low selling price of unit defective products
c	Manufacturer's unit production cost
k	Cost coefficient of unit sales effort level
π_r	Retailer's profit function
π_m	Manufacturer's profit function
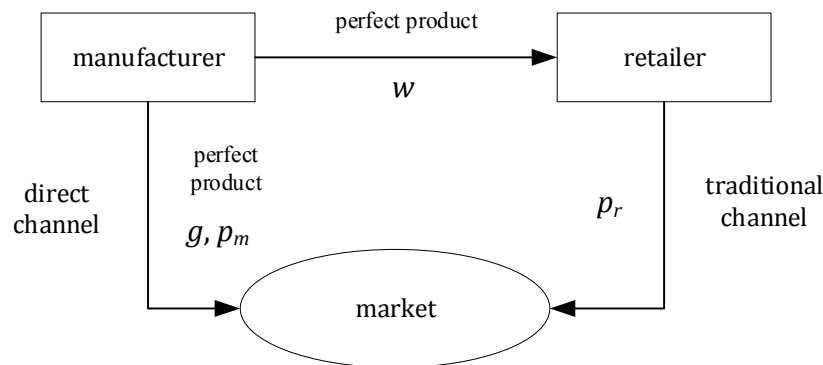
Fig. 1 DCSC structure

Research basic hypothesis:

- The DCSC actors are risk neutral, and both of them want to maximize their respective profits, similar to the RN model proposed by Jian [26].
- The wholesale price provided by the manufacturer is an exogenous variable, and the offline channel sales price is higher than that of the direct sales price. To make DCSC members profitable, we have $p_r > p_m > w > c$.
- $c > p_l$. Supposing that manufacturer's production cost is greater than that of the sale price of imperfect product.

- $c(g) = \frac{1}{2}kg^2$, $c(0) = 0$. The manufacturer's sales efforts cost function is convex, and when the manufacturer has no sales effort, its cost is 0.
- The cross-price elasticity of demand, b, is less than the self-price elasticity. In this paper, self-price elasticity is assumed to be 1, $0 \leq b \leq 1$.
- It is assumed that the product demand of the manufacturer and retailer is a linear function of price and sales effort. The manufacturer makes decision first to determine the price of direct channel and the level of product promotion effort. The retailer act as a follower and then decides the product price of the offline channel. Similar to Ranjan [14], their demand functions are: $D_m(p_r, p_m, g) = (1 - \rho)\alpha - p_m + bp_r + \tau g$, $D_r(p_r, p_m, g) = \rho\alpha - p_r + bp_m + (1 - \tau)g$.

3. Models for different game scenarios

This section mainly analyzes the profit function of DCSC members consisting a manufacturer and a retailer in three scenarios: (a) non-cooperative game model; (b) coordination model under revenue-sharing contract; (c) coordination model under profit-sharing contract. In order to gain some management insight, we analyze and discuss the optimal decision.

3.1 Non-cooperative game model

A non-cooperative game is played between the DCSC actors, and the manufacturer is the leader in this case. The manufacturer will produce defective products with a random ratio of $t(0 \leq t \leq 1)$, but it will sell imperfect products at a lower price p_l to reduce product quality losses in the secondary market. Some qualified products are sold directly to consumers at the price of p_m, while others are sold to the retailer at the wholesale price of w, and finally flow to consumers at the retail price of p_r. This paper used reverse induction so as to achieve Stackelberg equilibrium. To do this, we must first solve the problem of the follower, and then solve the problem of the manufacturer. The manufacturer and retailer maximize their profits by determining channel prices and sales effort for their products, so the profit equation of DCSC actors is as follows:

$$\pi_r = (p_r - w)D_r \tag{1}$$

$$\pi_m = wD_r + p_mD_m + \left(p_lE(t) - c(1 + E(t))\right)(D_r + D_m) - \frac{1}{2}kg^2 \tag{2}$$

Taking the second-order partial derivative about offline selling price p_r for retailer's profit π_r, we have $\frac{d^2\pi_r}{dp_r^2} = -2 < 0$. The Hessian matrix of π_m is obtained by calculation as shown below:

$$\begin{pmatrix} -k & b\left(-\frac{1}{2}\tau + \frac{1}{2}\right) + \tau \\ b\left(-\frac{1}{2}\tau + \frac{1}{2}\right) + \tau & b^2 - 2 \end{pmatrix}$$

If $0 < -k(b^2 - 2) - \left(b\left(-\frac{1}{2}\tau + \frac{1}{2}\right) + \tau\right)^2$, there is a maximum profit in the negative definite Hessian matrix, and π_m is concave with respect to p_m and g.

<u>Proposition 1:</u> In scenario 1, π_r is concave with respect to p_r, and π_m respect to p_m and g.

<u>Theorem 1:</u> Because the profit of each DCSC actor has a maximum value, the optimal channel pricing and sales efforts under non-cooperative game model are as follows:

$$g^{sg} = \frac{(-4 + (-4b + 4)\tau)w + B_1}{A_1} \tag{3}$$

$$p_m^{sg} = \frac{\left((-b + 2)\tau^2 + (2b - 2)\tau + (-4k - 1)b\right)w + B_2}{A_1} \tag{4}$$

$$p_r^{sg} = \frac{(b\tau^2 + (-b+4)\tau - 4k - 2)w + B_3}{A_1} \tag{5}$$

3.2 Coordination model under revenue-sharing contract

Similar to scenario 1, but the retailer seek to work with manufacturer to provide long-term customer demand and pay part of their revenue to manufacturer. By means of revenue-sharing contract to coordinate DCSC, the manufacturer receives a proportion of the retailer's revenues, ϕ. First, the offline selling price of optimal value is given by the retailer to maximize its expected profit. Then, considering the response of the retailer, the manufacturer, as the leader, determines the optimal direct selling price and the level of product sales effort to get its maximal profit. In model 2, we have the expected profit equation of DCSC actors as shown below:

$$\pi_r = \left((1 - \phi)p_r - w\right)D_r \tag{6}$$

$$\pi_m = wD_r + p_m D_m + \left(p_l E(t) - c\left(1 + E(r)\right)\right)(D_r + D_m) + \phi p_r D_r - \frac{1}{2}kg^2 \tag{7}$$

Taking the second-order partial derivative about offline selling price p_r for retailer's profit π_r, we have $\frac{d^2\pi_r}{dp_r^2} = -(1 - \phi) < 0$. Through the above analysis, we get the Hessian matrix of π_m under scenario 2:

$$\begin{pmatrix} \frac{1}{2}(\tau - 1)^2\phi - k & -\frac{1}{2}(\phi + 1)(\tau - 1)b + \tau \\ -\frac{1}{2}(\phi + 1)(\tau - 1)b + \tau & -2 + \frac{1}{2}(\phi + 2)b^2 \end{pmatrix}$$

If $\left(\frac{1}{2}(\tau - 1)^2\phi - k\right)\left(-2 + \frac{1}{2}(\phi + 2)b^2\right) - \left(-\frac{1}{2}(\phi + 1)(\tau - 1)b + \tau\right)^2 > 0$, the second principal minor is greater than zero, but the first principal minor is less than zero, so π_m has a maximum value.

<u>Proposition 2:</u> The retailer's profit of under the revenue-sharing contract is concave with respect to p_r, and π_m respect to p_m and g.

Theorem 2: It can be found from Proposition 2 that the optimal values of g, p_m, and p_r under model 2 are obtained as follows:

$$g^r = \frac{\left(\left((-2b^2 - 2b + 4)\tau + 2b^2 - 4\right)\phi + 4 + (4b - 4)\tau\right)w + B_4}{A_2} \tag{8}$$

$$p_m^{rs} = \frac{\left(\left((-2\phi + 1)b + 2\phi - 2\right)\tau^2 + \left((4\phi - 2)b - 2\varphi + 2\right)\tau - 2\left((k + 1)\phi - 2k - \frac{1}{2}\right)b\right)w + B_5}{A_2} \tag{9}$$

$$p_r^{rs} = \frac{\left(\left((4b - 4)\phi - b\right)\tau^2 + \left((-4b + 8)\phi + b - 4\right)\tau - 2b^2k\phi + 4k - 4\phi + 2\right)w + B_6}{A_2} \tag{10}$$

3.3 Coordination model under profit sharing contract

In this scenario, the manufacturer and retailer realize the coordination of DCSC through profit-sharing contract, so as to alleviate the cost of the manufacturer's product sales efforts and the loss of product quality. The retailer pay manufacturer a percentage of their profits θ for long-term cooperation. As in the previous two cases, Stackelberg game is played between DCSC participants, with the retailer being the follower and the manufacturer its leader. First, the retailer gives the optimal offline selling price p_r, and then the manufacturer combines the decision-making actions of the retail to get the sales effort g and the online selling price p_m. Different channel expected profit under the profit-sharing contract is respectively:

$$\pi_r = (1 - \theta)(p_r - w)D_r \tag{11}$$

$$\pi_m = wD_r + p_m D_m + \left(p_l E(t) - c(1 + E(t))\right)(D_r + D_m) + \theta(p_r - w)D_r - \frac{1}{2}kg^2 \tag{12}$$

Similar to Proposition 1 and 2, both the π_r and π_m are concave function of its decision variables. If $0 < \left(\frac{1}{2}\theta\tau^2 - \theta\tau + \frac{1}{2}\theta - k\right)\left(-\frac{1}{2}\theta b^2 + (b\theta + b)b - 2\right) - \left((b\theta + b)\left(-\frac{1}{2}\tau + \frac{1}{2}\right) + \tau\right)^2$, according to the Hessian matrix, the maximum value of the manufacturer can be obtained.

<u>Theorem 3:</u> In view of the above discussion, the optimal values of g, p_m, and p_r under the scenario 3 are obtained as follows:

$$g^{ps} = \frac{\left(\left((2b^2+2b-4)\tau-2b^2+4\right)\theta-4+(-4b+4)\tau\right)w+B_7}{A_3} \tag{13}$$

$$p_m^{ps} = \frac{\left(((2\theta-1)b-2\theta+2)\tau^2+((-4\theta+2)b+2\theta-2)\tau+2b\left((k+1)\theta-2k-1/2\right)\right)w+B_8}{A_3} \tag{14}$$

$$p_r^{ps} = \frac{\left((-b^2+5b-4)\tau^2+(2b^2-5b+4)\tau+(-4k-1)b^2+4k+A_3-2\right)w+B_9}{A_3} \tag{15}$$

The values of A_i and B_i are shown in the Appendix.

4. Parameter analysis

4.1 Imperfect product probability

In general, it is common for defective quality products to sell for less than their cost of production in marketing, so we assume $c > p_l$. In this paper, it is assumed that the distribution of defect rate of products t is uniformed, that is, $t \sim \cup (0.02, 0.2)$. Next, we analyze the effect of the expected probability density of defective products on the optimal decision in three game situations.

$$\frac{dp_m^{ps}}{dE(t)} = \frac{2\left(\frac{1}{2}(b-1)(b-2\theta-2)\tau^2+(-b^2+(\theta+1)b-2\theta+1)\tau+\left(k+\frac{1}{2}\right)b-2k+\theta\right)(c-p_l)}{A_3} \tag{16}$$

<u>Proposition 3:</u> If $\frac{-(b-1)(b-2\theta-2)\tau^2+(2b^2+(-2\theta-2)b+4\theta-2)\tau-b^2-b-2\theta}{2b^2+2b-4} < k$, then $\frac{dp_m^{ps}}{dE(t)} > 0$, so the probability of defective products has a positive effect on the direct selling price.

$$\frac{dp_r^{sg}}{dE(t)} = \frac{(c-p_l)((b^3+b^2-2b)k+(-\tau^2+\tau)b^2+(\tau^2+1)b-2\tau+2)}{A_1} \tag{17}$$

<u>Proposition 4:</u> If $k < \frac{b^2\tau^2-b^2\tau-b\tau^2-b+2\tau-2}{b(b^2+b-2)}$, then $\frac{dp_r^{sg}}{dE(t)} < 0$, so imperfect product probability has a negative effect on retail price.
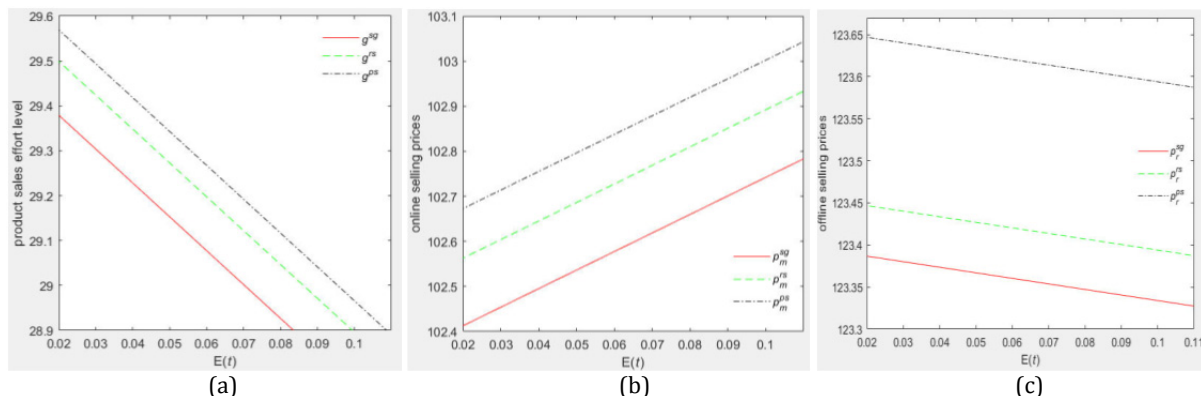

Fig. 2 The influence of defect rate on the optimal decision of (a) product sales effort level, (b) online selling prices and (c) offline selling prices

Obviously, as the expected probability density of defective products $E(t)$ increases, in order to offset the cost of quality loss and maximize their own profits, the manufacturer will reduce their sales efforts to products, Fig. 2(a), and increase the direct selling price of qualified products Fig. 2(b). However, in order to expand offline demand, the retailer will reduce retail prices, Fig. 2(c).

4.2 Consumer preference coefficient

The higher of the consumer's channel preference coefficient ρ, the more consumers are willing to experience or purchase products offline, so the demand of retail channel is more. Eq. (18) shows the first order derivative of the market demand of the offline channel in scenario 2, D_r^{rs}, with respect to consumer's preference coefficient, ρ.

$$\frac{dD_r^{rs}}{d\rho} = \frac{(\phi-1)(b^2k+(2k-\tau+1)b-4k+2\tau)\alpha}{A_2} \tag{18}$$

<u>Proposition 5:</u> If $\tau < \frac{kb^2+2kb-4k+b}{b-2}$, then $\frac{dD_r^{rs}}{d\rho} > 0$, so consumers' preference of offline channel has a positive effect on retailers' demand.

It can be concluded that the retailer increasing offline attraction to consumers, such as product experience, can increase the market demand for offline products and thus improve their expected profits.

4.3 The wholesale price

This sub-section analyzes the impact of manufacturer's wholesale prices on retailer's offline sales prices. Eq. (19) gives the first order derivative of offline selling prices under model 2, p_r^{rs}, with respect to the wholesale price, w.

$$\frac{dp_r^{rs}}{dw} = \frac{((4\phi-1)b-4\phi)\tau^2+((-4\phi+1)b+8\phi-4)\tau-2kb^2\phi+4k-4\phi+2}{A_2} \tag{19}$$

<u>Proposition 6:</u> If $\frac{4\tau^2b\phi-\tau^2b-4\tau^2\phi-4\tau b\phi+\tau b+8\tau\phi-4\tau-4\phi+2}{2(b^2\varphi-2)} < k$, then $\frac{dp_r^{rs}}{dw} > 0$, so the increase in wholesale prices has a positive impact on offline retail prices.

The increase of wholesale price proposed by the manufacturer will promote an increase in the offline selling price, and consumers will ultimately bear this part of the cost because of the retailer maximizing its profit.

5. Numerical simulation – Result and discussion

In this section, we will study the proposed 3 game model through numerical simulation and discuss the impact of key parameters. The parameter data is below in Table 2.

The sensitivity is mainly used to analyze the influence of direct channel demand sale efforts elasticity coefficient τ and sharing ratio (ϕ, θ) on the optimal values. At the same time, the paper analyzes the influence of sale efforts cost coefficient k on the profit of DCSC.

Table 2 Data of parameters

Parameter	ρ	α	$E(t)$	τ	b	p_l	c	k	ϕ	θ	w
Value	0.6	200	0.11	0.54	0.52	5	25	2	0.25	0.25	60

5.1 Direct channel demand sale efforts elasticity coefficient τ

To study the effects of sale efforts elasticity coefficient (τ), we donate $\phi = 0.25$，$\theta = 0.25$. For the given value of parameters, set the interval of τ to [0,1].

(a)

(b)

(c)

(d)
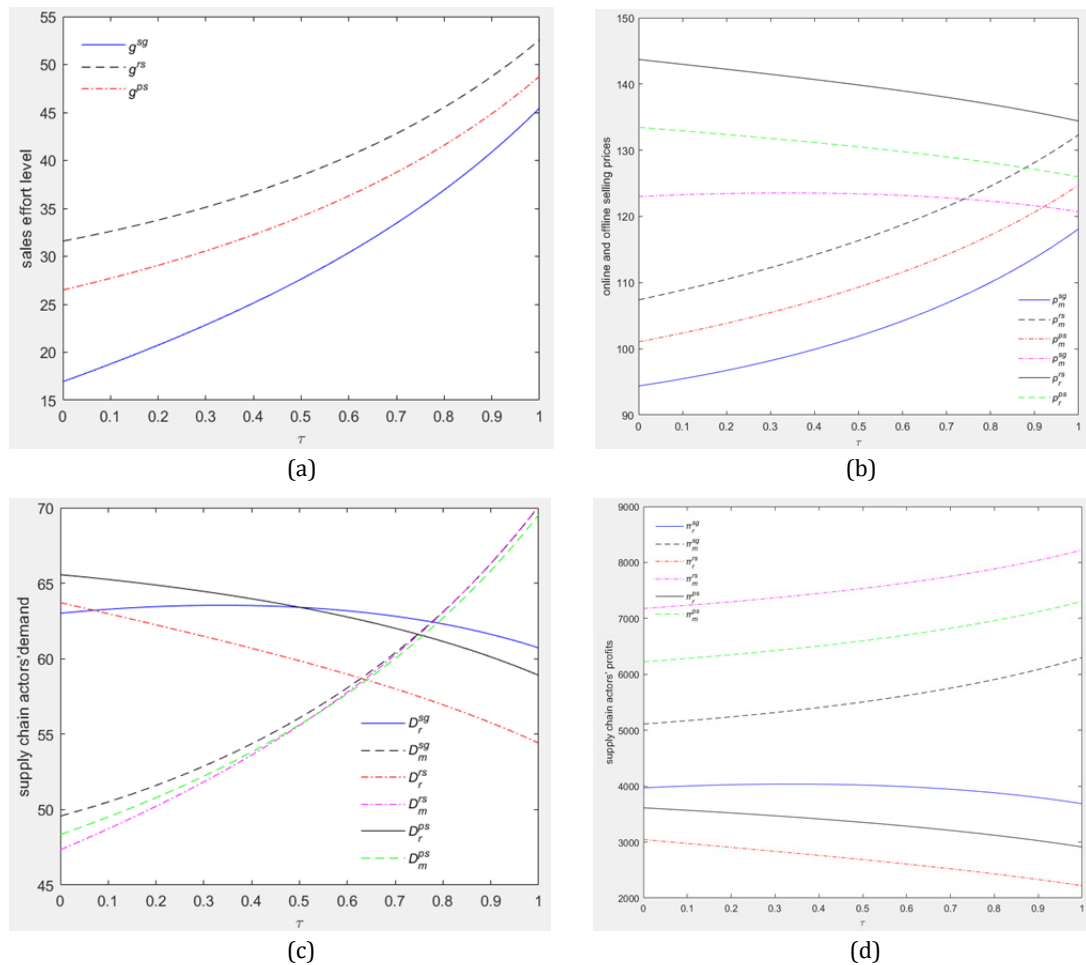
Fig. 3 The influence of sale efforts elasticity coefficient on the optimal decision of (a) sales effort level, (b) online and offline selling prices, (c) supply chain actors' demand, and (d) supply chain actors' profits

In Fig. 3(a), from the demand function of each channel, the sales effort level g increased with the sale efforts elasticity coefficient τ, but the cooperation model under scenario 2 had the highest level of sales effort. Because the larger τ value means the less possibility of free rider behavior, the more demand for direct sales channels, and the demand for traditional retail channels is decreasing, as shown in Fig. 3(c). As shown in Fig. 3(d), the retailer's profit is the lowest under scenario 2, but the overall profit of the DCSC can significantly improve. In Fig. 3(b), the online selling price increases with τ, but the offline selling price decreases with τ, and the traditional channel price is greater than the direct selling price.

5.2 Impact of the sharing ratio (ϕ, θ)

The sharing ratio (ϕ, θ) is also an important parameter influencing the optimal decision and demand in this study. Therefore, the manufacturer's sales effort elasticity coefficient (τ) is fixed at 0.54. In order to make the online sales price less than the offline sales price and the profit of DCSC members is positive, we set (ϕ, θ) belong to interval $[0.05, 0.45]$.

In Fig. 4(a), the sales effort level g increases with the sharing ratio (ϕ, θ), but the sales effort under the model 2 is greater than the other two scenarios. The manufacturer gets the most profit under the revenue-sharing contract, but the corresponding retailer's profit is the lowest, as shown in Fig. 4(d). Understandably, an increase in the sharing ratio (ϕ, θ) forces the retailer to increase offline selling prices, which in turn increases direct-sales prices, as shown in Fig. 4 (b). In Fig. 4(c), the increase in the proportion of manufacturer's revenue sharing will reduce the demand for retail channels and the demand for direct sales channels; However, the increase in the proportion of manufacturer's profit-sharing will increase the demand for retail channels and the demand for direct sales channels. Relatively speaking, the manufacturer is willing to use revenue sharing contracts, while the retailer prefers profit-sharing contracts.

(a)

(b)

(c)

(d)
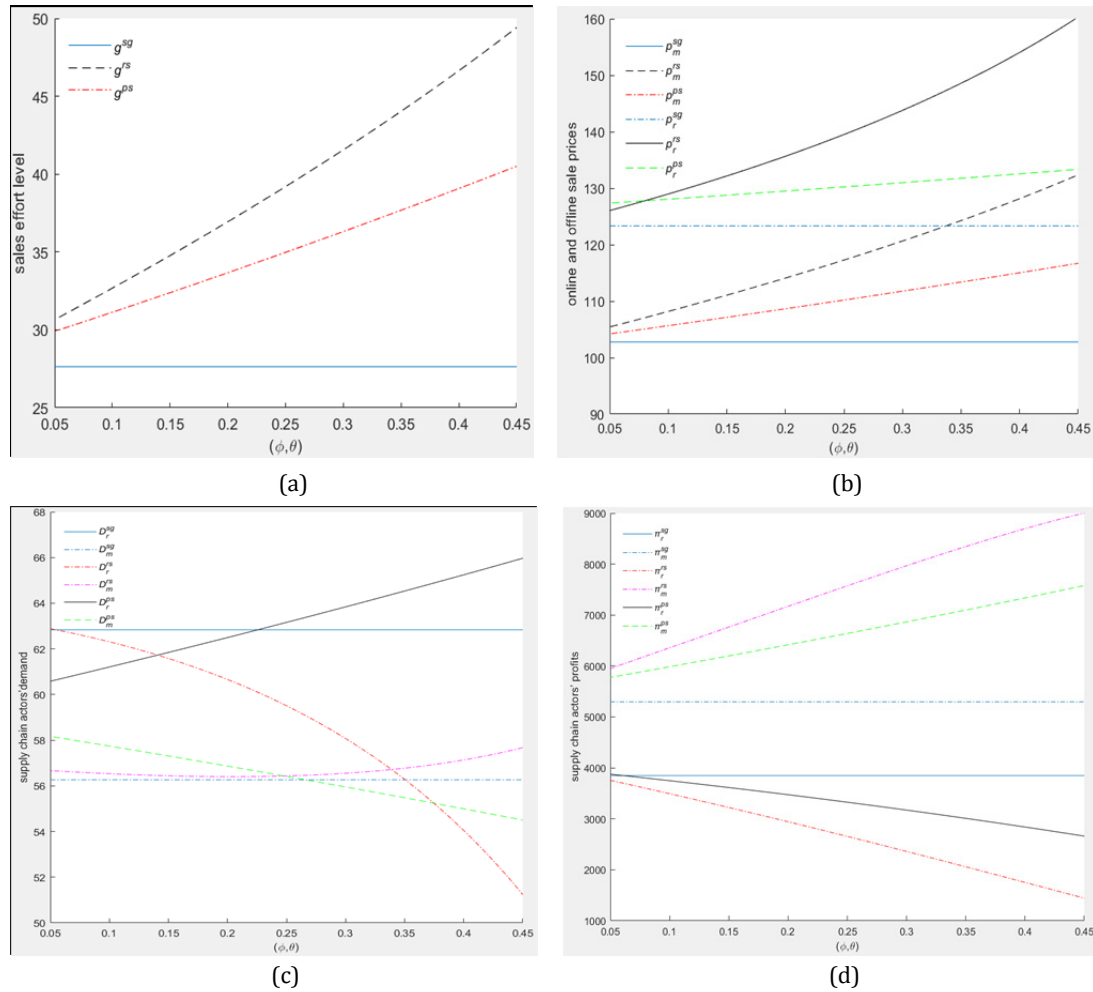
Fig. 4 The influence of sharing ratio on the optimal decision of (a)sales effort level, (b) online and offline sale prices, (c) supply chain actors' demand, and (d) supply chain actors' profits

5.3 Influence of k on the DCSC profit

Generally speaking, as the cost coefficient of sales effort k increases, manufacturer's motivation for promotion will be weakened.

(a)

(b)
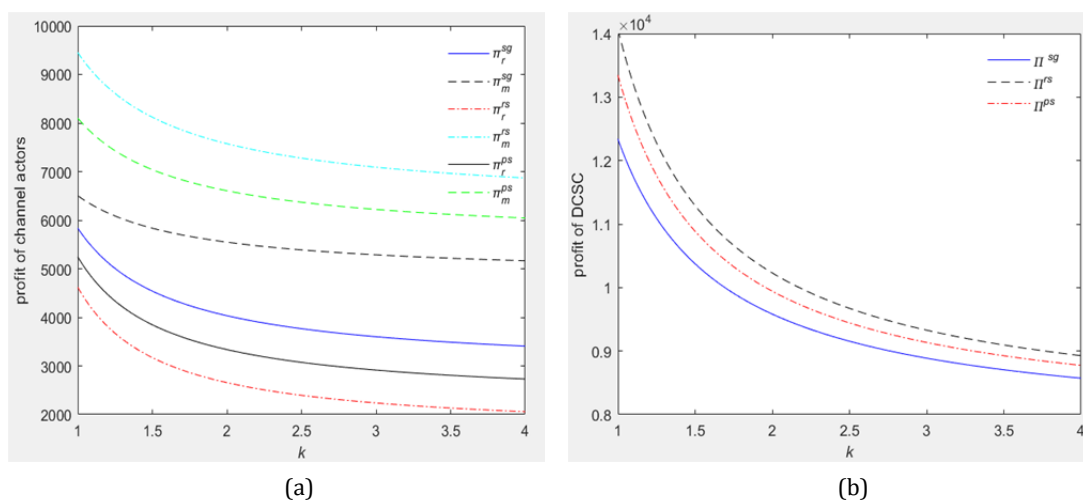
Fig. 5 The influence of cost coefficient of sales effort on profit of (a) channel actors, and (b) DCSC

As shown in Fig. 5, in the three game models, the profit of channel members will decrease with k, but the total profit of DCSC under scenario 2 is higher than other two models. If k increases, the level of manufacturer's sales effort will decrease, which brings about reducing the demand of direct sales channels. In order to mitigate the adverse impact of sales effort level on direct channel demand, the manufacturer reduces the online selling price(p_m). In addition, the demand in the offline channel will decline, prompting the retailer to reduce offline selling prices for expanding demand.

6. Conclusion

This paper discusses the pricing strategies and sales efforts with qualified product in a DCSC, which consists of a manufacturer and a retailer, and compared 3 game model. In addition, it considers that defective products are flow to the secondary market at a low price. The level of sale efforts and online selling price are the decision variables of the manufacturer, while the decision variable of retailer is offline selling price. We studied a competition and two coordination situations between DCSC members, determined their optimal strategies, and analyzed the model through numerical examples. The results showed that the product defect rate has considerable impact on pricing and sales efforts. For consumers who are pursuing price, competition between the DCSC actors is advantageous. In the light of DCSC profits, cooperation between the manufacturer and retailer is more profitable than channel competition, and they are more willing to make product sales efforts. In order to maximize profits, the manufacturer is more inclined to choose revenue-sharing contracts.

Although the model proposed in this paper is more in line with enterprise production management practices, there are still some shortcomings. This article only assumes that the product defect rate follows a uniform distribution, and does not consider more complicated situations, such as following the positive distribution. In addition, the flow of defective products to the secondary market may also have a certain impact on the demand for qualified products, which we have not taken into account. This paper only considers that the manufacturer set up online channels, which is just a form of DCSC, and does not study retailer building online channels.

Acknowledgement

References

[1] Milić, B., Rosi, B., Gumzej, R. (2019). An approach to E-marketplace automation, *Tehnički Vjesnik – Technical Gazette,* Vol. 26, No. 3, 639-649, doi: 10.17559/tv-20171201150248.

[2] Burinskiene, A. (2018). New challenges for supply chain: Electronic invoicing and its use perspective, *Journal of Logistics, Informatics and Service Science*, Vol. 5, No. 1, 31-42.

[3] Chen, J., Liang, L., Yao, D.-Q., Sun, S. (2017). Price and quality decisions in dual-channel supply chains, *European Journal of Operational Research*, Vol. 259, No. 3, 935-948, doi: 10.1016/j.ejor.2016.11.016.

[4] Taleizadeh, A.A., Khanbaglo, M.P.S., Cárdenas-Barrón, L.E. (2016). An EOQ inventory model with partial backordering and reparation of imperfect products, *International Journal of Production Economics*, Vol. 182, 418-434, doi: 10.1016/j.ijpe.2016.09.013.

[5] Modak, N.M., Panda, S., Sana, S.S. (2016). Three-echelon supply chain coordination considering duopolistic retailers with perfect quality products, *International Journal of Production Economics*, Vol. 182, 564-578, doi: 10.1016/j.ijpe.2015.05.021.

[6] Rad, M.A., Khoshalhan, F., Glock, C.H. (2018). Optimal production and distribution policies for a two-stage supply chain with imperfect items and price-and advertisement-sensitive demand: A note, *Applied Mathematical Modelling*, Vol. 57, 625-632, doi: 10.1016/j.apm.2016.11.003.

[7] Li, W., Chen, J., Liang, G., Chen, B. (2018). Money-back guarantee and personalized pricing in a Stackelberg manufacturer's dual-channel supply chain, *International Journal of Production Economics*, Vol. 197, 84-98, doi: 10.1016/j.ijpe.2017.12.027.

[8]   Hu, H., Wu, Q., Zhang, Z., Han, S. (2019). Effect of the manufacturer quality inspection policy on the supply chain decision-making and profits, *Advances in Production Engineering & Management*, Vol. 14, No. 4, 472-482, doi: 10.14743/apem2019.4.342.

[9]   Tsao, Y.-C. (2015). Cooperative promotion under demand uncertainty, *International Journal of Production Economics*, Vol. 167, 45-49, doi: 10.1016/j.ijpe.2015.05.023.

[10] De Giovanni, P. (2011). Quality improvement vs. advertising support: Which strategy works better for a manufacturer?, *European Journal of Operational Research*, Vol. 208, No. 2, 119-130, doi: 10.1016/j.ejor.2010.08.003.

[11] Pu, X., Gong, L., Han, X. (2017). Consumer free riding: Coordinating sales effort in a dual-channel supply chain, *Electronic Commerce Research and Applications*, Vol. 22, 1-12, doi: 10.1016/j.elerap.2016.11.002.

[12] Li, B., Hou, P.-W., Li, Q.-H. (2015). Cooperative advertising in a dual-channel supply chain with a fairness concern of the manufacturer, *IMA Journal of Management Mathematics*, Vol. 28, No. 2, 259-277, doi: 10.1093/imaman/dpv025.

[13] Chen, X., Zhang, W., Gu, W. (2019). Coordination of two-echelon pharmaceutical supply chain with dual-channel considering promotion behavior and consumer preference, *Industrial Engineering & Management*, Vol. 24, No. 139, 24-33.

[14] Ranjan, A., Jha, J.K. (2019). Pricing and coordination strategies of a dual-channel supply chain considering green quality and sales effort, *Journal of Cleaner Production*, Vol. 218, 409-424, doi: 10.1016/j.jclepro.2019.01.297.

[15] Wang, L., Song, Q. (2020). Pricing policies for dual-channel supply chain with green investment and sales effort under uncertain demand, *Mathematics and Computers in Simulation*, Vol. 171, 79-93, doi: 10.1016/j.matcom.2019.08.010.

[16] Nazifa, T.H., Ramachandran, K.K. (2019). Information sharing in supply chain management: A case study between the cooperative partners in manufacturing industry, *Journal of System and Management Sciences*, Vol. 9, No. 1, 19-47.

[17] Zhu, X.D., Li, B.Y., Wang, Z. (2017). A study on the manufacturing decision-making and optimization of hybrid-channel supply chain for original equipment manufacturer, *Advances in Production Engineering & Management,* Vol. 12, No. 2, 185-195, doi: 10.14743/apem2017.2.250.

[18] Cai, G., Zhang, Z.G., Zhang, M. (2009). Game theoretical perspectives on dual-channel supply chain competition with price discounts and pricing schemes, *International Journal of Production Economics*, Vol. 117, No. 1, 80-96, doi: 10.1016/j.ijpe.2008.08.053.

[19] Chen, J., Zhang, H., Sun, Y. (2012). Implementing coordination contracts in a manufacturer Stackelberg dual-channel supply chain, *Omega*, Vol. 40, No. 5, 571-583, doi: 10.1016/j.omega.2011.11.005.

[20] He, L., Zhang, X., Wang, Q.P., Hu, C.L. (2018). Game theoretic analysis of supply chain based on mean-variance approach under cap-and-trade policy, *Advances in Production Engineering & Management,* Vol. 13, No. 3, 333-344, doi: 10.14743/apem2018.3.294.

[21] Liu, H., Sun, S., Lei, M., Leong, G.K., Deng, H. (2016). Research on cost information sharing and channel choice in a dual-channel supply chain, *Mathematical Problems in Engineering*, Vol. 2016, Article ID 4368326, doi: 10.1155/2016/4368326.

[22] Ha, A., Long, X., Nasiry, J. (2016). Quality in supply chain encroachment, *Manufacturing & Service Operations Management*, Vol. 18, No. 2, 280-298, doi: 10.1287/msom.2015.0562.

[23] Jabarzare, N., Rasti-Barzoki, M. (2020). A game theoretic approach for pricing and determining quality level through coordination contracts in a dual-channel supply chain including manufacturer and packaging company, *International Journal of Production Economics*, Vol. 221, Article ID 107480, doi: 10.1016/j.ijpe.2019.09.001.

[24] Jafari, H., Hejazi, S.R., Rasti-Barzoki, M. (2016). Pricing decisions in dual-channel supply chain including monopolistic manufacturer and duopolistic retailers: A game-theoretic approach, *Journal of Industry, Competition and Trade*, Vol. 16, No. 3, 323-343, doi: 10.1007/s10842-016-0224-1.

[25] Zhou, J., Zhao, R., Wang, W. (2019). Pricing decision of a manufacturer in a dual-channel supply chain with asymmetric information, *European Journal of Operational Research*, Vol. 278, No. 3, 809-820, doi: 10.1016/j.ejor.2019.05.006.

[26] Jian, M., Wang, Y.L. (2018). Decision-making strategies in supply chain management with a waste-averse and stockout-averse manufacturer, *Advances in Production Engineering & Management,* Vol. 13, No. 3, 345-357, doi: 10.14743/apem2018.3.295.

Appendix

For the convenience of calculation, we let $X = \mathrm{E}(r)p_l - \big(1 + E(r)\big)c$. Since the price of the defective product is usually lower than the production cost, we have $X < 0$. Similarly, A_i represents the denominator of the optimal decision in the three scenarios, and B_i is obtained by numerator merging of similar items.

$$X = \mathrm{E}(r)p_l - \big(1 + E(r)\big)c \tag{A1}$$

$$A_1 = (\tau^2 + 4k - 2\tau + 1)b^2 + (-4\tau^2 + 4\tau)b + 4\tau^2 - 8k \tag{A2}$$

$$B_1 = \big((b-2)\tau - b\big)(b\rho - 2\rho + 2)\alpha - 4w(1 + (b-1)\tau) \tag{A3}$$

$$B_2 = \big((-\tau^2 - 2k + 2\tau - 1)b^2 + (3\tau^2 - 2k - 2\tau - 1)b - 2\tau^2 + 4k - 2\tau\big)X - 2k\alpha(b\rho - 2\rho + 2) \tag{A4}$$

$$B_3 = -kXb^3 + (\alpha k\rho - X(-\tau^2 + k + \tau))b^2 + ((-\tau^2 + (-\rho + 2)\tau + (2\rho - 2)k + \rho - 1)\alpha - X\tau^2 + X(2k - 1))b + (2\tau^2 + (2\rho - 2)\tau - 4\rho k)\alpha + 2X(\tau - 1) \tag{A5}$$

$$A_2 = 2\left(\left(\tfrac{1}{2}b^2 + (-2\phi - 2)b + 2\phi + 2\right)\tau^2 - (b - 2)(b - 2\phi)\tau + \left(k\phi + 2k + \tfrac{1}{2}\right)b^2 - 4k + 2\phi\right)(\phi - 1) \tag{A6}$$

$$B_4 = -(\phi - 1)\left(X(\tau - 1)b^3 + (-\rho(\tau - 1)\alpha + (-2X\phi - X)\tau - X)b^2 + \left(4(\tau + 1)\left(\left(\rho - \tfrac{1}{2}\right)\tau - \tfrac{1}{2}\rho + \tfrac{1}{2}\right)\alpha + 2X(\tau\phi - \phi + 1)\right)b + ((-4\rho\phi - 4\rho + 4)\tau + 4\rho\phi)\alpha + 4X\right) \tag{A7}$$

$$B_5 = -2\left(\left(\tfrac{1}{2}(b - 1)(b - 2\varphi - 2)\tau^2 + ((b - 2)\phi - b^2 + b + 1)\tau + \phi + \left(\tfrac{1}{2} + k\right)b^2 + \left(\tfrac{1}{2} + k\right)b - 2k\right)X + (-\tau^2\phi - \phi(\rho - 2)\tau + (bk\rho + \rho - 1)\phi + k(b\rho - 2\rho + 2))\alpha\right)(\phi - 1) \tag{A8}$$

$$B_6 = -(\phi - 1)\left(kXb^3 + (-\alpha k\rho + X(-\tau^2 + k + \tau))b^2 + ((\tau^2 + (\rho - 2)\tau + (-2\rho + 2)k - \rho + 1)\alpha + X\tau^2 + (-2k + 1)X)b + (-2\tau^2 + (-2\rho + 2)\tau + 4\rho k)\alpha - 2X(\tau - 1)\right) \tag{A9}$$

$$A_3 = (b^2 + (-4\theta - 4)b + 4\theta + 4)\tau^2 - 2(b - 2)(b - 2\theta)\tau + (2k\theta + 4k + 1)b^2 - 8k + 4\theta \tag{A10}$$

$$B_7 = -X(\tau - 1)b^3 + (\rho(\tau - 1)\alpha + (2X\theta + X)\tau + X)b^2 + \left(-4(\theta + 1)\left(\left(\rho - \tfrac{1}{2}\right)\tau - \tfrac{1}{2}\rho + \tfrac{1}{2}\right)\alpha - 2X(\tau\theta - \theta + 1)\right)b + ((4\rho\theta + 4\rho - 4)\tau - 4\rho\theta)\alpha - 4X$$
$$\tag{A11}$$

$$B_8 = (-(b - 1)(b - 2\theta - 2)\tau^2 + (2b^2 + (-2\theta - 2)b + 4\theta - 2)\tau + (-2k - 1)b^2 + (-2k - 1)b + 4k - 2\theta)X - 2\left(-\tau^2\theta - \theta(\rho - 2)\tau + k\rho(\theta + 1)b - 2\left(k - \tfrac{1}{2}\theta\right)(\rho - 1)\right)\alpha \tag{A12}$$

$$B_9 = -kXb^3 + (\alpha k\rho - X(-\tau^2 + k + \tau))b^2 + ((-\tau^2 + (-\rho + 2)\tau + (2\rho - 2)k + \rho - 1)\alpha - X\tau^2 + X(2k - 1))b + (2\tau^2 + (2\rho - 2)\tau - 4\rho k)\alpha + 2X(\tau - 1) \tag{A13}$$

Hybrid evolution strategy approach for robust permutation flowshop scheduling

Khurshid, B.[a], **Maqsood, S.**[b,*], **Omair, M.**[b], **Nawaz, R.**[a], **Akhtar, R.**[a]

[a]Department of Industrial Engineering, University of Engineering and Technology, Peshawar, Pakistan
[b]Department of Industrial Engineering, Jalozai Campus, University of Engineering and Technology, Peshawar, Pakistan

A B S T R A C T

In this paper, a robust schedule has been proposed to deal with uncertainities for *m*-machines permutation flow shop problems. A robust schedule ensures that the expected finish time is always less than the makespan. To use the global search ability of the evolution strategy (ES) and local search ability of Tabu Search (TS), a hybrid evolution strategy (HES) is proposed by combining Improved ES with TS to generate the robust schedules. The robust schedule is first generated using ES and then the solution is optimized using TS for maximum exploitation and exploration of the solution space. For maximum exploitation in ES, *(1+9)* reproduction operator and double swap mutation is used. Also variable mutation rate is used for fine tuning of the results. In TS, the length of Tabu list is fixed, also lower bound is used to save computational time. The hybrid algorithm is tested on Carlier and Reeves benchmark problems taken from the OR-library. Achieved results are compared with other famous techniques available in the literature, and the results show that HES performs better than other techniques and provides an affirmative percentage increase in the probability that the expected finish time is less than the makespan.

1. Introduction

Scheduling in services and manufacturing sectors refers to the allocation of tasks or activities to resources in a determined process for minimization of costs and optimizing operational efficiency [1]. Based on the structure of the environment, scheduling has many types. Flow shop scheduling has practical implementation in automobile, pharmaceutical, pump, chemical, steel industry and is addressed in this paper [2]. Permutation flow shop scheduling problems (PFSSP) has been the focus for most researchers in the recent past, however they have mostly focused on a deterministic environment. Study of deterministic PFSSP is relatively easier as all the parameters are known in advance [3].

However uncertain events arrive in real-life situations and the uncertainties are induced in processing times, which will affect the makespan of schedule [4]. Thus there are chances that some jobs will not be completed in the expected finish time and hence the production gets delayed. Hence more focus should be paid to uncertainties in PFSSP [5, 6].

In stochastic scheduling, processing times of jobs are random and till their finish they are unknown. Hence in scheduling, real-life situations should be able to deal with these stochastic events. A good scheduling environment should cope with these uncertain situations and produce a robust schedule. If the behavior of a schedule does not degrade significantly in the face of a

disruption it is termed as a robust schedule. Hence a robust schedule is insensitive to the occurrence of uncertain events. Robust scheduling is currently being used in various real-life situations to, i.e. manufacturing industry, airline crew scheduling, project scheduling, and process industry. The present research is focused on robust scheduling for the manufacturing industry.

The two common approaches presently used in robust scheduling are reactive and proactive scheduling [7]. In proactive scheduling, future disruptions are taken into account while generating the initial schedule. However reactive scheduling does not take future disruptions in account while generating the initial schedule, and the schedule is revised after the occurrence of a disruption. In this paper, a proactive approach is used for robust scheduling.

Since the deterministic PFSSP is classified as an NP-hard problem [8], therefore the stochastic PFSSP is also an NP-hard problem. Hence exact methods cannot be used to solve the large size problem, therefore approximation methods should be used for their solutions [9]. Under uncertainties, González-Neira *et al.* [6] carried out a detailed literature review of flow shop problems. He defined role of scheduling and guided further areas of research. He surveyed 100 papers and in most of the papers makespan was the main objective, while very limited papers were focused on multi objectives.

The remainder of the paper is organized as follows. A detailed literature review is provided in Section 2. Section 3 explains the problem statement while methodology is presented in Section 4. The robust schedule is explained in Section 5 while computational results are explained in Section 6. Finally, conclusions and recommendations are suggested in Section 7.

2. Literature review

Robustness of a schedule can be defined using different measures [10]. Mostly researchers have minimized the variation of a performance indicator [11-13]. However, the robust schedules do not guarantee that the performance indicator will not exceed limits as uncertainty occurs. Initially, Daniels and Carrillo [14] proposed a robust solution to address the uncertainties of processing times in a single machine environment using a Branch and Bound (B & B) method and a heuristic approach. They discovered the risk of the inferior system, by considering the variance and mean performance in appraising alternative schedules. An exact dynamic program was used by Yang and Yu [11] to find a robust schedule for a single machine environment with three performance measures. Kuo and Lin [15] Studied robustness for a single machine environment with total flow time as the objective function. The authors used a fractional programming framework to find robust schedules. Using an algorithm they suggested worst case scenario and worst case relative deviation, then a parametric programming algorithm was used to find robust schedule.

A robust multi-objective problem was studied by Jia and Ierapetritou [16] incorporating robustness, economic expectation and expected unsatisfied demand. Based on a Tabu Search (TS) algorithm, a robust and stable schedule was proposed by Goren and Sabuncuoglu [13]. For a single machine scheduling problem, the proposed algorithm-generated robust and stable schedules for three performance parameters, i.e. total flow time, makespan and total tardiness. The algorithm constitutes two parts, i.e. sequence generator and sequence evaluator. In order to cope with uncertain situations in a single machine environment, a robust schedule was proposed by Wu *et al.* [17] using dominance rules. The objective was to minimize the risk that makespan will not exceed the maximum threshold. He proposed three models, i.e. combined, primal and a dual model to solve the problem, however, the combined method was the most efficient one.

Mostly the research has been focused on a single machine and it doesn't represent actual cases of PFSSP. By increasing the number of machines, the effect of uncertainty in scheduling environment increases. A robust schedule for *m*-machines PFSSP was first studied by Liu *et al.* [7] using an improved genetic algorithm (IGA). The IGA used a new generation scheme to preserve the good characteristics of parents. The IGA was tested on Carlier and Reeves problems, and compared with the results of NEH heuristic. Results showed that IGA performed better than NEH and also produced an affirmative percentage that the expected finish time is always less than the makespan.

For machine breakdown uncertainty, Fazayeli *et al.* [18] proposed a Hybrid Meta heuristic for maximizing β-robustness of makespan, he hybridized genetic algorithm with simulated annealing and outperformed six other heuristics. For uncertain setup and processing times, Gholami-Zanjani *et al.* [19] suggested a Robust optimization and a Fuzzy Optimization approaches to minimize the weighted mean completion time. For two machine problem, Rahmani [20] used surrogate measures for uncertain processing times and machine failures. The algorithm worked in two step structure, initially a schedule was generated for processing times and then a reactive schedule was generated after machine failure. In view of the robust starting times, Cui *et al.* [21] Proposed a Weibull distribution considering machine failures to minimize makespan. The algorithm proceeded in two loop, first local serach is initialized using NEH and then genetic algorithm is used in second loop.

For the uncertainties of processing times in *m*-machines, Ma *et al.* [22] proposed a robust schedule based on an artificial bee colony algorithm (ABC). To enhance the exploitation and exploration of ABC, an improved local search scheme was introduced in ABC. The algorithm was tested on famous Carlier and Reeves problems and compared with the results of IGA and NEH. Results show that ABC finds a better robust schedule as compared to IGA and NEH. For stochastic processing times, González-Neira *et al.* [23] proposed a simheuristic approach to solve multi objective PFSSP. The objectives are minimization of expected deviation of tardiness and tardiness. Tabu Search is hybridized with a Monte Carlo simulation and a Pareto archived evolution strategy in the simheuristic approach and tested on 540 benchmark instances. In addition he applied the simheuristic approach on an optical laboratory case and found better results for expected and standard deviation as compared to the sequences used by the laboratory.

Recently various meta-heuristics have been used by numerous researchers for PFSSP and other related problems, e.g. GA, ABC, TS, ES [24-31]. Although GA is fast, however, their searchability is reduced due to their lack of local search adaptability. ABC algorithms are simple however they often get trapped in local optimum [22]. TS is a local search technique and is widely used for the discrete optimization problem, however, it becomes slow for large-sized problems. ES was developed by Rechenberg in 1970 for parameter optimization problems, however recently they have been applied to discrete problems. ES performs better for global search and contains information of the previous solutions, however sometime it gets trapped in a local minima after certain iterations, in this condition the ES jumps out of the local minima by using large mutation rate.

The two key parameters for the performance of any algorithm are: i) Exploiting the best solutions and ii) Exploring the search space. Hence the global search ability of ES should be combined with local search ability of TS for better performance. Hence in this paper, a hybrid evolution strategy (HES) is proposed by combining an ES with TS to find robust schedules for *m*-machines PFSSP. The ES is improved by using, *(1+9)* reproduction operator and double swap mutation operator, also variable mutation rate is used for fine tuning of the results. To save the computation time of TS, the length of Tabu list is fixed and lower bound is used. With all these improvements, the HES finds optimal solution in minimum computational time.

3. Problem statement

In a PFSSP, *n*-jobs are processed in fixed order on *m*-machines. At time zero all the jobs are available and they are independent. The first machine has no idle time and each machine can simultaneously process one job. The processing time of the job includes setup and transportation times. Each job has M operations and they are performed on different machines. The processing order of the job is the same on every machine. All machines are continuously available and preemption is not allowed. The due date for all jobs is the same and there is unlimited buffer space. Processing time of job I on machine j is represented at P_{ij} and the Corresponding finish time is represented at C_{ij}. The finish time for the last job is termed as makespan and is represented at C_{max}. Mathematically PFSSP can be represented as below:

$$C_{11} = P_{11} \tag{1}$$

$$Ci_1 = \sum_{r=1}^{i} P_{r_1} \qquad \text{where } i = 1,2,\dots,N \tag{2}$$

$$C_{1_j} = \sum_{r=1}^{j} P_{1_r} \qquad \text{where } j = 1,2,\dots,M \tag{3}$$

$$C_{max} = \max\{C_i(j-1), \qquad C(i-1)\} + P_{ij} \tag{4}$$

$$Objective = max\{Probability(C_{max} \leq Expected\ Finish\ Time)\} \tag{5}$$

4. Robust schedule

When the processing times for jobs are uncertain, then for *m*-machines PFSSP and *n*-jobs, a schedule which ensures maximum probability that the expected finish time is less that the makespan is termed as robust schedule. Mathematically, for a robust schedule the probability ($C_{max} \leq X$) is maximum.

The processing time uncertainty in a robust schedule can be presented by fuzzy logic or probabilistic technique. The probabilistic technique is normally used for processing time uncertainty, where the distribution describes the processing time uncertainty. Actual data is taken from the jobs processing time, and then it is analyzed to know the distribution of processing time. Ample processing time data through repeat production is required to know the distribution of processing time. The processing time uncertainty is an independent random variable and according to the central limit theorem, its distribution formed is a normal distribution. Hence job processing time follows normal distribution according to the central limit theorem. If two numbers *A* and *B* follow normal distribution then their sum *A + B* also follows a normal distribution. Hence makespan computed from normally distributed processing times follows a normal distribution as depicted in Fig. 1.

For normally distributed makespan, the probability that the expected finish time is less than makespan is calculated using Eq. 4.
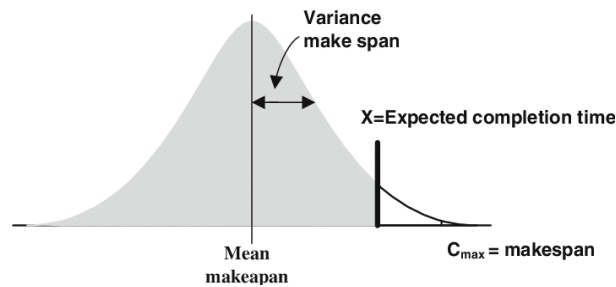
Fig. 1 Normal distribution curve for makespan

$$Probability\ (Cmax \leq X) = \frac{1}{2} + \varphi(z) \tag{6}$$

$$\text{where} \quad z \geq 0 \ \text{and} \ z = \frac{X - \mu Cnm}{6CnMx} \tag{7}$$

$$\text{and} \quad \varphi(z) = \frac{1}{\sqrt{2p}} \int_{-\infty}^{z} e^{-(t2/2)}\, dt \tag{8}$$

$$\emptyset(z) \approx \varphi(z) = \begin{cases} 0.1z(4.4 - z) & (0 \leq z \leq 2.2) \\ 0.49 & (2.2 \leq z \leq 2.6) \\ 0.50 & (z \geq 2.6) \end{cases} \tag{9}$$

It is difficult to find the value of *z* through the exact method. However, Hayter [32] proposed a mathematical equation to find its approximate value as shown in Eq. 9.

5. Methodology

5.1 Evolution strategy

Evolution strategy (ES) is a subclass of an evolutionary algorithm and was developed was Rechenberg [33]. ES is based on the Darwinian Paradigm of evolution and its performance depends on the strength of its various genetic operators, i.e. selection, reproduction, recombination, evaluation. ES operates with a population of size *(μ + λ)*, where *μ* represents individual parent and *λ* represents the offspring. ES is an iterative process developed for the numerical optimization process and the solution space is searched through the population of individual solutions. The mutation operator is the main genetic operator in ES [34]. In Literature different reproduction operators have been used for ES, i.e. *(1+1), (1+4), (1+9), (1+16)* ([35, 36]).

Two selection operators are normally used in ES, i.e. *(μ+λ)-ES* and *(μ, λ)-ES*. In *(μ+λ)-ES*, both the parents and offspring's take part in the selection process and it is recommended for combinatorial optimization problems. While in *(μ, λ)-ES* only the offspring's take part in the selection process and it is recommended for real value parameter optimization problems.

The performance of ES is heavily dependent on the strength of its mutation operator and is the main source of genetic variation in ES. The mutation operator is problem-dependent, and their appropriate selection is an art. Various mutation operators can be used for PFSSP, however, swap operators are best for PFSSP [37].

5.2 Improved evolution strategy (IES)

In order to maximize the exploration and exploitation of the solution space, the following improvements have been made (procedure for the IES is in Fig. 2):

Pseudocode for the IES
Input Parameters:
Total Number of generations
Mutation rate
Population size
Number of off springs to be produced from parent(λ=9)
Record Parameters: Total number of generations and best makespan
1:        Parent population randomly generated, Pp
2:        for gen =1: k
3:        Evaluate parent population
4:        If number of generations (k) is not achieved go to step 7
5:             else
6:        end
7:             for v= 2: μ
8:        Produce offsprings and apply mutation operator (double swap mutation operator)
9:             Update population, Pi
10:       Evaluate all offsprings
11:       end for
12:       Evaluate Pi and fittest individual should be termed as parent for new iteration
13:    If an offspring has minimum makespan it is termed as candidate (OS1-OS9=C)
14:       else
15:       Parent is termed as candidate (P=C)
16:       end
17:       Until number of iterations are achieved go to step 2
18:       Record Total number of generations and best makespan

Fig. 2 Pseudocode for IES

- For maximum exploitation of the solution space, *(1+9)* reproduction operator is used. From 1 parent 9 offspring's are generated.
- The selection scheme used is *(1+9)* instead of *(1, 9)*, hence the selection pool consists of 10 entities, and the best offspring is selected from the pool, so the parent can survive for many generations. In *(1, 9)* parents die out of the selection pool and only children are available for selection.
- In order to increase the genetic variation, the large mutation rate is used initially and then it is reduced for fine-tuning of global minima.
- To save computational time and for maximum exploitation of search space, double swap mutation operator is used.

5.3 Tabu search (TS)

TS is a local search technique where the neighborhood is deterministically selected. For combinatorial optimization problems, TS is one of the most effective local search techniques for finding near-optimal solutions [38]. The local search technique starts with a solution and then find the best solution in the neighborhood. TS is good to avoid local minima and improving the solution through iterations. TS helps in exploring the solution beyond local optimality. TS starts from a basic schedule and by searching its neighborhood, moves generate a set of iterations with the lowest makespan. The exploration is then started from the previous best iteration as a new iteration and the search process continues.

The key steps of the TS algorithm are an initial solution, evaluation, move, neighborhood search, memory, searching strategy and termination criteria.

To avoid duplication of job swaps, a record of moves is kept in the list termed as Tabu List. The key benefit of TS is the use of Tabu List to avoid duplication and overcoming local optima and guiding the solution to the region which have not been explored. The infinite length of the tabu list is not recommended as it slows down the algorithm. For finite Tabu List, FIFO strategy is used, so as new attributes are inserted the old attributes are removed. The algorithm is terminated if the number of iterations have reached, or the computational time has reached, or there is no improvement in makespan after significant iterations, or the neighborhood is empty. The performance and speed of convergence for any TS algorithm is based on the accurate design of its components.

Following improvements have been made in the basic TS algorithm:

- To save the computational time of our TS algorithm, we have used lower bound and a number of iterations instead of explicitly finding the best makespan.
- To avoid local minima, Tabu List having fixed length is used.
- Since the TS improves the solution found by IES, hence global search ability of ES is united with local search ability of TS to find the best results.

Move and neighborhood

Every solution in our algorithm is represented by iteration. Using a set of moves, the neighborhood of a solution is generated. Then, using the Move function, the solution is transformed into another solution. The subset of moves associated with a given solution produces a set of solutions known as neighborhood. At each iteration, the neighborhood is searched to find the best in the neighborhood. Again move is performed, and a solution is generated from the previous best solution and becomes the current solution and the iteration continues.

The two main types of moves for TS are i) E-move, Exchange Jobs at the ath and b^{th} position. ii) *L*-move, Remove a job at a^{th} position and put it at b^{th} position. Although E-move is complex however it provides a better result and has been used in this paper. Since ample computational time is required for the large neighborhood, hence to save computation time lower bounds are used instead of calculating makespan explicitly.

Tabu list

The primary purpose of Tabu list is used to prevent cycling during the search. In literature various methods are available for implementation of Tabu list: i) Pairs of executed iterations, ii) Job and its position, iii) Makespan of executed iterations, iv) Pair of jobs along with their positions. The design of the appropriate Tabu list is a major factor for the performance and convergence of the TS algorithm.

Based on problem type the length of Tabu List can be fixed or dynamic. In this paper fixed length has been used. Let *TL= (TL$_1$,…, TL$_t$)* be a fixed Tabu List with length *t*, and *Tj=(g, h)* is a pair of jobs. Initially, the Tabu List is started with zero elements *Tj= (0, 0)*, where *j=1,.., t*. Let *υ= (a, b)* a move performed from an iteration π, after this move the Tabu List will be updated *Tj=Tj+1* where *j=1,.., t-1*. Then set *Tt= (π (a), π (a+1))* if *a<b* and *Tt= (π (a-1), π (a))* if *a>b*. An iteration *β* cannot be performed from a move *υ= (a, b)* if minimum one pair *(β (j), β (a)), j=a+1,…, b* is in *T* if *a<b* and minimum one pair *(β (a), β (j)), j=b,..a-1* is in *T*.

Procedure for the TS is in Fig. 3:

Pseudocode for the TS
Input:
Number of iterations, k
Size of move list ((a1,b1), (ai+1,bi+1) where i=…n
Total generations, k
1:　　　Use the final sequence from ES as a starting sequence(So) for TS 　　　　　So= (J$_1$, J$_2$,.. J$_n$) where n=number of jobs
2:　　　for gen =1: k
3:　　　Evaluate sequence, G(So)
4:　　　Interchange adjacent wise pairs of So to generate new sequence(Sc) (Exchange Jobs at the ath and bth position)
5:　　　Evaluate candidate sequence G(Sc)
6:　　　IF
7:　　　　　　G(Sc)<G(So) 　　　Then　　　So=Sc
8:　　　　　　　Update move in Tabu List(a1≠a1+1≠b1≠b1+1)
9:　　　　　end
10:　IF
11:　　　　　C$_{max}$=LB
12:　　　　　Go to step 16
13:　　　　　Else Continue
14:　　　　　End
15:　　　repeat until loop (Go to step 2)
16:　　　Output C$_{max}$ and Total generations

Fig. 3 Pseudocode for TS

6. Computational results and discussion

To evaluate the robustness of HES, results are compared with other well-known techniques available in the literature. Probability ($C_{max} \leq X$) of HES is compared with the probability ($C_{max} \leq X$) of other known techniques. Robust schedule dealt is the paper was first presented by Liu, Ullah [7] for *m*-machines PFSSP, he used IGA to find a robust schedule and compared his results with the robust schedule generated by NEH heuristic [39]. The IGA performed better than NEH based on the objective of probability ($C_{max} \leq X$). An ABC algorithm was suggested by Ma, Wang [22] for *m*-machines PFSSP and found better results than IGA and NEH. Hence in order to validate HES for robust schedules it results will be compared with IGA, NEH, and ABC. Results of IGA and ABC are taken from their original papers. Results of HES cannot be compared with other technqiues as robust schedules for benchmark problems of Carlier [40] and Reeves [41] are only generated by IGA, NEH and ABC.

The expected finish time is required to compare the probability ($C_{max} \leq X$). Hence in order to compare the probability ($C_{max} \leq X$) of HES, IGA, NEH and ABC, some assumptions are made. The probability value for NEH schedule is assumed and the analogous z-value is computed using Eqs. 6 and 9. Using the z-value the expected finish time is calculated using Eq. 7. Then the expected finish time is used to compute the probability ($C_{max} \leq X$) of HES. Finally, the probability of HES, ABC, and IGA are compared with the probability of NEH.

The technique has been evaluated on famous benchmark problems of Carlier [40] and Reeves [41] and their data set has been taken from OR-Library. The processing times in the data set are deterministic, hence the deterministic times are assumed as the mean processing times. While the variance of processing times is calculated from an assumed interval [1, $\mu_{ij}/9$], where μ_{ij} is the mean processing time. The mean and variance of processing times for Car01 and Rec01 problems are shown in Tables 1 and 2.

The hybrid ES was coded in MATLAB and tested on Laptop with 2.1 GHz processor and 4 GB Ram. While the IGA, ABC, and NEH were all coded in Visual C. Three probabilities of 0.80, 0.85 and 0.90 were assumed for NEH Heuristic, hence for each problem three instances are used. The z-value for each instance is calculated using Eqs. 6 and 9. Each instance is first solved using NEH to find mean and variance and then expected makespan as shown in Tables 3 and 4. The expected finish time calculated using NEH is assumed to be the same for the HES, IGA and ABC. The mean and variance makespan is then calculated using HES. Then the z-values are calculated using Eq. 9. Finally, probability ($C_{max} \leq X$) is calculated using Eq. 9 for each instance.

Table 1 Processing times (mean and variance) for Car 1 (11×5) instance

Car 1 Problem										
Jobs		Mean processing times					Variance processing times			
	M1	M2	M3	M4	M5	M1	M2	M3	M4	M5
1	375	12	142	245	412	11	1	11	3	6
2	632	452	758	278	398	15	4	1	9	8
3	12	876	124	534	765	1	1	7	16	2
4	460	542	523	120	499	2	10	6	7	2
5	528	101	789	124	999	11	8	2	2	8
6	796	245	632	375	123	4	6	12	10	12
7	532	230	543	896	452	11	10	2	9	5
8	14	124	214	543	785	1	9	3	16	17
9	257	527	753	210	463	19	10	3	2	1
10	896	896	214	258	259	1	4	3	8	13
11	532	302	501	765	988	8	2	13	1	13

Table 2 Processing times (mean and variance) for Rec 1 (20×5) problem

Rec 1 Problem (20×5)										
Jobs		Mean Processing Times					Variance Processing Times			
	M1	M2	M3	M4	M5	M1	M2	M3	M4	M5
1	5	76	74	99	26	1	8	8	11	2
2	74	21	83	52	90	8	2	9	5	10
3	67	48	6	66	38	7	5	1	7	4
4	97	36	71	68	81	10	4	7	7	9
5	87	86	64	11	31	9	9	7	1	3
6	1	42	20	90	23	1	4	2	10	2
7	69	32	99	26	57	7	3	11	2	6
8	69	12	54	80	16	7	1	6	8	1
9	11	63	24	16	89	1	7	2	1	9
10	87	52	43	10	26	9	5	4	1	2
11	25	59	88	87	40	2	6	9	9	4
12	50	42	72	77	29	5	4	8	8	3
13	58	76	71	82	94	6	8	7	9	10
14	79	48	20	63	97	8	5	2	7	10
15	35	57	78	99	80	3	6	8	11	8
16	70	76	53	2	19	7	8	5	1	2
17	79	22	77	74	95	8	2	8	8	10
18	34	99	49	3	61	3	11	5	1	6
19	37	24	32	25	4	4	2	3	3	1
20	50	88	46	63	76	5	9	5	7	8

In Eq. 10, The proportion increase in probability ($C_{max} \leq X$) for each instance is introduced while using Eq. 11 the proportion decline in risk can be calculated. Both these parameters will be used to compare the proposed HES, IGA and ABC.

$$\%_{increase}\ Probability = \frac{\varphi(z)_{ES} - \varphi(z)_{NEH}}{\varphi(z)_{NEH}} \tag{10}$$

$$\%_{increase}\ Risk = \frac{(1 - \varphi(z)_{NEH}) - (1 - \varphi(z)_{ES})}{(1 - \varphi(z)_{ES})}\ x\ 100 \tag{11}$$

6.1 Carlier problems

From Table 3 it is evident that HES finds better robust schedules than NEH, IGA and ABC for Carlier Problems. HES finds minimum makespan for all instances as compared to NEH and IGA. Except Car-03 instance, makepan values found by HES for all other instances is minimum as compared to ABC. The probability found by HES is higher than the probabilities of HES and IGA. For instance Car-03, probability of ABC is better, while for all other instances probability of HES is higher than ABC. Probability is almost 100 % that the makespan is less than the expected finish time. Almost 100 % probability is attained due to the assumptions used for computing $\phi(z)$. With HES, the minimum percent increase in the probability of 15 % and 13.09 % decrease in risk for Car-01 problem. While the maximum increase in the probability of 66.67 % is obtained for Car-02, Car-04 and Car-08 problems. A maximum percent decrease in risk of -42.88 % is obtained for Car-02 problem.

From Figs. 4 and 5 it is evident that for schedules generated using HES, there is the maximum probability that the makespan is less than the expected finish time and also ensures that the decrease the risk of exceeding makespan from a large gap.

Table 3 Carlier problem results

| Prob	Size	Nawaz-Enscore-Ham Heuristic				Improved genetic algorithm			Artificial bee colony algorithm			Hybrid evolution strategy			Percent increase in probability with ES	Percent decrease in risk with ES
		Prob	ø(z)	Cmax	X	X	Cmax	Prob	X	Cmax	Prob	X	Cmax	Prob		
Car 01	11×5	0.8	0.3	7038	7152.73	7152.73	7050	0.87	7152.73	7040	0.862	7152.73	7038	0.88	26.67	13.46
		0.85	0.35	7038	7179.78	7179.78	7050	0.917	7179.78	7040	0.913	7179.78	7038	0.93	22.86	14.38
		0.9	0.4	7038	7212.56	7212.56	7059	0.934	7212.56	7040	0.957	7212.56	7038	0.96	15.00	13.09
Car 02	13×4	0.8	0.3	7376	7534.52	7534.52	7180	1	7534.52	7166	1	7534.52	7166	1	66.67	-4.97
		0.85	0.35	7376	7571.89	7571.89	7176	1	7571.89	7166	1	7571.89	7166	1	42.86	-24.55
		0.9	0.4	7376	7617.19	7617.19	7200	1	7617.19	7186	1	7617.19	7166	1	25.00	-42.88
Car 03	12×5	0.8	0.3	7399	7543.52	7543.52	7403	0.922	7543.52	7312	0.95	7543.52	7399	0.92	40.00	21.25
		0.85	0.35	7399	7577.59	7577.59	7312	0.925	7577.59	7312	0.972	7577.59	7399	0.96	31.43	21.23
		0.9	0.4	7399	7618.9	7618.90	7401	0.947	7618.90	7312	0.984	7618.90	7399	0.98	20.00	16.24
Car 04	14×4	0.8	0.3	8129	8270.02	8270.02	8024	1	8270.02	8011	1	8270.02	8003	1	66.67	32.63
		0.85	0.35	8129	8303.26	8303.26	8004	1	8303.26	8014	1	8303.26	8003	1	42.86	16.17
		0.9	0.4	8129	8343.56	8343.56	8018	1	8343.56	8106	1	8343.56	8003	1	25.00	-3.98
Car 05	10×6	0.8	0.3	7835	7946.51	7946.51	7758	0.969	7946.51	7727	0.966	7946.51	7720	0.98	60.00	34.83
		0.85	0.35	7835	7972.8	7972.80	7798	0.97	7972.80	7727	0.979	7972.80	7720	1	42.86	25.89
		0.9	0.4	7835	8004.67	8004.67	7758	0.99	8004.67	7727	0.99	8004.67	7720	1	25.00	13.71
Car 06	8×9	0.8	0.3	8773	8893.55	8893.55	8570	1	8893.55	8505	1	8893.55	8210	0.99	63.33	35.66
		0.85	0.35	8773	8921.97	8921.97	8570	1	8921.97	8505	1	8921.97	8210	0.99	40.00	25.74
		0.9	0.4	8773	8956.43	8956.43	8570	1	8956.43	8505	1	8956.43	8210	1	25.00	15.31
Car 07	7×7	0.8	0.3	6590	6702.77	6702.77	6590	0.754	6702.77	6590	0.881	6702.77	6490	0.95	50.00	27.80
		0.85	0.35	6590	6729.35	6729.35	6590	0.8	6729.35	6590	0.93	6729.35	6490	0.97	34.29	22.90
		0.9	0.4	6590	6761.58	6761.58	6590	0.85	6761.58	6590	0.968	6761.58	6490	0.98	20.00	16.00
Car 08	8×8	0.8	0.3	8564	8694.23	8694.23	8366	1	8694.23	8424	1	8694.23	7790	1	66.67	34.11
		0.85	0.35	8564	8724.94	8724.94	8366	1	8724.94	8420	1	8724.94	7790	1	42.86	23.41
		0.9	0.4	8564	8762.16	8762.16	8429	1	8762.16	8424	1	8762.16	7790	1	25.00	12.30
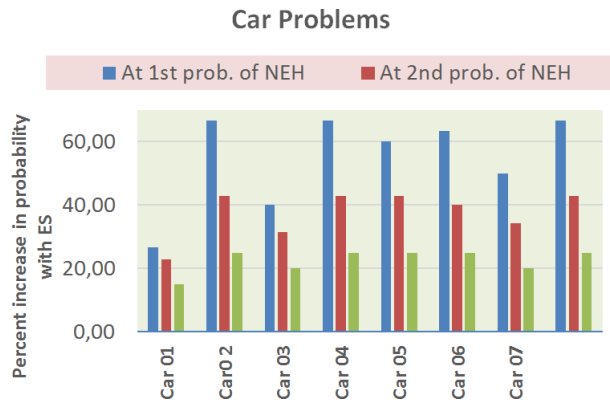
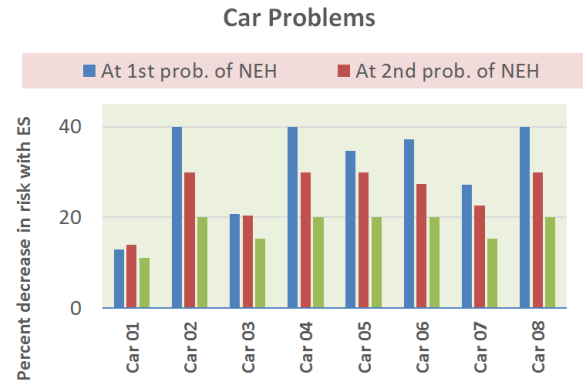Fig. 4 Comparison of Prob. on Carlier problems

Fig. 5 Comparison of risk on Carlier problems

6.2 Reeves problems

The results of HES for Reeves's problems are shown in Table 4. Results of the HES are better as compared to NEH, IGA and ABC. HES finds minimum makespan for all instances as compared to NEH, IGA and ABC. Also the probability found by HES is higher than the probabilities of HES, IGA and ABC. Using HES, the probability ($C_{max} \le X$) for all Rec problems is 100 %. Minimum increase in the probability of 25 % and a decrease in risk of 20 % is observed for Rec-01 problem. While maximum probability of 66.67 % is observed for Rec-01, Rec-03, Rec-05, Rec-07, Rec-09, Rec-11, Rec-13, Rec-15 and Rec-17 problems and maximum decrease in risk of 40 % is observed for Problem 1, 3, 5, 7, 9, 11, 13, 15 and 17 respectively.

From Figs. 6 and 7 it is evident that for schedules generated using HES, there is a maximum probability that the makespan is less than the expected finish time and also ensures that the decrease the risk of exceeding makespan from a large gap for Reeves problems.

Table 4 Reeves problem results

| Prob	Size	Nawaz-Enscore-Ham heuristic				Improved genetic algorithm			Artifical bee colony algorithm			Hybrid evolution strategy			Percent increase in probability with ES	Percent decrease in risk with ES
		Prob	ø(z)	Cmax	X	Cmax	ø(z)	Prob	Cmax	ø(z)	Prob	Cmax	ø(z)	Prob		
Rec 1	20×5	0.8	0.3	1320	1340.82	1271	0.5	1	1279	0.5	1	1249	0.5	1	66.67	40.00
		0.85	0.35	1320	1345.72	1268	0.5	1	1291	0.5	1	1249	0.5	1	42.86	30.00
		0.9	0.4	1320	1351.67	1288	0.5	1	1293	0.5	1	1249	0.5	1	25.00	20.00
Rec 3	20×5	0.8	0.3	1116	1133.02	1115	0.312	0.812	1111	0.452	0.952	1109	0.5	1	66.67	40.00
		0.85	0.35	1116	1137.03	1111	0.397	0.897	1112	0.475	0.975	1109	0.5	1	42.86	30.00
		0.9	0.4	1116	1141.89	1111	0.437	0.937	1113	0.49	0.99	1109	0.5	1	25.00	20.00
Rec 5	20×5	0.8	0.3	1296	1315.80	1255	0.5	1	1261	0.5	1	1245	0.5	1	66.67	40.00
		0.85	0.35	1296	1320.47	1247	0.5	1	1266	0.5	1	1245	0.5	1	42.86	30.00
		0.9	0.4	1296	1326.13	1268	0.5	1	1277	0.5	1	1245	0.5	1	25.00	20.00
Rec 7	20×10	0.8	0.3	1626	1645.89	1584	0.5	1	1584	0.5	1	1572	0.5	1	66.67	40.00
		0.85	0.35	1626	1650.58	1599	0.5	1	1584	0.5	1	1572	0.5	1	42.86	30.00
		0.9	0.4	1626	1656.26	1601	0.5	1	1596	0.5	1	1572	0.5	1	25.00	20.00
Rec 9	20×10	0.8	0.3	1583	1602.40	1580	0.340	0.840	1557	0.5	1	1537	0.5	1	66.67	40.00
		0.85	0.35	1583	1606.98	1575	0.448	0.948	1557	0.5	1	1537	0.5	1	42.86	30.00
		0.9	0.4	1583	1612.52	1574	0.464	0.964	1547	0.5	1	1537	0.5	1	25.00	20.00
Rec 11	20×10	0.8	0.3	1550	1569.91	1502	0.5	1	1502	0.5	1	1431	0.5	1	66.67	40.00
		0.85	0.35	1550	1574.60	1509	0.5	1	1509	0.5	1	1431	0.5	1	42.86	30.00
		0.9	0.4	1550	1580.29	1491	0.5	1	1491	0.5	1	1431	0.5	1	25.00	20.00
Rec 13	20×15	0.8	0.3	2002	2025.90	1981	0.465	0.965	1981	0.5	1	1935	0.5	1	66.67	40.00
		0.85	0.35	2002	2031.54	1969	0.5	1	1969	0.5	1	1935	0.5	1	42.86	30.00
		0.9	0.4	2002	2038.37	1979	0.5	1	1979	0.5	1	1935	0.5	1	25.00	20.00
Rec 15	20×15	0.8	0.3	2025	2045.59	1986	0.49	0.99	1986	0.5	1	1962	0.5	1	66.67	40.00
		0.85	0.35	2025	2050.45	1998	0.49	0.99	1998	0.5	1	1962	0.5	1	42.86	30.00
		0.9	0.4	2025	2056.33	1997	0.5	1	1997	0.5	1	1962	0.5	1	25.00	20.00
Rec 17	20×15	0.8	0.3	2019	2044.40	1992	0.484	0.984	1992	0.5	1	1939	0.5	1	66.67	40.00
		0.85	0.35	2019	2050.39	1986	0.5	1	1986	0.5	1	1939	0.5	1	42.86	30.00
		0.9	0.4	2019	2057.65	1992	0.5	1	1994	0.5	1	1939	0.5	1	25.00	20.00
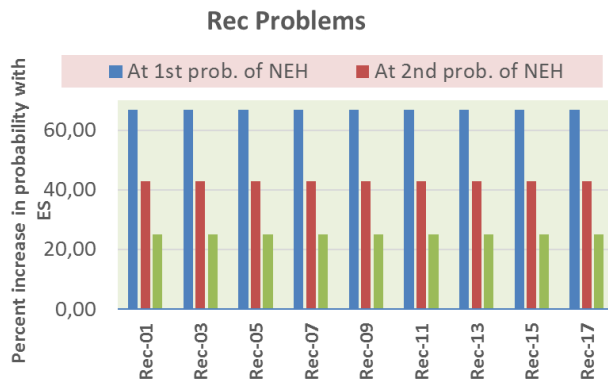
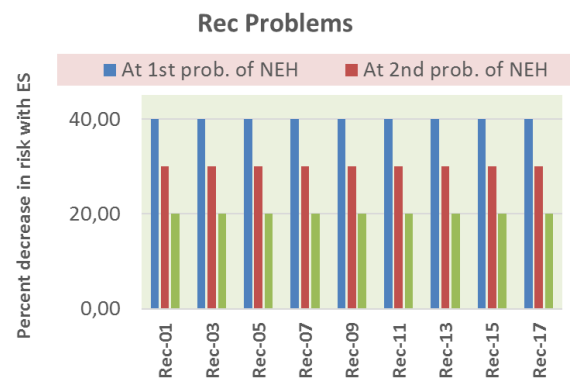**Fig. 6** Comparison of probabilities on Reeves problems

Fig. 7 Comparison of risk on Reeves problems

6.3 Overall results

Fig. 8 demonstrates the average rise in probability and average percentge decline in risk for all Carlier and Reeves problems. It is evident that for all Carlier and Reeves problems, HES provides better probability that the expected finish time is less than the makespan for Carlier and Reeves instances (more than 38 % and 42 % respectively). Also HES ensures a decline in risk that expected finish time will not exceed the makespan for Carlier and Reeves instances (more than 22 % and 29 % respectively). The overall results show that HES outperforms IGA, NEH and ABC and ensures that the robust schedules generated by HES gives higher probability that they will not exceed the expected finish time for Carlier and reeves problem. Also robust schedules generated using HES ensures the decline in risk that the makespan will exceed the expected finish time for Carlier and Reeves instances.
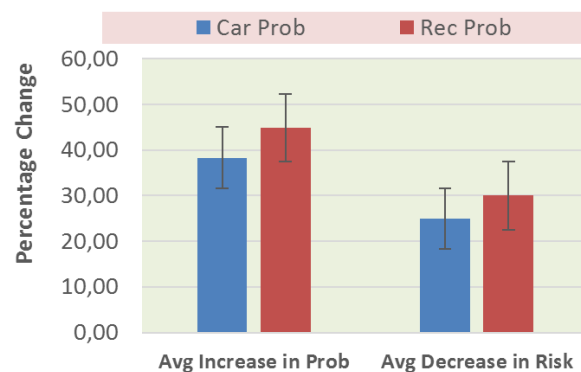

Fig. 8 Avg. percentage increase in Prob. and Avg. percentage decrease in risk by HES

7. Conclusion and recommendations

Robust schedules are generated for *m*-machines PFSSP to address the uncertainty of processing times. The objective is to ensure that the expected finish time is less than the makespan. As per the central limit theorem, processing time for uncertain jobs is normally distributed. A hybrid ES has been proposed and evaluated on famous benchmark problems of Carlier and Reeves. First ES is executed for 30,0000 iterations and then the solution is optimized using TS. The hybrid algorithm ensures maximum exploration as well as maximum exploitation of solution space. Results are compared with the NEH, IGA and ABC algorithms, and HES has outperformed all of them for all the Carlier and Reeves instances. The present research is focused on robust scheduling for the manufacturing industry, and it ensures that the expected finish time of jobs will not exceed the deadline as there are fluctuations in processing times of jobs in manufacturing industry. Hence the research is applicable to other industrial cases, i.e. process and chemical industry, pharmaceutical industry, steel industry etc. as the processing times in these industries are uncertain.

For simplicity it is assumed that finish time is same for all jobs, however, in actual flow shop, the finish times are different. Hence future research should be focused on PFSSP with all job

have different expected finish times. Also, the research can be extended to flow shop with other objectives, i.e. tardiness, and flowtime. So far robust schedules were generated for small size flow shop problems. Hence in the future, robust schedules should be generated for large size problems of Reeves, Taillard, and Valllada benchmark instances. Also robust schedules for job shop problems are also still pendent. In addition robust schedules can be generated for other performance measures, i.e. tardiness, flowtime etc.

References

[1] Pinedo, M.L. (2015). *Scheduling, Theory, Algorithms, and Systems,* Fifth Edition*,* Springer, New York, USA, doi: 10.1007/978-3-319-26580-3.
[2] Sturrock, D. (2012). New solutions for production dilemmas, *Industrial Engineer,* Vol. 44, No. 12, 47-52.
[3] Gourgand, M., Grangeon, N., Norre, S. (2003). A contribution to the stochastic flow shop scheduling problem, *European Journal of Operational Research*, Vol. 151, No. 2, 415-433, doi: 10.1016/S0377-2217(02)00835-4.
[4] Juan, A.A., Barrios, B.B., Vallada, E., Riera, D., Jorba, J. (2014). A simheuristic algorithm for solving the permutation flow shop problem with stochastic processing times, *Simulation Modelling Practice and Theory*, Vol. 46, 101-117, doi: 10.1016/j.simpat.2014.02.005.
[5] Elyasi, A., Salmasi, N. (2013). Stochastic flow-shop scheduling with minimizing the expected number of tardy jobs, *The International Journal of Advanced Manufacturing Technology*, Vol. 66, No. 1-4, 337-346, doi: 10.1007/s00170-012-4328-4.
[6] González-Neira, E.M., Montoya-Torres, J.R., Barrera, D. (2017). Flow-shop scheduling problem under uncertainties: Review and trends, *International Journal of Industrial Engineering Computations*, Vol. 8, No. 4, 399-426, doi: 10.5267/j.ijiec.2017.2.001.
[7] Liu, Q., Ullah, S., Zhang, C. (2011). An improved genetic algorithm for robust permutation flowshop scheduling, *The International Journal of Advanced Manufacturing Technology*, Vol. 56, No. 1-4, 345-354, doi: 10.1007/s00170-010-3149-6.
[8] Vallada, E., Ruiz, R., Minella, G. (2008). Minimising total tardiness in the *m*-machine flowshop problem: A review and evaluation of heuristics and metaheuristics, *Computers & Operations Research*, Vol. 35, No. 4, 1350-1373, doi: 10.1016/j.cor.2006.08.016.
[9] Yenisey, M.M., Yagmahan, B. (2014). Multi-objective permutation flow shop scheduling problem: Literature review, classification and current trends, *Omega*, Vol. 45, 119-135, doi: 10.1016/j.omega.2013.07.004.
[10] Sabuncuoglu, I., Goren, S. (2009). Hedging production schedules against uncertainty in manufacturing environment with a review of robustness and stability research, *International Journal of Computer Integrated Manufacturing*, Vol. 22, No. 2, 138-157, doi: 10.1080/09511920802209033.
[11] Yang, J., Yu, G. (2002). On the robust single machine scheduling problem, *Journal of Combinatorial Optimization*, Vol. 6, No. 1, 17-33, doi: 10.1023/A:1013333232691.
[12] Liu, L., Gu, H.-Y., Xi, Y.-G. (2007). Robust and stable scheduling of a single machine with random machine breakdowns, *The International Journal of Advanced Manufacturing Technology*, Vol. 31, No. 7-8, 645-654, doi: 10.1007/s00170-005-0237-0.
[13] Goren, S., Sabuncuoglu, I. (2008). Robustness and stability measures for scheduling: Single-machine environment, *IIE Transactions,* Vol. 40, No. 1, 66-83, doi: 10.1080/07408170701283198.
[14] Daniels, R.L., Carrillo, J.E. (1997). β-Robust scheduling for single-machine systems with uncertain processing times, *IIE transactions*, Vol. 29, No. 11, 977-985, doi: 10.1080/07408179708966416.
[15] Kuo, C.-Y., Lin, F.-J. (2002). Relative robustness for single-machine scheduling problem with processing time uncertainty, *Journal of the Chinese Institute of Industrial Engineers*, Vol. 19, No. 5, 59-67, doi: 10.1080/10170660209509359.
[16] Jia, Z., Ierapetritou, M.G. (2007). Generate Pareto optimal solutions of scheduling problems using normal boundary intersection technique, *Computers & Chemical Engineering*, Vol. 31, No. 4, 268-280, doi: 10.1016/j.compchemeng.2006.07.001.
[17] Wu, C.W., Brown, K.N., Beck, J.C. (2009). Scheduling with uncertain durations: Modeling β-robust scheduling with constraints, *Computers & Operations Research*, Vol. 36, No. 8, 2348-2356, doi: 10.1016/j.cor.2008.08.008.
[18] Fazayeli, M., Aleagha, M.-R., Bashirzadeh, R., Shafaei, R. (2016). A hybrid meta-heuristic algorithm for flowshop robust scheduling under machine breakdown uncertainty, *International Journal of Computer Integrated Manufacturing*, Vol. 29, No. 7, 709-719, doi: 10.1080/0951192X.2015.1067907.
[19] Gholami-Zanjani, S.M., Hakimifar, M., Nazemi, N., Jolai, F. (2017). Robust and fuzzy optimisation models for a flow shop scheduling problem with sequence dependent setup times: A real case study on a PCB assembly company, *International Journal of Computer Integrated Manufacturing*, Vol. 30, No. 6, 552-563, doi: 10.1080/0951192X.2016.1187293.
[20] Rahmani, D. (2017). A new proactive-reactive approach to hedge against uncertain processing times and unexpected machine failures in the two-machine flow shop scheduling problems, *Scientia Iranica*, Vol. 24, No. 3, 1571-1584, doi: 10.24200/sci.2017.4136.
[21] Cui, W., Lu, Z., Li, C., Han, X. (2018). A proactive approach to solve integrated production scheduling and maintenance planning problem in flow shops, *Computers & Industrial Engineering*, Vol. 115, 342-353, doi: 10.1016/j.cie.2017.11.020.

[22] Ma, S., Wang, Y., Li, M. (2019). A novel artificial bee colony algorithm for robust permutation flowshop scheduling, In: Li, X., Wong, K.C. (eds.), *Natural computing for unsupervised learning, Unsupervised and semi-supervised learning,* Springer, Cham, Switzerland,163-182, doi: 10.1007/978-3-319-98566-4_8.

[23] González-Neira, E.M., Urrego-Torres, A.M., Cruz-Riveros, A.M., Henao-García, C., Montoya-Torres, J.R., Molina-Sánchez, L.P., Jiménez, J.-F. (2019). Robust solutions in multi-objective stochastic permutation flow shop problem, *Computers & Industrial Engineering*, Vol. 137, Article No.106026, doi: 10.1016/j.cie.2019.106026.

[24] Lebbar, G., El Abbassi, I., Jabri, A., El Barkany, A., Darcherif, M. (2018). Multi-criteria blocking flow shop scheduling problems: Formulation and performance analysis, *Advances in Production Engineering & Management*, Vol. 13, No. 2, 136-146, doi: 10.14743/apem2018.2.279.

[25] Xu, H., Bao, Z.R., Zhang, T. (2017). Solving dual flexible job-shop scheduling problem using a Bat Algorithm, *Advances in Production Engineering & Management*, Vol. 12, No. 1, 5-16, doi: 10.14743/apem2017.1.235.

[26] Rathinam, B., Govindan, K., Neelakandan, B., Raghavan, S.S. (2015). Rule based heuristic approach for minimizing total flow time in permutation flow shop scheduling, *Tehnički Vjesnik – Technical Gazette,* Vol. 22, No. 1, 25-32, doi: 10.17559/TV-20130704132725.

[27] Ma, D.Y., He, C.H., Wang, S.Q. Han, X.M., Shi, X.H. (2018). Solving fuzzy flexible job shop scheduling problem based on fuzzy satisfaction rate and differential evolution, *Advances in Production Engineering & Management,* Vol. 13, No. 1, 44-56, doi: 10.14743/apem2018.1.272.

[28] Maqsood, S., Noor, S., Khan, M.K., Wood, A. (2012). Hybrid genetic algorithm (GA) for job shop scheduling problems and its sensitivity analysis, *International Journal of Intelligent Systems Technologies and Applications*, Vol. 11, No. 1-2, 49-62, doi: 10.1504/IJISTA.2012.046543.

[29] Khalid, Q.S,, Arshad, M., Maqsood, S., Jahanzaib, M., Babar, A.R., Khan, I., Mumtaz, J., Kim, S. (2019). Hybrid particle swarm algorithm for products' scheduling problem in cellular manufacturing system, *Symmetry*, Vol. 11, No. 6, 729, doi: 10.3390/sym11060729.

[30] Sarkar, B., Omair, M., Choi, S.-B. (2018). A multi-objective optimization of energy, economic, and carbon emission in a production model under sustainable supply chain management, *Applied Sciences*, Vol. 8, No. 10, 1744, doi: 10.3390/app8101744.

[31] Zubair, M., Maqsood, S., Omair, M., Noor, I. (2019). Optimization of material handling system through material handling equipment selection, *International Journal of Progressive Sciences and Technologies*, Vol. 15, No. 2, 235-243.

[32] Hayter, A. (2012). *Instructor solution manual, Probability and statistics for engineers and scientists,* 3rd edition, Nelson Education, Scarborough, Canada.

[33] Rechenberg, I. (1973). *Optimierung technischer systeme nach prinzipien der biologischen evolution*, Phd thesis, Technische Universität Berlin, Germany, doi: 10.1002/fedr.19750860506.

[34] Beyer, H.-G. (2001). *The theory of evolution strategies*, Natural Computing Series, Springer-Verlag, Berlin, Germany, doi: 10.1007/978-3-662-04378-3.

[35] Ahmad, A.M., Khan, G.M., Mahmud, S.A. (2013). Classification of arrhythmia types using cartesian genetic programming evolved artificial neural networks, In: Iliadis, L., Papadopoulos, H., Jayne, C. (eds.), *Engineering applications of neural networks, EANN 2013, Communications in computer and information science,* Vol. 383, Springer, Berlin, Germany, doi: 10.1007/978-3-642-41013-0_29.

[36] Paris, P.C.D., Pedrino, E.C., Nicoletti, M.C. (2015). Automatic learning of image filters using Cartesian genetic programming, *Integrated Computer-Aided Engineering*, Vol. 22, No. 2, 135-151, doi: 10.3233/ICA-150482.

[37] Murata, T., Ishibuchi, H., Tanaka, H. (1996). Genetic algorithms for flowshop scheduling problems, *Computers & Industrial Engineering*, Vol. 30, No. 4, 1061-1071, doi: 10.1016/0360-8352(96)00053-8.

[38] Grabowski, J., Pempera, J. (2007). The permutation flow shop problem with blocking. A tabu search approach, *Omega*, Vol. 35, No. 3, 302-311, doi: 10.1016/j.omega.2005.07.004.

[39] Nawaz, M., Enscore Jr., E.E., Ham, I. (1983). A heuristic algorithm for the m-machine, n-job flow-shop sequencing problem, *Omega*, Vol. 11, No. 1, 91-95, doi: 10.1016/0305-0483(83)90088-9.

[40] Carlier, J. (1978). Ordonnancements à contraintes disjonctives, *RAIRO-Operations Research*, Vol. 12, No. 4, 333-350, doi: 10.1051/ro/1978120403331.

[41] Reeves, C.R. (1995). A genetic algorithm for flowshop sequencing, *Computers & Operations Research*, Vol. 22, No. 1, 5-13, doi: 10.1016/0305-0548(93)E0014-K.

Systematic mitigation of model sensitivity in the initiation phase of energy projects

Đaković, M.[a], **Lalić, B.**[a], **Delić, M.**[a], **Tasić, N.**[a], **Ćirić, D.**[a]

[a]University of Novi Sad, Faculty of Technical Sciences, Novi Sad, Serbia

ABSTRACT

Early project risk identification and assessment is a complex issue based on decision-making methods that are methodically suitable for successful project delivery. Nevertheless, although there are several risk management assessment tools, in practice, this issue is still not taken seriously enough in the project initiation phase. Literature research reveals a need for an applicable systematic risk model approach, systematic sensitivity of mitigation action plans, considering the need for early systematic project risk awareness. This paper not only explains the evidence that a risk systematic model tool is essential in the project initiation phase but also narrows the gaps through the systematic sensitivity approach with the accent on the integrated risk systematic model. The sensitivity approach is taken in the project early preparation phase, where evaluation, the establishment of limits to which risks are controllable, is based on the stage-gate model. The stage-gate model evaluates which risks are specific to a certain analysis in the early project definition phase, leads to the conclusion that excluding any mitigation elements or probability of risk occurrence reflects on the outcomes, and presents an unrealistic picture of the given project targets. This research represents a reliable risk tool with improvements in resolving systematic risk system faults, 'stakeholders' subjective decision gaps, constricting project contingency, and shortening project schedule deviation. The research is based on two complex industry (case studies) projects within the energy industry.

1. Introduction

Various authors emphasize that a crucial part of risk management is a reaction plan, which ensures proactive problem solving [1, 2, 3]. Numerous studies, including authors such as Ward or Chapman, have shown a need for project risk management (PRM), including its benefits [4]. Various authors have found that the quality of stake estimates, assessment method tools, and scheduling are essential for proactivity in project management [5, 6]. In the last decade, risk project solving has significantly improved within the risk management tools, where a more reliable risk allocation is being facilitated [7]. Thus, gaps still exist, and improvements in risk management are necessary. These should include a more detailed or quantified approach, early reduction of risk and risk avoidance, and prompt systematic action of suitable integrated techniques to improve risk management practices [8, 9, 10]. Over the last years, risk management (RM) has attracted the attention of both scientists and practitioners. The Project Management Institute (PMI) included risk management as one of the ten knowledge areas in project management (PM) [11]. Considering the previously stated, this study aims to identify the major needs for a systematic risk model response within the energy industry, taking into account the

preparation projects phase and its impact on (time constraints) schedule with an emphasis on model sensitivity [12]. The results of different authors suggest that in the engineering industry, project risk management still having some ineffectiveness. Mainly it is related to the 'stakeholders' lack of involvement in the risk management appraisal, as well as the failure of projects with some specific elements of the outcome presented through the study of various risk tools and their technological doubts [4, 13, 14]. One of the uncertainties was the inadequate participation of all stakeholders from the initiation until project closure [4]. Dale, Stephen, Geoffrey, and Phil highlight that risk should be considered at the earliest stages of project planning to avoid correction later on in the execution phase. The authors mention that risk management activities should be continued throughout a project lifetime [13, 15]. It is also suggested that risk management focuses on identifying and assessing risks to a project and managing those risks to minimize the impact on project objectives. Therefore, the presented model takes into account all the mentioned gaps and collectively and systematically resolves the issue from the definition or initiation project phase.

Authors Zwikael and Ahn, considering the lack of provided solutions on the market, emphasize the need for tools that are easy to use and lead to better outcomes [16]. As proactivity is needed in the engineering industry, risk management tools have to overcome and actively solve potential problems in the early initiation, definition, and implementation phase of a project [10, 12, 17]. Systematic process model steps and criteria will allow risk-handling stage-gate strategy by selective elimination based on relevant available mitigation criteria (considering the contingency), including the objective probability of the desired successful project results. The desired successful project results are given through a detailed stage-gate systematic approach of establishing all risks according to the predefined and locked model criteria. The approaches and the final objective show that the new systematic process model will generate less deviation and improve the implementation of projects [18].

The objective of the early risk initiation phase is to prepare a plan of risk mitigation by identifying potential gaps, narrowing down all known and unknown risks before proceeding to the next stage [8, 10]. If we are looking from the qualitative standpoint of resolving these issues by using the existing software, the project definition does not differ from project planning with minimum information [19]. The degree of risk information varies with project complexity, the scope of work, timeframe, approved funds, and project location [15]. A few studies present risk management frameworks from the 'developers' perspective, integrating the software development cycle, and involving the concerned stakeholders [15, 19]. The main message from the findings is that successful projects resolving possible problems before they arise. That should be the most crucial task of project risk management, and the aim of the current presented study, with the focus on the given sensitivity systematic matrix tree [12, 20]. Even the overview of risk standards calls for further process improvements. Based on the David H. comparison of the risk standards limitation, it is apparent that risk standards have a great deal in common, and that with a universal consensus of risk management, gaps should be covered [21]. On the other hand, there are some, substantial gaps and material differences between them:

- The first is the general observation that none of the included risk standards covers all the fields regarding the ''stakeholders' involvement, communication, and collaboration into organization structured adoption of risk implementation.
- The second is that specific standards cover only the risk management process but not the establishment of organizational infrastructure to apply such processes.
- The third is the differentiation of the risk definition, an approach to risk both as a threat and an opportunity, as opposed to the approach that risk is only a threat.

What follows from all the above is that there is a broad consensus regarding the main steps and activities of the generic risk management process, but there is still room for a comprehensive approach that will cover the gaps. The contribution of the research is the effective and continuous involvement of stakeholders. The effectiveness is visible throughout the entire risk process. Predefined, concrete steps resolve possible systematic risk system faults with precision and functionality. The results show a leaner project contingency approach and shorten the project schedule deviations.

Risk model methodology approach

The objective of the research is proposed with a systematic risk management model that uses a quantitative technique with the active involvement of stakeholders throughout the entire risk management process (identification, analyses, and response to risks) [14, 22]. The systematic risk management model is an integration of the existing tools such as Risk Work Breakdown Structure (RWBS), Risk Registers (RR), Probability and Impact (PI), Analytic Hierarchy Process (AHP), Fault Tree Analysis (FTA) [23]. Two significant areas must be introduced through the model tree: early systematic risk assessment and the project stakeholders understanding what and how those steps may impact the project beyond its objectives [9, 10]. The entire method is based on the approach with one step ahead of any project definition and implementation. The risk model provides details, breakdown into actions that will support the research from the moment of decision-making, emphasizing the quantitative approach to risk evaluation with the effectiveness in bridging the gaps mentioned above.

The presented model involves advanced strategic steps for risk management. The advanced strategic steps practice corrections or mitigations of risks utilizing knowledge of the managerial resources, as well as the given model benchmarks [24]. With this quantitative methodology, considering quantitative risk elements and risk management integration, the risk model process will be developed through stage-gate. Such an approach contains steps that will enable better implementation of project risk management. A systematic approach to risk management is the most common problem in the pre-definition phase of the project management industry [12].

There is a concern with the policy prescription to remedy the problem to provide a deeper understanding of what constitutes systematic risk management and how it impacts on incentives and welfare measures. The purpose of the paper and the presented model in risk analysis is a data-level specification of a "more systematic risk 'treatment' including objectives of stakeholders. It is clarified through the matrix tree how the definition criteria differ from the existing definitions of systematic risk. The definition is applied to all steps in the model and the stage gates where criteria are well-coded to ensure the given option over random choice sets. The definition is also innovative, as opposed to the consideration of the existing random choice sets. In circumstances where a stakeholder has the option to discard risk identification for a well-defined reason, it is clear that risk treatment should be much more systematic [4, 14].

The systematic decision model tree represents the level of involvement and the level of predictability of risks, including the external and internal factors with the focus on all risk elements known, unknowns, known unknowns, and unknown unknowns. The weighted probability of risk categorization and mitigation is included in all stage gates following risk assessment according to all established criteria. The main aim of the research is to evaluate and establish limits to which level risks are manageable and the extent to which risks are specific to a certain analysis in the early project initiation stages [10, 13]. The study is focused on improving schedule deviation through the systematic process model approach for future preparation and implementation of projects. The most important motivation for the paper comes from the research gaps where risk management and risk assessment in the early stage is not thoroughly considered [8, 10, 17].

The paper addresses the problem of risk management in the field of energy industry projects using a knowledge-based approach. It proposes a systematic methodology based on five main segment criteria: systematic process matrix tree, risk registration, control flow plan, risk support documents, and data with applicable criteria. The expected mitigation and the presented risk response stage-gate strategy are there to eliminate uncertainty factors of the, anticipated new unwanted risks and their post evaluation. The first challenge is the modelling of the risk management function area managers (FAMs), criteria of its evaluation, and the possibility of integrating best practices into the model.

Therefore, the systematic process model tree and stage-gate criteria include risk events, risk reduction or elimination actions and their effects, interactions between the stage gates concerning risks and risk decision, and mitigation efforts [18]. The systematic process model stage-gate criteria allow the risk-handling stage-gate strategy by selective elimination based on relevant available mitigation criteria, including the objective probability of the desired successful project

results. The desired successful project, results are given through the detailed stage-gate systematic approach of establishing all risks in the model predefined criteria. The approaches and the final objective show that the new systematic process model generates less deviation show different levels of sensitivity results and improves the implementation of projects [20]. Further expectations are that the application of the proposed approach will allow functional area managers (FAMs) and end-users to develop project risk management functionality based on best practices and to improve the performance of the awareness.

The fundamental changes that are taking place today in the field of risk project management applications originate precisely in the area of the earlier risk identification work [25]. They are, on the one hand, positive and successful possibilities in project risk management, where such an approach can result in significant flexibility in operation (time savings) and cost reduction. The use of the earlier risk identification can be considered in terms of improving competencies based on which a company's primary strategy then develops and achieves a competitive edge and brings added value to the project management decision-makers. Risk management should be incorporated in the initial start-up phases of projects and continued throughout the project duration [26, 27].

Since risk can occur in three phases or levels, the initiation phase, the project risk definition phase and the day to day project operation phase, it is crucial, based on the conclusions of recognized authors, that risk should be considered at the earliest stages of project planning to avoid correction later in the execution phase [8-10, 12]. Project risk is always in the future, but if the risk is managed systematically and thoroughly in the early phase, project implementation should not have a vast deviation or corrections.

Scientific proofs illustrate that although there are well-developed, designed and implemented processes of project Risk Management (RM) such as risk management planning, risk identification, risk assessment, risk analysis, and risk response planning, in the construction project experience failure is always ascribed to a risk event [8, 28, 29]. Risk management is crucial in the planning stage of a project, and its scope and depth increase as the project moves towards the execution phase, while they decrease in the conclusion phase [30].

Section 1 presents an overview of the key research and objective glitches in a risk management society, based on the current technologies and the basic challenges of new tools as well. Summary of the methodology description, research, and data collection.

Section 2 presents the concept and assessment of the model. The particular emphasis has been put on the development, usage, and impact of applying the model to the existing risk management tools. The systematic and sensitivity approach, has been elaborated. Provides more insight into the model structure and implications. Also, discuss the model individual connections and model pattern demonstration.

Section 3 provides an overview of the two complex industry projects (case studies) as a key structure in any type of project management. Section 4 provides an overview of the given sensitivity results and comparison of the two complex industry projects (case studies), regarding the sensitivity capability RIO model itself. Section 5 presents the conclusions and discussion of the results obtained by research. The practical implications and limitations of the research are described and summarize the scientific contribution of the paper. Also, the directions for future researches are indicated. In the end, it shows the scientific literature that has been used during the research, also indicates the excellent structure of the due diligence path towards the findings.

2. Systematic risk model, risk identification oversight (RIO)

In the engineering industry, there is a wide range of risk management tools and techniques, all of which can add value to the performance in achieving project objectives [32]. The collected existing risk history data, together with the newly added risks, went through the checked Strengths, Weaknesses, Opportunities, and Threats (SWOT) analysis. SWOT analysis was used for identification, structuration, and comparison of the already existing data, their strong and weak sides so that it would be following the current project objectives. In this paper, the emphasis is not on computer model outcomes but rather on the interactions of the presented risk management

tools, their participants, who in this case are the functional area managers, and the effects of systematic interactions according to the model given criteria with the main impact on the project timeline outcomes. The model, RIO matrix diagram, graphically shows various combinations and conditions that may fix failures, such as decision making, analysis, information data, and possible gaps [10]. Potential gaps are overcome in the model matrix tree according to the defined and constructed logical connections including the return possibility If Yes, "then proceed to the next step or stage-gate, and If Not, "return to the designated step of the gate. The risk identification oversight model RIO includes a detailed evaluation of the possibilities of various failure events at each stage-gate step before proceeding to the task. Such gaps are filled with the precision of a well-defined support document; and based on one of the equations used in excel, the model can format and recheck the status of documents each time before it proceeds to the next step:

$$IF(OR(OR(\sum_{n=1}^{\infty} C_n = "X");OR(\sum_{n=1}^{\infty} D_n = "X");OR(\sum_{n=1}^{\infty} E_n = "X");$$

$$IF(OR(OR(\sum_{n=1}^{\infty} C_n = "X");OR(\sum_{n=1}^{\infty} D_n = "X");OR(\sum_{n=1}^{\infty} E_n = "X");$$

$$OR(\sum_{n=1}^{\infty} F_n = "X");OR(\sum_{n=1}^{\infty} G_n = "X");OR(\sum_{n=1}^{\infty} H_n = "X");$$

$$);"Check\ data!";"Document\ OK\ \checkmark") \tag{1}$$

The RIO model matrix tree follows a systematic logic technique, which attempts to see all possible outcomes of the possible gaps and all faults and to take the initiative [10]. The challenging part of the matrix is to foresee the impact of various potential events due to the complexity and uniqueness of most project targets where structured risk key owners enforce quality control correction before the document is applied to the model. The owner's possibility is to acknowledge the final document and to present the following outcomes through the model. The presented results or mitigation criteria are given to functional area managers (FAMs) or stakeholders for the final review and approval before any further steps are taken. Therefore, a possible fault is automatically mitigated since there are a few steps of quality control before the document is applied to the model. From the other point of view, the fault is mitigated by the involvement of functional area managers and their contribution to the mitigation selection and the possibility of decisions of where and when some of the steps need to be repeated to achieve realistic or correct results.

The main model breakdown of the risk management assessment and how the risks may be measured is given in [13]:

- In costs (budgetary risks)
- In time (delay risks for time management)
- Or quality (usually affecting contracts through the budgetary cost of improvement)

The focus of the paper is the time per given tasks and the delays. The model allows a (stage-gate) strategy for managing risk by selective elimination based on relevant available criteria (considering unforeseen events), considering objective probability.

This integrated approach and the final results show that the model generates systematic risk treatment as smoothly as possible, improves, and clearly indicates the sensitivity transformation parameters of the project time impacts. The paper does not deal with the impact of software solutions qualitatively in relation to quantitative, but only the quantitative approach is applied [19]. The expected results of the proposed approach will enable functional managers and clients to develop a project risk-based management function built on good practice, raising awareness of early risk detection [8].

The structure of the risk model matrix tree is explained and defined based on two main elements:

1. Methodological evaluation of factors that include a set of criteria for each step
2. The level of evaluation for each factor and its dimensions.

The presented model tree will have three main corrective groups:

- First group *: Systematic process map with stage gates one (1) through five (5)
- Second group **: Risk registration and control flow plan
- Third group ***: Risk documents and data with the applicable risk management existing tools

Each group of risk data files (***) must pass through the (**) risk registration and control flow plan before moving to the next step. The systematic process map (*) is developed in detail (each step has a note/task of explanations) to create more criteria for the decision of the flow plan (**) and supported by the risk data and the applied methods (***). At every step, risk documents will go through different risk data criteria sets. These documents aim to reduce the expansion of documentation and to make the existing documentation as simple and useful as possible. The advantage of the RIO model is that the tree is not significant and complicated, and it helps in visualizing the analysis, considering combinations of corrections, and determining occurrence probability for complex corrections. In the RIO, risk assessment is performed using quantitative methods, but also some aspects of qualitative methods, too.

Fig. 1 shows the stage-gate No. 1 and the first step in the risk management model process, where all stakeholders are involved from the beginning [14]. At this stage, all related project risks (known and unknown) are listed. Also, the historical documents of a previous project relevant to the scope it's included, as well. In stage-gate No. 1, risks are grouped by category, presenting the details of risks, the strategy of mitigation, the probability of occurrence, responsible individuals with their roles and responsibilities. Further down through the decision tree, risks are given a rating scale from the high-high to the low-low and categorized from the knowns, unknowns, and new risks. Costs are associated with each of the identified risks. At the end of the stage-gate No. 1, all risks are acknowledged by the stakeholders, with all the needed criteria that include the initial RWBS and schedule. Before any further step is taken, the owner of the risk assessment team confirms authorization towards the next stage gate.

Fig. 2 is the stage-gate No. 2, a step where only the unknown risks are treated. The stage-gate is developed based on certain flow steps with the possibility of checkpoints and corrections (workshops, decision tree analysis with an integrated approach, including brainstorming, checklist, probability impact matrices, objective judgment). A set of documents such as RWBS, RR, PI, AHP, FTA is prepared and implemented through the process [23]. The outcomes of the stage-gate No. 2 are: all identified risks at the end of the stage-gate are established as unknowns, including new risks that are selected as unknown and all applicable history unknown risks. The stage-gate provides the first summary of the unknowns results with the first estimated cost. At this stage-gate, all project unknowns are acknowledged.

Fig. 3 shows stage-gate No. 3, a step where only known risk is treated. The stage-gate is developed based on the firm flow steps with the possibility of checkpoints and corrections. A set of documents is introduced through a process that is almost identical to the stage-gate No. 2. The stage-gate outcome is: all new risks are selected as known, including all applicable history data of known risk [23]. At this stage-gate, all project knowns are acknowledged.
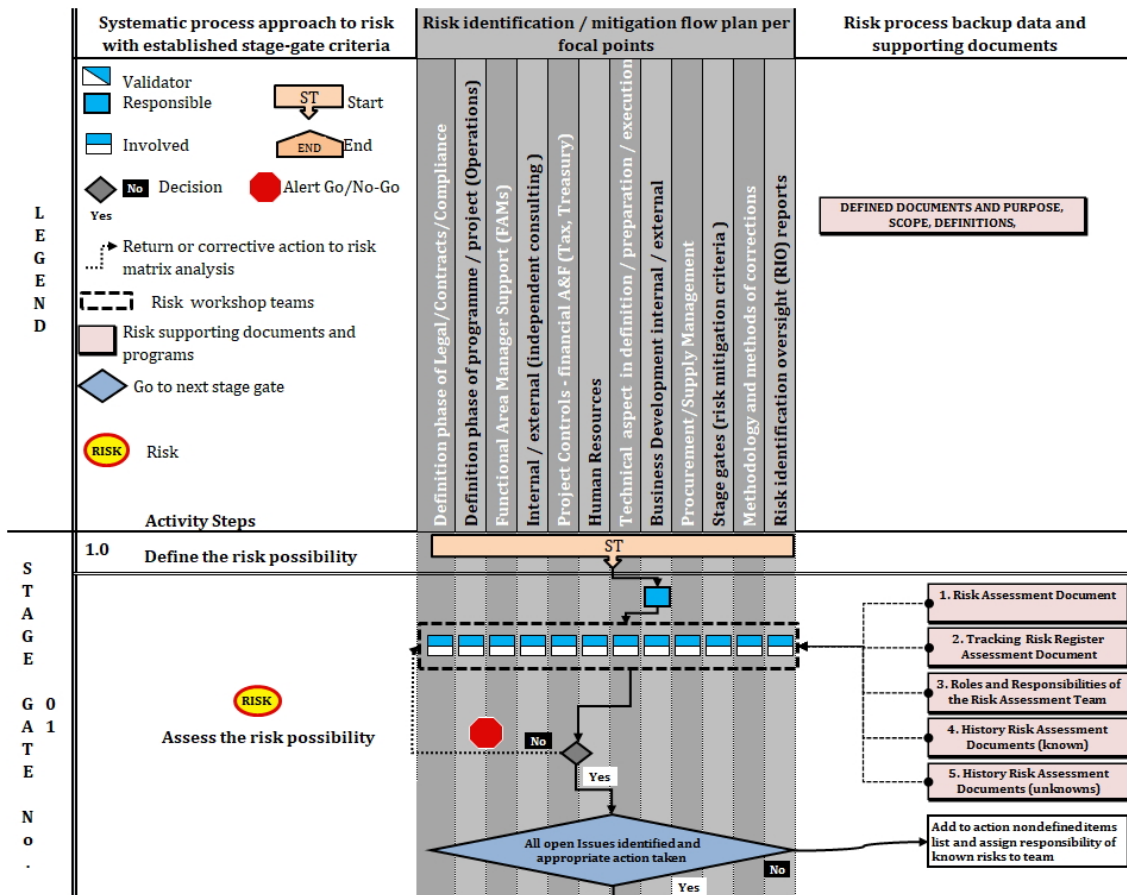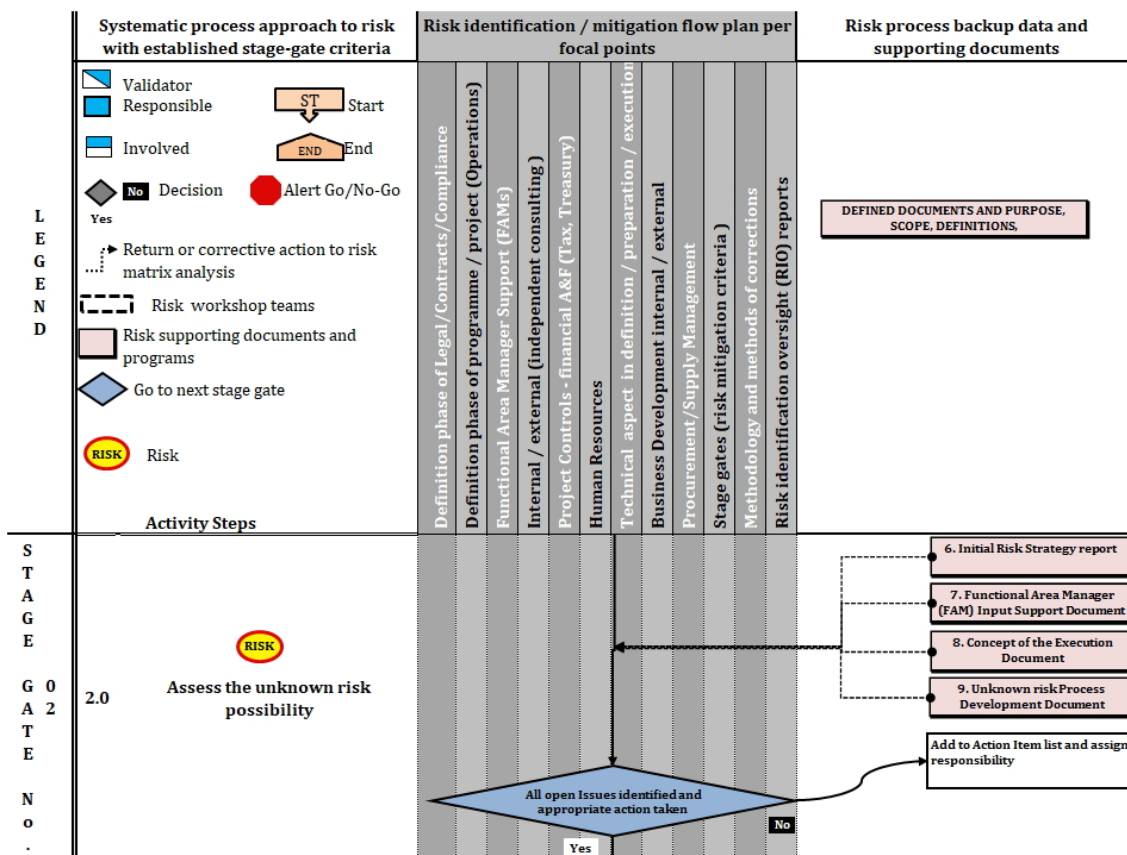
Fig. 1 Stage-gate matrix No. 1
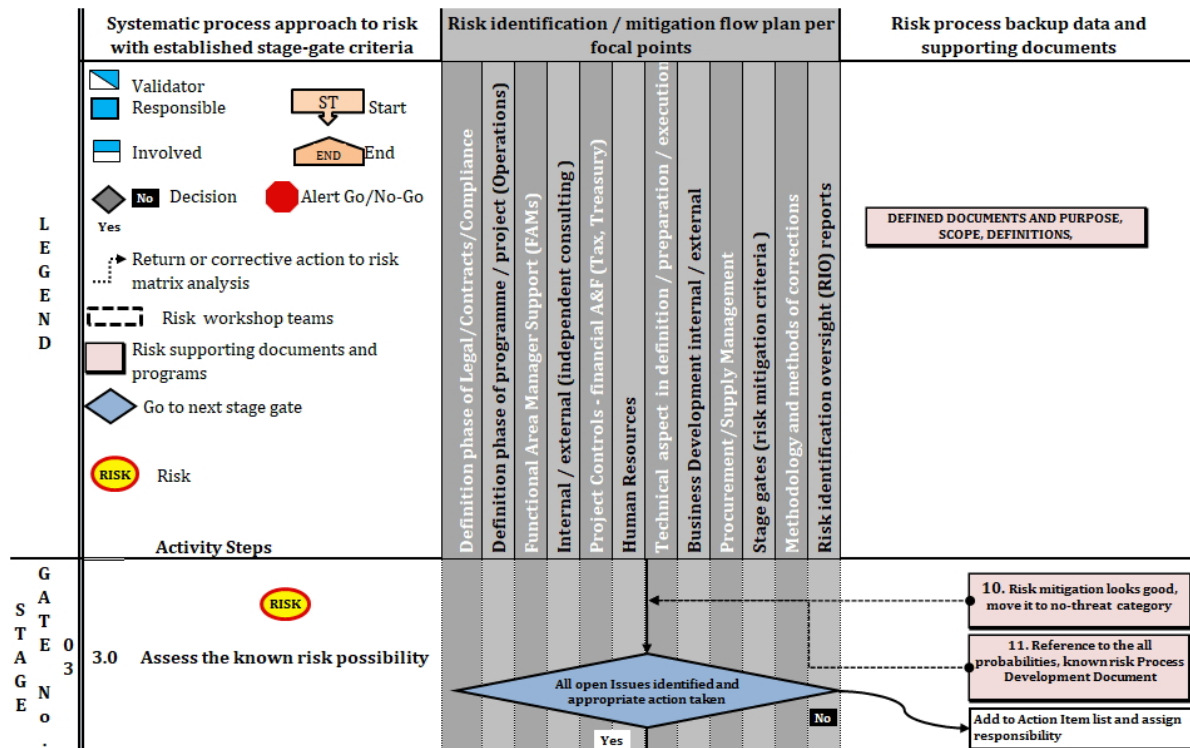

Fig. 2 Stage-gate matrix No. 2

Fig. 3 Stage-gate matrix No. 3

Fig. 4 shows stage-gate No. 4, where all initial reports are obtained, and deeper systematization and synthesis of risk are acquired, the result of which is greater knowledge about the project. The proposed analysis of risk mitigation is focused on the initial WBS and the proposed schedule timelines. All possible deviation, exceptions, and impacts are explained. The link between any documents, but with the emphasis on documents related to scheduling, is achieved using the built-in excel functionality that automatically searches for the source of data needed and used in the current stage gate. Each time the document is currently in use, its opening will require an update. This is achieved using formulas "Formulas> Edit links." All major risk impacts reflecting the schedule are updated, and the first mitigation on all knowns and unknowns is applied.

The formula for the validation of risks:

$$IF (AND(^="✓"), AND(NOT(^=""),NOT(^="")))," OK","")$$

$$IF (AND(^="✓"), AND(NOT(^=""),NOT(^="")))," OK","") \tag{2}$$

where the ^ is the excel file cell location.
Risk exposure factor using unified formulas [33]:

$$E = P \cdot I \tag{3}$$

where E is risk exposure, P risk probability, and I risk impact.
Risk exposure factor and the risk mitigation cost using unified formulas [34, 35]:

$$E = P \cdot I \left(\frac{RV}{PSF/8}\right) \cdot IC \tag{4}$$

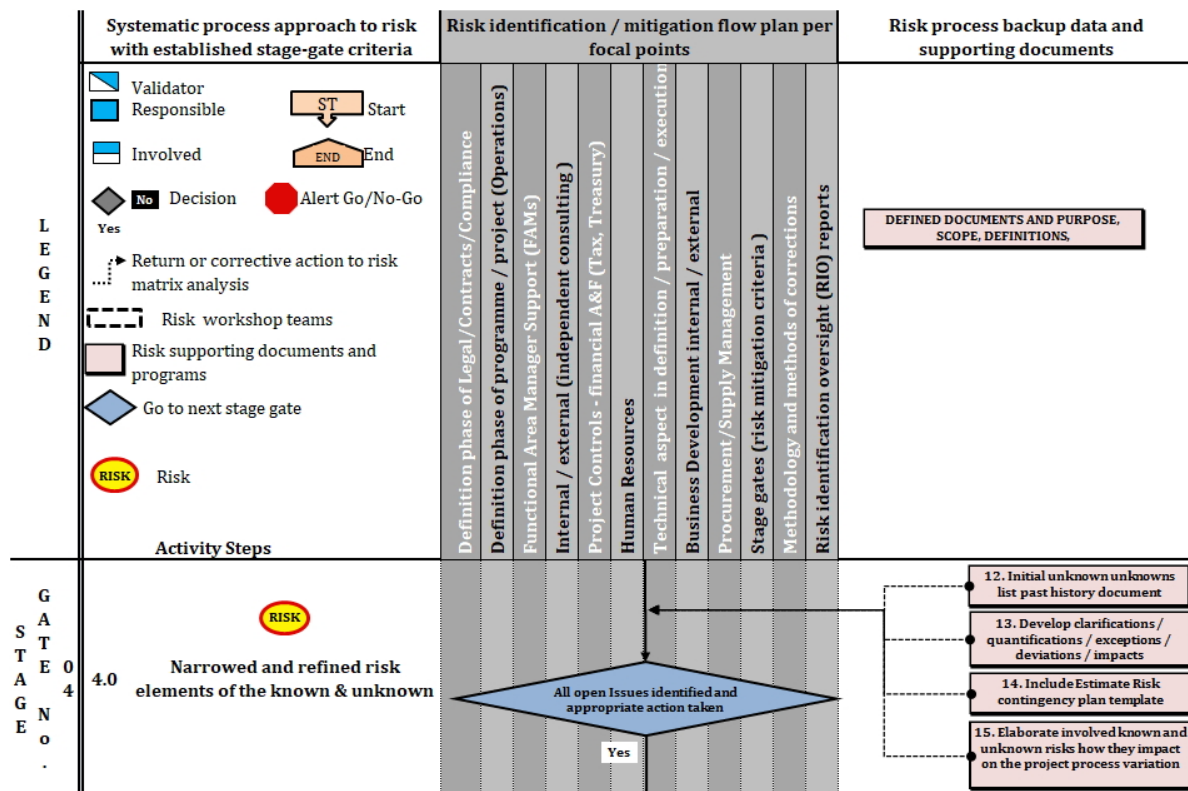where RV is risk weight, IC initial cost, and PSF proportional scale factor.
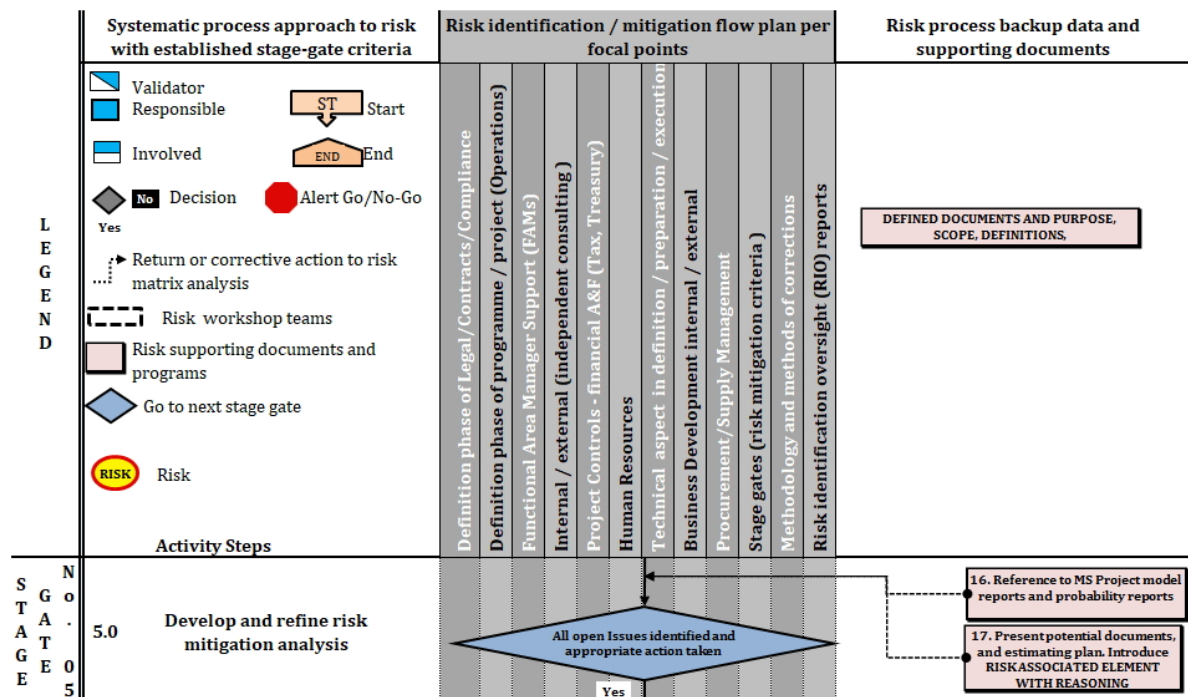
Fig. 4 Stage-gate matrix No. 4

Fig. 5 Stage-gate matrix No. 5

Fig. 5 is stage-gate No. 5, where all data is obtained. The first set of results and reports is examined. The acknowledgment of risk mitigation is derived from the stakeholders, and further actions and analyses are proposed.

All known and unknown risk final impacts are highlighted through the continued workshops [32]. At this stage, the focus is on the high-risk mitigation/probability corrections and the effects on the schedule-timeline built from the initial work breakdown structure and schedule. All possible deviations are presented and explained. The selected risk volumes are moved from the work

breakdown into schedule tool reports. At this stage, the results for the critical risks are confirmed with the data presented in Table 1 & Table 2 - Major risks for Project No. 1 & No. 2.

Fig. 6 shows stage-gate No. 6, where the results are combined, and all project-related risk results locked. At this stage, numerous reports are prepared, and data are archived and stored on the shared drive.
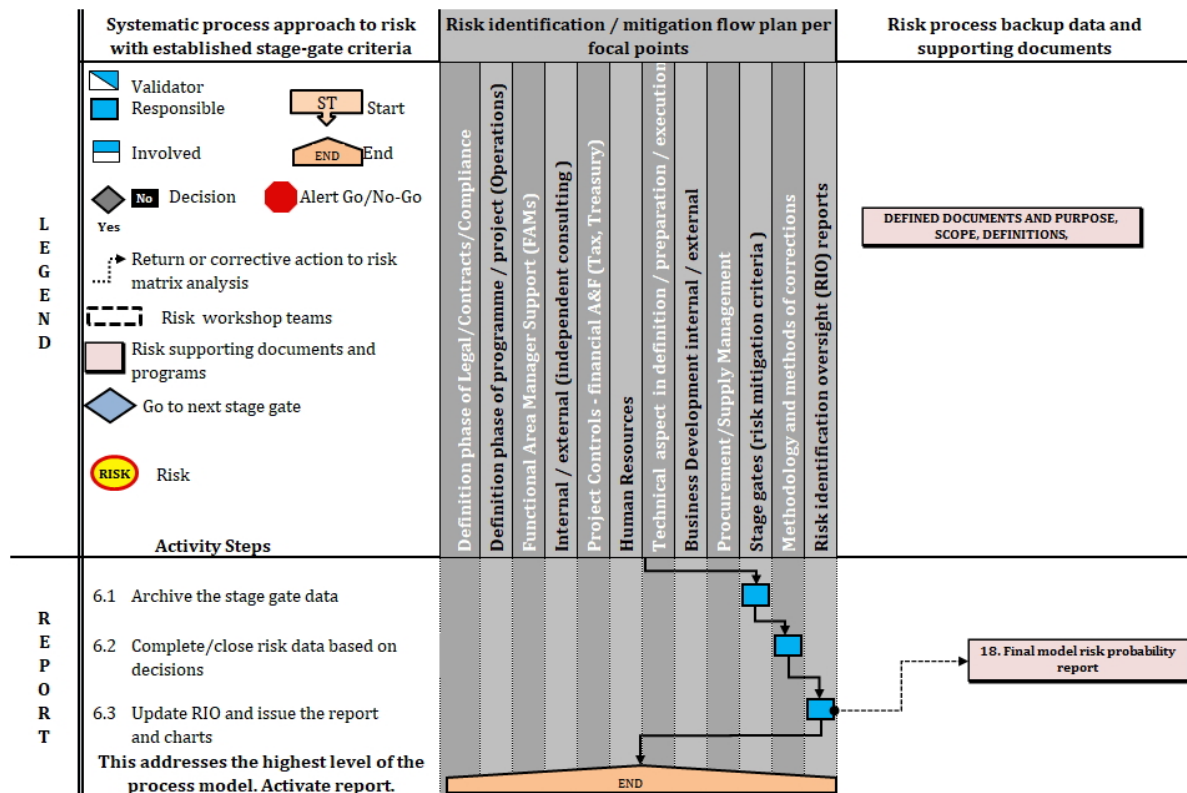

Fig. 6 Stage Gate Matrix No. 6

3. Case studies

3.1 Case study No. 1

Case study No. 1 is an industry project of a drilling platform reconstruction. The project consists of one hundred six scopes of work with the major reconstruction considering all relevant engineering disciplines. Project risk identification and assessment were performed through a set of documents such as RWBS, RR, PI, AHP, FTA, and integrated through the systematic process of the presented model [23, 31]. Starting with the initial three hundred two (302) identified risks, through data analyses, with the comparison of data which have been extracted from the existing history data file and processed through the matrix iterations and mitigation of changes, the final result was fifty-one (51) major selected risks. Fifty-one selected risks use the form of scheduling connection and the initial work breakdown structure (WBS), following the logic. All data is analyzed only concerning the schedule-timeline impacts. The presented changes use the embedded excel formula and pivot analysis of data on certain tasks in which changes occurred. Such a connection drives the preceding data to obtain the final excel table and graph views. As it can be seen in the column differences, going through the systematic model in the early project initiation phase, significant gaps regarding time durations can be observed.

Table 1 Major risks for the case study No. 1

Task ID No.	Description		Duration per tasks		
	Task	Baseline duration	Estimated duration	Difference in days	
1	Painting specialist consulting	216	271	55	
2	Painting specialist consulting WBS – Phase 1	62	57	-5	
3	Painting specialist consulting WBS – Phase 2	62	50	-12	
4	Painting specialist consulting WBS – Phase 3	62	56	-6	
5	Procurement LLI	272	394	122	
6	Procurement Other	142	432	290	
7	Project team – mobilization	13	15	2	
8	Legs scopes of work	171	201	30	
9	Leg #3	171	202	31	
10	Leg #2	144	159	15	
11	Leg #1	144	142	-2	
12	Main deck - steel renewal	129	208	79	
13	Removal of areas & welding of new steel	89	80	-9	
14	Removal of areas & welding of new steel Phase 1	27	15	-12	
15	Removal of areas & welding of new steel Phase 2	29	21	-8	
16	Removal of areas & welding of new steel Phase 3	31	22	-9	
17	Preload tanks	98	143	45	
18	Bow	70	86	16	
19	Tank #1	54	82	28	
20	Tank #2	58	83	25	
21	Tank #3	64	86	22	
22	STDB	71	90	19	
23	Tank #13	64	86	22	
24	Tank #17	69	93	24	
25	Tank #12	72	72	0	
26	Tank #14	74	63	-11	
27	Cable trays & supports – renewal	93	85	-8	
28	Refurbishment of cable trays and supports – phase 2	32	24	-8	
29	Refurbishment of cable trays and supports – phase 3	23	15	-8	
30	Helideck installation	77	36	-41	
31	Marine equipment & systems	123	218	95	
32	Jacking system	14	20	6	
33	Preload system – piping & dump valves repair/replacement	98	139	41	
34	Preload system – Phase 1	48	94	46	
35	Preload system – Phase 2	49	40	-9	
36	Drilling equipment & systems	114	151	37	
37	Top drive – overhaul	85	72	-13	
38	Top drive Trolley Beams	55	44	-11	
39	Well testing lines – repair / replacement	18	11	-7	
40	Mud pumps – overhaul	60	40	-20	
41	Safety equipment & systems	124	137	13	
42	Fast rescue boat – refurbishment	35	28	-7	
43	Installation of new davits, lifeboat stations 3 & 4	50	35	-15	
44	Fire alarm system upgrade	55	45	-10	
45	Deck cranes	125	65	-60	
46	STBD crane	41	31	-10	
47	Aft crane	41	37	-4	
48	Port crane	41	37	-4	
49	MCC – upgrade	112	100	-12	
50	Communications & data processing	86	259	173	
51	TV system – 'receiver's replacement	14	12	-2	

3.2 Case study No. 2

Case study No. 2 is an industry project of a drilling rig modernization. The project consists of forty-seven scopes of work with significant modernization considering all relevant engineering disciplines. Project risk identification and assessment were performed using the specific set of documents, as in case study No. 1, following the systematic model process [23, 31]. Starting with the initial two hundred fifty-two (252) identified risks, through data analyses, with the comparison of data which have been extracted from the existing history data file and processed through the matrix iterations and mitigation of changes, the result was thirty (32) major selected risks. Thirty introduced risks use a form of scheduling connection with a comparison of the initial WBS, and the analyzed results reflect only schedule-timeline impacts. The changes show differences in days between the initial estimation in the work breakdown structure WBS, then corrected based on the applied action of the model in the schedule, with an emphasis on durations with a negative impact, but in most cases with a positive impact on the scheduled durations. In every way, this corrective tool shows a realistic status of the planned activities.

Table 2 Major risks for the case study No. 2

Task ID No.	Description		Duration per tasks	
	Task	Baseline duration	Estimated duration	Difference in days
1	Project preparation phase	228	237	9
2	Wind wall	60	272	212
3	Triplex pumps	126	256	130
4	Third-party inspections	11	163	152
5	Substructure	61	118	57
6	R/U electrical power supply	167	121	-46
7	Procurement of rig	350	123	-227
8	Procurement of solids control equipment	160	193	33
9	Procurement of BOP control unit	276	209	-67
10	Procurement of BHA elements	226	117	-109
11	Outdoor high voltage and lighting system execution works	165	111	-54
12	Nested water tank manufacturing	140	184	44
13	MCC container manufacturing	144	113	-31
14	Mast and substructure	120	98	-22
15	Manufacturing of mud tank system	197	133	-64
16	Low pressure mud system	18	15	-3
17	Instrumentation system	95	-8	-103
18	Instrumentation and data system	130	55	-75
19	Install the HP lines & H. manifold	13	35	22
20	Hydraulic system modification	125	72	-53
21	High pressure mud system manufacturing	197	76	-121
22	Fuel tank system manufacturing	258	50	-208
23	Foldable mobile house manufacturing	114	85	-29
24	Finalize social & office containers.	81	86	5
25	Diesel supply system	114	13	-101
26	Caravan manufacturing	183	120	-63
27	BOP transport and testing skid	32	62	30
28	Air supply unit manufacturing	140	34	-106
29	Works prior to mast erection	13	74	61
30	Mast erection partial jobs	20	49	29

4. Results and discussion – Sensitivity transformation of the case studies

Lack of precision can lead to misleading conclusions. The RIO model excludes the possibility of precision errors. Therefore, if the risk assessment and treatments being taken in an inconsequential way by not following all predefined steps, it 'wouldn't be possible to treat the all-risk elements correctly through the RIO model process. In such a case that defined steps in the RIO model matrix have skipped the outcome of the results will lead to significant deviations. The RIO model

sensitivity transformation clearly shows how much systematic approach is needed. In case that such inconsequential way is continued through the entire RIO model matrix, it will be evident misguidance of the data. By enabling a more accurate, systematic treatment of the risks input and output sizes by reducing all possible faults, additional extended learning and vast correction processes can be prevented. Based on that, the accuracy and sensitivity of the model are shown in Fig. 7 to Fig. 10.

Fig. Seven and Fig. 8 show the graph and the amplitudes of the deviations for Project No. 1 and Project No. 2. Graphs in Fig. 9 and Fig. 10 are linked with Table 1 and Table 2 – Major risks for Project No. 1 and 2, where:

- the blue line shows task durations after all five stage gates,
- the red line shows the estimated durations from the initial WBS and schedule,
- the green shows achieved differences in days per task after the RIO process has been applied.

The tables show the main tasks, initial duration based on the WBS, and then the corrected and estimated length based on the RIO model mitigation. Fig. Seven and Fig. 8 clearly show the positive and negative deviations that have a direct impact on the schedule. Based on the results, it is clearly demonstrated that in the early stage of the project definition, risk management has a significant correction impact.

To present one more evidence of how much a systematic risk management tool is needed, Fig. 9 and Fig. 10 show sensitivity graph amplitudes, where some of the steps in the RIO risk matrix decision tree were overlooked and neglected. This shows that the presented model has to follow a precise systematic way of the predefined three steps [15]. Performance cases for both of the projects are negative, or projects are underperformed based on the initially given objectives. If the problem is addressed trivially, by taking only a few significant risks out of the total number of risks, to show deviation in cases when some steps are skipped, it is not possible to treat risk through the process [15]. There is abundant evidence that the early systematic model is needed [9]. A comparison of the graphs for each of the projects clearly shows a significant negative impact and deviation on the project task durations.
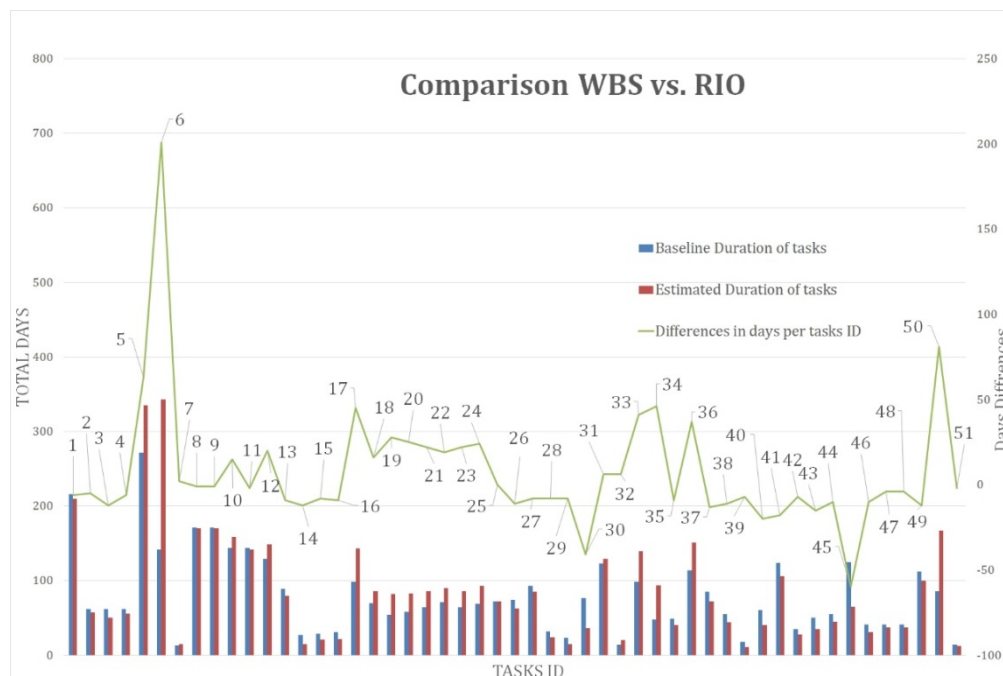

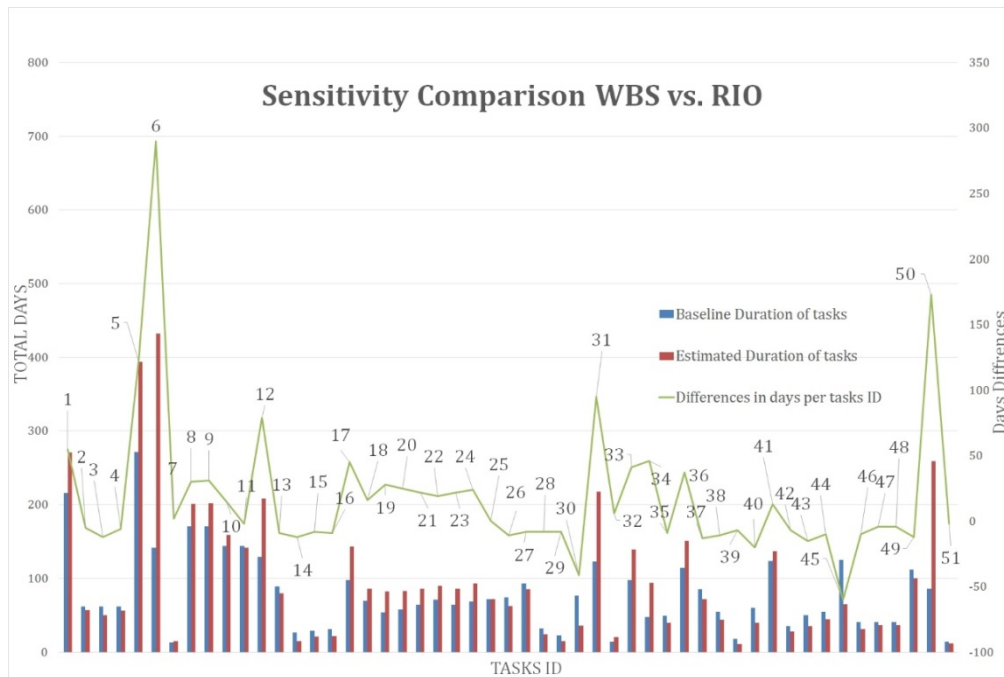**Fig. 7** Major risk deviations case study No. 1

Fig. 8 Sensitivity of major risk deviations case study No. 1
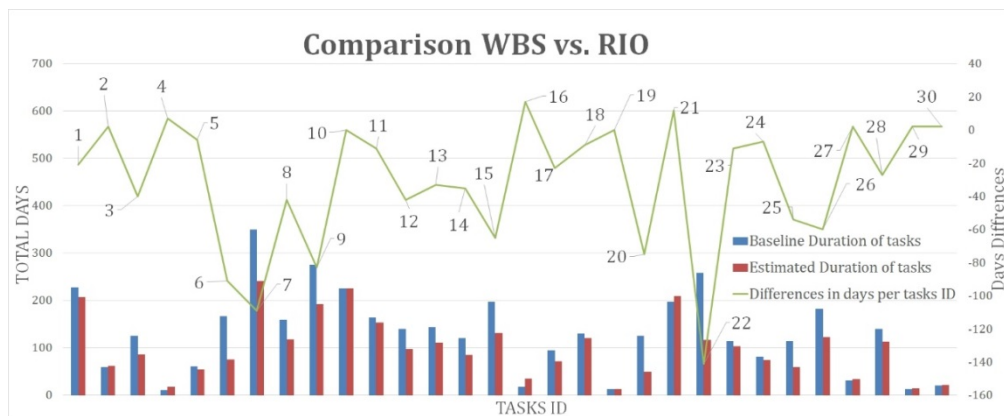

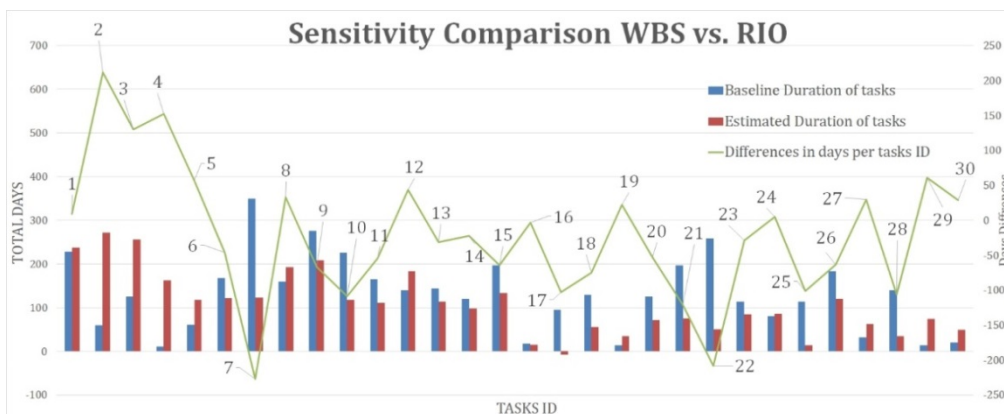**Fig. 9** Major risk deviations case study No. 2

Fig. 10 Sensitivity of major risk deviations case study No. 2

5. Conclusion

Systematic risk management is an ongoing process that should be implemented through all phases of projects [12, 32]. Thus, the lack of systematic formality is an obstacle to successful project implementation. The objective of this paper was to examine the sensitivity of the sys-

tematic risk management model with the involvement of stakeholders throughout the entire risk management process [14, 22]. This paper represents the development of the systematic risk model with references, collaboration quantitative tools system, and the impact of the mentioned systematic system on resolving the gaps and faults and organizational performance, which is based on the model of risk management system success. The paper clearly outlines what is needed in the industry for project management companies to successfully measure the effects of risk threats in any industrial technology [12]. It clearly shows an increased awareness of the sensitivity tools where only a few missed steps can have significant deviations from the original objectives [20]. The sensitivity of results opens a new area of research, but also provides organizations with additional knowledge that needs to be addressed with a systematic definition of the effectiveness of the adopted or existing models. Also, new systematic sensitivity effectiveness improvement of the collaboration system is influenced by the quality of the system model, user-friendliness, end-user involvement, and results in benefits. The paper shows how successful awareness and risk perceptions are necessary to improve future project preparation and future execution. The model uses a mixed approach to data collection with common and acknowledged risk management processes, with the objective parameters in combination with the subjective attitudes of the involved stakeholders, which allows better use of the documents criteria in the model [13]. The model modifies and complements the existing tools of systematic risk success assessment – effectiveness in the context of the structured, systematic system and provides information regarding relations between the stakeholders [4]. With such a systematic approach with locked steps, involving stakeholders from the beginning of the process, and narrowing down their objectives, it is obvious that the major gaps are covered. This research shows that it represents a valid and reliable step towards improving the measurement of the early systematic risk mitigation systems. The main limitation of the study comes from the level of data that is available at an early stage. The second limitation of the tool is the mitigation strategies identified by the stakeholders to accept risks according to which level of activity risks are controllable per the model stage gates. From the academic point of view, the limitation comes from the fact that RIO tool practice is not widespread in other engineering industries with the applicability through the different sets of risk data assessments. The future study will be made in a way of a methodical web-based application that companies can use and access the web-based tool through servers. If there was a need for it, the application could be further developed.

References

[1]   Karimi Azari, A.R., Mousavi, N., Mousavi, S.F., Hosseini, S.B. (2011). Risk assessment model selection in construction industry, *Expert Systems with Applications*, Vol. 38, No. 8, 9105-9111, doi: 10.1016/j.eswa.2010.12.110.

[2]   Peckiene, A., Komarovska, A., Ustinovicius, L. (2013). Overview of risk allocation between construction parties, *Procedia Engineering,* Vol. 57, 889-894, doi: 10.1016/j.proeng.2013.04.113.

[3]   Aleksić, A., Runić Ristić, M., Komatina, N., Tadić, D. (2019). Advanced risk assessment in reverse supply chain processes: A case study in Republic of Serbia, *Advances in Production Engineering & Management*, Vol. 14, No. 4, 421-434, doi: 10.14743/apem2019.4.338.

[4]   Taillandier, F., Taillandier, P., Tepeli, E., Breysse, D., Mehdizadeh, R., Khartabil, F. (2015). A multi-agent model to manage risks in construction project (SMACC), *Automation in Construction*, Vol. 58, 1-18, doi: 10.1016/j.autcon.2015.06.005.

[5]   Lu, S.-T., Kuo, Y.-C., Yu, S.-H. (2010). Risk assessment model for the railway reconstruction project in Taiwan, In: *Proceedings of 2010 International Conference on Machine Learning and Cybernetics*, Qingdao, China, 1017-1022, doi: 10.1109/ICMLC.2010.5580622.

[6]   Osipova, E., Eriksson, E.P. (2013). Balancing control and flexibility in joint risk management: Lessons learned from two construction projects, *International Journal of Project Management,* Vol. 31, No. 3, 391-399, doi: 10.1016/j.ijproman.2012.09.007.

[7]   Purnus, A., Bodea, C.-N. (2013). Considerations on project quantitative risk analysis, *Procedia-Social and Behavioral Sciences*, Vol. 74, 144-153, doi: 10.1016/j.sbspro.2013.03.031.

[8]   Bodicha H.H. (2015). How to measure the effect of project risk management process on the success of construction projects: A critical literature review, *The International Journal of Business & Management*, Vol. 3, No. 12, 99-112.

[9]   Kardes, I., Ozturk, A., Cavusgil, S.T., Cavusgil, E. (2013). Managing global megaprojects: Complexity and risk management, *International Business Review,* Vol. 22, No. 6, 905-917, doi: 10.1016/j.ibusrev.2013.01.003.

[10] Peixoto, J., Tereso, A., Fernandes, G., Almeida, R. (2014). Project risk management methodology: A case study of an electric energy organization, *Procedia Technology,* Vol. 16, 1096-1105, doi: 10.1016/j.protcy.2014.10.124.

[11] Project Management Institute (2011*). A guide to the project management body of knowledge (PMBOK Guide),* 5th edition*,* Project Management Institute, Newtown Square, Pennsylvania, USA.

[12] Yildiz, E.A., Dikmen, I., Birgonul, M.T., Ercoskun, K., Alten, S. (2014). A knowledge-based risk mapping tool for cost estimation of international construction projects, *Automation in Construction,* Vol, 43, 144-155. doi: 10.1016/j.autcon.2014.03.010.

[13] Benta, D., Podean, M., Mircean, C. (2011). On best practices for risk management in complex projects, *Informatica Economica,* Vol. 15, No. 2, 142-152.

[14] Todorović, M.L., Petrović, D.Č., Mihić, M.M., Obradović, V.L., Bushuyev, S.D. (2015). Project success analysis framework: A knowledge-based approach in project management, *International Journal of Project Management,* Vol. 33, No. 4, 772-783, doi: 10.1016/j.ijproman.2014.10.009.

[15] Dey, P.K., Kinch, J., Ogunlana, S.O. (2007). Managing risk in software development project: A case study*, Industrial Management & Data Systems,* Vol. 107, No. 2, 284-303, doi: 10.1108/02635570710723859.

[16] Porananond, D., Thawesaengskulthai, N. (2014). Risk management for new product development projects in food industry, *Journal of Engineering, Project, and Production Management,* Vol. 4, No. 2, 99-113, doi: 10.32738/JEPPM.201407.0005.

[17] Baynal, K., Sarı, T., Akpınar, B. (2018). Risk management in automotive manufacturing process based on FMEA and grey relational analysis: A case study, *Advances in Production Engineering & Management,* Vol. 13, No. 1, 69-80, doi: 10.14743/apem2018.1.274.

[18] Dey, P.K. (2012). Project risk management using multiple criteria decision-making technique and decision tree analysis: A case study of Indian oil refinery, *Production Planning & Control*, Vol. 23, No. 12, 903-921, doi: 10.1080/09537287.2011.586379.

[19] Jun, L., Qiuzhen, W., Qingguo, M. (2011). The effects of project uncertainty and risk management on IS development project performance: A vendor perspective, *International Journal of Project Management,* Vol. 29, No. 7, 923-933, doi: 10.1016/j.ijproman.2010.11.002.

[20] Hassanien, S.S., Skow, J.B. (2012). Quantitative risk assessment for projects schedules, In: *Proceedings of the 9ᵗʰ International Pipeline Conference, Volume 1: Upstream Pipelines; Project Management; Design and Construction; Environment; Facilities Integrity Management; Operations and Maintenance; Pipeline Automation and Measurement,* Calgary, Canada, 61-67, doi: 10.1115/IPC2012-90548.

[21] Irizar, J., Wynn, M. (2014). Centricity in project risk management: Towards a conceptual framework for improved practice, In: *Proceedings of CENTRIC 2014: The Seventh International Conference on Advances in Human-oriented and Personalized Mechanisms, Technologies, and Services*, Nice, France, 83-88.

[22] de Carvalho, M.M., Rabechini, Jr.R. (2015). Impact of risk management on project performance: The importance of soft skills, *International Journal of Production Research,* Vol. 53*,* No. 2, 321-340, doi: 10.1080/00207543.2014.919423.

[23] Burcar Dunović, I., Radujković, M., Vukomanović, M. (2013). Risk register development and implementation for construction projects, *Građevinar,* Vol. 65, No. 1, 23-35.

[24] Berg, H.-P. (2010). Risk management: Procedures, methods and experiences, *RT&A#2,* Vol. 1, No. 17, 79-95.

[25] Renuka, S.M., Umarani, C., Kamal, S. (2014). A review on critical risk factors in the life cycle of construction projects, *Journal of Civil Engineering Research*, Vol. 4, No. 2A, 31-36.

[26] Renault, Y.B., Agumba, J.N., Ansary, N. (2016). An assessment of enterprise risk management process in construction firms, In: *Proceedings of International Conference of Socio-economic Researchers ICSR,* Zlatibor, Serbia, 66-79.

[27] Janekova, J., Fabianova, J., Fabian, M. (2019). Assessment of economic efficiency and risk of the project using simulation, *International Journal of Simulation Modelling*, Vol. 18, No. 2, 242-253, doi: 10.2507/IJSIMM18(2)467.

[28] Yaraghi, N., Langhe, G.R. (2011). Critical success factors for risk management systems, *Journal of Risk Research*, Vol. 14, No. 5, 551-581, doi: 10.1080/13669877.2010.547253.

[29] Moreno, N., Salazar, F., Delgado, S. (2019). Comparative analysis of methodological trends in the management of software projects: Identification of the main variables, *Tehnički Vjesnik – Technical Gazette*, Vol. 26, No. 1, 80-86, doi: 10.17559/TV-20170824233730.

[30] Cagliano, A.C., Grimaldi, S., Rafele, C. (2015). Choosing project risk management techniques: A theoretical framework, *Journal of Risk Research,* Vol. 18, No. 2, 232-248, doi: 10.1080/13669877.2014.896398.

[31] Dey, P.K., Ogunlana, S.O. (2015). Selection and application of risk management tools and techniques for build operate transfer projects, *Industrial Management & Data Systems*, doi: 10.1108/02635570410530748.

[32] Goh, C.S., Abdul-Rahman, H., Abdul Samad, Z. (2013). Applying risk management workshop for a public construction project: Case study, *Journal of Construction Engineering and Management*, Vol. 139, No. 5, 572-580, doi: 10.1061/(ASCE)CO.1943-7862.0000599.

[33] Leopoulos, V.N., Kirytopoulos, K.A. (2004). Risk management: A competitive advantage in the purchasing function, *Production Planning & Control*, Vol. 15, No. 7, 678-687, doi: 10.1080/09537280412331298238.

[34] Roy G.G. (2004). A risk management framework for software engineering practice, In: *Proceedings of Australian Software Engineering Conference*, Melbourne, Australia, 60-67, doi: 10.1109/ASWEC.2004.1290458.

[35] Alberts, C.J. (2006). *Common Element of Risk, Technical Note CMU/SEI-2006-TN-014,* Software Engineering Institute, Carnegie Mellon University, Pittsburgh, USA, 1-26, doi: 10.1184/R1/6572627.v1.

A closed loop Stackelberg game in multi-product supply chain considering information security: A case study

Babaeinesami, A.[a], Tohidi, H.[b,*], Seyedaliakbar, S.M.[c]

[a,b,c]Department of Industrial Engineering, South Tehran Branch, Islamic Azad University, Tehran, Iran

A B S T R A C T

Realization of information security among supply chain components has always been one of the concerns of supply chain players. This research is the development of a mixed integer mathematical model for solving the problem of designing a multi-product network chain and balancing the separation line of parts in a closed loop supply chain. This model is responsive to market demand for finished products and spare parts simultaneously, and minimizes the transportation costs in forward and backward chains, product purchase costs in assembly section, costs of renewing collected products, and fixed costs of workplaces for the dividing the parts. This game consists of two players: the first player includes: Suppliers, assembly centers, retailers and customers, and the second player includes collection centers, renovation centers, separation centers and disposal centers. The payoff of each actor is minimizing their own objectives, and the objective of the model is the unawareness of the members of the chain from the objectives of other members (information security). The proposed model was solved in GAMS 24 software. Due to the nested model, the first model is solved first and the results of the model are entered into the second model. The results of the model solution show the good performance of the proposed model after implementation for the case study. Among the innovations of this research is the consideration of the Stackelberg game in multi-product closed loop supply chain along with the balance of the separation line of parts with the objective of minimizing all the cost elements.

1. Introduction

Over the past few years, the emergence of new technologies and massive changes in world markets have made supply chain management more necessary, in such a way that different organizations have to use supply chain management to create and maintain their competitive position. The information revolution and the emergence of new forms of mutual relationship between organizations and growth of customer expectations with regard to products and services cost, quality, delivery, technology and the committed cycle time, given the increasing competition in global markets and the like, are among the factors that have made organizations around the world to leave traditional purchase systems and move towards the supply chain management system [1].

Due to increased environmental and legal concerns (such as the prohibition of disposal of some products, along with the reduction of raw materials resources and the discovery of the profitable opportunity of recovering returned products), the scope of traditional supply chain

management has broadened the introduction of reverse logistics and the closed-loop supply chain [2]. Over the past few decades, many factories have paid particular attention to the retrieval, renewal, and reverse and closed-loop supply chain in a broad-spectrum of products (including steel, tire, printers, ships, disposable cameras, automotive parts, photocopiers, computers and cellphones) and have had a significant improvement in this field [3]. Renovation of the product can be investigated in two respects: the type of returned products or the type of activities. From the first point of view, the return of products may occur for various reasons throughout the life cycle of the product. Commercial returns are the products that customers return to retailers after 30, 60, or 90 days after purchase, requiring a minor fix for re-launch [4].

Generally and traditionally, manufacturers of products and items do not take any responsibility in relation to their goods after distribution and then consumption by consumers, and do not commit to their distributed and consumed products. Today, however, the volume of consumed products has caused significant damage to the environment, and everyone including consumers and authorities are concerned about the environmental conditions. So everyone expects from different manufacturers of goods and items to accept the cost of waste collection resulting from their products, or at least reduce the waste of consumed products [5]. This growing attention towards waste management and the introduction of new rules on waste products (especially in Europe) have led manufacturers to improve their production process, because the cost of disposal and cleaning the environment is very high. The present study seeks to design a multi-product closed loop logistics network [6]. Lessening transportation costs in forward and backward chains, product purchase costs in assembly section, costs of renewing collected products, and fixed costs of workplaces for the dividing the parts is the main goal of companies.

So this research is presented in 8 sections. In the first and second sections, the introduction and literature review are offered. Statement of the problem and the mathematical modeling are presented in the third and fourth section, respectively. The mechanism of the competition between players is reviewed in the fifth section, and the case study in the sixth section. To end with, computational results and conclusions are expressed in seventh and eighth sections, respectively.

2. Literature review

Zailani *et al.* [7] observed the design of the supply chain network, and proposed linear programming based on genetic algorithm. They used linear programming and also genetic operators. They showed that their method with cplex software is more successful than the traditional genetic algorithm. Saidinia *et al.* [8] proposed a nonlinear integer model with solving method of genetic algorithm for designing a reverse network emphasizing on the number and location of return centers with the objective of minimizing costs. They considered the balance between the discount rate of fare and the cost of inventory storage due to the transportation and integration to determine the exact time of integration of the main collection centers. Zhang *et al.* [9] presented an integer linear programming model for planning a supply chain network with stochastic demand and supply. They presented two-stage stochastic optimization approach based on the integer method, which evaluated location decisions and facility allocations in the first stage and the flow routing decisions in the second stage. Kalverkamp *et al.* [10] outlined a reverse logistics network considering two options of renovation, repair and production simultaneously. They showed that considering repair in the reverse logistics system along with re-production can have a great impact on network structure system and costs reduction. Guo *et al.* [11] studied the general supply chain network by formulating and optimizing the robust state of the network using variable non-uniformity theory. Jia *et al.* [12] investigated the design of the reverse logistics network under uncertainty and provided a two-stage probabilistic programming approach in which the solving method was the integrated SA heuristic method.

Sahebjamnia *et al.* [13] proposed a scenario-based stochastic optimization model for designing a supply chain network, in which demand, the number and quality of returns, and all stochastic variables were considered to be stochastic. Uncertainty in the quality of returned products was considered and a mixture of renewable and crushed in return flow were considered as

stochastic parameters. Pereira *et al.* [14] presented a multi-objective stochastic two-stage integer model for reverse logistics programming, considering multi-product, technology selection, and the transportation costs and the expansion of waste to be probabilistic. Bhattacharya *et al.* [15] presented an integer programming model for designing of a large-scale paper renovation network under uncertainty. Gu *et al.* [16] developed an integer programming model for simultaneous programming and designed a multi-product multi-cycle closed-loop supply chain in which the given time cycle was divided into strategic time units and these units themselves were divided to smaller parts. They also considered travel time of flows, processing time of facilities, categorization of product materials, product disassembly structure and environmental objectives imposed by law. Hajipour *et al.* [17] projected a strong optimization model for designing a closed-loop supply chain network that supposed the number of refunded products, customer demand, after market, and transportation costs in fluctuating stochastic sets. Hasanov *et al.* [18] studied the design of the reverse supply chain network by designing product components and different levels of quality. They considered the collection of returns from retailers in combination with the renovation of collected product components using the renovation service network. Ruiz-Torres *et al.* [19] provided a reverse supply chain network model that minimized the total cost of return process of electronic products. As'ad *et al.* [20] offered an integer linear programming model for designing a reverse supply chain system for programming the renewal of electronic products in the state of Texas and decreasing the waste flow. Their model measured the obsolescence of electronic products and the multitasking function of resources. Yu *et al.* [21] presented a mathematical model for inventory management in supply chain. They solved the presented mathematical model using Ant colony algorithm. Using fuzzy numbers in model is one of the contributions of model. Orščič *et al.* [22] presented a model for third-party logistics service providers in supply chains. Considering sustainability in green supply chain is one of the contributions of their research. he models incorporates the application of quality measurement standards and a PDCA cycle system of continuous improvement into indicators. Liang *et al.* [23] presented a stochastic mathematical model for remanufacturing in supply chain. Thy proposed the coordination mechanism to describe relationship between supplier and service provider. Finally the adaptive immune genetic algorithm was established to solve the model.

An account of the literature review is given in Table 1.

Table 1 A review of previous research

Author	Network structure	Decision-making factors	Modeling type	Data type	Planning type	Single / multi product	Capacity status	Objective function
Zailani (2019)	CLSC	LA	MIP	Dtr	MP	MC	UnCap	Min cost
Saedinia (2019)	CLSC	LA	MILP	Dtr	SP	SC	UnCap	Min profit
Jing (2019)	RSC	FL	MILP	Dtr	MP	MC/SC	Cap	Min cost
Jia *et al.* (2019)	CLSC	Rou	MIP	Dtr	SP	SC	Cap	Min cost
Ruiz-Torres (2019)	RSC	Flow	MINLP	Stoch	MP	SC	Cap	Min profit
Matthias (2019)	CLSC	Rou	MIP	Stoch	SP	MC	Cap	Min profit
Guo (2019)	CLSC	FL	MINLP	Dtr	SP	SC	UnCap	Min profit
Hajipour *et al.* (2019)	RSC	Allo	MIP	Dtr	SP	MC	Cap	Min cost
As'ad *et al.* (2019)	CLSC	Flow	MILP	Dtr	SP	SC	UnCap	Min cost
Bhattacharya *et al.* (2018)	RSC	FL	MILP	Stoch	MP	MC	Cap	Min cost
Gu *et al.* (2018)	CLSC	Allo	MILP	Dtr	SP	SC	Cap	Min cost
This paper	CLSC	Flow,Allo	MIP	scenario	MP	MC	Cap	Min cost

As the result of the review of previous research shows, the closed-loop supply chain problem has attracted many scholars so far. This attention has been intensified over the last few years due to the importance of economic savings as well as the consideration of environmental aspects and the increasing global attention to sustainable development of organizations. But the issue of multi-product closed-loop supply chain regarding the separation line balance has not been studied so far and is considered as an innovation of this research. Minimizing transportation costs in

forward and backward chains, product purchase costs in assembly section, costs of renovating the collected products, costs of customer refunds, collection costs and fixed costs of the workstations for separating the parts are the main objectives of the companies. Accordingly, given the intense competition, the necessity and importance of this research is quite obvious.

3. Statement of the problem

The problem under study in this research is the design of the multi-product closed-loop supply chain, considering the balance of the separation line of parts. In this study, an integrated model that mutually optimizes the strategic and tactical decisions of a multi-product closed loop supply chain is studied. Once defining decision is done, variables and related parameters, the mathematical model of the problem is established. In this problem, strategic level decisions link with programming the flow of products in the direct and reverse supply chain concurrently. Tactical level decisions are on the balance of separation lines of parts in the reverse chain. To reach a viable and competitive closed-loop supply chain network, the separation line of parts and reverse distribution processes should be able to work simultaneously. This research is the development of a mixed integer mathematical model for solving the problem of designing a multi-product network chain and balancing the separation line of parts in a closed-loop supply chain. This model is responsive to market demand for finished products and spare parts simultaneously, and minimizes the transportation costs in forward and backward chains, product purchase costs in assembly section, costs of renovating the collected product, and fixed costs of workstations for separation of parts. The uncertainty considered is a scenario based. In this type of uncertainty the proposed model is executed on the number of scenarios considered. Therefore, the proposed model considers all the scenarios and gives the optimal solution for all the scenarios. It is important to note that different scenarios are likely to occur with deferent possibility. Therefore, this uncertainty makes decisions at the macro and comprehensive level of supply chain.

As shown in Fig. 1, the raw materials are carried from suppliers to assembly centers. Then the products are sent to retailers and eventually to customers. Renewable products move to collection centers. Finally, these products are detracted from the collection centers to disposal and separation centers which the renovated products are directed to the assembly centers.
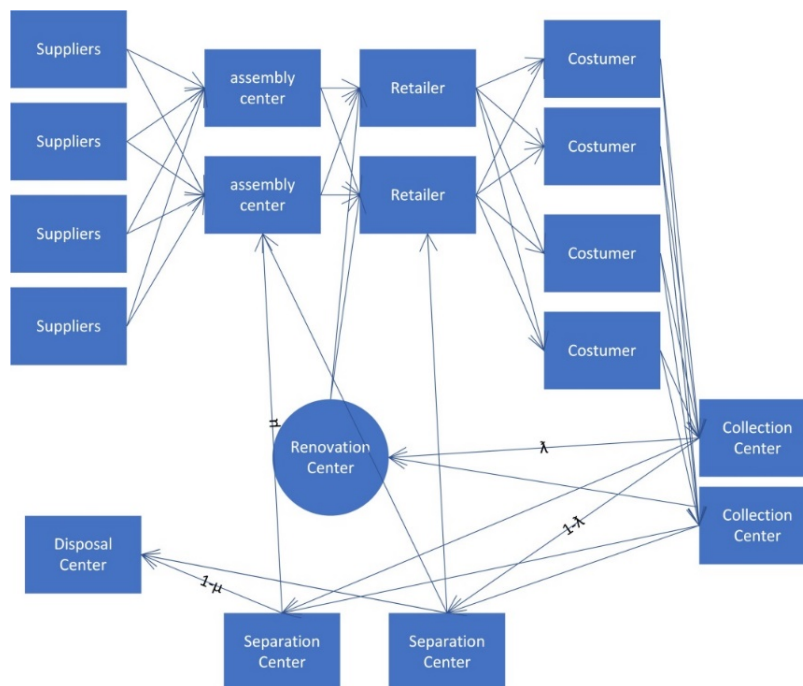

Fig. 1 The flow of products and raw materials in the problem

The main aim of this problem is to estimate the amount of products and parts transported from different centers to each other, as well as allocating and balancing the separation line of parts to minimize system costs.

The innovations of this research are as follows:

- regarding a Stackelberg game in the multi-level multi-product closed loop supply chain and multi-product closed loop,
- considering the balance of the separation line of parts with the objective of minimizing all cost elements,
- developing a model for a multi-product integrated supply chain considering disposal, renovation and collection centers,
- considering scenarios of market recession and boom,
- considering the information security in the supply chain using the game mechanism design.

4. Materials and methods

4.1 Background on the Stackelberg game

In a study on the market economy, Stackelberg used a hierarchical model to describe the market situation for the first time. The model of Stackelberg games is a type of economic games in which the first player initially moves, and then the second player. This model illustrates that there are different decision-makers in the market, and they act according to their own needs which often have different goals but are proportional to the decision of others. Suppose, in the simplest state, there are only two decision makers. So this model models a two-level hierarchy simultaneously, one of them independently managing the market and the other one acting independently (follower). In such games, the first player plays a leading role, and the second player follows the first player. In such games, the follower player observes the move of the leader player and then moves accordingly. Therefore, the best move of the second player is the same move that the Stackelberg balance predicts. A leader can dictate his objectives to the market, but has to wait for the consequences of this decision. The decision of customer determines the profits of the leader.

4.2 Mathematical modeling

Model assumptions are as follows:

- the capacity of all facilities in forward and backward flows is constrained and constant,
- the costs of transportation, purchase, renovation and workstations are definite and pre-identified,
- the rates of collection, disposal, and separation of parts are pre-identified and the amount of renovation is a certain percentage of customer demand and other parameters,
- all workstations can perform operations at the same cost,
- each product is completely separated.

Index

i	Suppliers	p	Index of scenario
j	Assembly centers	c	Index of parts
k	Retailers	g	Index of products
l	Consumers	s	Workstations for separation of parts
m	Collection centers	t	Index of separation operation
r	Renovation centers	a	Index of nodes
d	Separation centers		

Parameters

d_{ij}	Distance between supplier i and assembly center j
d_{jk}	Distance between assembly center j and retailer k

d_{kl}	Distance between retailer k and consumer l
d_{lm}	Distance between consumer l and collection center m
d_{mr}	Distance between collection center m and renovation center r
d_{md}	Distance between collection center m and separation center d
d_{rk}	Distance between renovation center r and retailer k
d_{dj}	Distance between separation center d and assembly center j
d_d	Distance between separation center d and disposal center
a_{gcip}	Capacity of supplier i for part c of product g in scenario p
b_{gip}	Capacity of assembly center j for product g in scenario p
c_{gkp}	Capacity of retailer k for product g in scenario p
u_{glp}	Demand of consumer l for product g in scenario p
e_{gmp}	Capacity of collection center m for product g in scenario p
f_{grp}	Capacity of renovation center r for product g in scenario p
g_{gcdp}	Capacity of separation center d for part c of product g in scenario p
tc	Transportation cost
s_{gci}	Purchase cost of part c of product g from supplier i
w_{gr}	Cost of renovation for product g at center r
cc_{glm}	Cost of collection for product g from consumer l to center m
pc_{gcd}	Cost of separation for part c of product g at center d
rf_{glm}	Cost of refund to customer l for product g to collect to center m
wdc_{gc}	Cost of disposal for part c of product g
o	Fixed cost of workstation
q_{gc}	Number of parts c in product g
θ_{max}	Maximum percentage of collected products
θ_{min}	Minimum percentage of collected products
γ	Percentage of the product sent from collection centers to renovation centers
μ	Percentage of parts sent from separation centers to assembly centers
A_a	Set of artificial nodes on chart of separation operation
B_t	Set of natural nodes on chart of separation operation
d_{B_t}	Time of separation operation t
S_{dp}	Maximum number of workstations in separation center d in scenario p
w_{time}	Working time

Variables

X_{gcijp}	Amount of part c of product g sent from supplier i to assembly center j in scenario p
y_{gjkp}	Amount of product g sent from assembly center j to retailer k in scenario p
w_{gklp}	Amount of product g sent from retailer k to consumer l in scenario p
a_{glmp}	Amount of product g sent from consumer l to collection center m in scenario p
b_{gmrp}	Amount of product g sent from collection center m to renovation center r in scenario p
s_{gmdp}	Amount of product g sent from collection center m to separation center d in scenario p
E_{grkp}	Amount of product g sent from renovation center r to retailer l in scenario p
z_{gcdjp}	Amount of part c of product g sent from separation center d to assembly center j in scenario p
F_{gcdp}	Amount of part c of product g disposed from separation center d in scenario p
T_{gcdp}	amount of part c obtained from the separation of product g at separation center d
CT_{dp}	Cycle time of separation center d in scenario p
M_{tsdp}	1, If the separation operation t is allocated to workstation s at separation center d in scenario p; otherwise 0
L_{tdp}	If the separation operation t is done at separation center d in scenario p.

$$Minz = tc\left(\sum_{g\in G}\sum_{c\in C}\sum_{i\in I}\sum_{j\in J}\sum_{p\in P} x_{gcijp} \cdot d_{ij} + \sum_{g\in G}\sum_{k\in K}\sum_{j\in J}\sum_{p\in P} y_{gjkp} \cdot d_{jk}\right.$$

$$\left. + \sum_{g\in G}\sum_{k\in K}\sum_{l\in L}\sum_{p\in P} w_{gklp} \cdot d_{kl} + \sum_{g\in G}\sum_{c\in C}\sum_{i\in I}\sum_{j\in J}\sum_{p\in P} x_{gcijp} \cdot s_{gci}\right) \tag{1}$$

$$\sum_{j\in J} x_{gcijp} \leq a_{gcip} \qquad\qquad \forall g \in G, c \in C, i \in I, p \in P \tag{2}$$

$$\sum_{k\in K} y_{gjkp} \leq b_{gip} \qquad\qquad \forall g \in G, i \in I, p \in P \tag{3}$$

$$\sum_{l\in L} W_{gklp} \leq c_{gkp} \qquad\qquad \forall g \in G, k \in K, p \in P \tag{4}$$

$$\sum_{k\in K} W_{gklp} \geq u_{glp} \qquad\qquad \forall g \in G, l \in L, p \in P \tag{5}$$

$$\sum_{j\in J} y_{gjkp} + \sum_{r\in R} e_{grkp} - \sum_{l\in L} W_{gklp} = 0 \qquad\qquad \forall g \in G, k \in K, j \in J, p \in P \tag{6}$$

Model of the first player

Objective Eq. 1 is the minimization of transportation costs between all facilities of closed-loop supply chain and the cost of purchasing parts from the supplier. Constraint Eq. 2 shows that the total amount of purchased parts from suppliers can't exceed their capacity in each scenario. Constraint Eq. 3 states that the production amount of finished products should not exceed the production capacity of the assembly center in each scenario. Constraint Eq. 4 ensures that the amount of products distributed by the retailer to the consumer can't exceed the distribution capacity of retailer. Constraint Eq. 5 ensures that the demand of all consumers is satisfied. Constraint Eq. 6 ensures that the amount of parts purchased from the supplier and the amount sent from the separation center to the assembly center is equal to the amount of product that was made at the center assembly of these parts and sent to the retailer.

Model of the second player

$$Minz = \sum_{g\in G}\sum_{m\in M}\sum_{l\in L}\sum_{p\in P} A_{glmp} \cdot d_{lm} + \sum_{g\in G}\sum_{m\in M}\sum_{r\in R}\sum_{p\in P} b_{gmrp} \cdot d_{mr}$$

$$+ \sum_{g\in G}\sum_{m\in M}\sum_{d\in D}\sum_{p\in P} S_{gmdp} \cdot d_{md} + \sum_{g\in G}\sum_{k\in K}\sum_{r\in R}\sum_{p\in P} e_{grkp} \cdot d_{rk}$$

$$+ \sum_{g\in G}\sum_{c\in C}\sum_{d\in D}\sum_{j\in J}\sum_{p\in P} z_{gcdjp} \cdot d_{dj} + \sum_{g\in G}\sum_{c\in C}\sum_{d\in D}\sum_{p\in P} f_{gcdp} \cdot d_{dc}$$

$$+ \sum_{g\in G}\sum_{m\in M}\sum_{r\in R}\sum_{p\in P} b_{gmrp} \cdot w_{gr} + \sum_{g\in G}\sum_{m\in M}\sum_{l\in L}\sum_{p\in P} A_{glmp} \cdot rf_{glm} \tag{7}$$

$$+ \sum_{g\in G}\sum_{m\in M}\sum_{l\in L}\sum_{p\in P} A_{glmp} \cdot cc_{glm} + \sum_{g\in G}\sum_{c\in C}\sum_{d\in D}\sum_{p\in P} f_{gcdp} \cdot wdc_{gc}$$

$$+ \sum_{s\in S}\sum_{d\in D}\sum_{p\in P} N_{sdp} \cdot O_{dp}$$

$$\sum_{r\in R} b_{gmrp} + \sum_{d\in D} S_{gmdp} \leq e_{gmp} \qquad\qquad \forall g \in G, m \in M, p \in P \tag{8}$$

$$\sum_{k\in K} E_{grkp} \leq f_{grp} \qquad\qquad \forall g \in G, r \in R, p \in P \tag{9}$$

$$f_{grp} + \sum_{d \epsilon D} z_{gcdjp} \leq g_{gcdp} \qquad \forall g \in G, c \in C, d \in D, p \in P \qquad (10)$$

$$\sum_{i \epsilon I} x_{gcijp} + \sum_{d \epsilon D} z_{gcdjp} - \sum_{l \epsilon L} y_{gklp} \cdot q_{gc} = 0 \qquad \forall g \in G, k \in K, p \in P \qquad (11)$$

$$\theta_{min} \sum_{k \epsilon K} W_{gklp} \leq \sum_{m \epsilon M} a_{gklp} \leq \theta_{max} \sum_{k \epsilon K} W_{gklp} \qquad \forall g \in G, l \in L, p \in P \qquad (12)$$

$$\gamma \sum_{l \epsilon L} a_{glmp} - \sum_{r \epsilon R} B_{gmrp} = 0 \qquad \forall g \in G, m \in M, p \in P \qquad (13)$$

$$\sum_{m \epsilon M} b_{gmrp} - \sum_{k \epsilon K} e_{grkp} = 0 \qquad \forall g \in G, r \in R, p \in P \qquad (14)$$

$$(1 - \gamma) \sum_{l \epsilon L} a_{glmp} - \sum_{d \epsilon D} s_{gmdp} = 0 \qquad \forall g \in G, m \in M, p \in P \qquad (15)$$

$$(1 - \mu) \sum_{m \epsilon M} s_{gmdp} \cdot q_{gc} - f_{gcdp} = 0 \qquad \forall g \in G, c \in C, d \in D, p \in P \qquad (16)$$

$$\mu \sum_{m \epsilon M} s_{gmdp} \cdot q_{gc} - \sum_{j \epsilon J} z_{gcdjp} = 0 \qquad \forall g \in G, c \in C, d \in D, p \in P \qquad (17)$$

$$\sum_{B_t \epsilon S(A_a)} L_{tdp} = 1 \qquad \forall a = 0, d \in D, p \in P, \forall t \in T \qquad (18)$$

$$\sum_{B_t \epsilon S(A_a)} L_{tdp} = \sum_{B_t \epsilon P(A_a)} L_{tdp} \qquad \forall a \neq 0, d \in D, p \in P, \forall t \in T \qquad (19)$$

$$\sum_{s \epsilon S} M_{tsdp} = L_{tdp} \qquad \forall t \in T, d \in D, p \in P \qquad (20)$$

$$\sum_{t \epsilon T} M_{tsdp} \cdot d_{B_t} \leq w_{time} / \left(\sum_{j \epsilon J} \sum_{c \epsilon C} z_{gcdjp} + \sum_{c \epsilon C} f_{gcdp} \right) \qquad \forall s \in S, d \in D, p \in P \qquad (21)$$

$$X_{gcijp}, y_{gjkp}, a_{glmp}, b_{gmrp}, s_{gmdp}, e_{grkp}, z_{gcdjp}, f_{gcdp} \geq 0 \qquad (22)$$

$$L_{tsdp}, L_{tdp} \in \{0, 1\} \qquad (23)$$

Objective function Eq. 7 is to minimize transportation between supply chain facilities, renovation costs of collected products, refund costs to the customer for the collection of products, costs of product collection and the cost of disposal of parts.

Constraint Eq. 8 indicates that the amount of products sent from the collection center to the renovation center can't exceed the capacity of the collection center. Constraint Eq. 9 indicates that the amount of products sent to the retailer from the renovation center can't exceed the capacity of the renovation center. Constraint Eq. 10 shows that the amount of parts sent from the separation center to the assembly and disposal center can't exceed the capacity of the separation center. Constraint Eq. 11 shows that the amount of products sent from the assembly center and the amount sent from the renovation center to the retailer is equal to the amount sent from the retailer to the consumer. Constraint Eq. 12 ensures that the amount of products collected from consumers should be between minimum and maximum of collection rates. Constraint Eq. 13 ensures that γ percent of the products collected from consumers is equal to the amount of products sent from the collection center to the renovation center. Constraint Eq. 14 ensures that the amount of products that is renovated in the renovation center is equal to the amount sent to the retailer from that center. Constraint Eq. 15 ensures that the remaining amount of the collected products is sent to the separation centers. Constraint Eq. 16 ensures that the amount of parts

that is obtained at the separation center and in unusual conditions is equal to the amount disposed. Constraint Eq. 17 ensures that the remaining amount of parts in the separation center in the usable conditions is equal to the amount sent from the separation center to the assembly center. Constraints Eq. 18 and Eq. 19 ensure that exactly one branch of the part separation graph is selected in each period. Constraint Eq. 20 ensures that each separation operation is exactly assigned to one of the work stations. Constraint Eq. 21 ensures that the time spent on each workstation should not be longer than the cycle time; the cycle time is obtained from dividing the working time into the amount of the separated parts. Constraint Eq. 22 implements the non-negativity constraint on decision variables. Constraint Eq. 23 shows binary variables.

4.3 Competition mechanism of players as Stackelberg game

Realization of information security among supply chain components has always been one of the concerns of supply chain players. Each member of the supply chain is trying to minimize their costs, but none of them are willing to inform other supply chain members of their objective functions and amount of cost minimization. So in this study, using a Stackelberg game, a game is designed to cover these objectives. This game consists of two players: the first player includes: Suppliers, assembly centers, retailers and customers, and the second player includes collection centers, renovation centers, separation centers and disposal centers. The payoff of each actor is minimizing their own objectives, and the objective of the game is the unawareness of the members of the chain from the objectives of other members (information security). Also due to the inherent uncertainty of the mentioned problem, the parameters and decision variables are considered as scenario-based. Therefore, the uncertainty used in this paper is scenario-based. The scenarios considered in this study include three scenarios:

- market recession,
- normal market conditions,
- market boom.

Table 2 shows design of scenarios:

Table 2 Design of scenarios

Scenario	Scenario description	Demand
Scenario1	market recession	Up to 2000
Scenario2	normal market	Up to 1000
Scenario3	market boom	Up to 500

So the designed game mechanism is as shown in Fig. 2.
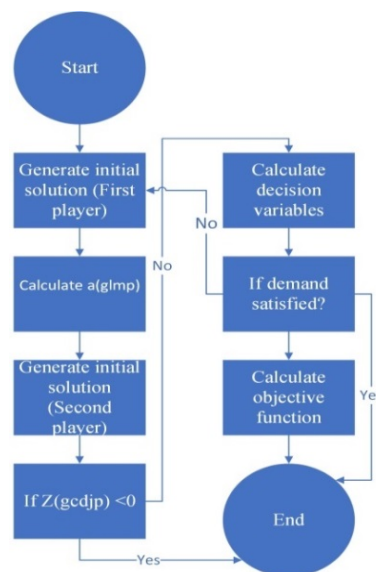

Fig. 2 Designed game mechanism

In order to implement the game mechanism, first, the first model (first player model) will be solved then the value of the variable a_{glmp} will be calculated. This value will enter into the second model, and then the model of the second player will be solved. If the value of z_{gcdjp} is negative, the solving mechanism is complete; otherwise the decision variables of the second model will be solved and if the demand is satisfied, the model is complete; otherwise, the first model will be solved again to satisfy the demand.

5. Results and discussion

5.1 Case study

Simachob company, the largest and only Iranian company in the field of wood industry, is located on an area of 50,000 square meters using the most advanced machinery, the most experienced specialists, employing 320 skilled workers, more than 30 contracting companies, having over half a century of experience in the field of designing and producing various types of park furniture (benches, trash cans and gazebos), park fitness equipment, polyethylene play tools for children, park granule flooring and equipping parks, passages and streets. This company has been investigated for the case study. The factory has 5 suppliers, 3 assembly centers, 6 retailers, 4 collection centers, 3 separation centers, 3 products, 3 renovation centers and 5 major customers.

Below are some of the parameters of the first model.

Table 3 shows the distance between the collection center m and the separation center d. The distances are in meters. For example, the distance between the collection center 3 and the separation center 2 is 8700 meters.

Table 4 shows the demand for the product from customers in different scenarios. As can be seen, the first scenario is market boom, the second scenario is normal conditions and the third scenario is market recession. Thus, according to the following table, the amount of demand for the first product in the third scenario for the fourth customer is 80 units.

Also, some of the parameters of the second model are as follows. For example, the capacity of the renovation center for the product g in the scenario p is given in Table 5. For example, the second product's capacity in the third scenario at the third renovation center is 800 units.

Also, each of the products of this factory consists of three separate parts. Therefore, the cost of disposing part c of product g is shown in Table 6. It should be noted that the costs mentioned are in dollars. For example, the cost of disposing the part 3 of the second product is $ 32.

Table 3 Distance between the collection center and the separation center

d / m	1	2	3	4
1	2500	6200	1000	4600
2	4100	2600	8700	9600
3	14200	9500	4800	6900

Table 4 Demand for each product by customers in each scenario

l / g.p	l1	l2	l3	l4	l5
g1.p1	950	860	900	790	880
g1.p2	550	420	450	350	510
g1.p3	120	200	90	80	150
g2.p1	650	710	600	750	790
g2.p2	500	480	530	480	450
g2.p3	230	200	250	300	220
g3.p1	500	550	600	580	560
g3.p2	220	250	260	300	200
g3.p3	100	150	90	120	110

Table 5 The capacity of the renovation center for the product in each scenario

l g.p	r1	r2	r3
g1.p1	1500	1500	1500
g1.p2	1000	1000	1000
g1.p3	800	800	800
g2.p1	1300	1300	1300
g2.p2	900	900	900
g2.p3	800	800	800
g3.p1	1800	1800	1800
g3.p2	1200	1200	1200
g3.p3	900	900	900

Table 6 Disposal cost for each part of the product

c g	c1	c2	c3
g1	8	15	23
g2	12	5	32
g3	11	9	30

5.2 Computational results

The problem is solved using the GAMS 24 software. Fig. 3 shows the results of the model's solution in various iterations. As can be seen, in the base model (first model), the amount of costs decreases with increasing the number of iterations. Also, by increasing the number of iterations, the cost of the second model gradually increases, and this trend continues until the costs are almost constant. The reason for the increase in costs in the second model is model's attempt to satisfy demand. In the solution approach, at first, the first model declares the amount of demand to the second model, and since the second model is not able to satisfy demand at first; it therefore tries to satisfy the demand as much as possible. And otherwise it will satisfy the rest of the demand in the next period.

Table 7 shows the amount of products sent from the assembly center to the retailer in each scenario. For example, the amount of products type 1 sent from the second assembly center to the fifth retailer in the first scenario is 628 units. Also, the amount of products type 2 sent from the first assembly center to the sixth retailer in the third scenario is 213 units. Moreover, the analysis of scenarios shows that the amount of products sent in the market boom scenario is much more than the other scenarios.

Fig. 4 shows the comparison of different scenarios in terms of the objective function. As previously mentioned, there are three scenarios including boom, normal conditions and recession in this study. As shown in Fig. 1, scenario 1 (market boom) has higher trend value of the objective function than other scenarios. Also, as expected, the second project is in balance and the objective function in this scenario is in intermediary state. Finally, in the third scenario, which is recession in the market, the objective function has its lowest value compared to the rest of the scenarios. It is natural that, when the market is in recession, the values of objective functions are less than the boom state, since in the event of recession, transportation costs and other costs are greatly reduced.
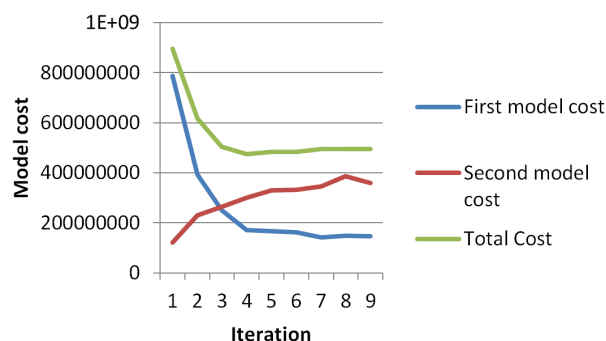

Fig. 3 Results of model solution for different iterations

Table 7 The amount of products sent from the assembly center to the retailer in each scenario

g.j.k	$p = 1$	$p = 2$	$p = 3$
g1.j2.k1	669	371	-
g1.j3.k2	686	368	142
g1.j3.k3	-	323	-
g1.j2.k5	628	-	102
g1.j3.k5	632	-	213
g2.j1.k5	-	323	247
g2.j1.k6	616	-	213
g2.j2.k1	684	-	104
g2.j2.k2	665	339	247
g2.j2.k3	700	322	-
g2.j2.k4	-	382	119
g2.j2.k6	-	338	119
g2.j3.k2	608	-	-
g2.j3.k3	644	302	-
g3.j3.k3	-	301	177
g3.j1.k4	696	-	193
g3.j1.k6	652	363	-
g3.j2.k1	699	321	138
g3.j2.k2	-	333	238
g3.j2.k4	655	-	187
g3.j3.k1	617	331	-
g3.j3.k4	-	302	105
g3.j3.k5	607	-	231
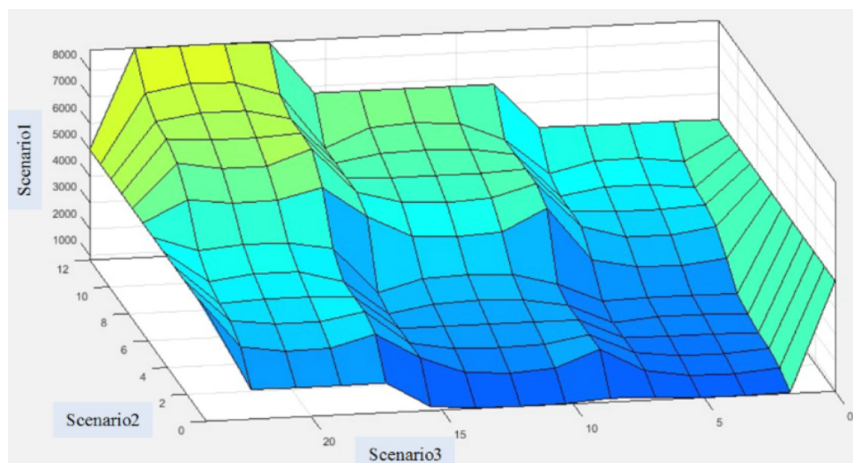
Fig. 4 Comparison of the costs of different scenarios

Sensitivity analysis of mathematical models shows the sensitivity and importance of effective parameters on objective functions and model variables. Here, the effects of changes in demand are examined in two models. As can be seen, with demand increasing, the costs of the first and second models and the total model will increase. According to Fig. 5, a 30 % reduction in demand will result in a cost of 12490000 for the first model and a cost of 29319900 for the second model. An increase of 10 % in demand will lead to an increase in the costs of the first model to 23711000 and an increase in the second model to 34420000. Eventually, an increase in demand up to 30 percent will result in an increase in total costs to 58131000.

Fig. 6 shows the effect of disposal costs on the two models. As can be seen, with the in-crease in disposal costs, the costs of the first and second models and the total model will increase. According to Fig. 4, a 30 % reduction in disposal costs will result in a cost of 31150000 for the second model and a cost of 10374000 for the first model. Also, a 10 % increase in the disposal costs will lead to an increase in the cost of the first model to 18711000 and an increase in the second model to 38950000. Eventually, the increase in the disposal costs up to 30 % will lead to an in-crease in the costs of the first and second models to 21415000 and 45105000 respectively.
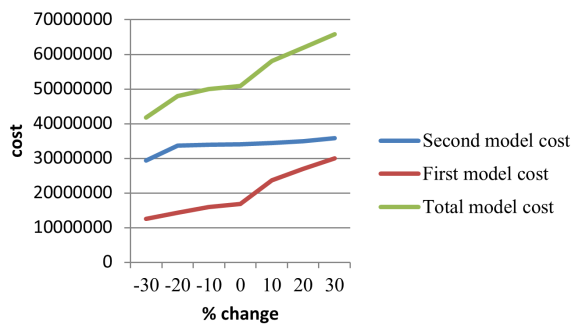
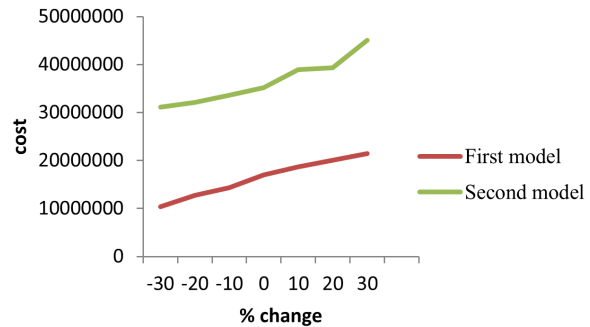**Fig. 5** Sensitivity analysis of the amount of demand

Fig. 6 The effect of disposal costs on two models

The reason for the increase in costs in the second model is the attempt to satisfy demand. In the solution approach, at first, the first model declares demand to the second model; and since the second model is not able to satisfy demand at first, it tries to solve the model with more iterations which increases the amount of costs.

6. Conclusion

Reverse logistics management and closed-loop supply chains are of the important and vital aspects of every business and ensure the production, service distribution, and support of every kind of products. In today's business market, which the life cycle of products shortens every day, product return policies are defined with quick response times and customer service and more emphasis on return management, renovation and re-storage of the finished products. New government laws and green laws that associate with to return and removal of materials also need high-level logistics managers and supply chain processors to concentrate more on the reverse logistics process and the closed-loop supply chain. This survey is the development of a mixed integer mathematical model for solving the problem of designing a multi-product chain network and balancing the separation line of parts in a closed-loop supply chain. This model is responsive to the market demand for finished products and parts simultaneously and minimizes transportation costs in forward and backward chains, product purchase costs in the assembly section, the costs of renovating the products, and fixed cost of workstations for separation of parts. According to the importance of the information, a Stackelberg game including two models is presented. The case study of this research is Simachob, which has 5 suppliers, 3 assembly centers, 6 retailers, 4 collection centers, 3 separation centers, 3 products, 3 renovation centers and 5 major customers. So the amount of problem variables has been computed. For example, the amount of products type 1 sent from the second assembly center to the fifth retailer in the first scenario is 628 units. Also, the amount of products type 2 sent from the first assembly center to the sixth retailer in the third scenario is 213 units. Sensitivity analysis results indicate that a 30 % reduction in demand will result in a cost of 12490000 for the first model and a cost of 29319900 for the second model. An increase of 10 % in demand will lead to an increase in the costs of the first model to 23711000 and an increase in the second model to 34420000. Eventually, an increase in demand up to 30 percent will result in an increase in total costs to 58131000. One of the constraints of this research is the lack of access to accurate cost information. The following are also suggested for future studies:

- Considering other types of uncertainty for example stochastic or fuzzy.
- Considering other games in the closed-loop supply chain, for example Nash equilibrium.
- Solving closed-loop supply chain problem using meta-heuristic approaches such as ant colony algorithm and genetic algorithms.
- Considering the failure rate in disposal centers and separation centers.

References

[1] Li, J., Wang, Z., Jiang, B., Kim, T. (2017). Coordination strategies in a three-echelon reverse supply chain for economic and social benefit, *Applied Mathematical Modelling,* Vol. 49, 599-611, doi: 10.1016/j.apm.2017.04.031.

[2] Kim, J., Chung, B.D., Kang, Y., Jeong, B. (2018). Robust optimization model for closed-loop supply chain planning under reverse logistics flow and demand uncertainty, *Journal of Cleaner Production,* Vol. 196, 1314-1328, doi: 10.1016/j.jclepro.2018.06.157.

[3] Flygansvær, B., Dahlstrom, R., Nygaard, A. (2018). Exploring the pursuit of sustainability in reverse supply chains for electronics, *Journal of Cleaner Production,* Vol. 189, 472-484, doi: 10.1016/j.jclepro.2018.04.014.

[4] Heydari, J., Govindan, K., Sadeghi, R. (2018). Reverse supply chain coordination under stochastic remanufacturing capacity, *International Journal of Production Economics,* Vol. 202, 1-11, doi: 10.1016/j.ijpe.2018.04.024.

[5] Phuc, P.N.K., Yu, V.F., Tsao, Y.-C. (2017). Optimizing fuzzy reverse supply chain for end-of-life vehicles, *Computers & Industrial Engineering,* Vol. 113, 757-765, doi: 10.1016/j.cie.2016.11.007.

[6] Shi, J., Zhou, J., Zhu, Q. (2019). Barriers of a closed-loop cartridge remanufacturing supply chain for urban waste recovery governance in China, *Journal of Cleaner Production,* Vol. 212, 1544-1553, doi: 10.1016/j.jclepro.2018.12.114.

[7] Zailani, S., Iranmanesh, M., Foroughi, B., Kim, K., Hyun, S.S. (2019). Effects of supply chain practices, integration and closed-loop supply chain activities on cost-containment of biodiesel, *Review of Managerial Science*, 1-21, doi: 10.1007/s11846-019-00332-9.

[8] Saedinia, R., Vahdani, B., Etebari, F., Nadjafi, B.A. (2019). Robust gasoline closed loop supply chain design with redistricting, service sharing and intra-district service transfer, *Transportation Research Part E: Logistics and Transportation Review,* Vol. 123, 121-141, doi: 10.1016/j.tre.2019.01.015.

[9] Zhang, Z.-C., Guo, L., Wu, Q.-Q., Gong, L.-M., Ni, T.-T., Guo, P.-H. (2019). Dynamic pricing with reference quality effects in closed-loop supply chain, In: Huang, G., Chien, C.F., Dou, R. (eds), *Proceeding of the 24th International Conference on Industrial Engineering and Engineering Management,* Springer, Singapore, 549-557, doi: 10.1007/978-981-13-3402-3_58.

[10] Kalverkamp, M., Young, S.B. (2019). In support of open-loop supply chains: Expanding the scope of environmental sustainability in reverse supply chains, *Journal of Cleaner Production,* Vol. 214, 573-582, doi: 10.1016/j.jclepro.2019.01.006.

[11] Guo, J., He, L., Gen, M. (2019). Optimal strategies for the closed-loop supply chain with the consideration of supply disruption and subsidy policy, *Computers & Industrial Engineering,* Vol. 128, 886-893, doi: 10.1016/j.cie.2018.10.029.

[12] Jia, F., Gong, Y., Brown, S. (2019). Multi-tier sustainable supply chain management: The role of supply chain leadership, *International Journal of Production Economics*, Vol. 2017, 44-63, doi: 10.1016/j.ijpe.2018.07.022.

[13] Sahebjamnia, N., Fathollahi-Fard, A.M., Hajiaghaei-Keshteli, M. (2018). Sustainable tire closed-loop supply chain network design: Hybrid metaheuristic algorithms for large-scale networks, *Journal of Cleaner Production,* Vol. 196, 273-296, doi: 10.1016/j.jclepro.2018.05.245.

[14] Pereira, M.M., Machado, R.L., Ignacio Pires, S.R., Pereira Dantas, M.J., Zaluski, P.R., Frazzon, E.M. (2018). Forecasting scrap tires returns in closed-loop supply chains in Brazil, *Journal of Cleaner Production,* Vol. 188, 741-750, doi: 10.1016/j.jclepro.2018.04.026.

[15] Bhattacharya, R., Kaur, A., Amit, R.K. (2018). Price optimization of multi-stage remanufacturing in a closed loop supply chain, *Journal of Cleaner Production,* Vol. 186, 943-962, doi: 10.1016/j.jclepro.2018.02.222.

[16] Gu, X., Ieromonachou, P., Zhou, L., Tseng, M.-L. (2018). Developing pricing strategy to optimise total profits in an electric vehicle battery closed loop supply chain, *Journal of Cleaner Production,* Vol. 203, 376-385, doi: 10.1016/j.jclepro.2018.08.209.

[17] Hajipour, V., Tavana, M., Di Caprio, D., Akhgar, M., Jabbari, Y. (2019). An optimization model for traceable closed-loop supply chain networks, *Applied Mathematical Modelling*, Vol. 71, 673-699, doi: 10.1016/j.apm.2019.03.007.

[18] Hasanov, P., Jaber, M.Y., Tahirov, N. (2019). Four-level closed loop supply chain with remanufacturing, *Applied Mathematical Modelling,* Vol. 66, 141-155, doi: 10.1016/j.apm.2018.08.036.

[19] Ruiz-Torres, A.J., Mahmoodi, F., Ohmori, S. (2019). Joint determination of supplier capacity and returner incentives in a closed-loop supply chain, *Journal of Cleaner Production,* Vol. 215, 1351-1361, doi: 10.1016/j.jclepro.2019.01.146.

[20] As'ad, R., Hariga, M., Alkhatib, O. (2019). Two stage closed loop supply chain models under consignment stock agreement and different procurement strategies, *Applied Mathematical Modelling,* Vol. 65, 164-186, doi: 10.1016/j.apm.2018.08.007.

[21] Yu, W., Hou, G., Xia, P., Li, J. (2019). Supply chain joint inventory management and cost optimization based on ant colony algorithm and fuzzy model, *Tehnički Vjesnik – Technical Gazette,* Vol. 26, No. 6, 1729-1737, doi: 10.17559/TV-20190805123158.

[22] Orščič, J., Rosi, B., Jereb, B. (2019). Measuring sustainable performance among logistic service providers in supply chains, *Tehnički Vjesnik – Technical Gazette*, Vol. 26, No. 5, 1478-1485, doi: 10.17559/TV-20180607112607.

[23] Liang, Y., Qiao, P.L., Luo, Z.Y., Song, L.L. (2016). Constrained stochastic joint replenishment problem with option contracts in spare parts remanufacturing supply chain, *International Journal of Simulation Modelling,* Vol. 15, No. 3, 553-565, doi: 10.2507/IJSIMM15(3)CO13.

Calendar of events

- 6th International Conference and Expo on Ceramics and Composite Materials, June 8-9, 2020, Frankfurt, Germany.

- 26th International Conference on Advanced Materials, Nanotechnology and Engineering, June 17-18, 2020, Brisbane, Australia.

- 34th annual European Simulation and Modelling Conference (ESM®'2020), October 21-23, 2020, Toulouse, France.

- 14th International Conference on Flow Production, Processing and Industrial Applications, August 13-14, 2020, Venice, Italy.

- International Conference on Innovative Manufacturing and Manufacturing Methodology, September 17-18, 2020, Paris, France.

- 21st International Conference and Exhibition on Materials Science, Nanotechnology and Engineering, September 21-22, 2020, Milan, Italy.

- 31st DAAAM International Symposium – Virtual Online Edition, October 18-25, hosted from Mostar, Bosnia and Herzegovina.

- 15th International Conference on Green Supply Chain Management Applications, January 18-19, 2021, Rome, Italy.

This page intentionally left blank.

Notes for contributors

General

Articles submitted to the *APEM journal* should be original and unpublished contributions and should not be under consideration for any other publication at the same time. Manuscript should be written in English. Responsibility for the contents of the paper rests upon the authors and not upon the editors or the publisher. Authors of submitted papers automatically accept a copyright transfer to *Chair of Production Engineering*, *University of Maribor*. For most up-to-date information on publishing procedure please see the *APEM journal* homepage *apem-journal.org*.

Submission of papers

A submission must include the corresponding author's complete name, affiliation, address, phone and fax numbers, and e-mail address. All papers for consideration by *Advances in Production Engineering & Management* should be submitted by e-mail to the journal Editor-in-Chief:

Miran Brezocnik, Editor-in-Chief
UNIVERSITY OF MARIBOR
Faculty of Mechanical Engineering
Chair of Production Engineering
Smetanova ulica 17, SI – 2000 Maribor
Slovenia, European Union
E-mail: editor@apem-journal.org

Manuscript preparation

Manuscript should be prepared in *Microsoft Word 2010* (or higher version) word processor. *Word .docx* format is required. Papers on A4 format, single-spaced, typed in one column, using body text font size of 11 pt, should not exceed 12 pages, including abstract, keywords, body text, figures, tables, acknowledgements (if any), references, and appendices (if any). The title of the paper, authors' names, affiliations and headings of the body text should be in *Calibri* font. Body text, figures and tables captions have to be written in *Cambria* font. Mathematical equations and expressions must be set in *Microsoft Word Equation Editor* and written in *Cambria Math* font. For detail instructions on manuscript preparation please see instruction for authors in the *APEM journal* homepage *apem-journal.org*.

The review process

Every manuscript submitted for possible publication in the *APEM journal* is first briefly reviewed by the editor for general suitability for the journal. Notification of successful submission is sent. After initial screening, and checking by a special plagiarism detection tool, the manuscript is passed on to at least two referees. A double-blind peer review process ensures the content's validity and relevance. Optionally, authors are invited to suggest up to three well-respected experts in the field discussed in the article who might act as reviewers. The review process can take up to eight weeks on average. Based on the comments of the referees, the editor will take a decision about the paper. The following decisions can be made: accepting the paper, reconsidering the paper after changes, or rejecting the paper. Accepted papers may not be offered elsewhere for publication. The editor may, in some circumstances, vary this process at his discretion.

Proofs

Proofs will be sent to the corresponding author and should be returned within 3 days of receipt. Corrections should be restricted to typesetting errors and minor changes.

Offprints

An e-offprint, i.e., a PDF version of the published article, will be sent by e-mail to the corresponding author. Additionally, one complete copy of the journal will be sent free of charge to the corresponding author of the published article.

APEM
journal

Advances in Production Engineering & Management

Contents